Pipe Interaction with the Backfill Envelope

PUBLICATION NO. FHWA-RD-98-191

JUNE 1999

U.S. Department of Transportation
Federal Highway Administration

Research, Development, and Technology
Turner-Fairbank Highway Research Center
6300 Georgetown Pike
McLean, VA 22101-2296

FOREWORD

The project involved a study of the effects of pipe installation methods on pipe performance. Both laboratory and full-scale field tests were conducted. Pipes used in the tests were donated by Contech Construction Products, CSR/New England, Hancor, Inc., and Plexco/Spirolite, Inc. These pipes are representative of those widely used in practice for drainage applications. The results of the study, including a review of present practices, were used to develop recommendations for improving installation practices. This work is important to pipe design because proper design has to consider the effects of the installation process.

T. Paul Teng

T. Paul Teng P.E.
Director, Office of Infrastructure
Research and Development

NOTICE

Technical Report Documentation Page

1. Report No.	2. Government Accession No.	3. Recipient's Catalog No.
FHWA-RD-98-191		

4. Title and Subtitle	5. Report Date: June 1999
Pipe Interaction with the Backfill Envelope	6. Performing Organization Code: NSF98-444F
7. Author(s): Timothy J. McGrath, Ernest T. Selig, Mark C. Webb, and Glenn V. Zoladz	8. Performing Organization Report No.
9. Performing Organization Name and Address: University of Massachusetts-Amherst, Dept. of Civil & Environmental Engineering, Amherst, Massachusetts 01003-5205	10. Work Unit No. (TRAIS): 3D1d 11. Contract or Grant No.: DTFH61-93-Y-00100
12. Sponsoring Agency Name and Address: National Science Foundation, Arlington, VA 22230; Federal Highway Administration, McLean, VA 22101 & Sterling, VA 20166; California, Iowa, Kansas, Louisiana, Massachusetts, Minnesota, New York, Ohio, Oklahoma, Pennsylvania & Wisconsin State DOT's	13. Type of Report and Period Covered: Final Report June 1993 - Feb. 1998 14. Sponsoring Agency Code

15. Supplementary Notes

Contracting Officer's Technical Representative (COTR): John O'Fallon (HNR-10); John B. Scalzi (NSF)

16. Abstract

This report summarizes a study of installation practices for buried (culvert) pipes. Current practice was reviewed through a literature search and a survey of users, manufacturers, and other involved in the use of buried pipes.

Typical backfill materials were characterized through standard and variable effort compaction tests, CBR tests, penetration tests and one-dimensional compression tests. Standard classification systems were compared and standard groups of backfill materials were evaluated. The soil properties that were used to develop the AASHTO SIDD designs are proposed for use as standard properties for application to the installation of all types of pipes. The Constrained Modulus, M_s, is proposed as the standard measure of soil stiffness replacing the empirical Modulus of Soil Reaction E'.

Laboratory soil box tests and full-scale field tests were conducted to investigate soil behavior during installation. Variables include pipe type (concrete, steel, plastic) and size (600 & 1,500 mm (36 & 60 in.)), in-situ soil condition, trench width, backfill type, compactive effort, haunching effort, and bedding condition. The tests showed that all of the backfill-related test variables have a significant effect on pipe behavior. Tests with controlled low-strength materials showed this to be an excellent type of backfill. Computer modelling demonstrated that the finite element analysis can effectively model installation effects as well as effects of the fill over the pipe. The elastic solution for behavior of buried pipe, developed by Burns and Richard, shows promise as a basis for a simplified design method.

Recommendations for future practice include the use of soft bedding under the bottom of the pipe and of uncompacted fill over the top. Selection of trench width must consider the ability to place and compact backfill in the haunch zone and at the sides of the pipe. Hand tampers, sized differently for different backfills, were shown to be useful for providing haunching effort. It was shown that relatively small changes in backfill density can have significant effects on backfill stiffness.

The project shows that pipe performance is controlled by installation practices. Implementation of a design process that realistically assesses how a project will be built, and construction that understands and implements the design, is imperative for successful long-term culvert performance.

17. Key Words	18. Distribution Statement
Culvert, pipe, backfill, bedding, compaction, soil, trench	No restrictions. This document is available to the public through the National Technical Information Service (NTIS) Springfield, Virginia 22161

19. Security Classif. (of this report)	20. Security Classif. (of this page)	21. No. of Pages	22. Price
Unclassified	Unclassified	269	

Form DOT F 1700.7 (8-72) Reproduction of completed page authorized

SI* (MODERN METRIC) CONVERSION FACTORS

APPROXIMATE CONVERSIONS TO SI UNITS

Symbol	When You Know	Multiply By	To Find	Symbol
		LENGTH		
in	inches	25.4	millimeters	mm
ft	feet	0.305	meters	m
yd	yards	0.914	meters	m
mi	miles	1.61	kilometers	km
		AREA		
in²	square inches	645.2	square millimeters	mm²
ft²	square feet	0.093	square meters	m²
yd²	square yards	0.836	square meters	m²
ac	acres	0.405	hectares	ha
mi²	square miles	2.59	square kilometers	km²
		VOLUME		
fl oz	fluid ounces	29.57	milliliters	mL
gal	gallons	3.785	liters	L
ft³	cubic feet	0.028	cubic meters	m³
yd³	cubic yards	0.765	cubic meters	m³
NOTE: Volumes greater than 1000 l shall be shown in m³.				
		MASS		
oz	ounces	28.35	grams	g
lb	pounds	0.454	kilograms	kg
T	short tons (2000 lb)	0.907	megagrams (or "metric ton")	Mg (or "t")
		TEMPERATURE (exact)		
°F	Fahrenheit temperature	5(F-32)/9 or (F-32)/1.8	Celcius temperature	°C
		ILLUMINATION		
fc	foot-candles	10.76	lux	lx
fl	foot-Lamberts	3.426	candela/m²	cd/m²
		FORCE and PRESSURE or STRESS		
lbf	poundforce	4.45	newtons	N
lbf/in²	poundforce per square inch	6.89	kilopascals	kPa

APPROXIMATE CONVERSIONS FROM SI UNITS

Symbol	When You Know	Multiply By	To Find	Symbol
		LENGTH		
mm	millimeters	0.039	inches	in
m	meters	3.28	feet	ft
m	meters	1.09	yards	yd
km	kilometers	0.621	miles	mi
		AREA		
mm²	square millimeters	0.0016	square inches	in²
m²	square meters	10.764	square feet	ft²
m²	square meters	1.195	square yards	yd²
ha	hectares	2.47	acres	ac
km²	square kilometers	0.386	square miles	mi²
		VOLUME		
mL	milliliters	0.034	fluid ounces	fl oz
L	liters	0.264	gallons	gal
m³	cubic meters	35.71	cubic feet	ft³
m³	cubic meters	1.307	cubic yards	yd³
		MASS		
g	grams	0.035	ounces	oz
kg	kilograms	2.202	pounds	lb
Mg (or "t")	megagrams (or "metric ton")	1.103	short tons (2000 lb)	T
		TEMPERATURE (exact)		
°C	Celcius temperature	1.8C + 32	Fahrenheit temperature	°F
		ILLUMINATION		
lx	lux	0.0929	foot-candles	fc
cd/m²	candela/m²	0.2919	foot-Lamberts	fl
		FORCE and PRESSURE or STRESS		
N	newtons	0.225	poundforce	lbf
kPa	kilopascals	0.145	poundforce per square inch	lbf/in²

* SI is the symbol for the International System of Units. Appropriate rounding should be made to comply with Section 4 of ASTM E380.

(Revised September 1993)

TABLE OF CONTENTS

TABLE OF CONTENTS (continued)

Chapter **Page**

TABLE OF CONTENTS (continued)

Chapter **Page**

LIST OF FIGURES

Figure **Page**

LIST OF FIGURES (continued)

Figure **Page**

Figure **Page**

LIST OF FIGURES (continued)

Figure **Page**

LIST OF FIGURES (continued)

Figure **Page**

LIST OF TABLES

LIST OF TABLES (continued)

Table		Page

LIST OF TABLES (continued)

Table **Page**

CHAPTER 1
INTRODUCTION

1.1 Background

The long-term behavior of buried culverts and other gravity flow pipes is significantly affected by installation practice. While designers often think of the design process as design of a pipe, they are in fact designing a "pipe-soil system" where structural performance depends on structural characteristics of both the pipe and the soil. Rarely, with products in use today, can any rigid or flexible pipe carry all superimposed loads without depending in some way on the surrounding soil for support. Bedding must be uniform to prevent point loads, and lateral soil pressure at the sides of the pipe must be of sufficient magnitude to restrain deformation. Even the loads imposed on a buried pipe are related to the practices used at the time of construction. Thus, designing a buried pipe requires the simultaneous design of the surrounding backfill. Further, if the backfill conditions are important in the design phase, then, it becomes incumbent upon the designer and builder to see that the backfill assumptions made in design are implemented in the field during construction. This is the pipe-soil system design process.

Installation standards for buried pipe have not been thoroughly reviewed from a geotechnical perspective for many years, and some current installation standards use terminology that is outdated and unsuitable for current construction contracts. Also, many industries have proposed their own design and installation standards, suggesting that different types of pipes are fundamentally different and require separate treatment. This is a situation which creates confusion for both designers and installers. Present practice in these two areas needs to be reviewed for updating where necessary and for making standards as uniform as possible across all types of pipes.

A great deal of effort has been expended by the pipe industry and others on the development of mathematical models that describe pipe-soil interaction; however, most of this work has been on the properties of soil after compaction and does not evaluate the soil and pipe behavior that result from the application of compaction forces. Information is needed to correct this deficiency.

The overall goal of this research is to develop a fundamental understanding of the interactions between a buried pipe, the backfill soil around it, and the in situ soil in which the pipe/backfill system is installed. This improved understanding can in turn be used to develop more reliable and economical pipe installation and design methodologies based on improving the control of installation procedures during construction. Development of improved tools for use by designers in assessing the potential performance of installations is also a goal.

1.2 Objectives

The overall objective of the research was to investigate the fundamental interactions that take place during the process of excavating a trench, preparing the subgrade, installing the pipe, and then placing and compacting backfill around it. The materials and procedures used in this part of a pipe installation will strongly influence pipe performance as the balance of the fill is placed above the top of the pipe. An improved understanding of these fundamentals will aid designers in developing technically better and more economical specifications.

Specific objectives of this research were to:

1. Examine current pipe installation practices;
2. Evaluate the implications of current pipe installation practices on pipe performance and assess the potential benefit of new techniques;
3. Define bedding alternatives for buried pipe installations and their effect on pipe performance;
4. Develop improved compaction specifications relating compacted soil density to soil stiffness; and
5. Develop improved procedures for including installation effects in the design of buried pipe.

1.3 Scope

This research investigated the interactions that take place during soil placement around buried pipe and the soil properties that result from the installation process. This included:

1. Gathering information through literature review and survey of individuals and organizations involved in current projects;

2. Characterizing backfill materials in terms of desired soil properties for good pipe support;

3. Conducting laboratory tests to study significant installation parameters in a controlled environment;

4. Conducting full-scale field tests to evaluate findings from the literature review and laboratory tests and to investigate pipe installation techniques; and

5. Completing analyses and evaluations of field results and synthesis of findings into improved guidelines for design and installation of buried pipe.

1.4 Contents

Chapter 2 presents a review of the state of the art of current pipe installation practice among users and manufacturers, and where appropriate, a review of the design practice that is pertinent to installation. Chapter 3 describes the tests conducted on backfill soils, compares soil models, and proposes a set of design soil moduli based on the constrained (one-dimensional) modulus as a substitute for historical values based on the modulus of soil reaction. Chapter 4 presents the procedures and results of the laboratory and field tests conducted as part of this project to document installation behavior. Chapter 5 presents analysis of the field data with an idealized closed form elasticity solution for buried pipe and with finite element modeling of the actual test conditions. Chapter 6 presents a discussion of several key issues that are touched on in multiple chapters of this report. Finally, conclusions are drawn in chapter 7.

CHAPTER 2
STATE OF THE ART

This chapter presents the current state of the art of pipe installation practice based on a review of the literature, a limited survey of current users and specifiers, and review of current installation standards.

The technical literature related to buried pipe and culverts was collected by Selig, et. al., in preparation for the NSF Pipeline Workshop, held at the University of Massachusetts in 1987. This was compiled in an extensive document called "Bibliography on Buried Pipelines." The information provided in the bibliography will only be repeated as is pertinent to this study.

While the intent of the proposed research was to study installation practices, it is impossible to study the subject without also addressing pipe design practice because the two areas are so closely related. Pipe designers make implicit assumptions about installation materials and procedures to assess the pipe strength required for a given project. For example, in the case of rigid pipe design, the selection of a bedding factor involves an assumption of the lateral soil pressures applied to the pipe after installation. Thus, design issues are addressed as required to evaluate installation practice.

Terminology used in this report is defined in Fig. 2.1. Definitions of important terms follow:

Bedding is the soil on which the pipe is placed. The bedding may be in situ soil, but, in areas where naturally occurring soils are variable, it is preferred to use placed soil.

Embedment zone backfill includes all backfill that is in contact with the pipe.

Foundation is the soil which supports the embedment zone backfill. It must provide a firm stable surface and may be in situ soil or placed backfill. It may also serve as the bedding.

Haunch zone is the region of the backfill above the bedding and directly below the springline of the pipe. It is a region where hand placement and compaction methods are normally required for the backfill.

Initial backfill is the material placed at the sides and immediately over the pipe after it is installed on the bedding.

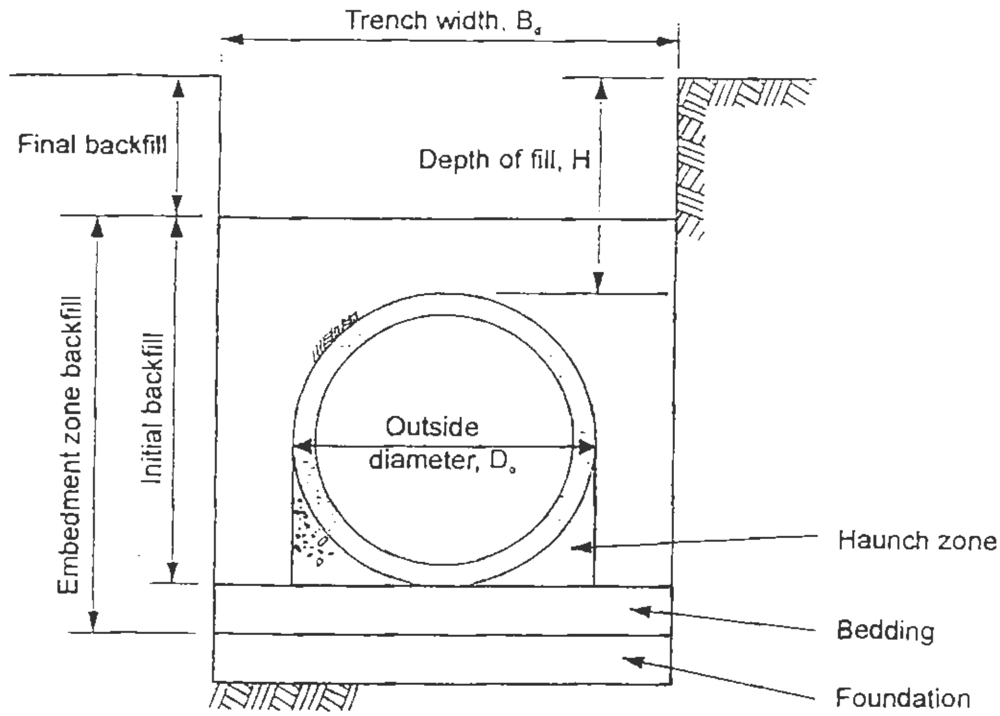

Figure 2.1 Standard Trench Terminology

Rigid Versus Flexible Pipe – This report uses the descriptive terms "rigid" and "flexible" to describe two general classes of pipes. These terms have traditionally been used to differentiate between a pipe with high flexural stiffness (rigid pipe) that carries load primarily through internal moments, and a pipe with low flexural stiffness (flexible pipe) carrying load through internal hoop thrust forces. Flexible pipe develop higher lateral soil pressures at the sides than do rigid pipe. The flexural stiffness of a pipe is described by the parameter EI/R^3, where E is the modulus of elasticity of the pipe material, I is the moment of inertia of the pipe wall, and R is the centroidal radius of the pipe. Concrete and clay pipes are examples of a rigid pipe, with values of EI/R^3 on the order of 7 MPa to 70 MPa (1,000 psi to 10,000 psi), while corrugated metal and plastic pipes are examples of a flexible pipe with EI/R^3 values on the order of 15 kPa to 700 kPa (2 psi to 100 psi). There are two problems with this classification system: (1) the actual response of a system is a function of the relative stiffness of the pipe and soil rather than just the pipe stiffness; and (2) there are no true boundaries to the flexural stiffnesses covered by the classifications, rather there is a transition region where both types of behavior contribute to the overall pipe response. These issues will be discussed further in later chapters.

2.1 Current Design and Installation Practice

The state of the art of current installation practice was evaluated by a survey of users, represented by the States and organizations that sponsored the project, public standards such as American Water Works Association (AWWA), American Society of Civil Engineers (ASCE), and American Society for Testing and Materials (ASTM), and the recommended practices of pipe producers.

2.1.1 General

Rigid Pipe - The most commonly used installation specifications for rigid pipes are derived from the work of Marston, Spangler, and others during the first half of the twentieth century (1913, 1917, 1920, 1926, 1930, 1932, 1933, 1950, 1953). Bedding conditions presented in current references such as the ASCE *Manual of Practice No. 37*, (ASCE, 1970), and the American Concrete Pipe Association's (ACPA) *Concrete Pipe Design Manual* (ACPA 1987a), and *Concrete Pipe Handbook* (ACPA 1987b) continue to present installation details based on this early work, (Fig. 2.2). These details are outdated in that they include such vague terms for soils as "granular material," "backfill," "fine granular fill," and even "soil." The compaction requirements in these beddings are also vague, using terminology such as "densely compacted," "carefully compacted," "lightly compacted," "compacted," and "loose." This terminology of backfill materials and compaction levels are difficult to interpret in modern construction contracts.

Heger (1988) proposed new "standard" installations for concrete pipes in the embankment condition, based on parametric studies with the finite element computer program SPIDA. These are called SIDD for Standard Installation Direct Design. The SIDD installations have been adopted in ASCE Standard 15-93, "Standard Practice for Direct Design of Buried Precast Concrete Pipe Using Standard Installations," (ASCE, 1994).

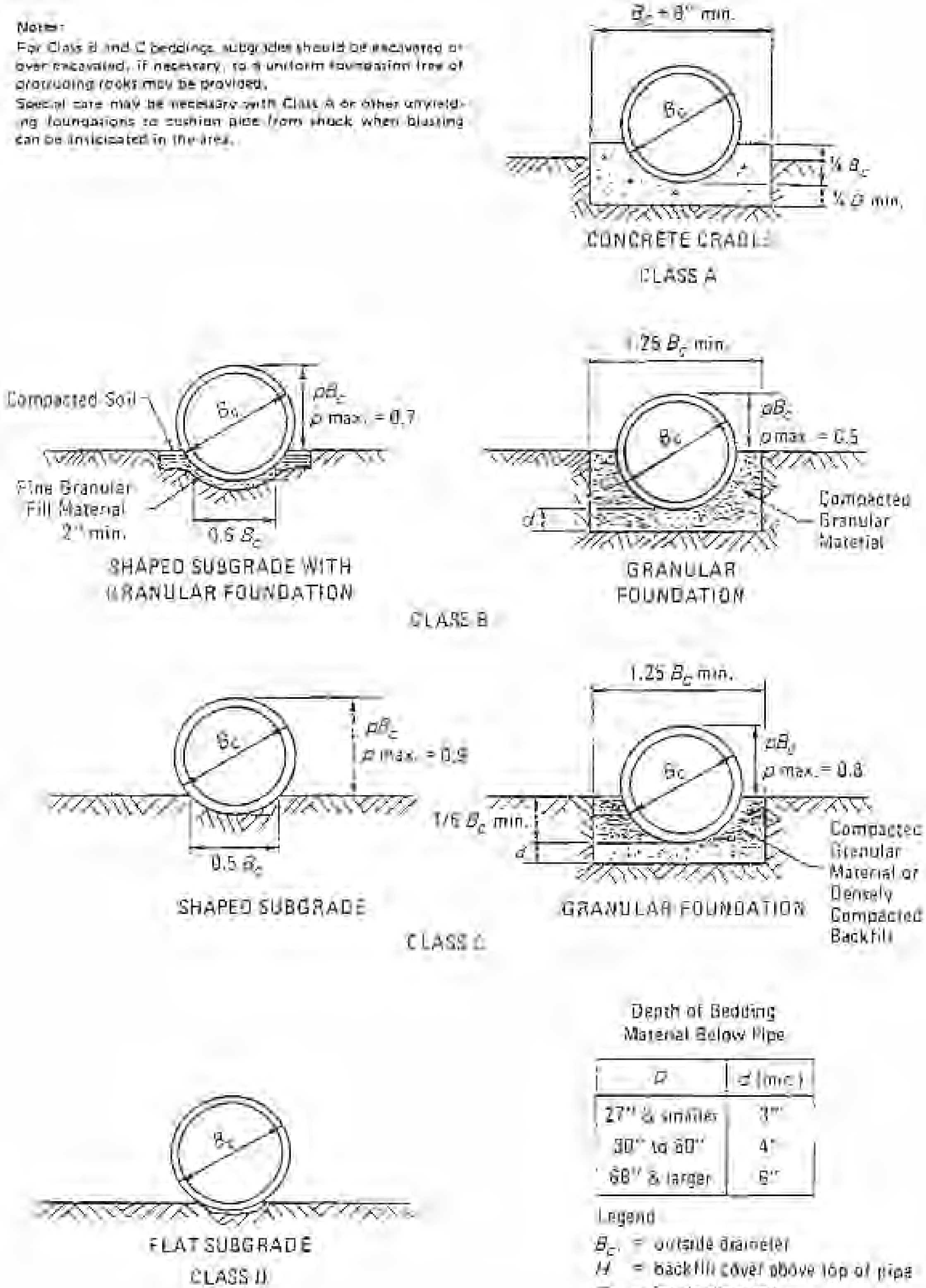

Notes:
For Class B and C beddings, subgrades should be excavated or over excavated, if necessary, so a uniform foundation free of protruding rocks may be provided.
Special care may be necessary with Class A or other unyielding foundations to cushion pipe from shock when blasting can be anticipated in the area.

Depth of Bedding Material Below Pipe

D	d (min.)
27" & smaller	3"
30" to 60"	4"
66" & larger	6"

Legend
B_c = outside diameter
H = backfill cover above top of pipe
D = inside diameter
d = depth of bedding material below pipe

Figure 2.2 Traditional Beddings for Rigid Pipe (ACPA 1987a)

"AASHTO Standard Specifications for Highway Bridges," 16th edition (AASHTO, 1996, hereafter called the Standard Specifications), and the AASHTO LRFD Bridge Design Specifications (AASHTO, 1994, hereafter called the LRFD Specifications). This approach is embodied in the Heger pressure distribution, Fig. 2.3, which shows significant variations in the pressure at the pipe-soil interface, particularly in the lower 180 degrees. Table 2.1 provides coefficients that describe the specific distributions for four standard installations. A Type 1 installation is constructed with coarse-grained, well compacted materials, a Type 4 installation is constructed with little control of backfill type or compaction, and Types 2 and 3 installations represent intermediate quality. Specific backfill and material requirements for each type of installation are presented in Fig. 2.4 and Table 2.2. Features of this approach are:

- Soil types and compaction levels are defined in accordance with accepted soil classification systems (AASHTO M 145 and ASTM D 2487), which are easily cited in contracts.
- The area of reduced pressure in the lower haunch zone acknowledges that, even with substantial effort during installation, it is unlikely that installers will achieve the same level of soil compaction as at the sides and bottom of the pipe.
- As the quality of backfill and the compaction level decrease, the invert pressure increases (note the relative values of the coefficients A1 and A2 which define the relative portion of the total load in each zone) and the lateral pressure decreases (note the coefficients A4, A5, and A6).

Liedberg (1991) has published detailed test results that evaluate the Heger work and concluded that the work is valid for embankment installations. Heger's findings should be applicable to pipes in trench installations as well, but the presence of trench walls and the influence of preexisting soils will also influence the selection of appropriate bedding conditions. In spite of the limited verification, the ASCE Standard 15-93 has incorporated the results of Heger's research and extended it to the trench condition. The trench installation is more complex than the embankment case because of the less predictable influence of the preexisting soils, the increased presence of groundwater problems, and the restricted space in which to work. ASCE does require that trench installations be designed for the embankment load condition that is conservative.

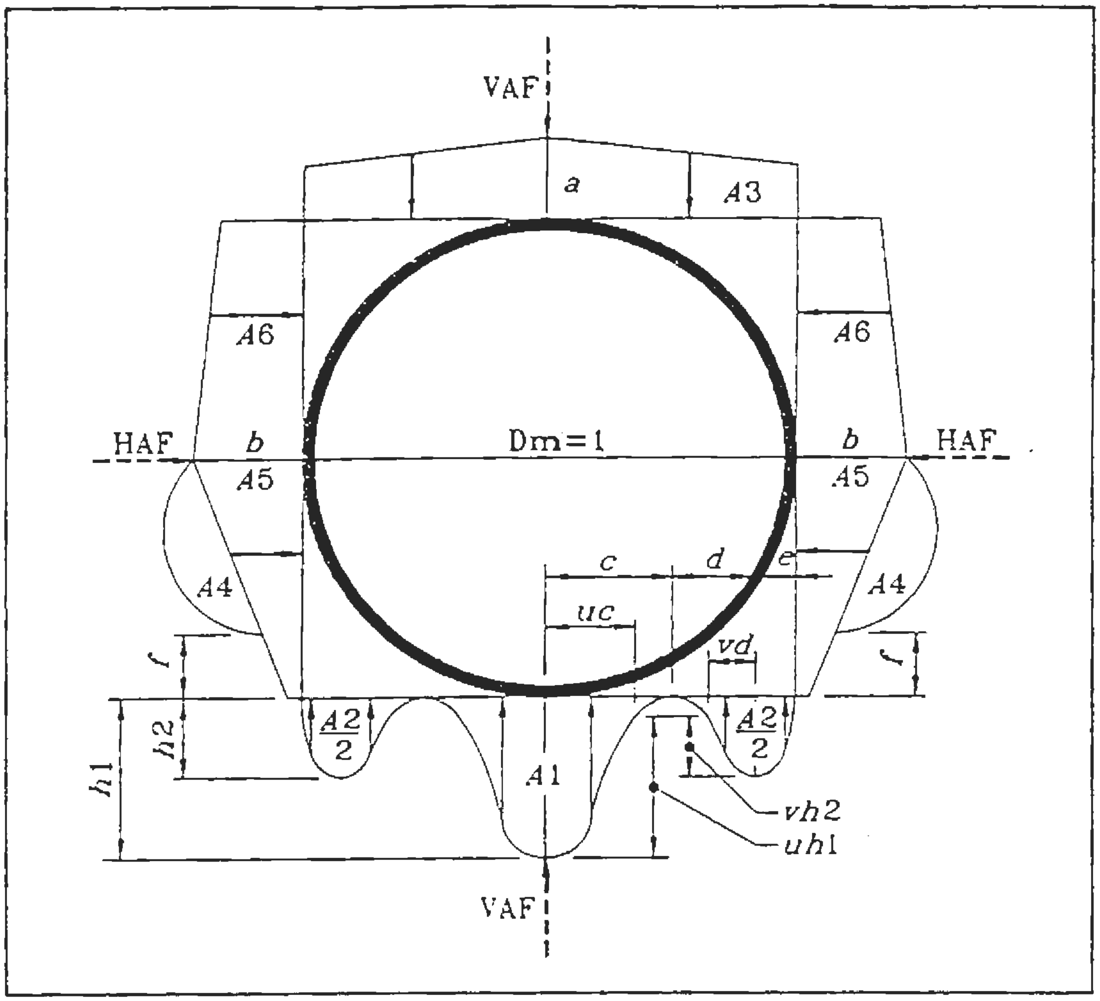

Figure 2.3 Heger Pressure Distribution for SIDD Installations (Heger 1988)

Table 2.1

Design Coefficients for Heger Pressure Distribution (Heger 1988)

Installation Type	VAF	HAF	A1	A2	A3	A4	A5	A6	a	b	c	e	f	u	v
1	1.35	0.45	0.62	0.73	1.35	0.19	0.08	0.18	1.40	0.40	0.18	0.08	0.05	0.80	0.80
2	1.40	0.40	0.85	0.55	1.40	0.15	0.08	0.17	1.45	0.40	0.19	0.10	0.05	0.82	0.70
3	1.40	0.37	1.05	0.35	1.40	0.10	0.10	0.17	1.45	0.36	0.20	0.12	0.05	0.85	0.60
4	1.45	0.30	1.45	0.00	1.45	0.00	0.11	0.19	1.45	0.30	0.25	0.00	-----	0.90	-----

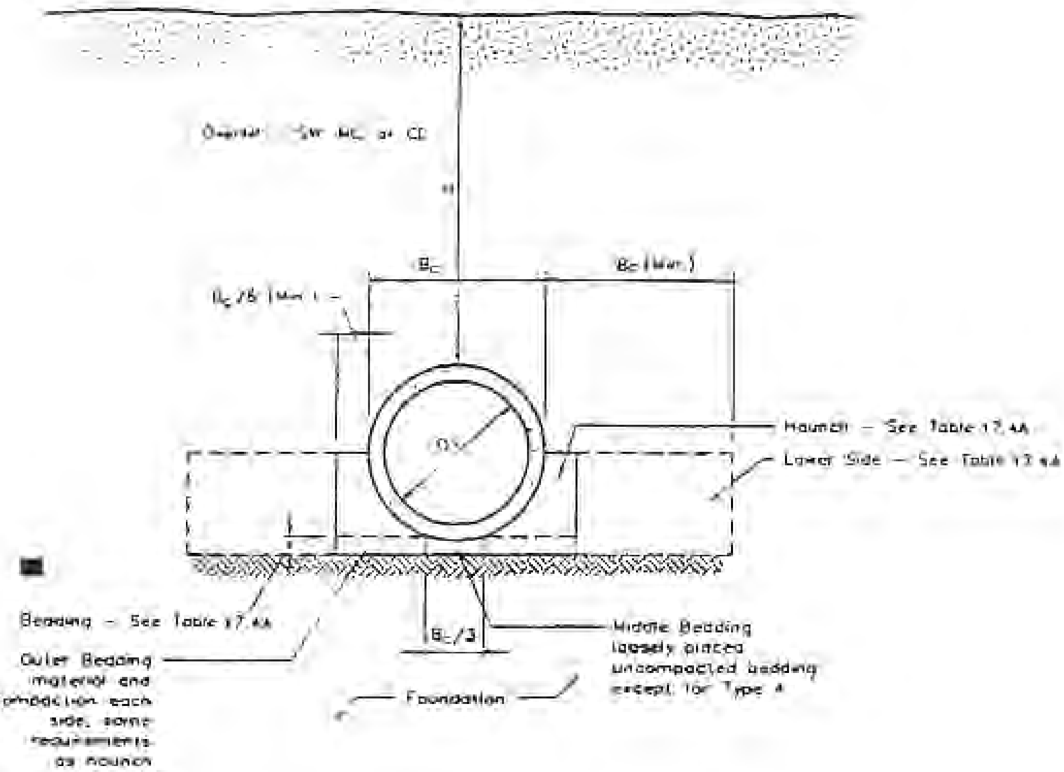

Figure 2.4 SIDD Type Embankment Installation

Table 2.2
SIDD Requirements for Embankment Installations

Installation Type	Bedding Thickness	Haunch and Outer Bedding	Lower Side
Type 1	B_c/24" (600 mm) minimum, not less than 3" (75 mm). If rock foundation, use B_c/12" (300 mm) minimum, not less than 6" (150 mm).	95% SW	90% SW, 95% ML, or 100% CL
Type 2 (See Note 3.)	B_c/24" (600 mm) minimum, not less than 3" (75 mm). If rock foundation, use B_c/12" (300 mm) minimum, not less than 6" (150 mm).	90% SW or 95% ML	85% SW, 90% ML, or 95% CL
Type 3 (See Note 3.)	B_c/24" (600 mm) minimum, not less than 3" (75 mm). If rock foundation, use B_c/12" (300 mm) minimum, not less than 6" (150 mm).	85% SW, 90% ML, or 95% CL	85% SW, 90% ML, or 95% CL
Type 4	No bedding required, except if rock foundation, use B_c/12" (300 mm) minimum, not less than 6" (150 mm).	No compaction required, except if CL, use 85% CL	No compaction required, except if CL, use 85% CL

The SIDD method divides backfill soils into three general categories that use the designations SW, ML and CL. The category names are the Unified Soil Classification System (USCS) classifications (ASTM D 2487) of three soils characterized by Selig (1988) and used in the development of the SIDD standard installations. Table 2.3 (AASHTO, 1996) suggests a grouping of all other USCS soil classifications and AASHTO (AASHTO M 145) soil classifications into the three categories. The particular soils were selected as having strength and stiffness properties on the lower end of other soils in the same classification, thus they should be conservative in design.

Loads on rigid pipe in the SIDD system are computed using the Vertical Arching Factor, or VAF. The VAF is the ratio of the total load on the pipe, taken as the springline thrust, to the weight of the soil prism load. The soil prism load is the weight of the soil directly over the pipe. The soil prism load, total load, and VAF are defined in equation form as:

$$W_{sp} = \gamma_s D_o (H + 0.11 D_o) , \tag{2.1}$$

$$W_p = 2 T_{sl} , \tag{2.2}$$

and

$$VAF = \frac{W_p}{W_{sp}} , \tag{2.3}$$

where

W_{sp}	=	weight of soil prism over pipe, kN/m, lb/ft,
γ_s	=	unit weight of soil, kN/m^3, lb/ft^3,
D_o	=	outside diameter of pipe, m, ft,
H	=	depth of fill over top of pipe, m, ft,
W_p	=	total load on pipe, m, ft,
T_{sl}	=	thrust force at springline in pipe wall, kN/m, lb/ft, and
VAF	=	vertical arching factor.

Suggested vertical arching factors for reinforced concrete pipes installed in embankment conditions vary from 1.35 to 1.45 (see table 2.1).

Table 2.3

Equivalent USCS and AASHTO Soil Classifications for SIDD Soil Designations (ASCE 1994)

	Representative Soil Types		Percent Compaction	
SIDD Soil	USCS	AASHTO	Standard Proctor	Modified Proctor
Gravelly Sand (SW)	SW, SP GW, GP	A1, A3	100 95 90 85 80 61	95 90 85 80 75 59
Sandy Silt (ML)	GM, SM, ML Also GC, SC with less than 20% passing No. 200 sieve	A2, A4	100 95 90 85 80 49	95 90 85 80 75 46
Silty Clay (CL)	CL, MH, GC, SC	A5, A6	100 95 90 85 80 45	90 85 80 75 70 40
	CH	A7	100 95 90 45	90 85 80 40

Flexible Pipe – Historically, installation trench details for flexible pipe were less detailed than those for rigid pipe. For example, ASCE Manual No. 37 (ASCE 1970) contains no suggested trench details for flexible pipe. In recent years, installation standards for flexible pipe in general and plastic pipe in particular have become far more detailed and provide excellent guidance for the installation process and for evaluating the potential support that can be derived from soil (see ASTM D 2321 and D 3839).

Flexible pipe design theories continue to rely on the work of Spangler (1941), Watkins and Spangler (1958), and White and Layer (1960). Spangler developed the Iowa formula for calculating pipe deflection under earth load, which uses the modulus of soil reaction, E', as the principal soil parameter. This formula is:

$$\Delta x = \frac{D_l K W}{EI/R^3 + 0.061 E'} \qquad (2.4)$$

where

Δx = change in horizontal diameter, m, in.,

D_l = deflection lag factor,

K = bedding factor

W = load on pipe, MN/m, lb/in.,

E = modulus of elasticity of pipe material, MPa, psi,

I = moment of inertia of pipe wall, mm^4/mm, $in.^4/in.$,

R = centroidal radius of pipe, mm, in., and

E' = modulus of soil reaction, MPa, psi.

While E' has been used successfully, it is not a true soil property and efforts to characterize it (Krizek, et al. 1971) have been unsuccessful. Howard (1977, 1996, see section 2.3) showed that E' is a function of soil density and soil type and provided a table of values that have come into common usage; however, these values are back calculated from field deflection measurements and undoubtedly represent the effects of installation practices as well as soil behavior and pipe properties. Hartley and Duncan (1987) used the close relationship between the one-dimensional modulus, M_s, and E' to show that soil stiffness varies with depth. The one-dimensional modulus represents the soil stiffness under uniaxial strain conditions. It is related to Young's modulus of elasticity, E_s, and Poisson's ratio, ν_s, through the relationship:

$$M_s = \frac{E_s(1 - \nu_s)}{(1 + \nu_s)(1 - 2\nu_s)} . \tag{2.5}$$

The Iowa formula also uses a bedding factor that is a function of the radial angle at the bottom of the pipe over which a uniform soil pressure is applied to represent the soil reaction. The bedding factor changes from 0.083 for 180 degree bedding to 0.110 for 0 degree bedding, thus, using the Iowa formula, a change from a high bedding angle to a small bedding angle could increase the calculated deflection by about 33 percent.

White and Layer introduced the ring compression theory which assumes that the load carried by a pipe is equal to the soil prism load (VAF = 1.0). This load assumption is widely used for flexible pipe design.

Design and installation standards for flexible pipe generally divide soil types into four or five general groups. ASTM D 2321 describes five soil "Classes." Class I is manufactured coarse graded material, Class II is gravel or sandy soil with less than 12 percent fines. Class III is gravel or sandy soil with 12 percent to 50 percent fines, and Classes IV and V are silts and clays, and organic soils, respectively. Classes I to III are considered good pipe backfills; some Class IV soils are acceptable as backfill under some conditions. The Howard E' table, noted above, classifies soils into four groups based on field data on pipe performance. Soil properties are discussed in more detail in section 2.3.

2.1.2 State and Federal Practice

Each State develops its own pipe design and installation standards based on local practice and conditions. Most States develop their own standards by adapting the general design guidelines contained in AASHTO Standards, historically the Standard Specifications. AASHTO has recently developed a load and resistance factor design method that is incorporated in the LRFD Specifications. Not all States use these specifications as yet; however, the culvert provisions are not substantially different. The following sections present the practice of individual States and the overall AASHTO specifications.

2.1.2.1 Departments of Transportation

Current practice among State Departments of Transportation was evaluated by surveying the practices of the project sponsors. This included 10 geographically diverse States and the Eastern Federal Lands of the Federal Highway Administration. Each organization was sent a questionnaire that inquired as to types of pipe used in highway practice, design methods and standards, backfill materials, methods of installation, and standards for controlling the quality of installations.

Design Practice – Questionnaire responses show that all but one respondent design rigid pipe by indirect design methods (determination of an equivalent three-edge bearing load). Some sponsors reference AASHTO and some reference ACPA literature. Pennsylvania has recently adopted the new SIDD direct design method for concrete pipes, and has developed fill height tables based on this method. California allows direct design (design based on an assumed pressure distribution) as well as indirect design for concrete pipes.

All respondents use AASHTO Sec. 12 for design of corrugated metal pipe. Three respondents include deflection checks for metal pipes even though not required by current AASHTO Specifications.

Seven respondents design plastic pipes by AASHTO Sec. 18, and four respondents limit plastic pipes to depths of fill between 3.5 m and 4.5 m (11 ft and 15 ft).

Other aspects of design practice from the questionnaire include:

- Eight use negative projecting installations but some do so only for reasons of ease of construction, rather than control of load on the culvert;
- Six use the induced trench method but one reports problems with this method; and
- Seven use the modulus of soil reaction, E', as a measure of soil stiffness:
  - Two use the Howard table of E' with values from 0.35 MPa to 21 MPa (50 psi to 3,000 psi) depending on the soil type and compaction level); and
  - Five use one or two values of E', varying between 7.2 MPa and 11.7 MPa (1,050 psi and 1,700 psi); however, three of these five are seeking better methods of determining soil stiffness.

Backfill – All respondents use "granular" backfill, however, the definitions of granular material vary. Materials that are allowed include large particle size, open graded aggregates (AASHTO No. 3), and some with fines content up to 15 percent. Names include select granular fill, granular backfill, gravel borrow, and select material. Some sponsors have separate gradations for select and granular materials. Four sponsors allow installation with fine-grained materials for some products or some situations. One sponsor allows select material to have up to 60 percent silt content.

Other information related to backfill materials used by the questionnaire respondents include:

- Three sponsors allow backfill with native material under some conditions;
- Compaction requirements generally vary from 90 to 100 percent of AASHTO T-99;
- Eight of eleven respondents use controlled low strength materials (CLSM), also called flowable fill, under some conditions;

- Some sponsors specify minimum trench widths as low as the outside diameter plus 150 mm (6 in.). Most sponsors specify maximum trench widths (generally O.D. plus 0.9 m (3 ft)) or three times the outside diameter. Some distinguish between flexible and rigid pipes and some have trench dimensions dependent on the diameter;
- Ten of eleven require or recommend inspection during backfilling;
- Two of eleven require mandrel tests after backfill of flexible pipe;
- Eight of eleven require compaction testing; and
- Two of eleven have specifications concerning groundwater control.

The most common need, based on the respondents' perception of current practice, was a better method to determine E'. Other issues include need for improved flexible pipe design procedures and better treatment of materials outside of the trench.

Of less overall importance but still desired by some respondents were:

- Refinement of the induced trench installation;
- Improved backfill procedures to achieve good support without developing excessive lateral pressures;
- Specifications that allow use of lower quality materials; and
- Better quality joints.

2.1.2.2 AASHTO

AASHTO Standards have been written around three product types: corrugated metal, concrete, and thermoplastic. The AASHTO standards for corrugated metal and reinforced concrete were largely developed by industry trade organizations and then adopted by AASHTO, while the standards for thermoplastic pipes were developed based on the metal pipe standards, presumably on the assumption that thermoplastic and corrugated metal pipes were both flexible conduits and behaved in the same fashion. The construction specifications for AASHTO set forth the installation requirements; however, many installation criteria are selected based on decisions made during the design process; thus, both the design and installation practices must be examined.

Corrugated Metal Pipe Design and Installation - AASHTO design methods for corrugated metal pipe consider hoop compression stresses, for yield and buckling analysis, and the flexibility coefficient, defined as:

$$FF = \frac{R^2}{EI} , \tag{2.6}$$

where

FF = flexibility coefficient, m/kN, in./lb,
R = centroidal pipe radius, mm, in.,
E = pipe modulus of elasticity, MPa, psi, and
I = pipe wall moment of inertia, mm^4/mm, $in.^4/in.$.

The flexibility coefficient is a flexural stiffness criterion that is intended to assure sufficient stiffness for the pipe to withstand handling and installation forces. The classical formula for a ring under diametrally opposed line loads (the parallel plate test) is:

$$\frac{F}{\Delta y} = \frac{EI}{0.149 R^3} , \tag{2.7}$$

where

F = line load, kN/m, lb/in., and
Δy = change in vertical diameter, mm, in.

By rearranging it to the form:

$$\frac{R^2}{EI} = \frac{\Delta y / R}{0.149 F} = FF , \tag{2.8}$$

it can be seen that the flexibility factor is proportional to the percent deflection ($\Delta y/R$) resulting from a unit line load (F), while the pipe stiffness ($F/\Delta y$) used to characterize thermoplastic pipe is the absolute deflection resulting from a line load. Limiting values for the flexibility coefficient have been set empirically based on experience.

Of current AASHTO criteria for metal culvert design, only the buckling equation considers soil stiffness. In the past, corrugated metal pipes were designed for deflection using the Iowa formula and the modulus of soil reaction, E'. This calculation was dropped from the specifications on the basis that if a pipe is properly installed it will not deflect more than the allowable value.

Reinforced Concrete Pipe Design and Installation - Traditional beddings for reinforced concrete pipes were noted above. These bedding conditions are associated with "bedding factors" that relate the load on the actual pipe to a load in a three-edge bearing test that will produce the same bending moment at the pipe invert. The pipe is then designed to resist the three-edge bearing load. This is called indirect design and is the predominant method of concrete pipe design. Alternatively, pipes can be analyzed and designed for the in-ground forces. This is direct design. It is used in some parts of the United States and is the preferred method of design for special conditions such as high fills.

The SIDD installations were actually developed as a direct design method; however, because of a long history of experience and confidence in indirect methods, bedding factors were developed for these installations and have been incorporated into AASHTO specifications. SIDD installations specify soil types in terms of AASHTO and ASTM soil classifications and compaction in terms of a percent of maximum Proctor density. Haunching effort is required for Installation Types 1 to 3. No special fill or compaction is required above the springline, except as required for support of surface pavement or other structures.

Thermoplastic Pipe Design and Installation - AASHTO developed a thermoplastic pipe design procedure on the assumption that thermoplastic pipes were flexible conduits and could be designed in the same manner as corrugated metal pipes. Issues pertinent to thermoplastic pipe design include:

- Design for total tensile strain, which is not considered for metal pipe, is required because not all thermoplastic pipes are ductile; and
- Design is currently based on the soil prism load, which is a common assumption for flexible pipe; however, Hashash and Selig (1990) have shown that loads on corrugated polyethylene pipes can be significantly less than the soil prism load.

2.1.3 Other Installation Practice

Different industries and specific pipe manufacturers have taken different approaches to the design of buried pipe installations. General practice of the corrugated metal, concrete, and thermoplastic pipe industries was explored above. Other industry practices of interest include:

Clay Pipe – Installation practice of the clay pipe industry is defined in ASTM C 12 Standard Practice for Installing Vitrified Clay Pipe. This standard focuses on support of the invert and haunch zones, as do standards for concrete pipes. The standard proposes beddings classified as B, C, D, crushed stone encasement, and controlled density fill (herein this material will be called CLSM for Controlled Low Strength Material).

The B, C, and D beddings are very much like the traditional reinforced concrete beddings, and use somewhat vague terminology such as "carefully placed material" and select material. A bedding using crushed stone encasement, suggesting a backfill material with angular particles, is shown to provide better support to a pipe with simply "gravel" backfill, such as a GW soil. This is consistent with the Howard table of E' values of soil stiffness for flexible pipe. The standard is the only one for pipe installation that currently provides a bedding detail for CLSM, as shown in Fig. 2.5. The detail shows the pipe laid on crushed stone bedding. This is a relatively simple installation from the point of labor, but allows the invert to have a potentially harder support point than the haunches which is undesirable. If the pipe is backfilled prior to the CLSM curing than the pipe could develop a line load at the invert and become overstressed. The standard also calls for a CLSM 28 day compressive strength of 700 to 2100 kPa (100 to 300 psi). This is high if the CLSM is to be considered excavatable. See Section 2.2.4 for additional discussion of CLSM.

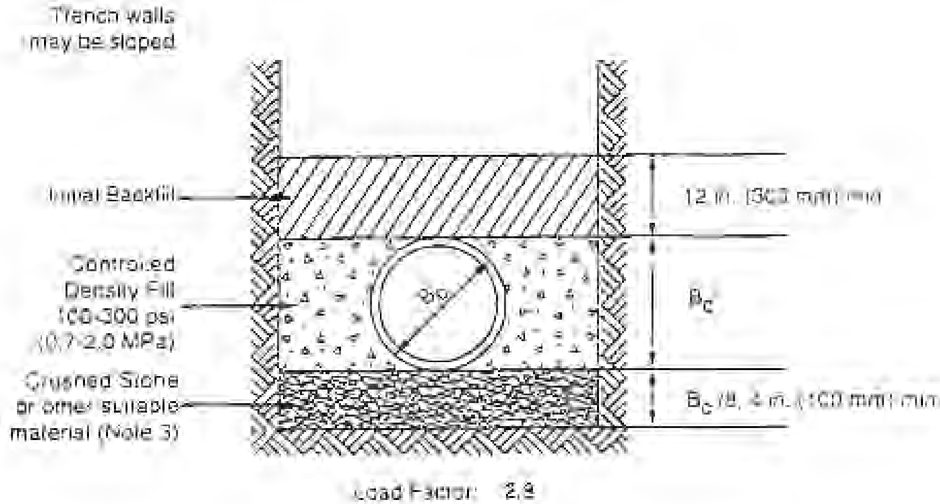

Figure 2.5 Bedding Detail for Clay Pipe with CLSM Backfill (ASTM C 12)

Fiberglass Pipe – Glass fiber reinforced plastic pipe, historically called GRP or FRP but now called simply fiberglass pipe in the United States, can be customized by changing the relative quantity of glass, resin, and, in some cases, sand filler. This allows the industry to produce a wide range of pipe stiffness which in turn allows a broader approach to installation, allowing several trench configurations and backfill conditions. This is documented in part in AWWA Manual M45 (AWWA 1996). One manufacturer's suggested installation details based on pipe stiffness and depth of fill are shown in table 2.4 and fig. 2.6. Fiberglass pipe is more strain sensitive than thermoplastic pipe, thus, more effort has been invested in the prediction of strains in this type of pipe and the design methods are more thorough than is traditionally the case for thermoplastic pipes. The design and installation procedures should be of interest to culvert designers, even if not specifically using fiberglass pipe.

Table 2.4
Installation Requirements for Hobas Fiberglass Pipe

NATIVE SOIL[2,5]	COVER DEPTH (ft.)	EMBEDMENT CONDITION[3]			
		1	2	3	4
	10 & <				SN 72
Rock	10 to 15	SN[6] 36			
Stiff to V. Hard Cohesive	15 to 20			SN[6] 46	
Compact to V. Dense Granular	20 to 25		SN[6] 46		
(Blows/ft.[4] > 8)	25 to 30	SN[6] 46			
	30 to 40		SN[6] 72	ALTERNATE INSTALLATION[7]	
	40 to 50				
	10 & <	SN[6] 36			SN[6] 72
Medium Cohesive	10 to 15		SN[6] 46	SN[6] 46	
Loose Granular	15 to 20	SN[6] 46			
(Blows/ft.[4] 4 to 8)	20 to 25		SN[6] 72	ALTERNATE INSTALLATION[7]	
	25 to 30				
	10 & <	SN[6] 36 to 46		SN[6] 72	
Soft Cohesive	10 to 15	SN[6] 72			
Very Loose Granular	15 to 20				
(Blows/ft.[4] 2 to 4)	over 20			ALTERNATE INSTALLATION[7]	

[1] Assuming minimum trench width per Figure 2.
[2] Blow counts should be representative of weakest condition.
[3] Defined in Figure 3. If a cement stabilized sand pipe zone surround is utilized, use column 1 in the highest soils category.
[4] Standard penetration test per ASTM D1586.
[5] For v. soft or v.v. loose soils with blow counts less than 2 use alternate installation per section 13, ¶ A8.
[6] SN is nominal stiffness in psi.
[7] Alternate installation per section 13, ¶ A8.

1 ft = 0.305 mm

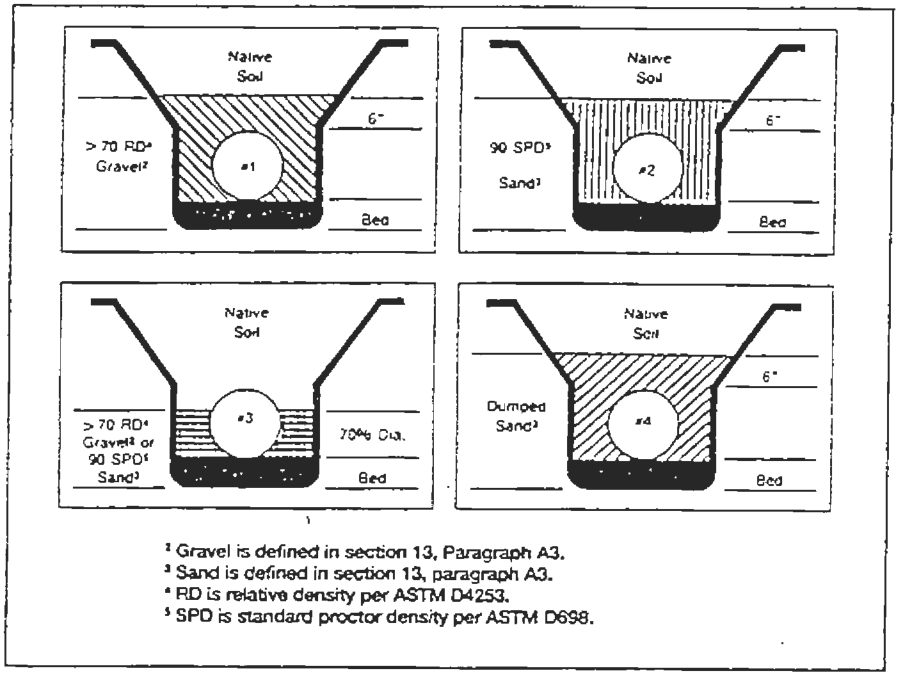

Figure 2.6 Trench Cross-Sections for Hobas Fiberglass Pipe

2.2 Classification and Characterization of Backfill Soils

Backfill materials are usually characterized in terms of gradation and density, and, in the case of fine-grained materials, Atterberg limits. The results of these standard tests are used to estimate a number of mechanical properties used in design. The most important property needed in the design of buried culverts is the soil stiffness; however, it is rare for specifications to require tests specifically for soil stiffness. Engineers often rely on simple empirical relations, such as gradation and density, to establish the soil stiffness. In the field, the importance of the soil stiffness often gets lost in the concern to meet a specification construction requirement for density or gradation. This section reviews standard practices for characterizing soils used as pipe backfill.

2.2.1 Classification Systems

The first step in engineering with soils is typically to characterize the material based on grain size and Atterberg limits (AASHTO M 145, T 88, T 89, and T 90, and the corresponding ASTM D 422, D 2487, D 2488, and D 4318). These tests and classification systems delineate some of the most basic differences among soil types, i.e., particle size and plasticity.

While the AASHTO and ASTM tests listed above for determining grain size and Atterberg limits are equivalent, the soil classification systems based on those test results are not. The AASHTO soil classification system (M 145) was developed for soils to be used as subgrades in road construction, while the ASTM system (D 2487, also called the Unified Soil Classification System or USCS) was developed for broader engineering purposes. Both systems rely on the percentage of material passing a No. 200 sieve (0.075 mm particle size) as the delineation between coarse-grained soils and fine-grained soils; however, each system considers a different percentages as critical. Behavior of coarse-grained soils is best described by particle size while behavior of fine-grained soils is best described by the liquid limit and plasticity index. The quantity of material passing the No. 200 sieve is called the percent fines.

The AASHTO classification system is shown in table 2.5. A soil is classified by using the table from left to right. The first group from the left to fit the soil is the correct AASHTO classification. In addition, the AASHTO system uses a group index based on the plasticity index and liquid limit. The group index is not often used in specifying pipe backfills and is not discussed further here. The AASHTO system classifies any soil with more than 35-percent fines a silt-clay material and any soil with less than 35-percent fines a granular material.

The ASTM classification system is shown in tables 2.6 and 2.7 for coarse and fine grained soils, respectively. A given soil is classified based on the grain size distribution, plasticity index, and liquid limit. The ASTM system classifies any soil with more than 50-percent fines as a fine-grained soil and any soil with less than 50-percent fines as a coarse-grained soil. Coarse-grained soils are characterized based on the coefficient of uniformity, C_u, and the coefficient of curvature, C_c. These coefficients are used to determine if a soil is uniformly or gap graded. Backfill soils are often specified in terms of the two letter group symbol (e.g., SW), however, much more information is available if the group name is used.

Table 2.5
AASHTO Soil Classification System (AASHTO M 145)

General Classification	Granular Materials (35% or Less Passing 0.075 mm)							Silt-Clay Materials (More than 35% Passing 0.075 mm)			
	A-1			A-2							A-7
Group Classification	A-1-a	A-1-b	A-3	A-2-4	A-2-5	A-2-6	A-2-7	A-4	A-5	A-6	A-7-5, A-7-6
Sieve analysis, percent passing:											
2.00 mm (No. 10)	50 max.	—	—	—	—	—	—	—	—	—	—
0.425 mm (No. 40)	30 max.	50 max.	51 min.	—	—	—	—	—	—	—	—
0.075 mm (No. 200)	15 max.	25 max.	10 max.	35 max.	35 max.	35 max.	35 max.	36 min.	36 min.	36 min.	36 min.
Characteristics of fraction passing 0.425 mm (No. 40)											
Liquid limit	—		—	40 max.	41 min.	40 max.	41 min.	40 max.	41 min.	40 max.	41 min.
Plasticity index	6 max.		N.P.	10 max.	10 max.	11 min.	11 min.	10 max.	10 max.	11 min.	11 min.*
Usual types of significant constituent materials	Stone fragments, gravel and sand		Fine sand	Silty or clayey gravel and sand				Silty soils		Clayey soils	
General Ratings as Subgrade	Excellent to Good							Fair to poor			

* Plasticity index of A-7-5 subgroup is equal to or less than LL minus 30. Plasticity index of A-7-6 subgroup is greater than LL minus 30 (see Figure 2).

Table 2.6
ASTM Classification System for Coarse Grained Soils (ASTM D 2487)

				GROUP SYMBOL		GROUP NAME
GRAVEL % gravel > % sand	<5% fines	Cu≥4 and 1≤Cc≤3		GW	<15% sand	Well-graded gravel
					≥15% sand	Well-graded gravel with sand
		Cu<4 and/or 1>Cc>3		GP	<15% sand	Poorly graded gravel
					≥15% sand	Poorly graded gravel with sand
	5-12% fines	Cu≥4 and 1≤Cc≤3	fines=ML or MH	GW-GM	<15% sand	Well-graded gravel with silt
					≥15% sand	Well-graded gravel with silt and sand
			fines=CL, CH, (or CL-ML)	GW-GC	<15% sand	Well-graded gravel with clay (or silty clay)
					≥15% sand	Well-graded gravel with clay and sand (or silty clay and sand)
		Cu<4 and/or 1>Cc>3	fines=ML or MH	GP-GM	<15% sand	Poorly graded gravel with silt
					≥15% sand	Poorly graded gravel with silt and sand
			fines=CL, CH, (or CL-ML)	GP-GC	<15% sand	Poorly graded gravel with clay (or silty clay)
					≥15% sand	Poorly graded gravel with clay and sand (or silty clay and sand)
	>12% fines		fines=ML or MH	GM	<15% sand	Silty gravel
					≥15% sand	Silty gravel with sand
			fines=CL or CH	GC	<15% sand	Clayey gravel
					≥15% sand	Clayey gravel with sand
			fines=CL-ML	GC-GM	<15% sand	Silty, clayey gravel
					≥15% sand	Silty, clayey gravel with sand
SAND % sand ≥ % gravel	<5% fines	Cu≥6 and 1≤Cc≤3		SW	<15% gravel	Well-graded sand
					≥15% gravel	Well-graded sand with gravel
		Cu<6 and/or 1>Cc>3		SP	<15% gravel	Poorly graded sand
					≥15% gravel	Poorly graded sand with gravel
	5-12% fines	Cu≥6 and 1≤Cc≤3	fines=ML or MH	SW-SM	<15% gravel	Well-graded sand with silt
					≥15% gravel	Well-graded sand with silt and gravel
			fines=CL, CH, (or CL-ML)	SW-SC	<15% gravel	Well-graded sand with clay (or silty clay)
					≥15% gravel	Well-graded sand with clay and gravel (or silty clay and gravel)
		Cu<6 and/or 1>Cc>3	fines=ML or MH	SP-SM	<15% gravel	Poorly graded sand with silt
					≥15% gravel	Poorly graded sand with silt and gravel
			fines=CL, CH, (or CL-ML)	SP-SC	<15% gravel	Poorly graded sand with clay (or silty clay)
					≥15% gravel	Poorly graded sand with clay and gravel (or silty clay and gravel)
	>12% fines		fines=ML or MH	SM	<15% gravel	Silty sand
					≥15% gravel	Silty sand with gravel
			fines=CL or CH	SC	<15% gravel	Clayey sand
					≥15% gravel	Clayey sand with gravel
			fines=CL-ML	SC-SM	<15% gravel	Silty, clayey sand
					≥15% gravel	Silty, clayey sand with gravel

Table 2.7
ASTM Classification System for Fine Grained Soils (ASTM D 2487)

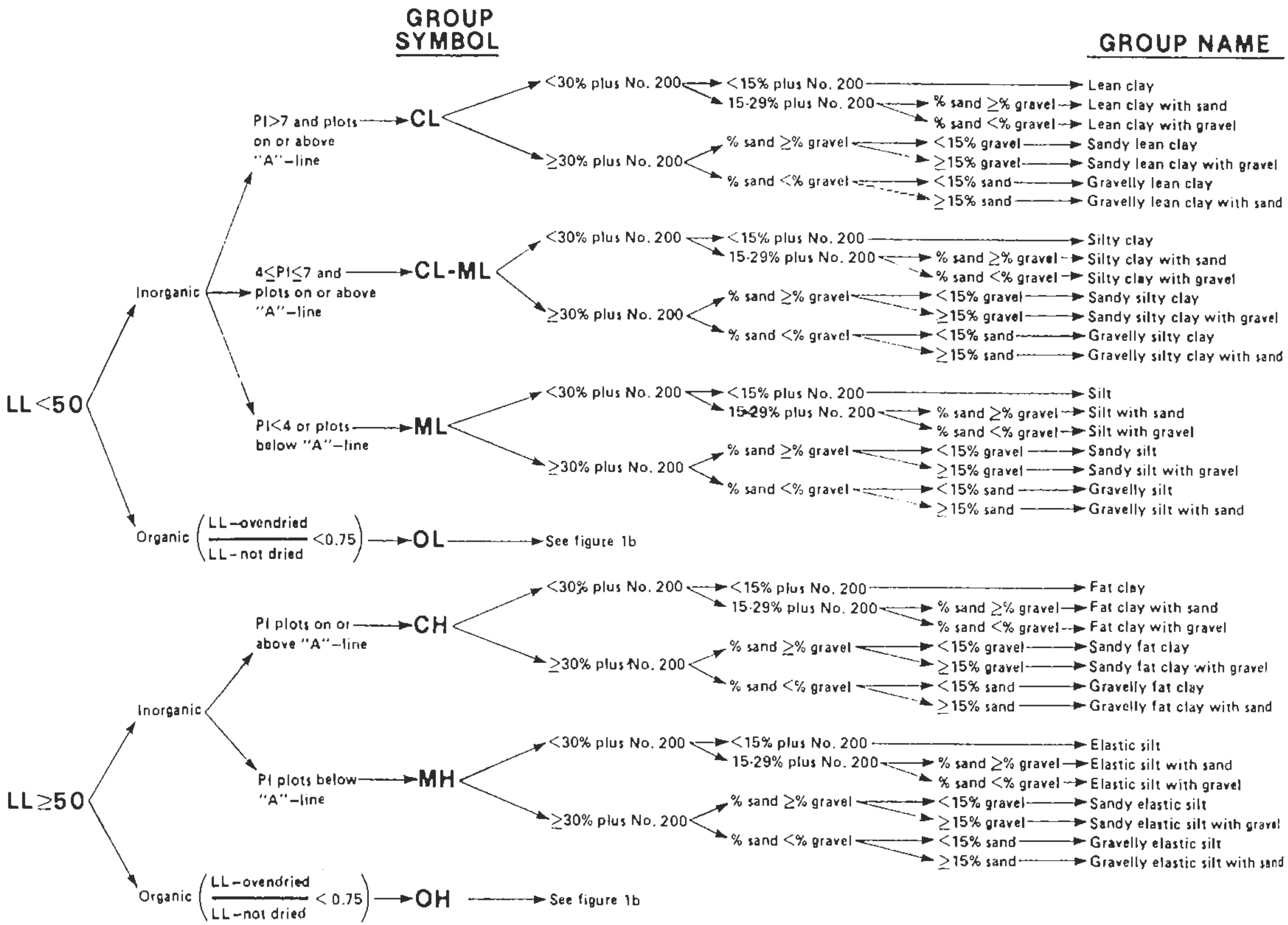

As noted above, a principal criterion for classification of soils is the quantity of fines. Fig. 2.7 compares the AASHTO and ASTM classification systems with the previously discussed soil groups made for structural purposes as assigned by Howard and SIDD based on the fines content. Observations based on this figure include:

- In the ASTM system, fines content is definitive as a first step in classification, i.e., a given soil with certain percentage of fines can only be classified into certain groups. The system uses fines content of 5, 12, and 50 percent as the principle limits; additional limits are available if the group names are used.
- The AASHTO system allows soils with limited fines to fall into one of several classifications as a function of other criteria, and depends on using table 2.5 from left to right to make the necessary distinctions.
- The Howard soil groups correspond closely to ASTM, except that an additional dividing point based on soils with more or less than 30 percent coarse-grained material is introduced, and the aforementioned grouping based on angularity.
- The SIDD soil groups use fines to distinguish between the SW group and both the ML and CL groups; however, for soils with more than 20 percent fines, Atterberg limits are used to distinguish among soils in the ML and CL groups.
- The SIDD soil groups do not specifically call out to which group soils with 5 to 12 percent fines should be assigned.
- The SIDD system puts all A-2 soils into the ML group. The A-2 soil classification group is very broad. It would be more consistent with assignment of ASTM soils if the A-2-6 and A-2-7 soils are reclassified in the CL group.

Review of the data on which the SIDD soil groupings were developed (Selig, 1988) shows that the soil used as the model for the "ML" classification had more than 30 percent coarse-grained material and that the soil used as the model for the "CL" soil classification had less than 30 percent coarse-grained material. This means that they would also fall into separate classification groups according to the E' soil table. The two systems should be reviewed to see if the criteria of silt versus clay, as used in SIDD, or the 30 percent coarse-grained material criteria used for E' is more appropriate as a backfill classification system.

Fig. 2.8 compares the AASHTO and ASTM systems based on plasticity as determined by the Atterberg limits. The figure shows that, while there are differences in details, the two systems generally have similar boundaries to distinguish between different types of behavior.

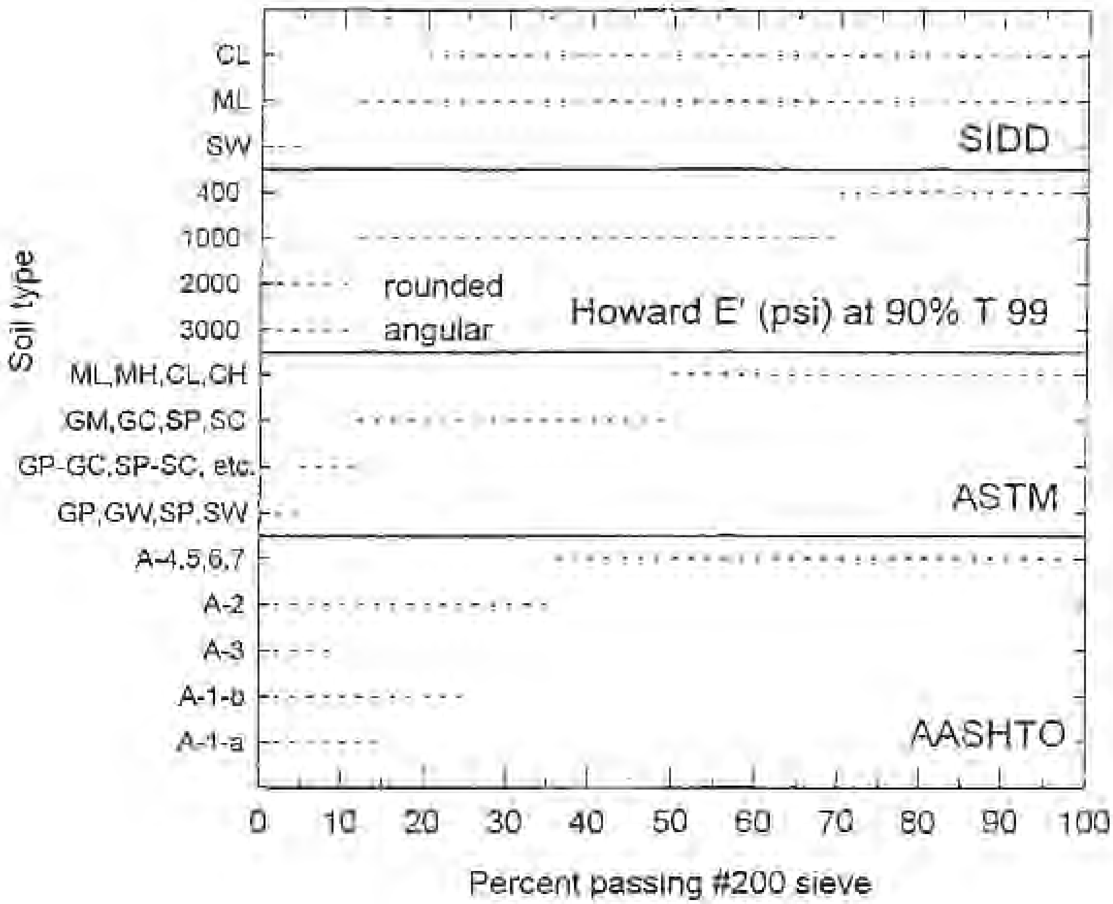

Notes:

SIDD soil groups:

CL includes A-5, A-6, CL, MH, GC, SC

ML includes GM, SM, ML, (and GC and SC if less than 20% fines), A-2, A-4

SW includes A-1, A-3, GW, SW, GP, SP

Howard soil groups:

E' = 400 includes CL, ML with less than 30% coarse particles

E' = 1000 includes CL, ML with more than 30 % coarse particles, and GM, GC, SM, SC

E' = 2000 inlcudes GW, GP, SW, SP and dual symbol groups GW-GC,etc.

E' = 3000 includes angular processed materials

Figure 2.7 Soil Classifications Based on Fines Content Compared to Howard Soil Stiffnesses and SIDD Soil Types

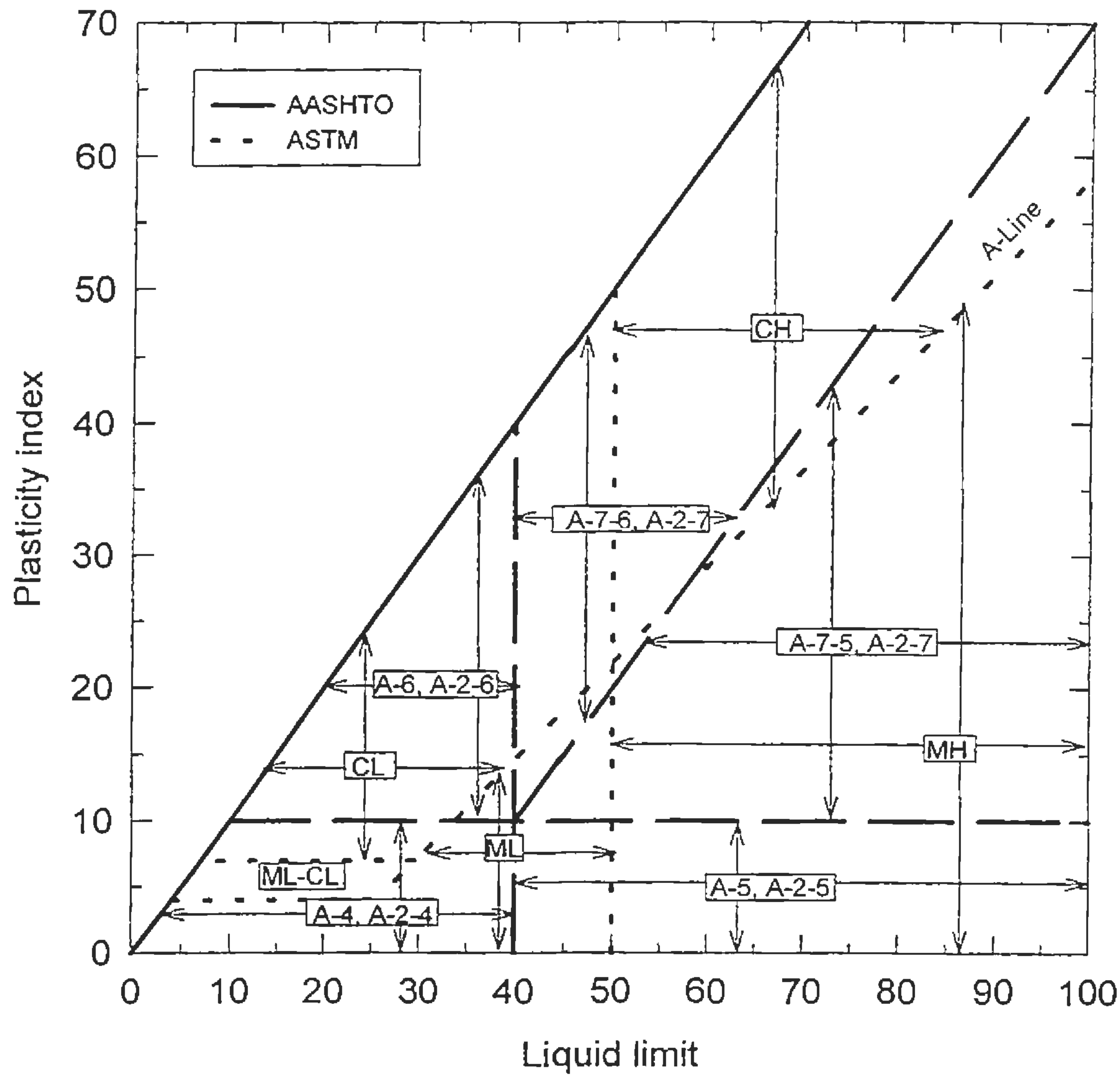

Figure 2.8 Comparison of Plasticity Charts for AASHTO and ASTM Classification

2.2.2 Compaction and Compactibility

Soils that are to be placed and compacted as part of engineered fills, such as pipe backfill, are also tested for moisture-density relationships due to compaction energy (AASHTO T 99 and T 180, and the equivalent ASTM D 698 and D 1557, called the standard and modified Proctor tests, respectively, herein). The density achieved during compaction of some coarse-grained soils with limited fines content (less than about 5 percent) is insensitive to moisture content. These soils are characterized using the relative density tests (ASTM D 4253 and D 4254).

A soil that achieves good stiffness characteristics with minimal compactive effort is said to be readily compactible. This generally applies to coarse grained materials such as A-1, A-2 and A-3 in the AASHTO system and GW, GP, SW, and SP in the USCS system. As grain size decreases and fines content increases the compactive effort required to achieve adequate stiffness increases and the maximum stiffness that can be achieved with compaction decreases. Selig (1988) demonstrated this in tests where the compactive effort was varied from 0 to 100 percent of the energy required by the standard Proctor test. McGrath (1990) developed this concept further to demonstrate the energy required to achieve a given level of soil stiffness (E') with various types of soil. Achieving an E' of 1000 psi with CL soil requires more than seven times the compactive energy of achieving the same E' with SW soil. This subject is explored more thoroughly in chapter 3.

2.2.3 Stiffness and Strength

Methods of modeling soil behavior for design of buried pipe vary from very simple procedures that assume linear, elastic soil behavior and do not consider strength, to very sophisticated models that consider true non-linear, stress-dependent soil behavior and strength parameters.

An example of a simple soil model is the above mentioned table of values for the modulus of soil reaction, E' (table 2.8), developed by Howard (1977) for use with the Iowa formula (Spangler, 1941). Howard's table divides soils into four principal groups and assigns values of E' as a function of the soil group and the density, which is expressed as function of the maximum density determined in a reference test, such as AASHTO T 99. The table makes a distinction, not made in the ASTM or AASHTO classification systems,

Table 2.8

Howard Design Values for Modulus of Soil Reaction, E' (Howard, 1977)

Soil type-pipe bedding material (Unified Classification System)[1]	E' for degree of compaction of bedding ($lb/in.^2$)			
	Dumped	Slight <85% Proctor <40% relative density	Moderate 85-95% Proctor 40-70% relative density	High >95% Proctor >70% relative density
Fine-grained soils (LL>50)[2] Soils with medium to high plasticity CH, MH, CH-MH	No data available; consult a competent soils engineer; otherwise use E'=0			
Fine-grained soils (LL<50) Soils with medium to no plasticity, CL, ML, ML-CL, with less than 25% coarse-grained particles	50	200	400	1000
Fine-grained soils (LL<50) Soils with medium to no plasticity, CL, ML, ML-CL, with more than 25% coarse-grained particles *Coarse-grained soils with fines* GM, GC, SM, SC[3] contains more than 12% fines	100	400	1000	2000
Coarse-grained soils with little or no fines GW, GP, SW, SP[3] contains less than 12% fines	200	1000	2000	3000
Crushed Rock	1000	3000		
Accuracy in terms of percent deflection[4]	±2%	±2%	± 1	± 0.5%

[1] ASTM Designation D 2487, USBR Designation E-3.
[2] LL = liquid limit.
[3] Or any borderline soil beginning with one of these symbols (i.e., GM-GC, GC-SC).
[4] For ± 1% accuracy and predicted deflection of 3%, actual deflection would be between 2% and 4%.

Note:
- A. Values applicable only for fills less than 50 ft.
- B. Table does not include any safety factor.
- C. For use in predicting initial deflections only, appropriate deflection lag factor must be applied for long-term deflections.
- D. If bedding falls on the borderline between two compaction categories, select lower E' value or average the two values.
- E. Percent Proctor based on laboratory maximum dry density from test standards using about 12,500 $ft\text{-}lb/ft^3$ (ASTM D-698, AASHTO T-99, USBR Designation E-11).

1 MPa = 145 psi, 1 $kN\text{-}m/m^3 = 20.9\ ft\text{-}lb/ft^3$

between "crushed rock" and other granular soils. This table is widely cited in the literature. Other variations of this table have been proposed. The Water Research Centre (WRc) in the United Kingdom published table 2.9 (DeRosa et al., 1988). This is similar to the Howard table but distinguishes uniform gravel from single size gravel. The single size gravel is seen to have a higher initial stiffness prior to compaction while the graded gravel is able to achieve a higher stiffness after compaction.

Table 2.9

Water Research Centre Values for Modulus of Soil Reaction (DeRosa et al., 1988)

EMBEDMENT MATERIAL		MODULUS OF SOIL REACTION (MN/m^2)				
DESCRIPTION	CASAGRANDE GROUP SYMBOL	UNCOMPACTED	80% Mp	85% Mp	90% Mp	95% Mp
Gravel - single size	GU	5	7	7	10	14
Gravel - graded	GW	3	5	7	10	20
Sand and coarse grained soil with less than 12% fines	GP SW SP	1	3	5	7	14
Coarse grained soil with more than 12% fines Fine grained soil (LL <50%) with medium to no plasticity and containing more than 25% coarse grained particles	GM GC SM CL, ML, mixtures ML/CL and ML/MH	–	1	3	5	10
Fine grained soil (LL <50%) with medium to no plasticity and containing less than 25% coarse grained particles	CL, ML, mixtures ML/CL, CL/CH and ML/MH	–	–	1	3	[illegible]

All values valid for semi-rigid pipe design.
D applies to cover depths in the range 0.9 to 10.0m.

Range of E' values recommended for flexible pipe design.

Note: 1 MN/m^2 = 145 psi

An example of a sophisticated soil model for use in buried pipe design is the hyperbolic model (Duncan et al., 1980), which is used in most finite element models for analysis of buried pipe. The hyperbolic model uses nine separate parameters to completely define the stress-strain behavior of soil, including both strength and stiffness parameters. The Duncan model used a power law rule to model the bulk modulus which represents the volumetric behavior of soil. Selig (1988) found a hyperbolic model for the bulk modulus could more accurately represent the volumetric behavior and presented a set of parameters that were used to develop the soil groupings for the SIDD installations. Selig (1990) later proposed an alternative set of properties for the hyperbolic bulk modulus model that he recommended for use with flexible pipe.

2.2.4 Controlled Low Strength Material

Controlled Low Strength Material, or CLSM, also known as flowable fill, is a special material manufactured to have good flow characteristics. Typical mix designs use cement sand, fly ash, and water; however, the cement content is on the order of 30 to 60 kg/m^3 (50 to 100 lbs/yd^3), extremely low relative to structural concrete mixes. The fly ash is the key ingredient to create the good flow characteristics. An alternative to fly ash is to use high quantities of air. Twenty to thirty percent air content, with reduced or no fly ash, has also been found to produce mixes with good flow characteristics (Grace, 1996). Applications of CLSM have been discussed by Howard (1996) and Brewer (1993).

CLSM gains strength and stiffness over time. McGrath and Hoopes (1997) published recommended hyperbolic soil model properties and design values of bedding factors and E' values at ages of 16 hours, 7 days, and 28 days for CLSM mixes with high air contents. The values were based on triaxial and one-dimensional compression testing, and finite element analysis. The mix designs used in that study are presented in table 2.10. The proposed soil properties are presented in tables 2.11, 2.12, and 2.13.

Table 2.10

CLSM Test Program Variables (McGrath and Hoopes, 1997)

Parameter	Conditions
CLSM Mix 1	cement: 59 kg/m^3, Type 1; sand: 1480 kg/m^3; air: 25-30%
CLSM Mix 2	cement: 30 kg/m^3, Type 1; fly ash: 150 kg/m^3; sand: 1480 kg/m^3; air: 27%
Age at test	16 hours, 7 days, 28 days
Triaxial confining stress	20, 40, and 60 kPa (3, 6, and 9 psi)

Table 2.11

Hyperbolic Soil Model Parameters for Air-Modified CLSM (McGrath and Hoopes, 1997)

Parameter Symbol	Value		
	16 hours	7 days	28 days
K	630	800	1000
n	0.8	0.75	0.65
R_f	0.86	0.6	0.55
C, kPa (psi)	0 (0)	28 (4)	42 (6)
ϕ, deg	38	38	38
$\Delta\phi$, deg.(Note 1)	0	0	0
B_i/Pa	19	40	450
ϵ_u	0.17	0.15	0.09

Notes

1. The term $\Delta\phi$ accounts for the non-linear Mohr-Coulomb failure envelope observed in many soils. The scope of the testing program was not sufficient to determine the shape of the envelope for CLSM, thus it is assumed to be linear by setting $\Delta\phi$=0.

Table 2.12

Rigid Pipe Bedding Factors for Air-Modified CLSM (McGrath and Hoopes, 1997)

Age	Installation Type	
	Trench	Embank.
16 hours	1.8	2.5 to 2.8
7 days	2	3.0 to 3.4
28 days	2.5	4.0 to 4.8

Table 2.13

Modulus of Soil Reaction Values for CLSM, MPa (psi)

Mix	Age		
	16 hours	7 days	28 days
Air-modified CLSM	7 (1,000)	14 (2,000)	21 (3,000)

2.3 Influence, Properties, and Modeling of Pre-existing Soil

For pipes installed in trenches, the stiffness and strength properties of the in situ soils that form the trench bottom and trench wall can influence the pipe behavior. Characterizing these materials has posed a significant problem for designers, as the variability of in situ soils is immense. In addition to the variability in particle size and plasticity described by the soil classification systems, natural soils have highly variable moisture contents, tend to change stiffness with age, and may range in stiffness from wet runny conditions to solid rock. Unlike backfill soils, which can be selected for a project, the designer must accept the natural soils as a part of the design. From a structural point of view, it is often desirable to use wide trenches to isolate a pipe from poor natural soils; however, the increase in excavation and backfill costs can be significant and the question of how wide a trench must be is important.

AWWA Manual M45, The Fiberglass Pipe Design Manual (1996) has attempted to provide guidance on soil stiffness for in situ soils based on the unconfined compressive strength and the standard penetration test (commonly called blow counts). Table 2.14 provides suggested modulus values ranging from 350 kPa to 138 MPa (50 to 20,000 psi).

Table 2.14
AWWA Manual M45 Values for Modulus of Soil Reaction of In Situ Soils

Native in Situ Soils*				
Granular		Cohesive		E'_n (psi)
Blows/ft †	Description	q_u(Tons/sf)	Description	
>0-1	very, very loose	>0-0.125	very, very soft	50
1-2	very loose	0.125-0.25	very soft	200
2-4		0.25-0.50	soft	700
4-8	loose	0.50-1.0	medium	1,500
8-15	slightly compact	1.0-2.0	stiff	3,000
15-30	compact	2.0-4.0	very stiff	5,000
30-50	dense	4.0-6.0	hard	10,000
>50	very dense	>6.0	very hard	20,000

* The modulus of soil reaction E'_n for rock is ≥ 50,000 psi.
† Standard penetration test per ASTM D1586.

For embankment installation $E'_b = E'_n = E'$

Note: 1 m = 3.28 ft, 1 kN/m^2 = 0.010 tons/sq. ft, 1 MPa = 145 psi

Evaluating in situ soils in simplified design methods generally requires that the soil stiffness at the side of a pipe be represented by a single modulus value, which is a result of the composite behavior of the trench backfill and the natural soil. Very little work has been done on this issue. Leonhardt (1979) used the layered elastic theory to develop a simplified method to compute an "effective" E' value based on the relative value of the stiffness of the in situ and backfill soils and the trench width, expressed as a ratio of the width to the outside diameter of the pipe. The expression is:

$$E'_{design} = \zeta E'_b \ , \tag{2.9}$$

where

E'_{design} = value of E' used in Iowa formula, MPa, psi,
ζ = Leonhardt factor, and
E'_b = value of E' for backfill.

The Leonhardt factor is computed as:

$$\zeta = \frac{1.662 + 0.639\left(\dfrac{B_d}{D_o} - 1\right)}{\left(\dfrac{B_d}{D_o} - 1\right) + \left[1.662 + 0.361\left(\dfrac{B_d}{D_o} - 1\right)\right]\dfrac{E'_b}{E'_n}} \ , \tag{2.10}$$

where

B_d = trench width, m, ft,
D_o = pipe outside diameter, m, ft, and
E'_n = value of E' for in situ material.

The Leonhardt approach is thought to be conservative. AWWA Manual M45 presents a table of slightly less conservative values.

In computer analyses, in situ soils are often treated as exhibiting linear elastic behavior. This usually produces acceptable accuracy, because the imposed stresses are often not greater than the previous maximum stress experienced by the soil mass and because the in situ soil is separated from the pipe by the trench backfill and therefore has less impact on the behavior. Designers should be aware of instances where these two conditions do not exist and may wish to investigate more sophisticated assumptions.

2.4 Pipe-Soil Interaction Software

A number of finite element method (FEM) computer programs have been written specifically for the analysis of buried pipe problems, among these are CANDE (Katona, 1976, and Musser et al. 1989), and SPIDA (Heger et al. 1985). These programs are considered representative of the types of features that are available in other programs.

CANDE was developed under contract from the Federal Highway Administration. It was originally written for main frame computers but has since been modified to run on personal computers (Musser et al. 1989). It considers all types of pipe materials, including both rigid and flexible pipes. Several elastic soil models are available, including linear elastic, overburden dependent, and hyperbolic. CANDE has three solution levels. Level 1 does not utilize finite elements. It is an implementation of the elastic plate solution developed by Burns and Richard (1964). Level 2 is a finite element solution with a predefined mesh. The automated mesh assumes symmetry about the centerline of the pipe and models only half of the structure using ten bending elements, each 15 degrees long. Level 3 is a fully user defined finite element solution. CANDE is publicly available.

The Burns and Richard solution has received a great deal of attention as a simplified design method that is based on a theoretically sound development and can address the entire range of pipe stiffnesses. It is a closed form solution for an elastic circular ring embedded in an infinite homogenous, elastic, isotropic medium. The theory describes the pipe in terms of the hoop (axial) stiffness:

$$PS_H = \frac{EA}{R}, \tag{2.11}$$

where

PS_H	=	Pipe hoop stiffness, MN/m^2, psi,
E	=	Pipe material modulus of elasticity, MPa, psi,
A	=	Pipe wall area per unit length, mm^2/mm, in.^{2}/in., and
R	=	Centroidal radius of pipe, mm, in.

and the pipe bending stiffness, which is defined here in terms of standard U.S. practice as the stiffness in the parallel plate test:

$$PS_B = \frac{EI}{0.149\,R^3}, \tag{2.12}$$

where

PS_B = Pipe bending stiffness, MN/m/m, lbs/in./in., and

I = Moment of inertia of pipe wall, mm^4/mm, in.^{4}/in..

The pipe stiffness are combined with the soil stiffness, using the constrained modulus, M_s, to define the overall pipe-soil system stiffnesses, which are the hoop stiffness parameter, S_H:

$$S_H = \frac{M_s R}{EA} , \tag{2.13}$$

and the bending stiffness parameter, S_B:

$$S_B = \frac{M_s R^3}{EI} . \tag{2.14}$$

These parameters are very useful in understanding behavior, as will be discussed in later sections.

SPIDA was developed jointly by Simpson Gumpertz & Heger Inc. and the University of Massachusetts under contract from the American Concrete Pipe Association. It assumes symmetry about the centerline of the pipe using 17 bending elements varying in arc length from 7.5 degrees near the crown and invert, to 10 degrees near the springline, to 15 degrees at 45 degrees from the crown and invert. SPIDA uses an automatic mesh generator that can define trench and embankment installations. For installations that fall within the limits of the mesh generator it is easier to use than CANDE, but it does not have an option with the versatility of CANDE Level 3. The soil options in SPIDA are linear elastic and hyperbolic. SPIDA is a proprietary program, owned by the ACPA.

CANDE and SPIDA both allow modeling soil behavior using the Duncan hyperbolic Young's modulus soil model with the Selig hyperbolic bulk modulus. This is an elastic model that incorporates non-linear behavior as a function of the soil strength parameters. Properties for use in this model have been developed from tests on previously compacted soil. It is an elastic model.

CHAPTER 3
CHARACTERIZATION OF BACKFILL MATERIALS

Current practice in characterizing backfill materials focuses on soil classification and compaction characteristics. This was discussed in chapter 2 but, also noted, was the fact that the properties of interest for pipe backfill are stiffness and strength. A program of characterizing backfill materials by both the classical tests and other tests that may be more revealing about stiffness and strength properties was undertaken to explore changes to practice that might allow a more direct correlation between the measured properties and the desired properties.

A second effort in correlating backfill properties is to relate the more sophisticated soil models used in finite element analysis of buried pipe to the simplified properties used in hand calculations. The hyperbolic models of Duncan (1980) and Selig (1988) are complicated and require significant testing to develop the data necessary to characterize a soil, while the modulus of soil resistance values of Howard (1977) are readily determined and applied but empirical in nature and have not been successfully correlated to true soil properties. The relationship between the modulus of soil reaction and the hyperbolic soil model is explored.

3.1 Materials Tested

A total of 12 processed backfill materials and naturally occurring soils were collected for testing (for simplicity they will all be called "soils" below). The soil gradations, classifications and common names by which they are sold are listed in Table 3.1. They are described as follows:

- Soils 1 to 3 are angular crushed stone with widely varying gradations. All three soils were crushed from the same material, a local deposit called trap rock with a specific gravity of 2.9.
- Soil 4 is a uniform rounded stone.
- Soils 5 and 8 are rounded and subrounded sands. Soil 5 is manufactured as fine concrete aggregate and Soil 8 for use on roads in winter.

Table 3.1

Soil Gradation Characteristics and ASTM and AASHTO Classifications

Soil No.	Common name	D_{60}	D_{30}	D_{10}	C_u	C_c	Gradation (% passing)				ASTM D 2487	AASHTO
							#4	#10	#40	#200		
1	gravel trap rock	9.10	7.50	5.80	1.57	1.07	2	<1	<1	<1	GP - poorly graded gravel	A-1-a
2	sand trap rock	1.05	0.34	0.09	11.67	1.22	100	85	35	8	SW-SM - well graded sand with silt	A-1-b
3	shoulder stone	4.80 (3.30)	1.60 (1.30)	0.20 (0.20)	24.00 (11.00)	2.67 (1.71)	59 (72)	35 (44)	13 (12)	3 (4)	SW - well graded sand with gravel	A-1-a
4	pea gravel	8.90	7.00	5.20	1.71	1.06	8	1	<1	<1	GP - poorly graded gravel	A-1-a
5	concrete sand	0.69	0.34	0.20	3.45	0.84	97	89	39	2	SP - poorly graded sand	A-1-b
6	rewash	0.10	0.07	0.06	1.72	0.90	100	100	100	23-33	SM - silty sand	A-2-4
7	glacial till	2.80	1.10	0.30	9.33	1.44	71	51	8	<1	SW - well graded sand with gravel	A-1-b
8	winter sand	0.92	0.47	0.26	3.54	0.92	94	82	25	2	SP - poorly graded sand	A-1-b
9	top clay									90	CL - lean clay	A-6
10	varved clay									93	CL - lean clay	A-6
11	red sandstone	1.30	0.55	0.27	4.81	0.86	92	75	21	2	SP - poorly graded sand	A-1-b
12	native sand	0.76	0.27	0.08	9.50	1.20	92	85	43	9	SW-SM well graded sand w/ silt	A-1-b

Note: Two sieve analyses were made for Soil Nos. 3 and 6. Both analyses are reported for Soil No. 3. For Soil No. 6 only the percent finer than the No. 200 sieve varied significantly and is reported.

- Soil 6 is a uniform, fine sand with rounded particles, all just smaller or just larger than the # 200 sieve. This soil was obtained from two separate stockpiles. One stockpile was recently manufactured while the other had been left to weather for several years. The latter had some grass and small stones that were picked out before laboratory testing. The two materials were similar in gradation and they are not distinguished herein.

- Soils 9 and 10 were taken from clay deposits on the University of Massachusetts Campus. Soil 9 had been used as fill. It had been in place for about 20 years. Soil 10 is a naturally occurring varved clay deposit. The varved clay was mixed and all of the structure of the varves was destroyed prior to laboratory testing.

- Soils 11 and 12 were taken from naturally occurring sand deposits on the University of Massachusetts Campus. The native sand was hard but readily excavated. The red sandstone was cemented and excavated only with some difficulty. All of the cementation was broken down while mixing the samples for testing. The particles of both sands are subrounded.

The results of sieve analyses conducted on each of the coarse-grained soils (Soils 1 to 8 and 11 and 12) in accordance with AASHTO T 88 (ASTM D 422) are presented in figs. 3.1 and 3.2. Atterberg limits of the fine grained soils (Soils 9 and 10) were determined in accordance with AASHTO T 89 and T 90 (ASTM D 4328) and are summarized in table 3.2. The quantity of coarse-grained material in the fine grained soils was estimated using the visual manual procedures of ASTM D 2488.

Table 3.2

Atterberg Limits for Fine Grained Soils

Soil No.	Common name	Liquid limit	Plasticity index
9	top clay	34	13
10	varved clay	37	18

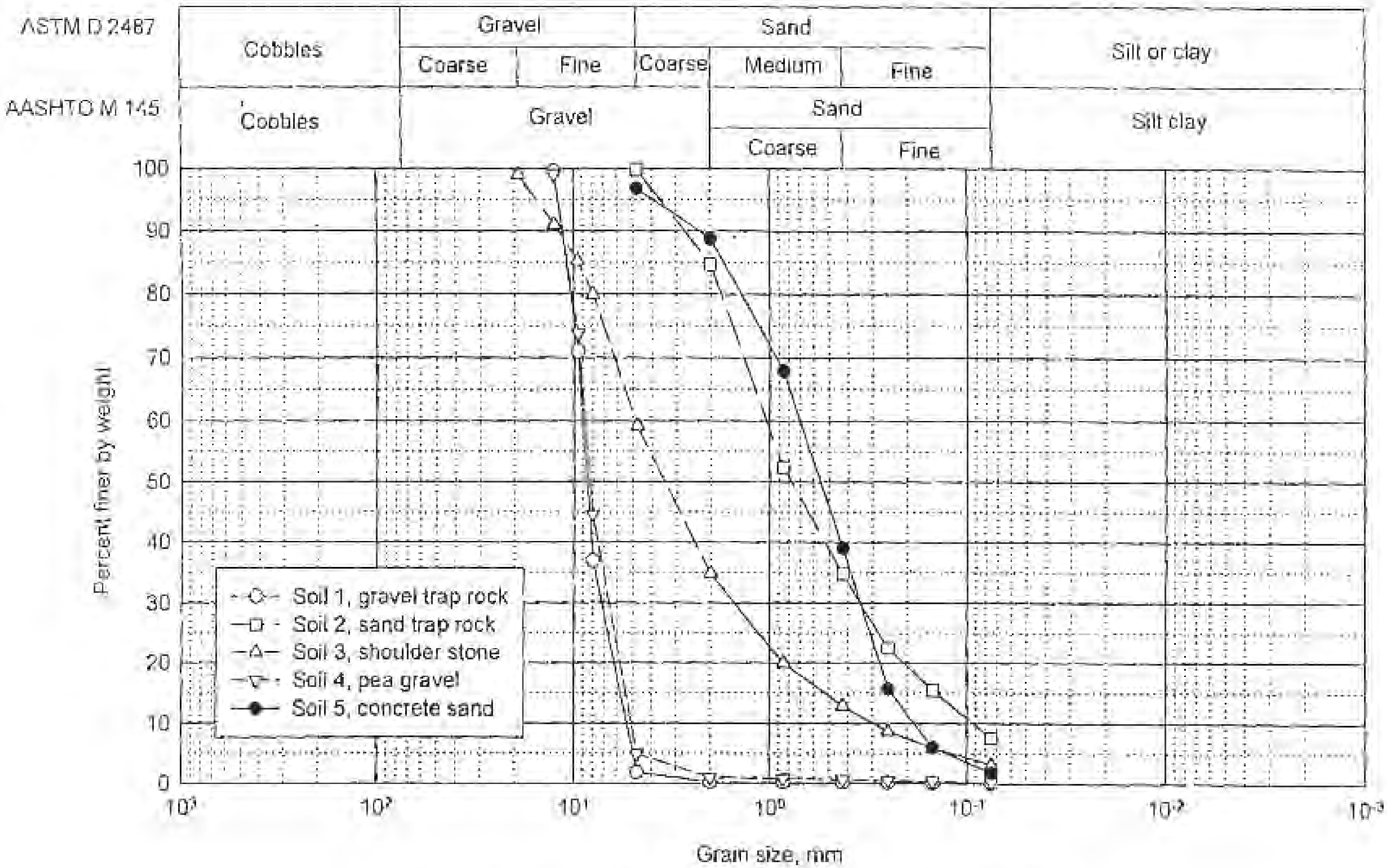

Figure 3.1 Grain Size Distribution for Soil Nos. 1 to 5

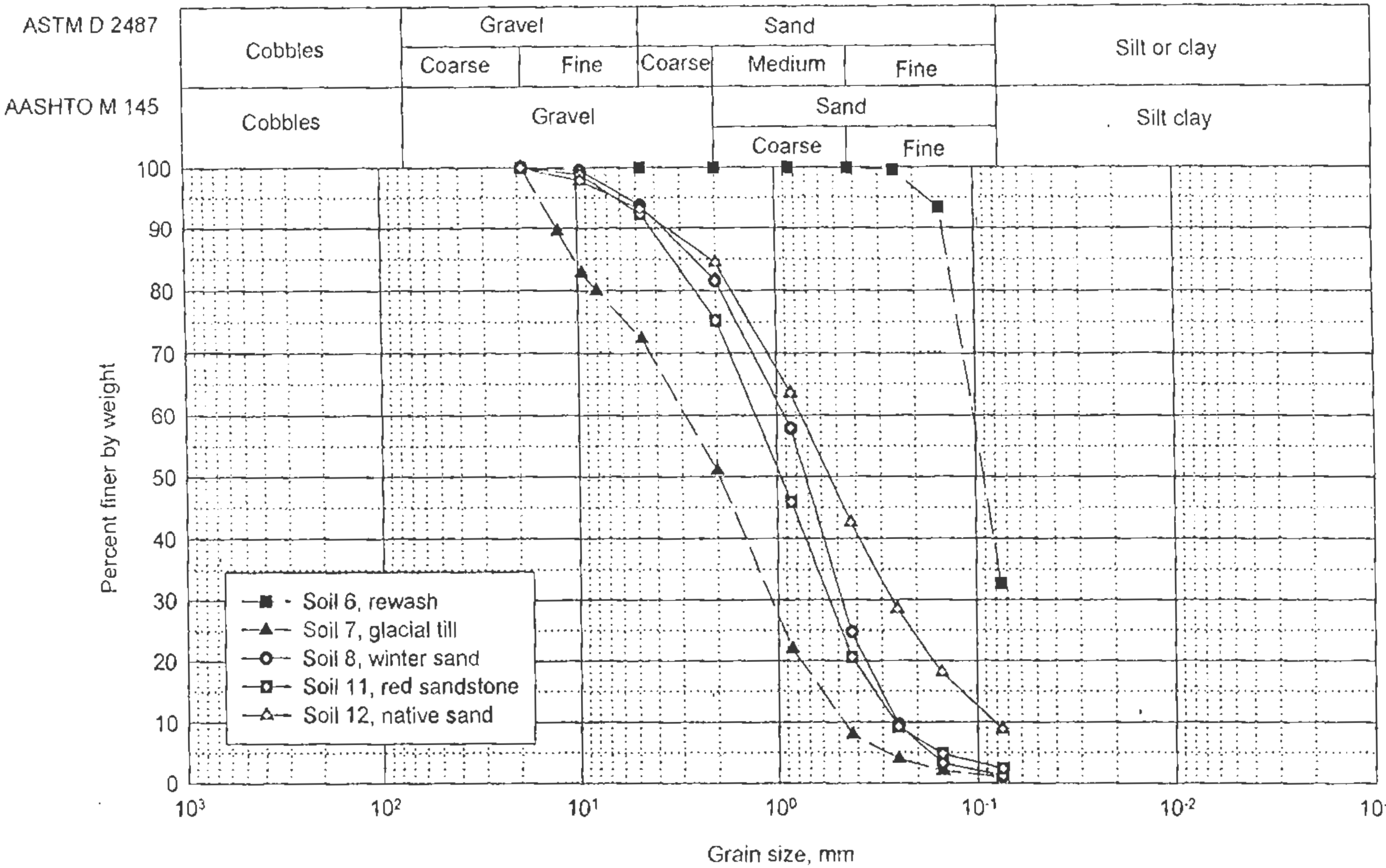

Figure 3.2 Grain Size Distribution for Soil Nos. 6 to 12

3.2 Characterization Tests

The tests for characterizing backfill materials included the traditional compaction tests as well as a number of tests that are not typically considered for pipe installation. These include the moisture-density relations using standard Proctor effort, California Bearing Ratio test, compaction tests conducted with variable effort, one-dimensional compression tests, and penetration tests. The CLSM material was tested for unconfined compression strength.

3.2.1 Compaction Characterization

Compaction characteristics of the test soils were determined in accordance with the standard Proctor test (AASHTO T 99, ASTM D 698). The Proctor tests were all conducted in 150 mm (6 in.) diameter molds suitable for conducting CBR tests (see section 3.3) after compaction. New soil was used for each test. Soils 1 to 6 were also characterized by relative density tests (ASTM D 4253 and D 4254). The maximum index density test was conducted on a cam driven vertically vibrating table using dry soil (Method 2A).

3.2.2 Variable Compactive Effort

After determination of maximum dry density and optimum water contents, compaction tests using variable levels of effort were conducted to determine the relationship of dry density to compactive effort. These tests were conducted on Soil Nos. 1 to 6. New soil was used for each test. All tests were conducted at near optimum water content as determined from the standard effort test and in 150 mm (6 in.) diameter molds with a mold volume of 0.0021 m^3 (0.075 ft^3). Compactive energy varied from none to the modified test energy, 2,700 kN-m/m^3 (56,000 ft-lb/ft^3), as summarized in table 3.3. CBR tests were conducted after completion of the compaction tests (See section 3.2.3).

Table 3.3
Parameters for Variable Compactive Effort Tests

Energy level	Weight (N)	Height of drop (m)	Blows per layer	Layers	Energy (kN-m/m^3)
Loose	0	0	0	1	0
0.25 * Std Proctor	24.5	0.305	14	3	150
0.50 * Std Proctor	24.5	0.305	28	3	300
0.75 * Std Proctor	24.5	0.305	42	3	440
1.00 * Std Proctor	24.5	0.305	56	3	590
2.19 * Std Proctor	44.8	0.457	27	5	1300
3.38 * Std Proctor	44.8	0.457	42	5	2000
4.58 * Std Proctor (Mod. Proctor)	44.8	0.457	56	5	2700

3.2.3 California Bearing Ratio

Soils 1 to 6 were tested by the California Bearing Ratio (CBR) test, AASHTO T 193 (ASTM D 1883). The test was conducted on specimens as compacted, without soaking, and with a 76.5 N (17.2 lb) surcharge (0.6 psi). The CBR was computed for a penetration depth of 5 mm (0.2 in.).

3.2.4 Penetration Tests

Soil Nos. 6 and 8 to 12 were also tested for penetration resistance in accordance with ASTM D 1558. The size of the penetrometer tip varied as a function of the density and soil type. The penetration force was read at a penetration depth of 50 mm (2 in.). The penetration test is similar to the CBR, except that the load is applied to a smaller bearing area with less control and there is no confining surcharge.

3.2.5 Results of Characterization Tests

Results of the standard Proctor compaction tests are given in table 3.4. The values are reported as unit weights (kN/m^3) rather than density (kg/m^3) to simplify calculation of loads and stress which are computed as force per unit length (kN/m) and force per unit area (kN/m^2), respectively. Table 3.4 also presents the results of the relative density tests in terms of the percentage of maximum standard Proctor density that was achieved and the loose density when soil was placed in the Proctor mold at optimum moisture content with no compaction. The data for Soils 1 to 6 is presented graphically in Fig. 3.3. This figure shows that the soils with less than 1 percent fines, whether dry or wet, are at 80 percent or more of maximum standard Proctor density when placed loose with no compactive effort. For the pea gravel in particular, which is uniformly graded and rounded, the soil is at 85 to 90 percent density when loosely placed. As the fines content increases, the loose density decreases. This demonstrates that, as the fines content increases, the loose density decreases which in turn increases the importance of applying proper compactive effort. Note also that the minimum relative density is not necessarily a lower bound for loosely placed soils. When moisture is added the soil can bulk, resulting in a lower density. In the case of Soil 6, the bulking is substantial, resulting in a loose density of about 55 percent of maximum standard Proctor density.

Table 3.4

Comparison of Relative Density and Standard Proctor Test Results

Soil No.	Common name	AASHTO T 99 max. unit weight,	AASHTO T 99 Optimum moisture	Maximum relative density	Minimum relative density	Placed loose at optimum moisture
		kN/m^3 (lb/ft^3)	(%)	% of maximum standard Proctor density		
1	gravel trap rock	16.6 (106)	2	97	81	83
2	sand trap rock	20.3(129)	12	96	75	58
3	shoulder stone	22.0(140)	9	94	70	71
4	pea gravel	16.9(108)	1	97	85	91
5	concrete sand	17.9(114)	10	107	86	70
6	rewash	15.0(96)	22 20	104	76	54
7	glacial till					
8	winter sand	17.6(112)	10			
9	top clay	17.1(109)	20			
10	varved clay	15.9(101)	22			
11	red sandstone	19.0(121)	12			
12	native sand	19.8(126)	9			

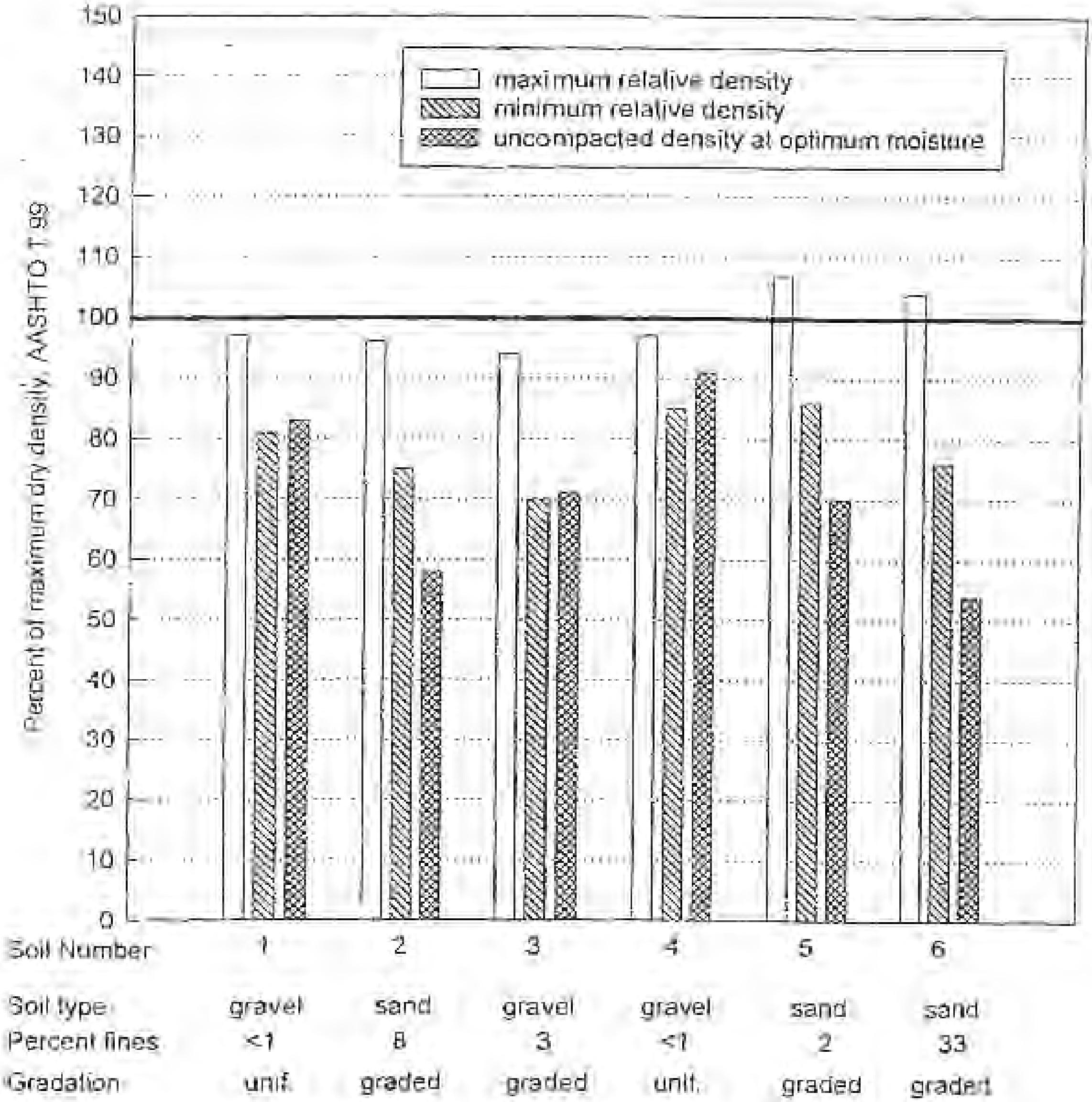

Figure 3.3 Loose and Compacted Density of Backfill Soils

Moisture-density and moisture-CBR relations for Soil Nos. 1 to 6 are presented in fig. 3.4. Soil No. 6, with 30 percent fines, shows the classical moisture-density relation, while the other soils, with few fines, have a much less distinct, or no relationship between moisture content and unit weight (fig. 3.4b). The CBRs show a trend of increasing at a modest rate until the moisture content nears optimum and then dropping rapidly (fig 3.4a). Fig. 3.5 shows the same data but with the CBR on the x-axis and all parameters normalized based on the value at 100 percent standard Proctor unit weight. The figure suggests that the

CBR is not a good indicator of unit weight for these soils in the range of 90 to 100 percent of maximum standard Proctor density.

Moisture-density relations and moisture-penetration resistance relations for Soil Nos. 6 and 8 to 12 are shown in figs. 3.6 and 3.7. Fig. 3.7 suggests that a relationship exists between moisture content and penetration resistance, and also between density and penetration resistance for the soils with more than 7 percent fines (Nos. 6, 9, 10, and 12). The penetration resistance varies almost 100 percent as the density varies between 90 and 100 percent of maximum standard Proctor density. The results for the two sands without fines (Nos. 8 and 11) show no correlation.

Together, figs. 3.4 to 3.7 indicate that relationships between penetration resistance (or CBR) could be established for soils with more than a few percent fines; however, the data in fig. 3.7 also show a strong relationship to moisture content, which may be the dominant variable.

Normalized results of the variable compactive effort tests are shown for individual soils in fig. 3.8 and for all data in fig. 3.9. Where the moisture content does not vary, a relation between CBR and density is present, as both parameters show an increase for compaction energy up to 100 percent of standard Proctor effort. Only Soil No. 5 shows a clear trend of continued increase in density as the compactive energy further increases from the standard effort to the modified effort; however, the data shows scatter. None of the soils show an increase in CBR over the range of standard to modified range of compactive energy. This lack of increase for compactive energies greater than the standard effort could have been anticipated as all of the tests were conducted at optimum moisture content determined from the standard test. Had the test been conducted at a lower moisture content a trend of increasing density and CBR value may have been evident over this range.

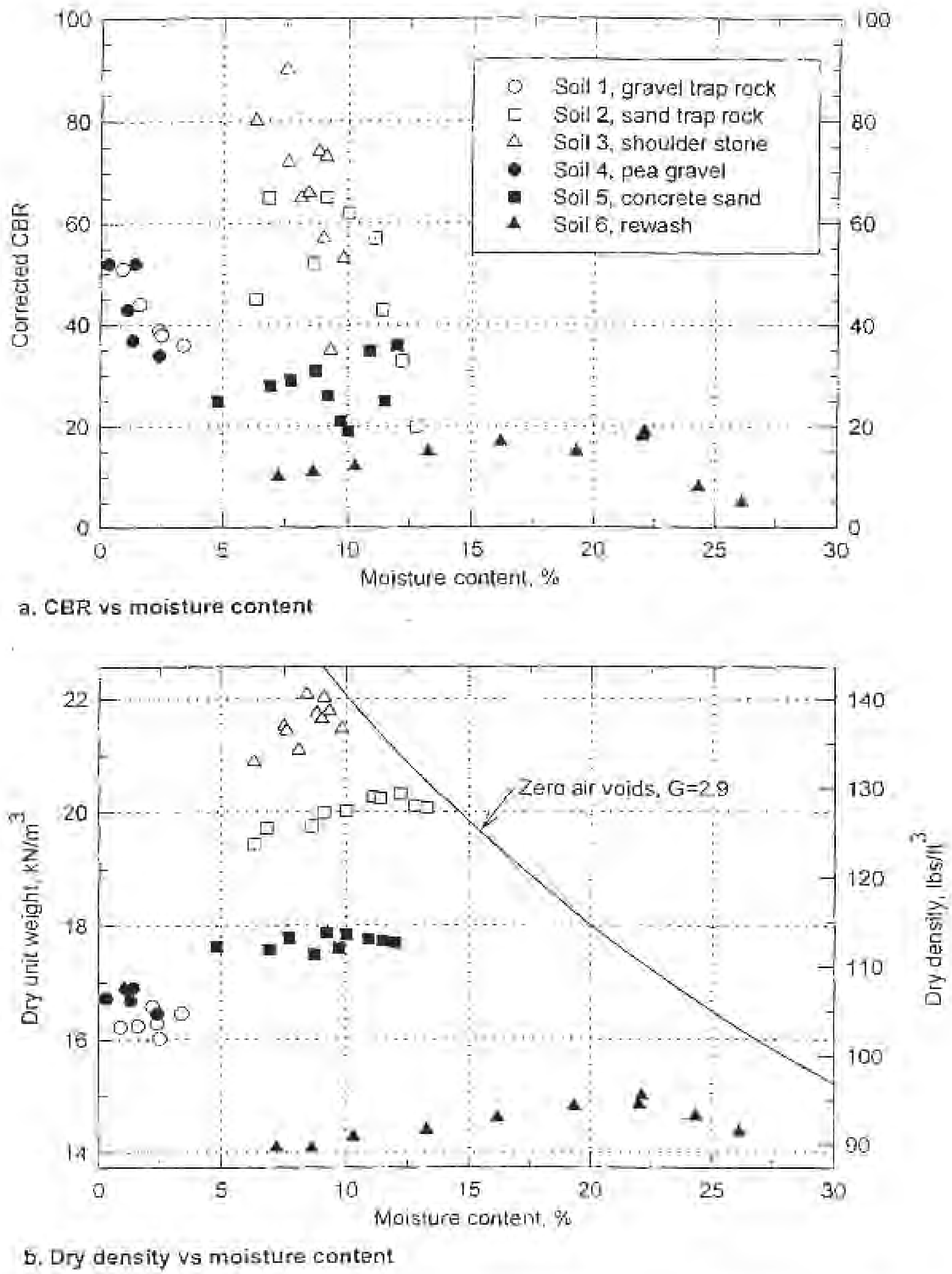

Figure 3.4 Moisture Content Versus Standard Effort Unit Weight and CBR

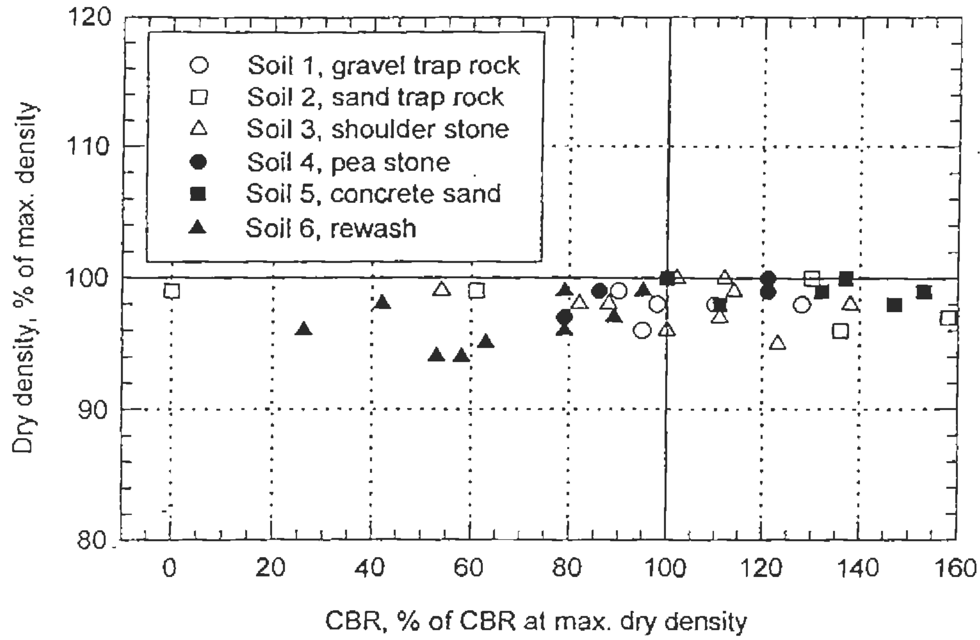

a. Dry density vs CBR

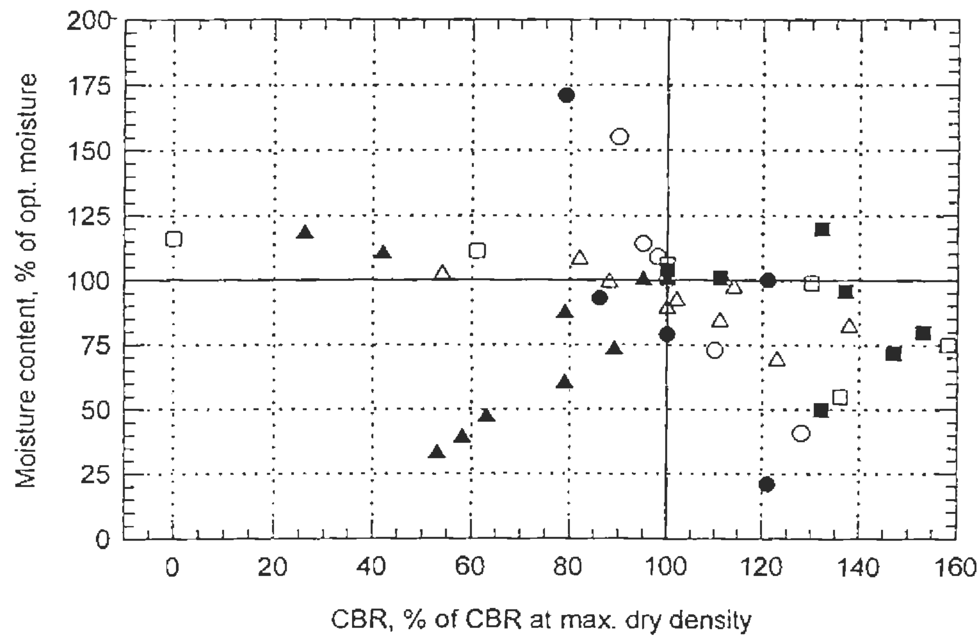

b. Moisture content vs CBR

Figure 3.5 CBR Versus Standard Effort Unit Weight and Moisture Content

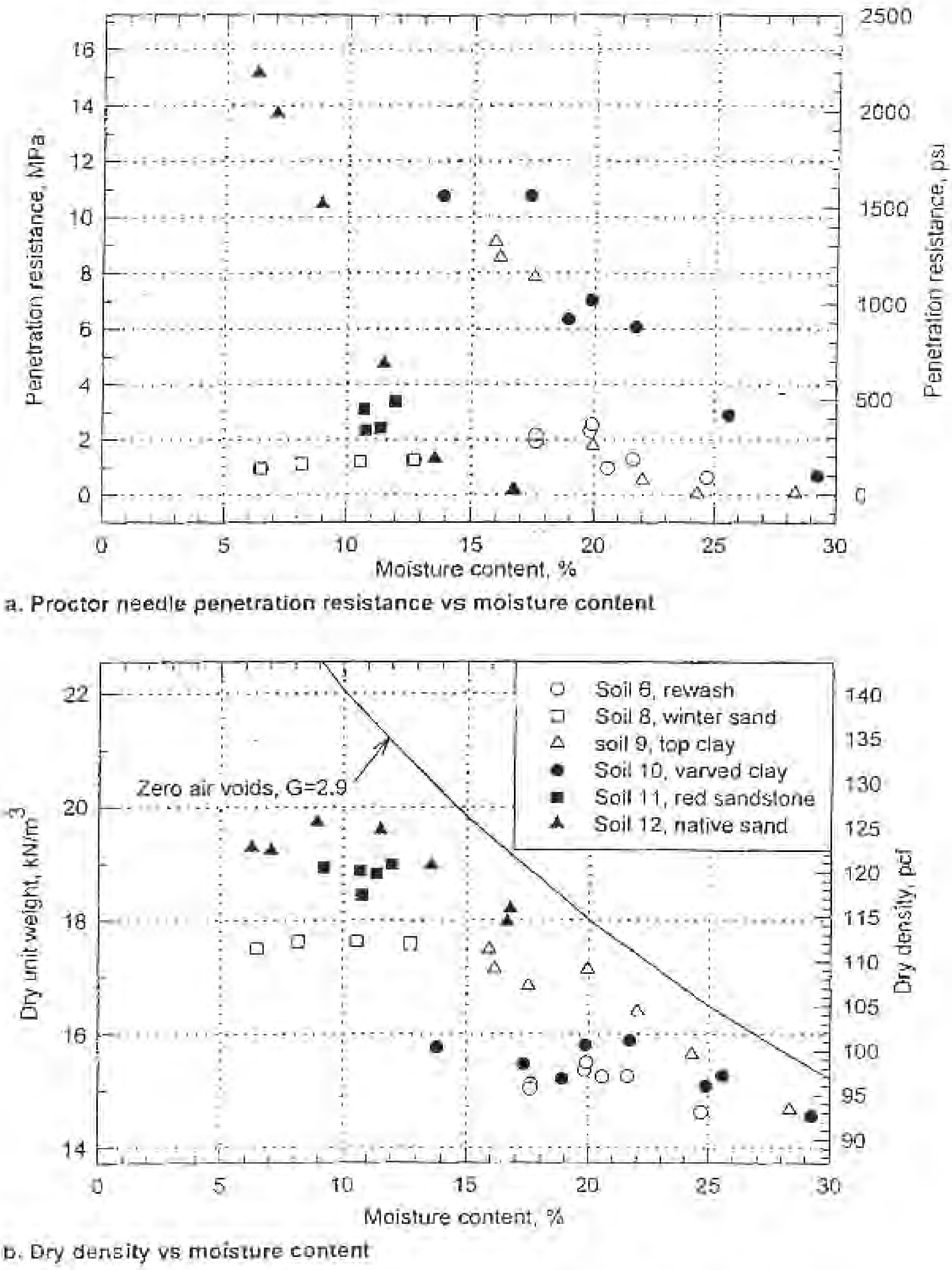

a. Proctor needle penetration resistance vs moisture content

b. Dry density vs moisture content

Figure 3.6 Moisture Content Versus Standard Effort Unit Weight and Penetration Resistance

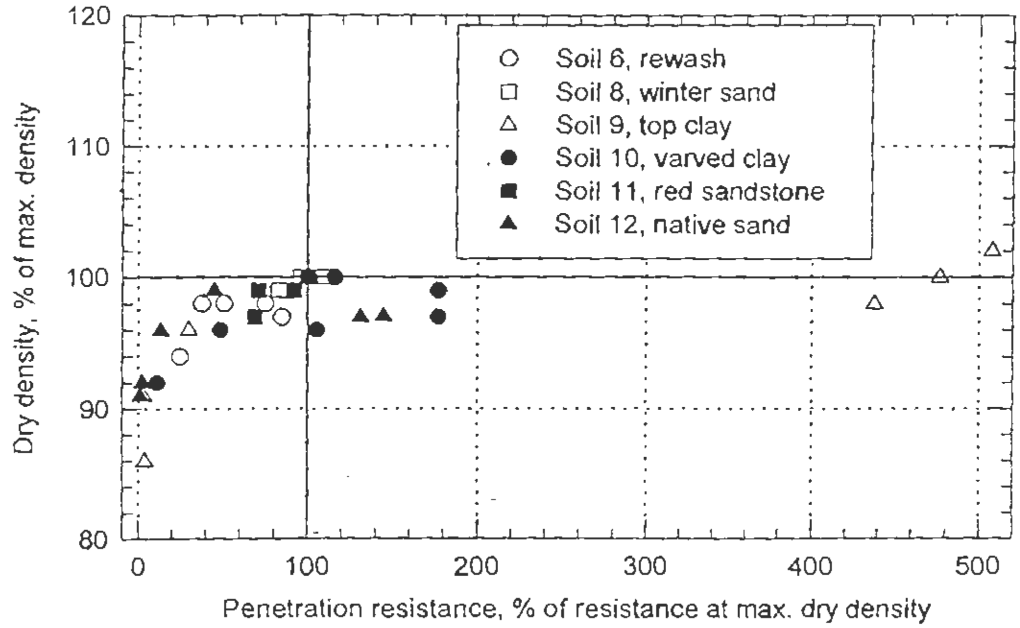

a. Proctor needle penetration resistance versus dry density

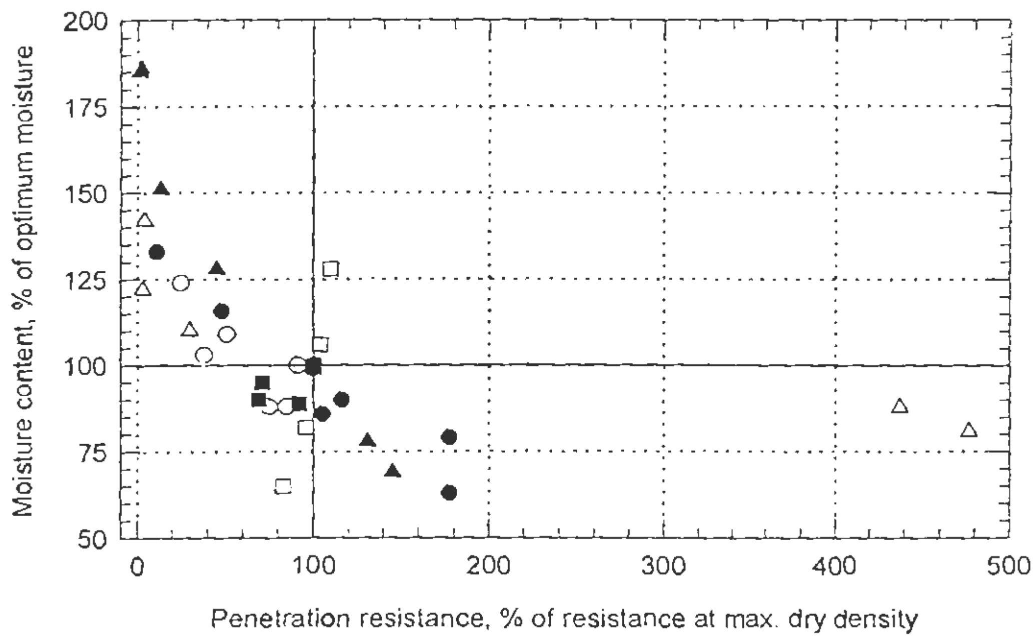

b. Proctor needle penetration resistance versus moisture content

Figure 3.7 Penetration Resistance Versus Moisture Content and Standard Effort Unit Weight

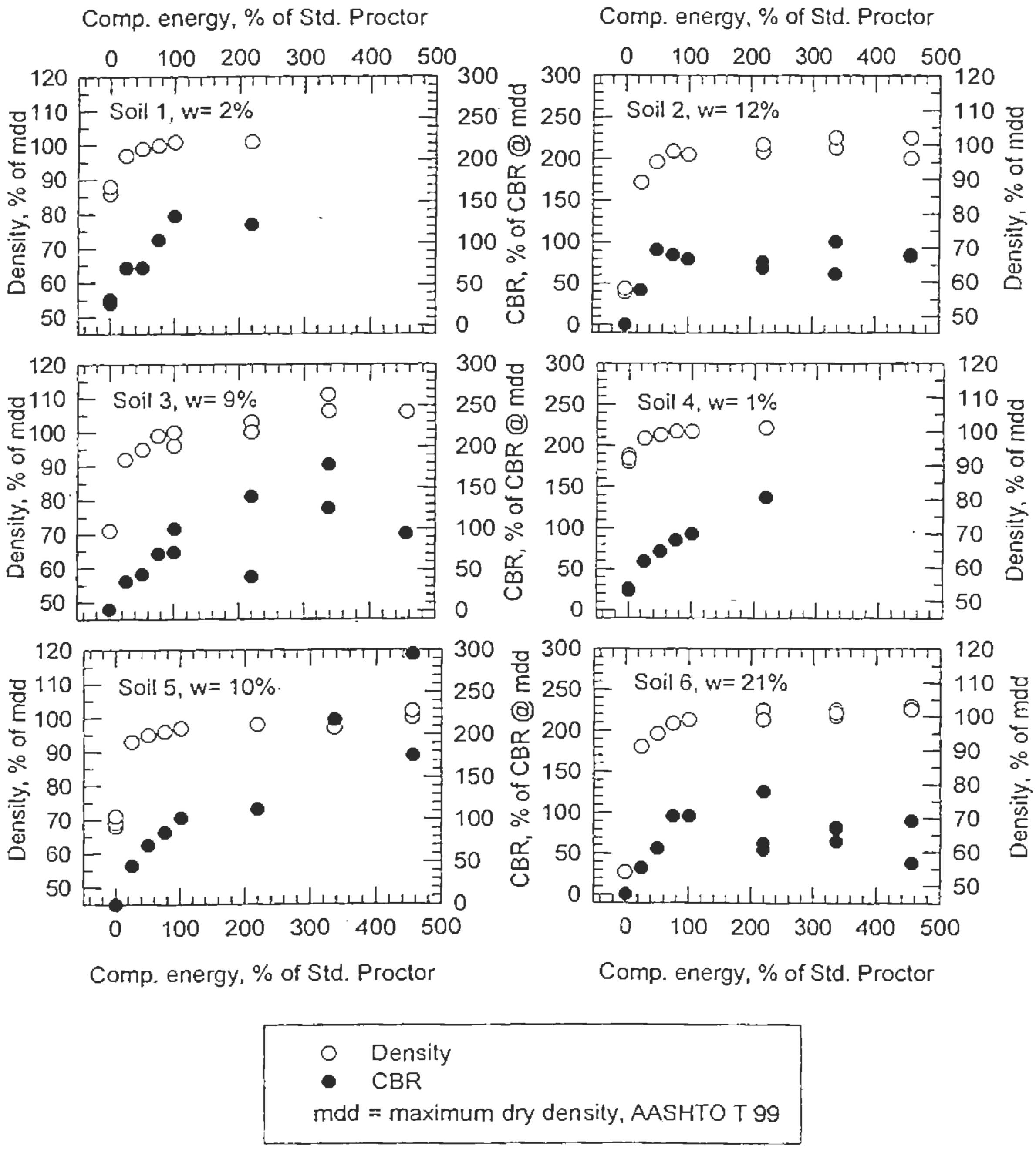

Figure 3.8 Variable Effort Compaction and CBR Conducted at Optimum Moisture Content

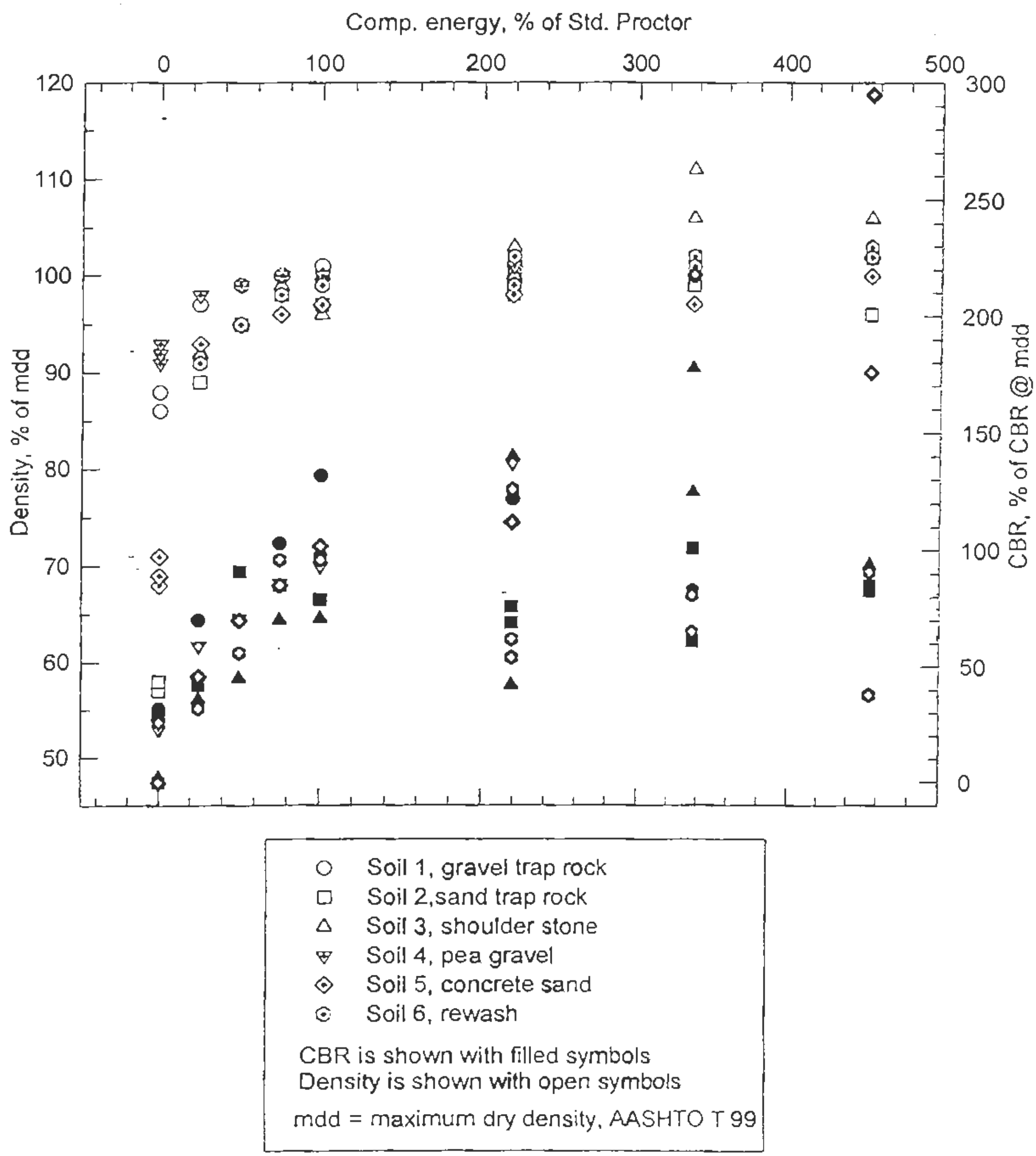

Figure 3.9 Normalized Variable Effort Compaction and CBR Test Results at Optimum Moisture Content

3.3 One-Dimensional Compression Tests

The variability of backfill materials and the lack of quality control on construction projects generally leads designers to accepting "standard" properties for soils, such as the hyperbolic properties of Duncan(1980) and Selig (1988, 1990) used in finite element analyses and the modulus of soil reaction values developed by Howard (1977). For some projects, however, it is desirable to conduct tests on actual backfill materials to determine the properties. The triaxial compression test is considered the most effective test to determine stiffness properties of soils; however, equipment for this test is not readily available to many pipe designers and the testing is relatively complex and time consuming. A relatively simple alternate to the triaxial test is the one-dimensional compression test which consists of compressing soil in a rigid mold that allows no lateral strain. This is essentially the oedometer test used for determining consolidation characteristics of clays.

The one-dimensional compression test is not typically used for coarse-grained soils because the standard mold is small relative to the particle sizes, because of edge effects at the soil-mold interface, and because of difficulty in leveling the sample surface and getting uniform contact with the loading plates. Even though these problems are known to exist, several of the backfill soils were evaluated with the one-dimensional compression test (Courtney, 1995, and Ramsay, 1994) and the results demonstrate important characteristics of backfill behavior.

3.3.1 Procedures

The test apparatus is shown in fig. 3.10. Tests were conducted in a 155 mm (6.11 in.) diameter mold with a height of 50.8 mm, (2 in.). All specimens were prepared at the optimum moisture content determined from the results of the standard Proctor test. Two methods of compaction of the compression test specimens were evaluated:

- Clay samples were compacted by static compression. This was accomplished in layers. The first layer of soil was placed in the mold and subjected to a static compression force in the compression testing machine until it reached the desired density. This was then repeated for the second layer of the specimen.

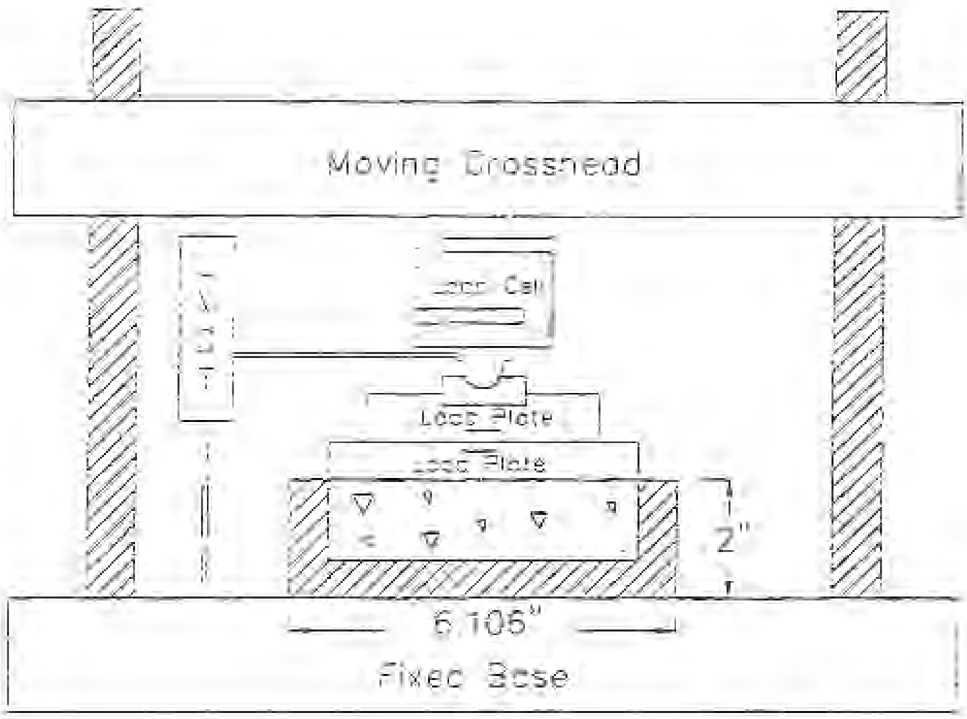

1 in. = 25.4 mm

Figure 3.10 Configuration of One-Dimensional Compression Test

- Coarse-grained soils were compacted by vibration. The full test amount of soil was placed in the test mold which was then secured to a vibrating table. The specimen was then vibrated at 60 hertz until the sample reached the desired density.

After preparation, samples were tested in a 53.3 kN (12,000 lb) capacity Tinius Olsen screw-drive compression machine. Load and strain were recorded at closely spaced intervals using an Artech 44.5 kN, (10,000 lb) load cell and a Hewlett Packard LVDT with a computerized data acquisition system. A test consisted of three load-unload cycles over a compression stress range from 0 to 1,000 kPa (0 to 145 psi).

Tests were conducted on the shoulder stone, rewash, winter sand, and top clay at several densities.

3.3.2 Results

All data was plotted by considering any load up to a stress level of 7 kPa (1 psi) as a seating effect. The stress and strain at this point on the raw data curves was subtracted from the remaining data prior to plotting. Stress-strain curves at a density of about 90 percent of maximum dry density are presented for each of the four soils tested in fig. 3.11, which shows the following:

- As the particle size decreases the total strain at 1,000 kPa (150 psi) increases. This demonstrates the relative stiffness of the soils.
- The high stiffness of the shoulder stone relative to the other soils is demonstrated by the high slope of the initial portion of the curve in the first load cycle.
- The slope of the curves for all three cycles of the coarse-grained soils are much higher than for the corresponding cycles of the clay. This also suggests the better performance of the coarse-grained materials.
- The stress-strain curve for the clay material shows a decrease in slope at about 4 percent strain. This "wave" is thought to be the result of the compaction method.

The stress-strain curves of the four soils in the lower stress region where pipes are typically installed are shown in fig. 3.12. This figure clearly shows the greater stiffness of the shoulder stone. The performance of the clay is much better than expected, showing a stress-strain curve similar to that of the winter sand and rewash. This is thought to be an effect of the differences in the compaction methods. The clay had been compacted using static compression, while the coarse grained soils were compacted using vibration. Thus, the stress-strain behavior of the sand represents a first load cycle while the clay is already on a second load cycle. The decrease in slope for the clay stress-strain curve at a strain level of about 3 percent supports this explanation.

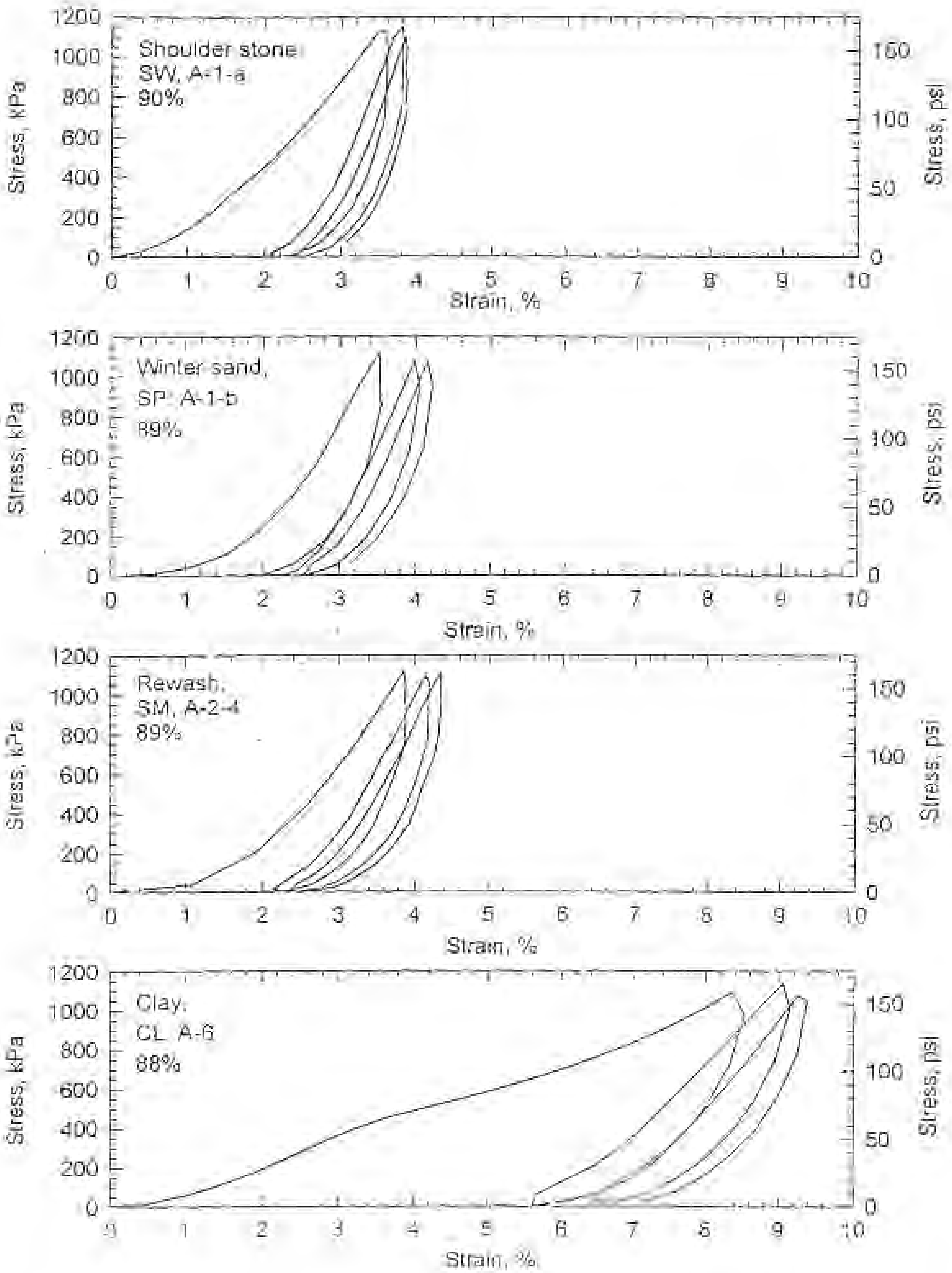

Figure 3.11 One-Dimensional Stress-Strain Curves at Approximately 90 Percent of Maximum Standard Proctor Density

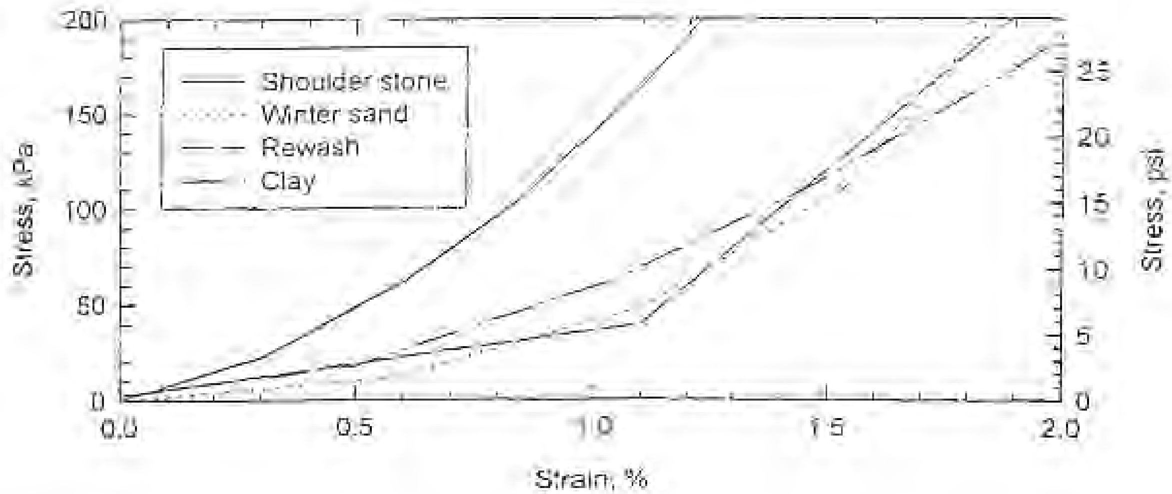

Figure 3.12 Stress-Strain Curves at Typical Stress Ranges, 90 Percent Density

Table 3.5 shows the secant constrained modulus, computed as the slope of the secant from the origin of the stress-strain curve to the "applied stress" level shown in the left hand column of the table. Modulus values are presented for several densities for each material. These values demonstrate the expected trends with changing density; however, the moduli are substantially lower than expected based on the predicted values from standardized soil properties, such as those used to develop the SIDD designs for reinforced concrete pipe, particularly those for the shoulder stone and winter sand. This will be discussed further in section 3.5.

Table 3.5
Constrained Modulus Values (MPa) from One-Dimensional Compression Tests

Applied stress (kPa)	Shoulder stone — Compaction level (% of maximum standard Proctor)				
	97%	90%	84%	75%	
7	7.3	5.6	3.3	1.9	
14	7.9	6.3	3.7	1.9	
34	9.3	8.2	4.9	2.1	
69	10.3	10.5	6.6	2.5	
138	12.6	13.8	9.3	3.1	
276	16.0	18.9	12.9	4.1	
413	18.7	21.7	14.9	5.0	
689	23.3	26.6	18.7	6.4	
1034	27.6	31.3	22.6	7.9	
Applied stress (kPa)	**Winter sand — Compaction level (% of maximum standard Proctor)**				
	94%	91%	89%	85%	63%
7	3.2	1.1	0.8	2.5	0.05
14	3.8	1.7	0.9	3.1	0.08
34	5.7	3.0	1.9	5.0	0.2
69	7.6	5.0	3.0	6.4	0.3
138	11.4	8.1	5.2	8.5	0.6
276	17.8	13.0	8.8	11.6	1.0
413	23.0	16.8	12.2	14.4	1.5
689	31.1	22.5	17.6	18.3	2.3
1034	38.8	28.2	23.8	22.0	3.3
Applied stress (kPa)	**Rewash — Compaction level (% of maximum standard Proctor)**				
	89%	84%	53%		
7	0.9	1.9	0.06		
14	1.6	2.1	0.09		
34	3.3	3.6	0.2		
69	5.1	5.9	0.3		
138	8.4	9.4	0.5		
276	13.0	13.7	0.9		
413	16.4	16.2	1.3		
689	22.2	19.2	2.1		
1034	27.8	22.0	3.0		

Table 3.5 (Cont.)
Constrained Modulus Values (MPa) from One-Dimensional Compression Tests

Applied stress (kPa)	Clay				
	Compaction level (% of maximum standard Proctor)				
	89%	84%	53%		
7	3.2	1.1	0.8		
14	3.8	1.7	1.0		
34	5.7	3.0	1.9		
69	7.6	5.0	3.0		
138	11.4	8.1	5.2		
276	17.8	13.0	8.8		
413	23.0	16.8	12.2		
689	31.1	22.5	17.6		
1034	38.8	28.2	23.8		

1 psi = 6.9 kPa, 1 psi = 0.0069 MPa

3.4 Correlation of Modulus of Soil Reaction with One-Dimensional Modulus

Most finite element analyses of pipes and culverts use soil models that represent the non-linear behavior of soils with reasonable accuracy. The hyperbolic model is used most in the United States. It models non-linear stress strain behavior and considers both strength and stiffness. Simplified pipe design has not progressed as far and still relies on the empirical modulus of soil reaction, E', as a measure of soil stiffness. The modulus of soil reaction is based on Spangler's Iowa formula and values are determined by back calculation from test results. As noted in chapter 2, the relationship between the modulus of soil reaction and true soil properties such as Young's modulus, E_s, or the constrained modulus, M_s has been investigated by a number of researchers. While not yet a consensus, there is a growing belief that the modulus of soil reaction can be related to the constrained modulus, which is reasonable since the soil around a pipe is generally well confined. The relationship between M_s, as expressed by the hyperbolic model, and E' was investigated and is reported here.

Two constants are required to define behavior of an elastic material. The hyperbolic model uses Young's modulus and the bulk modulus as the parameters. These parameters are both affected by the soil strength and state of stress. The basic equations for stress-vertical strain, and volumetric strain, as presented in Selig (1988), are:

$$(\sigma_1 - \sigma_3) = \frac{\epsilon_v}{\dfrac{1}{E_i} + \dfrac{\epsilon_v}{(\sigma_1 - \sigma_3)_u}} \quad , \tag{3.1}$$

where

σ_1 = major principal stress, kPa, psi,
σ_3 = minor principal stress, kPa, psi,
$(\sigma_1 - \sigma_3)$ = deviator stress, kPa, psi,
ϵ_v = vertical strain, mm/mm, in./in.,
E_i = initial tangent Young's modulus, kPa, psi, and
$(\sigma_1 - \sigma_3)_u$ = ultimate deviator stress, kPa, psi,

and

$$\sigma_m = \frac{B_i \, \epsilon_{vol}}{1 - \dfrac{\epsilon_{vol}}{\epsilon_u}} \quad , \tag{3.2}$$

where

σ_m = mean stress = $(\sigma_1 + 2\,\sigma_3)/3$, kPa, psi, (3.3)
B_i = initial bulk modulus, kPa, psi,
ϵ_{vol} = volumetric strain, and
ϵ_u = ultimate volumetric strain.

The one-dimensional compression test imposes the additional restriction that the volumetric strain is equal to the vertical strain because the lateral strains are zero:

$$\epsilon_{vol} = \epsilon_v \quad , \tag{3.4}$$

Substituting Eq. 3.4 into Eq. 3.2 yields:

$$\sigma_m = \frac{B_i \, \epsilon_v}{1 - \dfrac{\epsilon_v}{\epsilon_u}} \tag{3.5}$$

Eq. 3.3 can be rearranged to:

$$\sigma_3 = \frac{3\,\sigma_m - \sigma_1}{2} \tag{3.6}$$

substituted into Eq. 3.1, and simplified to:

$$\sigma_1 = \frac{0.667\,\epsilon_v}{\dfrac{1}{E_i} + \dfrac{\epsilon_v}{(\sigma_1 - \sigma_3)_u}} + \sigma_m \tag{3.7}$$

The initial Young's modulus, a function of the hyperbolic model soil parameters, K and n, and the confining stress, σ_3 is:

$$E_i = K\ P_a(\sigma_3/P_a)^n \tag{3.8}$$

Substituting Eq. 3.6 into Eq. 3.8 gives:

$$E_i = K\ P_a\left(\frac{3\,\sigma_m - \sigma_1}{2\,P_a}\right)^n \tag{3.9}$$

The ultimate deviator stress is a model parameter that is a function of the actual deviator stress at failure and the model parameter, R_f. In the hyperbolic model this is written as:

$$(\sigma_1 - \sigma_3)_u = \frac{(\sigma_1 - \sigma_3)_f}{R_f} \tag{3.10}$$

where the deviator stress at failure is a function of the soil friction angle, ϕ, the cohesion intercept, C, and the confining stress, σ_3, as follows:

$$(\sigma_1 - \sigma_3)_f = \frac{2\,C\,(\cos\phi) + 2\,\sigma_3(\sin\phi)}{1 - \sin\phi} \quad . \tag{3.11}$$

Substituting Eq. 3.6 into Eq. 3.11, and the result into Eq. 3.10 gives the expression:

$$(\sigma_1 - \sigma_3)_u = \frac{2\,C\,(\cos\phi) + 2\left(\dfrac{3\,\sigma_m - \sigma_1}{2}\right)\sin\phi}{(1 - \sin\phi)\,R_f} \quad . \tag{3.12}$$

Finally, the major principal stress, σ_1, can be expressed in terms of the vertical strain (which by definition of the one-dimensional compression test is the volumetric strain), by substituting Eqs. 3.12 and 3.9 into Eq. 3.7:

$$\sigma_1 = \frac{0.667\,\epsilon_v}{\dfrac{1}{K\;P_a\left(\dfrac{3\,\sigma_m - \sigma_1}{2P_a}\right)^n} + \dfrac{\epsilon_v}{\left(\dfrac{2\,C\,(\cos\phi) + 3\,\sigma_m \sin\phi - \sigma_1 \sin\phi}{(1 - \sin\phi)\,R_f}\right)}} + \sigma_m \quad . \tag{3.13}$$

This is the expression for the one-dimensional stress-strain curve and can be used to compute the constrained modulus, M_s.

The above solution is based on the assumption of a linear failure envelope (constant soil friction angle at all stress levels). To incorporate the effect of a curved failure envelope, the expression for ϕ may be corrected by introducing a stress sensitive model parameter, $\Delta\phi$, where:

$$\phi = \phi_o - \Delta\phi\ \log_{10}\,(\sigma_3/P_a) \ . \tag{3.14}$$

Substituting Eq. 3.6 into Eq. 3.14 gives:

$$\phi = \phi_o - \Delta\phi\ \log_{10}\left(\frac{3\ \sigma_m - \sigma_1}{2\ P_a}\right) \ . \tag{3.15}$$

Substituting Eq. 3.15 into Eq. 3.13 produces a complete equation that can be solved for the stress-strain curve under confined conditions. The complete expression is complex but is solved by publicly available mathematics software packages such as MathCad.

From the stress-strain curve the secant constrained modulus can be computed at various stress levels. The secant modulus is considered most appropriate for simplified design of buried pipe as it represents average soil behavior over the stress range of interest. Four sets of soil parameters were compared:

- Hyperbolic soil properties proposed by Selig (1988) were used to develop the SIDD design method for reinforced concrete pipe. They are referred to as the Selig/SIDD properties.
- Another set of hyperbolic soil properties proposed by Selig (1990) were developed based on research focused on flexible pipe. These properties have been incorporated into the finite element program CANDE and are the default values if the Selig soil model is selected within CANDE. These properties are referred to as the Selig/CANDE properties.
- E' values proposed by Duncan and Hartley (1987) were developed based on finite element analyses using hyperbolic soil properties previously proposed by Duncan et al. (1980). They are referred to as the Duncan properties.
- E' values proposed by Howard (1977) were developed based on back calculation, using the Iowa deflection formula, from measured deflections on a large number of projects. They are called the Howard properties.

The two sets of Selig soil properties include three general classifications of soil. Each general classification is given the name of the soil group which was actually tested, i.e., SW, ML, and CL. The two digit designation following the soil classification is the density as a percent of maximum standard Proctor density. A similar system is used to identify the Duncan Soil properties. Values of M_s and E', using the above four sets of data, are compared for different compaction levels in fig. 3.13, which indicates the following:

- The Selig/CANDE properties produce values of M_s that are consistently about twice the values produced by the Selig/SIDD properties.
- At stress levels less than about 70 kPa (10 psi) the Selig/SIDD properties are consistently similar to the values back calculated by Howard based on actual installations.

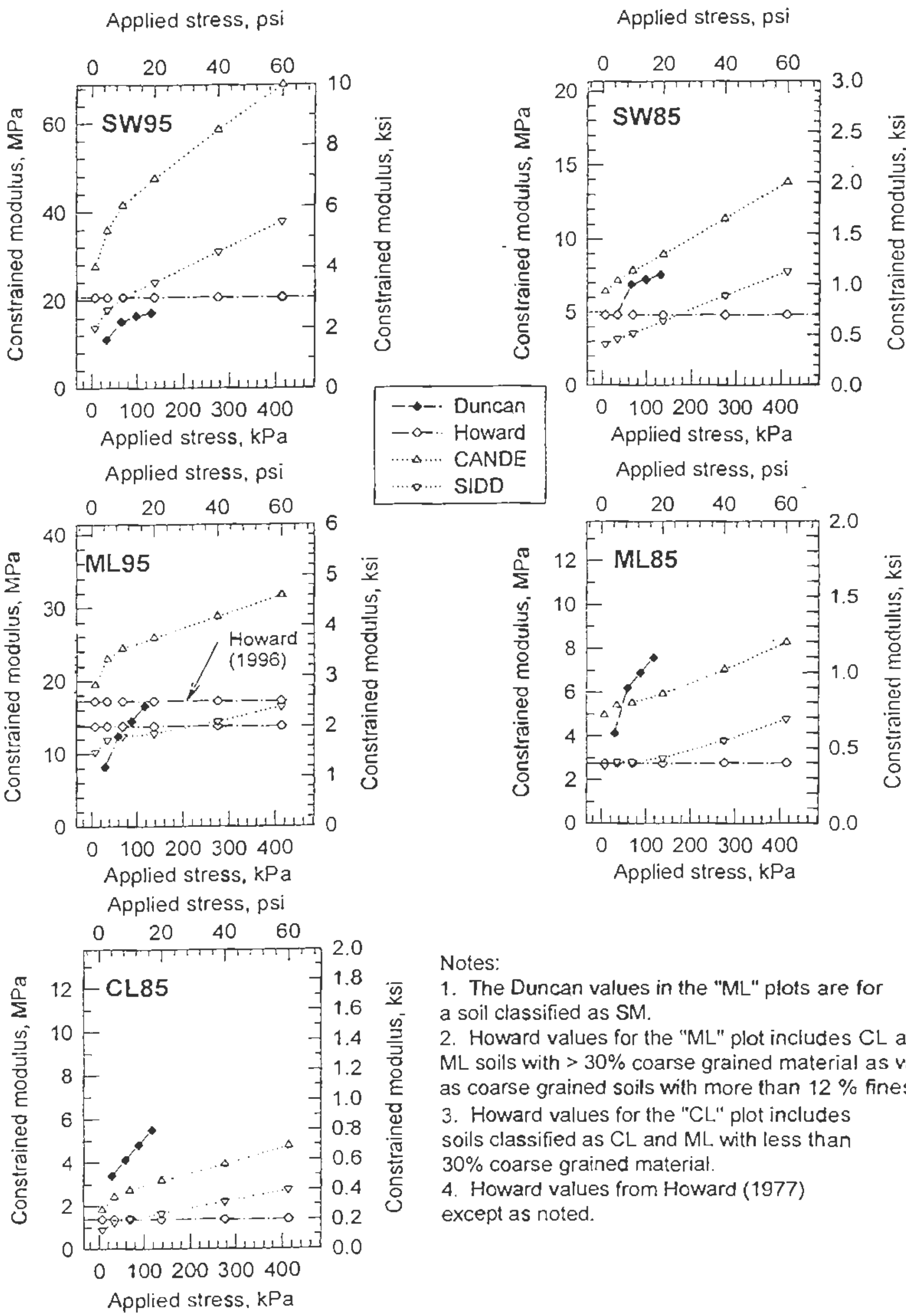

Notes:
1. The Duncan values in the "ML" plots are for a soil classified as SM.
2. Howard values for the "ML" plot includes CL and ML soils with > 30% coarse grained material as well as coarse grained soils with more than 12 % fines.
3. Howard values for the "CL" plot includes soils classified as CL and ML with less than 30% coarse grained material.
4. Howard values from Howard (1977) except as noted.

Figure 3.13 Comparison of Models for Secant Constrained Modulus

- The Duncan properties are somewhat erratic relative to all three of the other sets of properties.

The comparison in Fig. 3.13 suggests that for design purposes E' can be assumed equal to M_s and that the Selig/SIDD properties are roughly equivalent to the Howard values which represent a substantial amount of field data. This association further suggests that the same soil model could be used for simplified design of rigid and flexible pipe. This is a significant positive step in bringing together the currently diverse design methods used by different industries. Tabulated design values for M_s, computed from the Selig/SIDD properties at different stress levels are presented in table 3.6. These values can be used as a direct substitute for E' in design equations such as the Iowa formula.

The design values proposed in table 3.6 are compared with those determined by one-dimensional compression test and reported in table 3.5 and in fig. 3.14. This figure shows a poor match of properties from the two different sources. As noted previously, the problem is thought to be with the procedures used for the one dimensional testing, rather than the hyperbolic soil properties, which have had considerable successful use in design.

Table 3.6

Suggested Design Values for Constrained Soil Modulus, M_s

Stress level	Soil type and Compaction Condition		
	SW95	SW90	SW85
kPa (psi)	MPa (psi)	MPa (psi)	MPa (psi)
7 (1)	13.8 (2,000)	8.78 (1,275)	3.24 (470)
35 (5)	17.9 (2,600)	10.3 (1,500)	3.59 (520)
70 (10)	20.7 (3,000)	11.2 (1,625)	3.93 (570)
140 (20)	23.8 (3,450)	12.4 (1,800)	4.48 (650)
275 (40)	29.3 (4,250)	14.5 (2,100)	5.69 (825)
410 (60)	34.5 (5,000)	17.24 (2,500)	6.9 (1,000)

Table 3.6 (Cont.)
Suggested Design Values for Constrained Soil Modulus, M_s

Stress level	ML95	ML90	ML85
kPa(psi)	MPa (psi)	MPa (psi)	MPa (psi)
7 (1)	9.76 (1,415)	4.62 (670)	2.48 (360)
35 (5)	11.5 (1,670)	5.10 (740)	2.69 (390)
70 (10)	12.2 (1,770)	5.86 (750)	2.76 (400)
140 (20)	13.0 (1,880)	5.45 (790)	2.97 (430)
275 (40)	14.4 (2,090)	6.21 (900)	3.52 (510)
410 (60)	15.9 (2,300)	7.07 (1,025)	4.14 (600)
Stress level	**CL95**	**CL90**	**CL85**
kPa(psi)	**MPa (psi)**	**MPa (psi)**	**MPa (psi)**
7 (1)	3.68 (533)	1.76 (255)	0.90 (130)
35 (5)	4.31 (625)	2.21 (320)	1.21 (175)
70 (10)	4.76 (690)	2.45 (355)	1.38 (200)
140 (20)	5.10 (740)	2.72 (395)	1.59 (230)
275 (40)	5.62 (815)	3.07 (460)	1.97 (285)
410 (60)	6.17 (895)	3.62 (525)	2.38 (345)

3.5 CLSM Mix Design Study

A small scale study of CLSM mix designs was undertaken to investigate key elements of CLSM behavior and provide guidance in the selection of a mix design for the field studies reported in chapter 4. The study involved nine trial batches with different quantities of sand, fly ash, cement, and water. Testing was done for flowability and compressive strength. Materials were obtained from a nearby concrete batch plant.

The sand was fine aggregate for concrete batching per ASTM C 33. The component quantities for the nine trial mixtures are shown in table 3.7a. The quantities listed are for batch sizes of approximately 1 m^3; however, the actual batch sizes were much smaller.

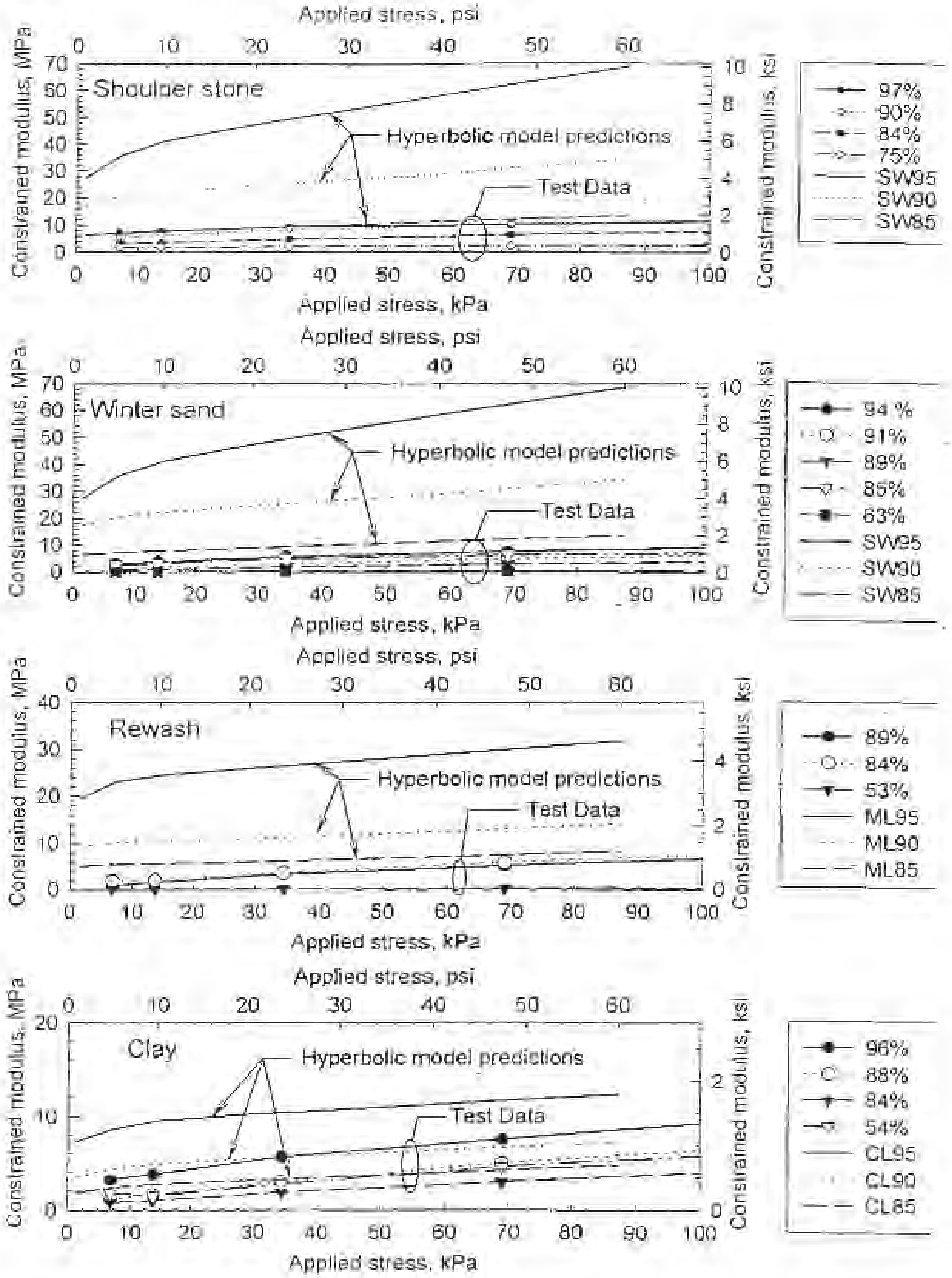

Figure 3.14 Comparison of Test Data for One-Dimensional Modulus with SIDD Soil Properties

Table 3.7

Mix Component Quantities and Strength Results

a) Mix Constituents (kg)

Material	Mix designation								
	Nom	A	B	C	D	E	F	X	Y
Cement	44	30	59	44	44	44	44	36	44
Fly Ash	296	148	296	222	296	296	296	148	148
Sand	1570	1570	1570	1570	1720	1570	1570	1570	1570
Water	296	296	296	296	296	237	355	296	296
w/c (1)	6.7	9.9	5.0	6.7	6.7	5.4	8.1	8.2	6.7
w/(c+fa) (1)	0.87	1.7	0.83	1.1	0.87	0.70	1.0	1.6	1.5

b) Test Results

7 Day compr. strength, kPa (psi)	1055 (153)	NT (2)	1410 (205)	515 (75)	825 (120)	1435 (209)	515 (75)	205 (30)	NT (2)
28 Day compr. strength, kPa (psi)	1890 (275)	350 (51)	2710 (393)	1645 (239)	1295 (188)	2900 (421)	1115 (162)	540 (79)	295 (43)
Segre-gation	None	Yes	Very little	Little	Little	Very little	Little	Yes	Yes
Spread, mm	380	No spread	250	280	220	No spread	315	–	No spread

Notes:
1. c = cement, w = water, fa = fly ash
2. Specimens A and Y were very fragile at an age of 7 days and broke up during the removal of the plastic molds and/or capping. NT – not tested.
3. ASTM Provisional Standard PS 28-95, Test Method for Flow Consistency of Controlled Low Strength Material
4. 6.89 kPa = 1 psi, 0.45 kg = 1 lbs, 25.4 mm = 1 in.

Specimen Preparation and Testing – Specimens were prepared in accordance with *ASTM Standard Test Method for Preparation and Testing of Soil-Cement Slurry Test Cylinders* (D 4832 - 88). The CLSM was mixed in a bowl with an egg beater type paddle for 2-3 minutes. Water was added to the mixer first, followed by sand, then cement, and finally fly ash. The addition of fly ash to the mix resulted in an enormous increase in flowability.

Flowability tests were conducted on all trial batches by placing a freshly mixed sample of CLSM in a 75 mm (3 in.) diameter by 150 mm (6 in.) high open ended tube, quickly lifting the tube vertically, and allowing the CLSM sample to flow into a circular mound. The circular sample spread was then measured. A minimum acceptable spread of 200 mm (8 in.) and no segregation of water were adopted acceptance criteria based on guide specifications of the Texas Aggregates and Concrete Association (TACA, 1989). These criteria have been adopted by other agencies as well.

The cylinders for compression testing were prepared and tested as follows:

1. The fresh mix was placed in three or four cylindrical plastic molds 100 mm diameter and 200 mm high (4 in. by 8 in.);
2. Specimens were allowed to set for 10 to 15 minutes, after which additional CLSM was added to displace bleed water and a lid was placed loosely on the filled mold;
3. Specimens were allowed to cure overnight in the laboratory and were then moved to a moist room;
4. Seven days after batching, two specimens of each mix were removed from the moist room, the plastic molds were stripped, and the test cylinders allowed to air dry for about 4 hours; and
5. The specimens were then capped with sulfur on both ends and tested in compression up to the ultimate strength.

Strength tests were conducted in the same fashion on the remaining test cylinders at an age of 28 days. In addition to monitoring load the cylinder strain was monitored with an LVDT for determination of modulus of elasticity.

Results – Compression and flowability test results are summarized in table 3.7b, along with observations of segregation. Findings include:

- Water to cement plus fly ash ratios greater than or equal to 1.5 produced the lowest compressive strengths. For example at an age of 7 days the strength of Specimen X was 205 kPa (30 psi) and Specimens Y and A broke up while being removed from the plastic molds. An inability to conduct compression tests does not mean that the mix is not suitable, only that the compression testing may not be an appropriate method of quality control.

- A 33 percent increase in cement content resulted in a 34 percent increase in the 7 day compressive strength and a 43 percent increase in the 28 day compressive strength (Specimens Nominal and B).

- A 25 percent decrease in the amount of the Class F fly ash resulted in about a 50 percent decrease in compressive strength (Specimens Nominal and C).

- A 10 percent increase in the amount of fine aggregate in the mix resulted in a 22 percent decrease in compressive strength (Specimens Nominal and D).

- A 20 percent reduction in the amount of water resulted in a 36 percent increase in compressive strength (w/c ratio of 0.87 for Specimen Nominal and 0.70 for Specimen E). Conversely, a 20 percent increase in the amount of water in the mix (w/c ratio of 0.87 for Specimen Nominal and 1.0 for Specimen F) resulted in about a 50 percent decrease in compressive strength when keeping the amount of cement and fly ash the same.

- Water segregated from the mixes with low amounts of fly ash as indicated by Specimens X, Y, and A. Specimen F which had more water than the others showed little water segregating from the mix. The remaining specimens, all of which had w/(c+fa) ratios of less than about 1.0, showed little or no segregation.

- Conversely, specimens with high amounts of fly ash (222 kg (488 lb) or greater) in the mix met minimum spread requirements of 200 mm (8 in.) except for Specimen E which fell over and which had the least amount of water. Specimens Y, X, and A having 148 kg (326 lb) of fly ash did not meet the 200 mm (8 in.) requirement.

The importance of fly ash in improving flowability, controlling water segregating from the mix, and increasing the compressive strength, is clearly indicated by these test results. Also, even though class F fly ash has no cementitious properties, an increase in compressive strength for increasing amounts of fly ash due to the pozzolanic reaction is clearly evident. The w/(c+fa) ratio (including the amount of fly ash) is a good indicator of expected material strength. Based on the results of this study, the mix design selected for the CLSM field test had 46 kg/m^3 (78 lb/ft^3) of cement and a water to cement plus fly ash ratio of 0.93. Additional details of the CLSM field test are provided in chapter 4.

CHAPTER 4
INSTALLATION TESTS

Pipe installation practices were evaluated through field and laboratory tests. The tests were designed to investigate the effects of different backfill materials and methods on pipe performance.

4.1 Laboratory Soil Box Tests

Twenty-five tests were conducted in a specially designed indoor test facility, called the "soil box," which allowed backfilling and compaction of materials around test pipes in a manner simulating certain aspects of field conditions. The soil box was designed for testing pipes with an outside diameter equal to or less than approximately 910 mm (36 in.) and trench widths varying from 1.5 to 2.5 pipe diameters. Tests were conducted with 760 mm (30 in.) inside diameter pipes. Test variables included trench wall stiffness, backfill material, method of compaction, haunching techniques, and bedding condition. The pipe, soil, and trench walls were monitored with a wide variety of instruments. The laboratory tests were conducted in part to evaluate the performance of pipe instrumentation being developed for the field test program described in section 4.2. The laboratory test procedures and data are presented in more detail in Zoladz (1995) and Zoladz et al. (1995).

4.1.1 Test Pipe

Three different types of pipes were included in the test program: (1) reinforced concrete (concrete); (2) corrugated, smooth interior wall, high density polyethylene (plastic); and (3) corrugated steel (metal). All test pipes were 760 mm (30 in.) in nominal inside diameter and 0.9 m (3 ft) in length.

The three types of pipes tested in this program span a wide range of pipe hoop stiffness and bending stiffness values and exhibit a wide range of pipe performance. The plastic and metal pipes are considered flexible in bending, whereas the concrete pipe is stiff in bending; however, the concrete and metal pipes are considered to have high hoop stiffness whereas the plastic pipe has a low hoop stiffness. Based on the bending stiffness values, plastic and metal pipes are typically considered flexible and the concrete pipe is considered rigid.

The reinforced concrete pipe was supplied by CSR/New England. Properties of the pipe are summarized in table 4.1. The concrete compressive strength and the concrete modulus of elasticity are estimated values, not test results.

Table 4.1
Section Properties of a Concrete Pipe for Laboratory Tests

Inside diameter, D_i, mm (in.)	760 (30)
Wall and thickness, mm, (in.)	Wall B, 89 (3.5)
Compressive strength, f_c', MPa (psi)	28 (4,000)
Modulus of elasticity, E_c, MPa (psi)	25,000 (3.7×10^6)
Cross-sectional area, A, mm^2/mm ($in.^2/in.$)	89 (3.5)
Wall moment of inertia, I, mm^4/mm ($in.^4/in.$)	58,700 (3.6)
Weight per unit length, W_p, kN/m (lb/ft)	5.6 (380)

The 900 mm (36 in.) diameter plastic pipe was supplied by Hancor, Inc. The pipe wall profile is shown in fig. 4.1a. Section properties were calculated based on measurements and the idealized geometry shown in fig. 4.1b, and are summarized in table 4.2. Two sets of section properties are provided; one assumes that the unbonded portion of the liner (element 1) is effective in carrying stress, and the second assumes that the unbonded portion is not effective. It is likely that the actual effectiveness of the liner is at an intermediate level that will vary with the relative liner thickness. McGrath, et al. (1994) have shown that for some corrugations the structural performance of the pipe is better represented by section properties computed assuming the liner is not effective. The modulus of elasticity is time dependent and can be estimated based on McGrath, et al. (1994). The value for the modulus of elasticity presented in table 4.2 is the AASHTO specified short term modulus.

The galvanized corrugated steel pipe was supplied by CONTECH Construction Products, Inc. Table 4.3 summarizes the pipe wall properties based on AASHTO (1996).

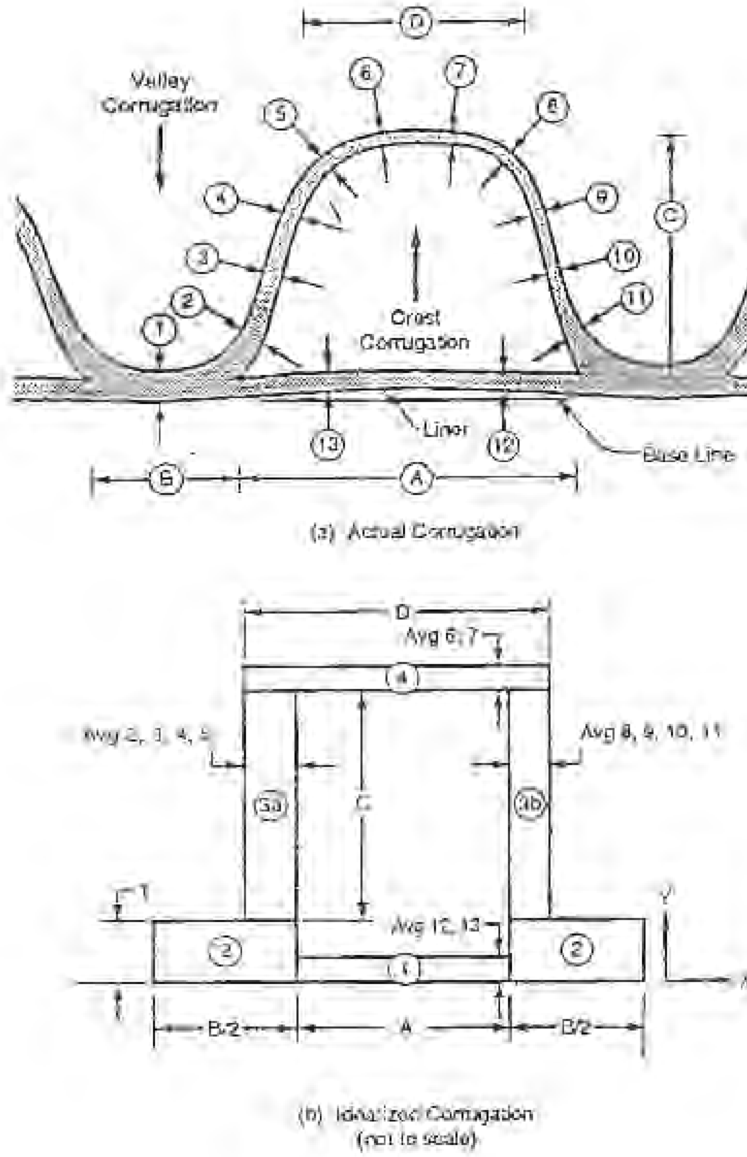

Figure 4.1 Plastic Pipe Corrugation Profile

Table 4.2
Section Properties of a Plastic Pipe for Laboratory Tests

Property	Liner effective	Liner ineffective
Inside diameter, D_i, mm (in.)	760 (30)	
Distance from inside surface to centroid, Y , mm (in.)	28 (1.1)	32 (1.3)
Short term modulus of elasticity, E, MPa (psi)	780 (1.1×10^5)	
Wall height, H, mm (in.)	76 (3.0)	
Width of corrugation L_c, mm (in.)	100 (3.9)	
Cross-sectional area A, mm^2/mm ($in.^2/in.$)	9.4 (0.4)	8.1 (0.3)
Wall moment of inertia I, mm^4/mm ($in.^4/in.$)	6,100 (0.37)	5,100 (0.31)
Section modulus to inner surface, S_i, mm^3/mm ($in.^3/in.$)	220 (0.34)	160 (0.24)
Section modulus to outer surface, S_o, mm^3/mm ($in.^3/in.$)	130 (0.20)	120 (0.18)
Weight per unit length, W_p, kN/m (lb/ft)	0.27 (18.4)	

Table 4.3
Section Properties of a Metal Pipe for Laboratory Tests (AASHTO 1996)

Inside diameter, D_i, mm (in.)	760 (30)
Corrugation size (in. x in., gage)	2-2/3 x 1/2, 16 gage
Modulus of elasticity, E, MPa (psi)	205,000 (3.0×10^7)
Specified thickness, mm (in.)	1.63 (0.064)
Cross-sectional area, A, mm^2/mm ($in.^2/ft.$)	1.64 (0.064)
Wall moment of inertia, I, mm^4/mm ($in.^4/in.$)	31 (0.0019)
Weight per unit length, W_p, kN/m (lb/in.)	0.35 (24.3)

The section properties of the test pipe and the bending stiffness and hoop stiffness are compared in table 4.4

Table 4.4
Summary of Properties of Laboratory Test Pipe

a. SI units

Pipe Type	E (MPa)	Wall height (mm)	A (mm^2/mm)	I (mm^4/mm)	PS_H (kN/m/m)	PS_B (kN/m/m)
Concrete	25,000	89	89	58,700	$5.2x10^6$	$1.3x10^5$
Plastic (w/ liner)	780	76	9.4	6,100	$1.8x10^4$	$4.3x10^2$
Metal	205,000	12.7	1.64	31.0	$8.7x10^5$	$7.3x10^2$

b. English units

Pipe Type	E (psi)	Wall height (in.)	A ($in.^2/in.$)	I ($in.^3/in.$)	PS_H (lb/in./in.)	PS_B (lb/in./in.)
Concrete	$3.7x10^6$	3.5	3.5	3.6	750,000	19,000
Plastic	$1.1x10^5$	3.0	0.4	0.37	2,600	62
Metal	$3.0x10^7$	0.5	0.06	0.0019	130,000	110

4.1.2 Soil Box

The soil box facility was designed to allow backfilling and compaction of the test pipe in a manner representative of actual practice. The box was designed for the pipe with an outside diameter of approximately 910 mm (36 in.) and trench widths varying from 1.5 to 2.5 pipe diameters. Fig. 4.2 is a schematic drawing of the primary elements of the soil box. For any given test, the trench walls were fixed, but the cross-trench walls could be raised, along with a platform surrounding the soil box, in 150 mm (6 in.) increments. This allowed compaction equipment to move from the platform at one end of the test pipe across the backfill to the platform on the other side of the test pipe, producing a reasonably realistic representation of a compactor moving along an actual pipe.

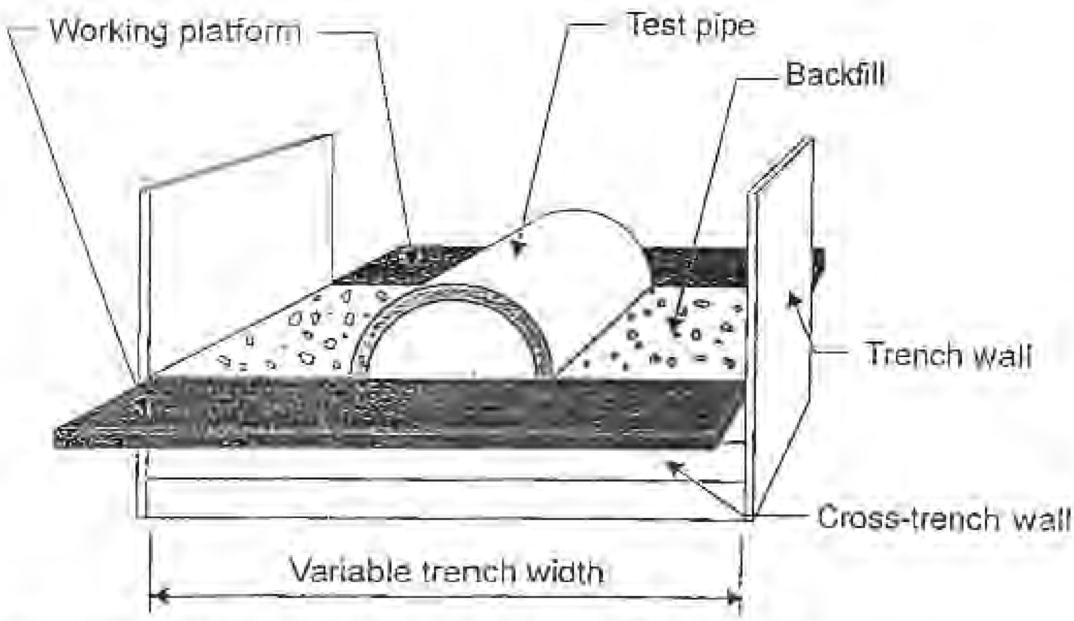

Figure 4.2 Primary Elements of the Soil Box

Trench Conditions - The soil box was designed to have two trench widths, a wide trench, nominally 2.3 m (7.5 ft) wide, and a narrow trench nominally, 1.5 m (5 ft) wide. In situ soils were modeled with three different trench wall stiffnesses by incorporating foam material into the trench walls. Bare plywood walls were used as a "hard" trench wall test. A very soft 100 mm (4 in.) thick foam rubber with a modulus of elasticity determined in unconfined compression of 10 kPa (1.5 psi) was used for the "soft" trench wall tests and a 19 mm (0.75 in.) thick foam rubber with a modulus of elasticity determined to be 340 kPa (49 psi) was used in tests with "intermediate" trench wall stiffness.

The narrow trench was constructed by placing two wooden inserts at each end of the trench. The inserts have a height of 1.6 m (5.3 ft), length of 0.9 m (3 ft), and width of 130 mm (15 in.) when the three 90 mm by 90 mm (U.S. 4x4 nominal lumber) posts are in place. When bolted to the wide trench walls, the inserts reduce the width of the trench by 760 mm (30 in.).

Dimensions for each trench condition are illustrated in fig. 4.3. Values are given as a function of the outside diameter of the pipe. The ranges are between concrete and metal pipe.

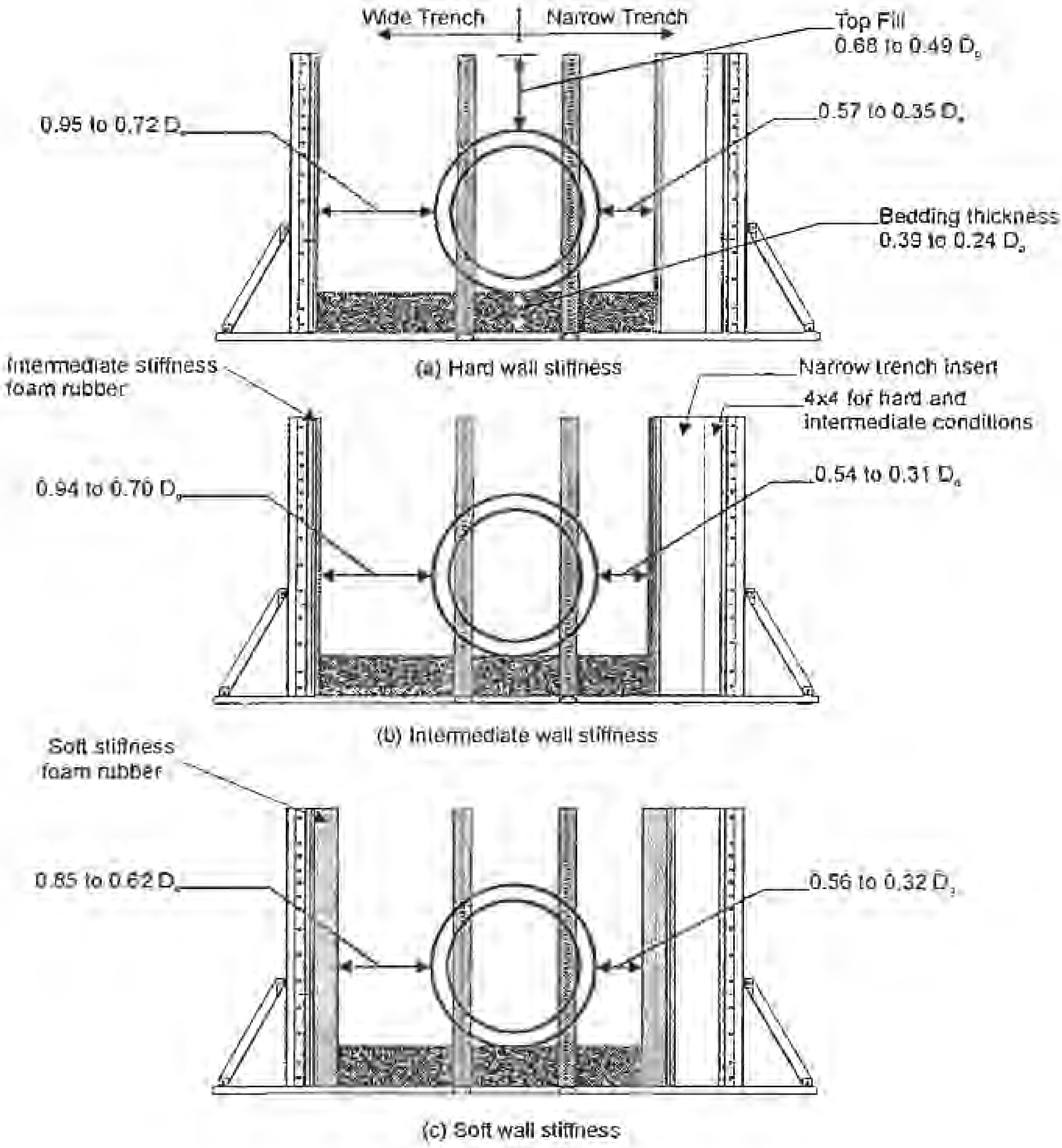

Figure 4.3 Trench Box Wall Conditions

which had the largest and smallest outside diameters, respectively, of the three pipe tested. The posts behind the narrow trench inserts are removed in the soft wall setup to compensate for the thickness of the foam.

4.1.3 Instrumentation

The behavior of the test pipe and the surrounding soil were monitored with several types of instrumentation during backfill placement. These instruments are described in more detail by Zoladz, (1995) and McGrath and Selig, (1996). Instruments included:

- A profilometer, using an LVDT, to measure pipe deflections and overall changes in pipe shape at 1-degree intervals around the pipe circumference.
- Visual extensometers mounted in the plastic pipe to measure changes in the pipe's diameter and verify the accuracy of the profilometer.
- Strain gages mounted in the plastic pipe.
- Pipe-soil interface pressure cells installed in the concrete (fluid filled earth pressure cells mounted in the pipe wall) and metal pipes (custom designed wall cutouts supported on instrumented support beams).
- Pressures cells mounted in the trench walls to measure horizontal soil stresses.
- Inductance coil strain gages mounted on the soft foam liner to measure soft wall displacements.
- A nuclear density gage to measure backfill moisture and soil density.
- A Proctor needle to measure soil strength in the haunch and bedding.
- Spring clamps mounted on the soil box were used to monitor gross pipe movements.

4.1.4 Backfill Materials and Compaction Equipment

Tests were conducted with pea gravel and rewash, characterized as Soil Nos. 4 and 6 in chapter 3. Hand tampers and shovel slicing were used to compact backfill in the pipe haunch zone.

Two types of hand-operated compaction equipment were used to compact the backfill: a rammer compactor (rammer) and a vibratory plate compactor (vibratory plate). The rammer is a Wacker model BS 60Y powered by a 1900 Watt (2.7 horsepower), two-cycle engine (Wacker Corporation). The 280 mm (11 in.) wide and 330 mm (13 in.) long ramming shoe is driven into contact with the soil at a percussion rate of about 10 blows per second. The operating mass of the rammer is 60 kg (132 lb). The manufacturer's literature indicates that the generated dynamic force per blow is 10.2 kN (2,300 lb).

The vibratory plate is a Wacker model VPG 160B (Wacker Corporation) powered by a 3000 Watt (4 horsepower), four-cycle engine driving counter-rotating eccentric weights producing about 5,700 vibrations per minute. The vibratory plate compactor has an operating mass of 78.5 kg (173 lb) and, per the manufacturer's literature delivers a centrifugal force of 10.5 kN (2,350 lb). The contact area of the plate is 535 mm by 610 mm, (21 in. by 24 in.).

Compactor calibration tests were conducted in the soil box with pea gravel and silty sand to determine the soil unit weight achieved by varying the number of coverages with each compactor (fig. 4.4). Based on these results, the pea gravel was compacted with one coverage of the rammer or three coverages of the vibratory plate, while the silty sand was compacted with three coverages of the rammer or five of the vibratory plate. The increased number of passes required for the vibratory plate is a function of the much lower contact pressures. Filz and Brandon (1993, 1994) tested almost identical compactors and found that the peak force applied by the rammer was about four times greater than that applied by the vibratory plate, even though the catalog values for dynamic force are equal. The vibratory plate applied one half of the catalog value while the rammer applied twice the catalog value.

For tests where compaction of the haunch zone was required, two types of haunching effort were used. With pea gravel backfill, a procedure called "shovel slicing" was used, where the blade of a standard dirt shovel was sliced into the haunch material repeatedly. For tests backfilled with rewash, both shovel slicing and "rod tamping" were used. Rod tamping consisted of striking the backfill in the haunch zone with a 150 mm by 300 mm (3 in. by 6 in.) steel plate attached to a 2.4 m (8 ft) long steel pipe.

4.1.5 Test Procedures

Test variables included pipe type, trench width, trench wall stiffness, backfill material, method of compaction, method of haunching, and bedding condition.

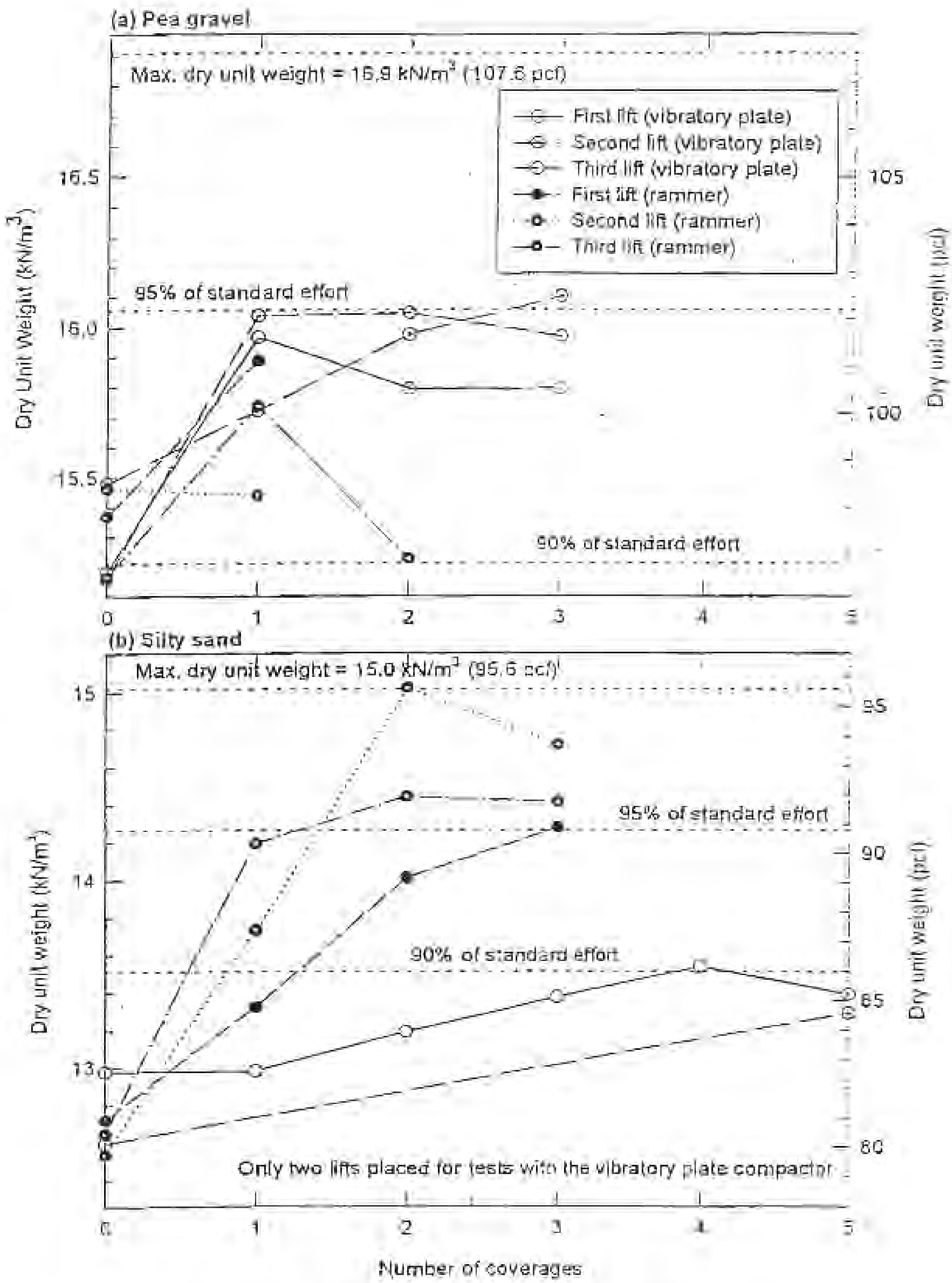

Figure 4.4 Compactor Calibration Test Results

The notation system, defined in table 4.5, was set up to identify test variables quickly. Figures and tables in this chapter use this system and identify variables in the order of test number, pipe type, trench condition, backfill, compactor, and haunching effort. Variables are removed from the label when indicated elsewhere in a figure. In addition to this notation, the backfill depth is often reported in terms of the normalized backfill depth, (NBD). This is the depth of the backfill relative to the top of the pipe divided by the outside diameter of the pipe. This simplifies interpreting the test results, as a normalized backfill depth of -1.0 is the bottom of the pipe, -0.5 is the springline, and 0.0 is the top of the pipe.

A total of 25 tests were conducted with the test variables listed in table 4.6. Because of the number of variables involved, it was impossible to test all combinations. The research team made selections of which combinations could provide the most information. Some tests were conducted primarily to evaluate the effects of compaction and haunch effort in the haunch zone. The backfill for these tests was brought only to a level at or near the springline. Other tests were backfilled to about 150 mm, (12 in.) over the top of the pipe.

Table 4.5
Notation System for Laboratory Test Variables

Test variable	Symbol	Definition
Test No.	1-25	
Pipe type	CP	Concrete pipe
	MP	Metal pipe
	PP	Plastic pipe
Trench conditions	WH	Wide trench with hard walls
	WI	Wide trench with intermediate wall stiffness
	WS	Wide trench with soft wall stiffness
	NH	Narrow trench with hard walls
	NI	Narrow trench with intermediate wall stiffness
	NS	Narrow trench with soft wall stiffness
Backfill material	PG	Pea gravel
	SS	Silty sand
Method of compaction	RM	Rammer compactor
	VP	Vibratory plate compactor
	XC	No compaction
Haunching effort	RT	Rod tamping
	SH	Shovel slicing
	XH	No haunching

Table 4.6
Variables for Laboratory Tests

Test No.	Pipe	Trench condition	Backfill	Lift thickness mm, (in.)	Compactor	Haunch effort	Bedding	Final backfill depth (NBD)
1	CP	WH	PG	305 (12)	XC	XH, SH	C	-0.68
2	CP	WH	PG	150 (6)	VP, RM	XH	C	-0.51
3	PP	WH	PG	305 (12)	XC	XH, SH	C	-0.33
4	PP	WH	PG	150 (6)	VP	XH	C	-0.33
5	PP	WH	PG	150 (6)	RM	XH	C	-0.33
6	PP	NH	PG	150 (6)	RM	XH	C	-0.33
7	MP	WH	PG	150 (6)	VP	XH	C	0.65
8	MP	WH	PG	150 (6)	RM	XH	C	0.65
9	PP	WH	PG	305 (12)	RM	XH	C	0.50
10	CP	WS	PG	305 (12)	RM	XH	C	0.30
11	CP	WH	PG	305 (12)	RM	XH	U	0.30
12	PP	WS	PG	305 (12)	RM	XH	U	0.33
13	CP	NS	PG	305 (12)	RM	XH	U	0.30
14	PP	NS	PG	305 (12)	RM	XH	U	0.33
15	PP	NH	PG	305 (12)	RM	XH	C	0.33
16	CP	NH	PG	305 (12)	RM	XH	C	0.30
17	CP	WH	SS	305 (12)	XC	XH, SH	C	-0.35
18	CP	WH	SS	305 (12)	VP, RM	XH	C	-0.35
19	CP	WH	SS	305 (12)	VP, RM	SH	U	-0.35
20	MP	WH	SS	305 (12)	VP	XH	C	-0.32
21	MP	WI	SS	305 (12)	VP	RT	C	-0.32
22	MP	NH	SS	305 (12)	RM	SH	U	-0.32
23	CP	NH	SS	305 (12)	RM	SH	U	-0.35
24	CP	NI	SS	305 (12)	RM	RT	C	-0.35
25	MP	NI	SS	305 (12)	RM	RT	C	-0.32

Tests were typically conducted in the following steps. Deviations from these procedures for specific tests are noted later.

1. Assemble soil box to required trench conditions.

2. Place and compact required bedding. Concrete and plastic pipes required a 230 mm (9 in.) bedding thickness, the metal pipe required a 305 mm (12 in.) thickness. Take density measurements at sidefill and invert locations.

3. Place pipe in trench and center the pipe between the lateral posts. The concrete and metal pipes required "in-air" readings of the interface pressure cells prior to placement. Take initial readings of all other instruments after placement.

4. Place first lift 305 mm (12 in.) deep for the concrete and metal pipes and 230 mm (9 in.) deep for the metal pipe. If haunching is to be conducted, place half the layer and haunch, then place the rest of the backfill.

5. Level off the lift and take uncompacted backfill readings. Uncompacted backfill readings are taken for the horizontal soil stresses, pipe-soil interface pressures, and soft wall displacements only.

6. Compact backfill as required and take compacted backfill readings. Compacted backfill readings are taken for all the instruments.

7. Repeat sequence of placing backfill, taking uncompacted readings, compacting, and taking compacted backfill readings until the final desired backfill depth is reached.

8. Remove backfill to at least 250 mm (10 in.) below springline and inspect the haunch zone. For tests with pea gravel, this consisted of carefully excavating under the pipe by hand. For tests with rewash, the pipe was removed and the backfill stiffness was evaluated with the Proctor penetrometer.

Deviations from Typical Tests Procedures – Variations from the standard procedures included the following:

- *Tests 1, 2, 3, 17, 18, 19* – Tests were conducted with a different compactors and/or different haunching method on each side of the pipe. Five of these tests were conducted with concrete pipe as it was felt that the compaction effects on one side of the pipe would not have any effect on the other side. The other test was conducted with polyethylene pipe with no mechanical compaction but with different haunching technique on each side of the pipe.

- *Instrumentation* – Electrical problems resulted in tests 3, 4, and 5 being conducted without the profilometer. Profilometer measurements were not conducted for the concrete pipe after test 16, as the concrete pipe did not show any measurable deflections. Horizontal soil stress cells were not installed in the trench walls until after test 9.

4.1.6 Results

This section presents and compares results from the 25 laboratory tests. Section 4.1.6.1 presents examples of each type of measurement taken, presented as a function of backfill depth. Complete results of each test are presented separately in Zoladz, et al. (1995). Subsequent sections compare results from different tests to demonstrate significant findings from the tests.

4.1.6.1 Examples of Test Results

Backfill Unit Weight, Pipe Deflections, and Gross Pipe Movement – Figs. 4.5a to 4.5e show examples of the variations in several monitored parameters with increasing depth of backfill for test 9, conducted with pea gravel backfill and compaction with the rammer. Fig. 4.5 (a) indicates that the dry unit weight of the backfill was relatively uniform for each layer placed. Fig. 4.5 (b) shows the deflection versus depth of fill and indicates that while placing sidefill at elevations between the springline and the crown the pipe peaked (increased in vertical diameter and decreased in horizontal diameter), and deflected only slightly due to backfill over the top of the pipe. Figs. 4.5 (c) and 4.5 (d) show the lateral pipe movement at the springline relative to the soil box and indicates that the pipe springlines moved inward as backfill was placed from the springline to the crown. This is consistent with the deflections reported in Fig. 4.5 (b). Fig. 4.5 (e) indicates the change in elevation of the pipe invert as backfill is placed and indicates that the pipe is lifted up off the bedding as backfill is placed from the invert to about the springline level.

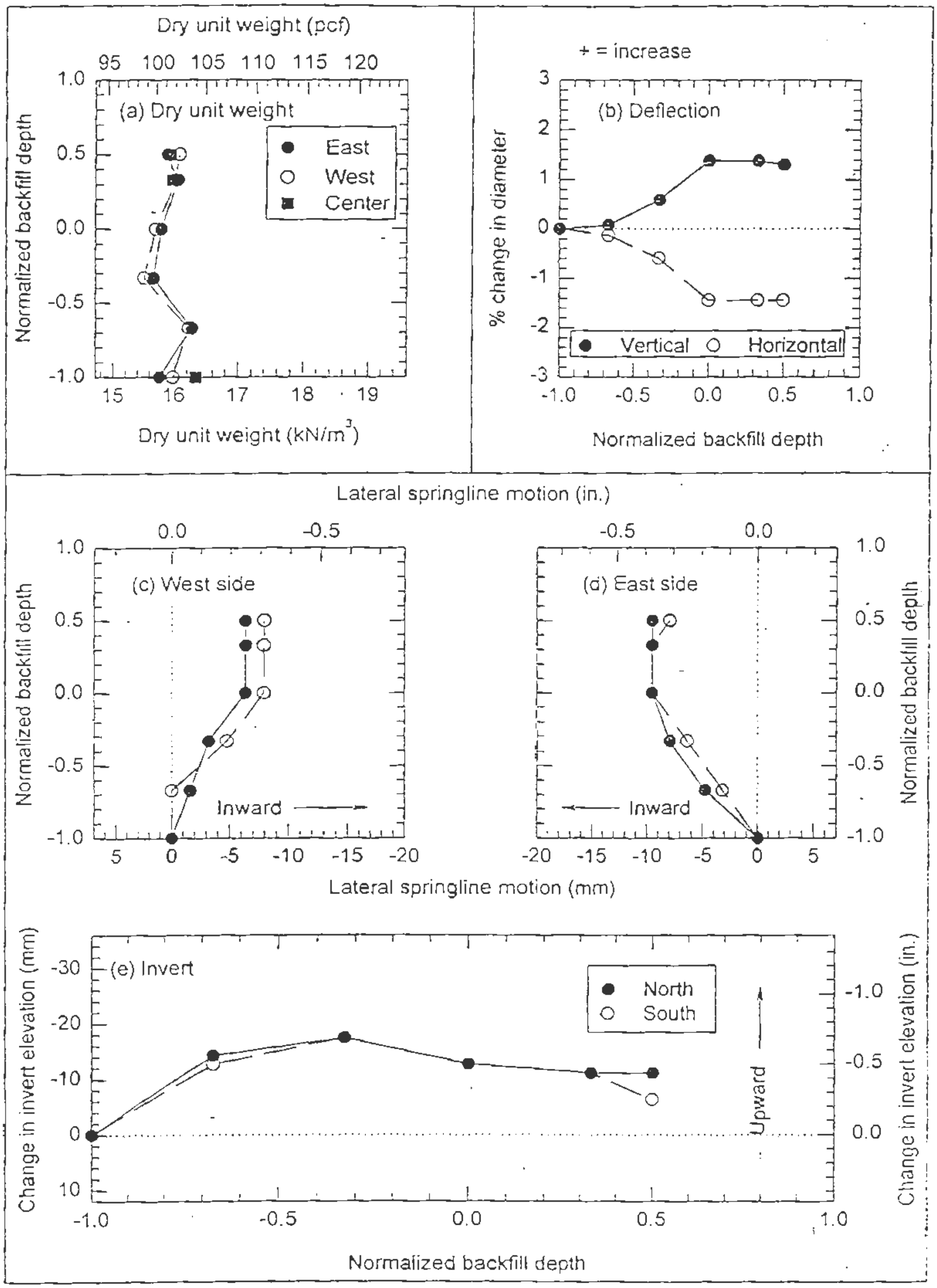

Figure 4.5 Soil Unit Weight, Pipe Deflections, and Pipe Movement (Lab Test 9)

Profilometer Data – Fig. 4.6 illustrates results of the profilometer measurements. The data from each profile measurement was smoothed by computing a running average of five degrees over the entire circumference of the pipe. The deformed shape is magnified ten times to improve readability. After magnification, the figures were aligned at the invert. Profilometer data were also used to determine changes in vertical and horizontal deflection.

Horizontal Soil Stresses at the Trench Wall – Fig. 4.7 presents average horizontal soil stresses at the trench wall, before and after compaction, from test 11 which was conducted using the concrete pipe placed in a wide trench with hard walls, pea gravel backfill, compaction with the rammer, and no haunching effort.

Pipe-Soil Interface Pressures – Fig. 4.8(a) presents the concrete pipe-soil interface pressures at the springline and 45 degrees below the springline (called the haunch in the figure) from test 11, both before and after compaction of each backfill lift. The figure suggests that even without haunching, when the rammer compactor is used with a free flowing material such as the pea gravel, significant radial pressures can develop at the haunch.

Further, Fig. 4.8(b) suggests that the rammer compactor is capable of lifting the concrete pipe sufficiently to lower the invert pressures, during compaction of the first lift. This is beneficial toward developing a uniform pressure distribution around the pipe.

Plastic Pipe Strains – Fig. 4.9 presents the plastic pipe strains measured during test 15, conducted with the plastic pipe placed in a narrow trench with hard walls, pea gravel backfill compacted with the rammer, and no haunching effort. Positive strains indicate tension. The strains are consistent with the other data, i.e., they indicate very little deformation during backfilling below the springline and then indicate that the pipe is being squeezed inward at the sides during compaction above the springline. The outside strains are higher than the inside strains which is consistent with the location of the neutral axis. Longitudinal strains are about 50 percent of the magnitude of the circumferential strains.

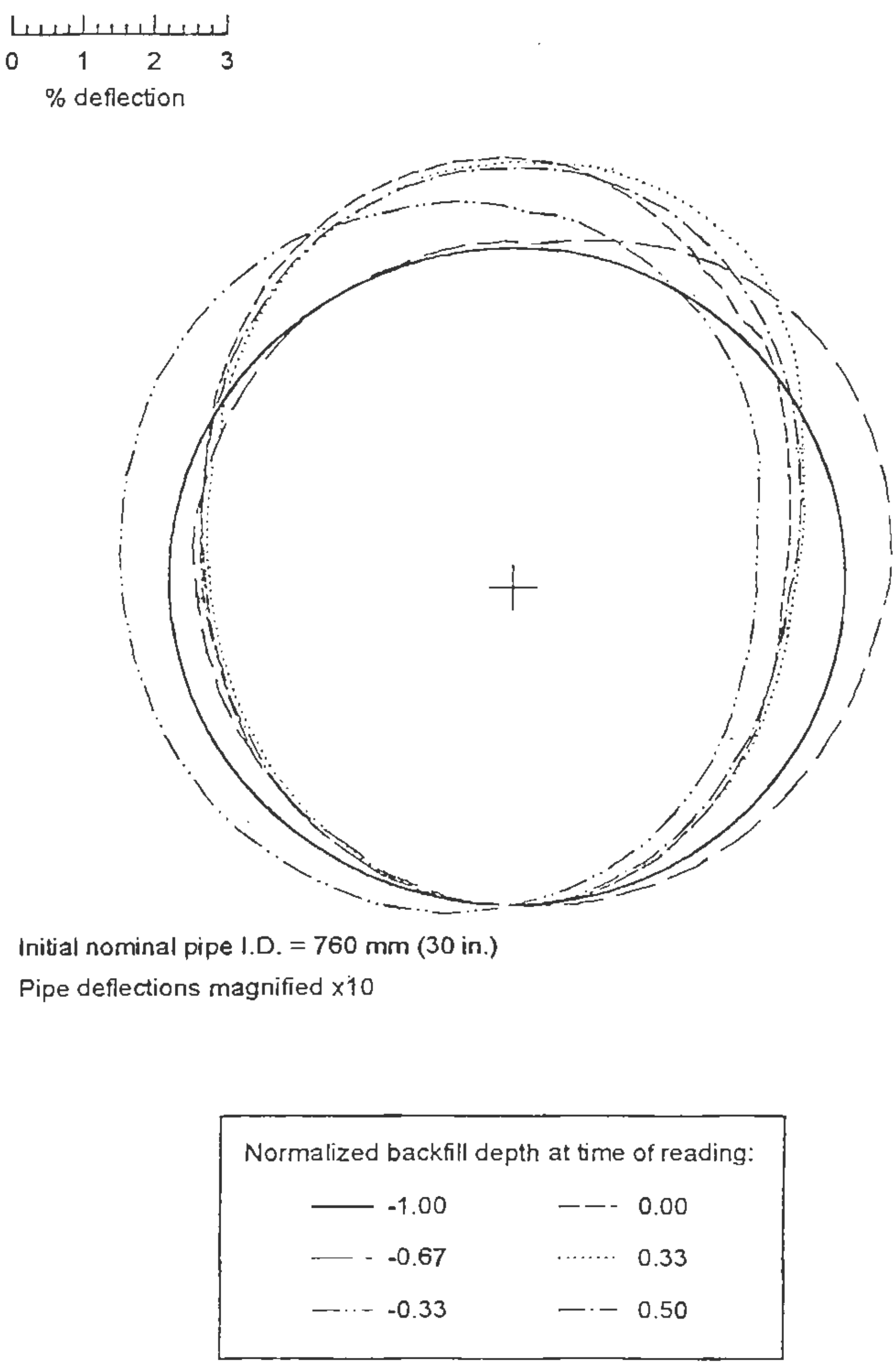

Figure 4.6 Magnified Plastic Pipe Profiles (Lab Test 9)

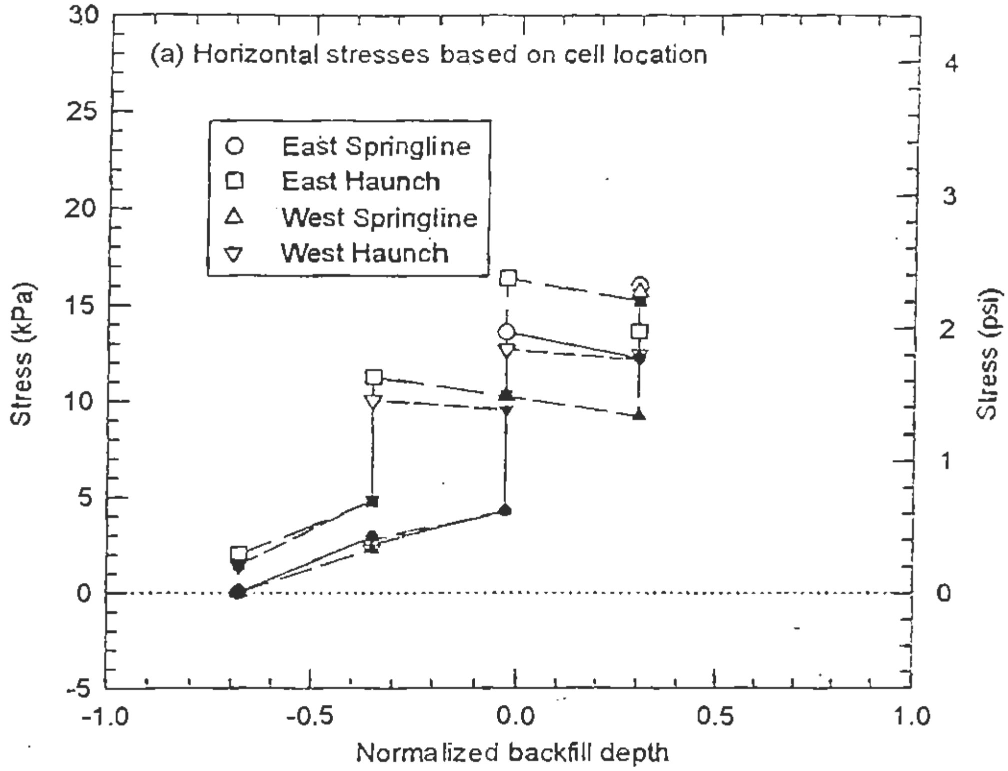

Note: Filled symbols represent readings taken prior to compaction of backfill

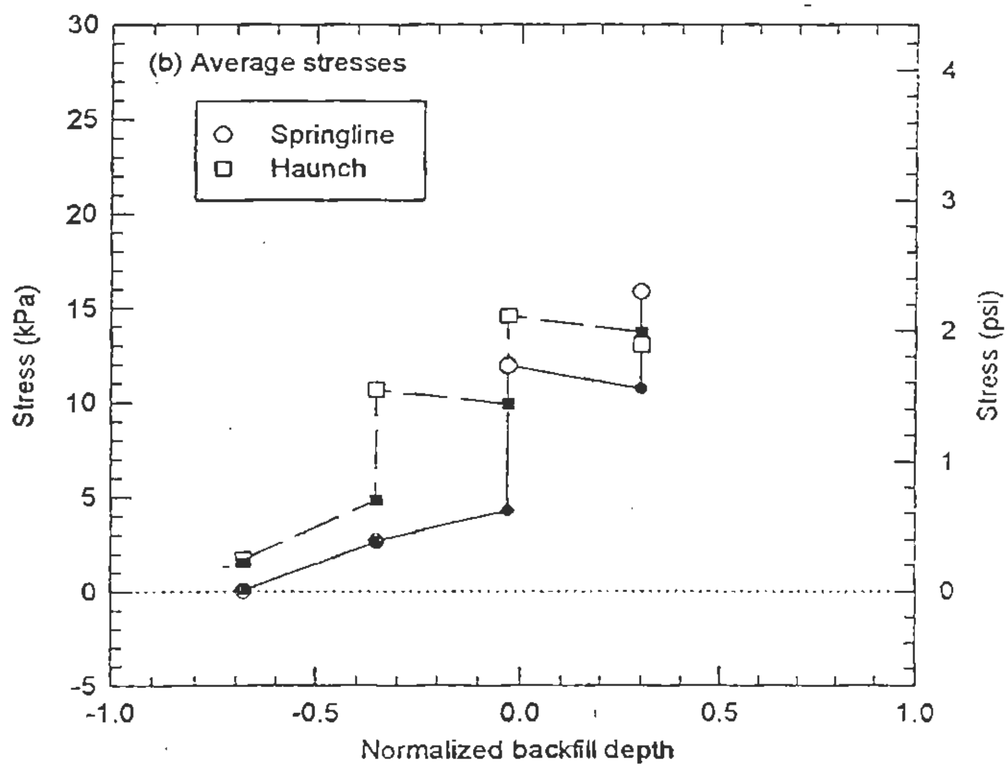

Figure 4.7 Horizontal Soil Stresses at the Trench Wall (Lab Test 11)

Note: Filled symbols represent readings taken prior to compaction of backfill

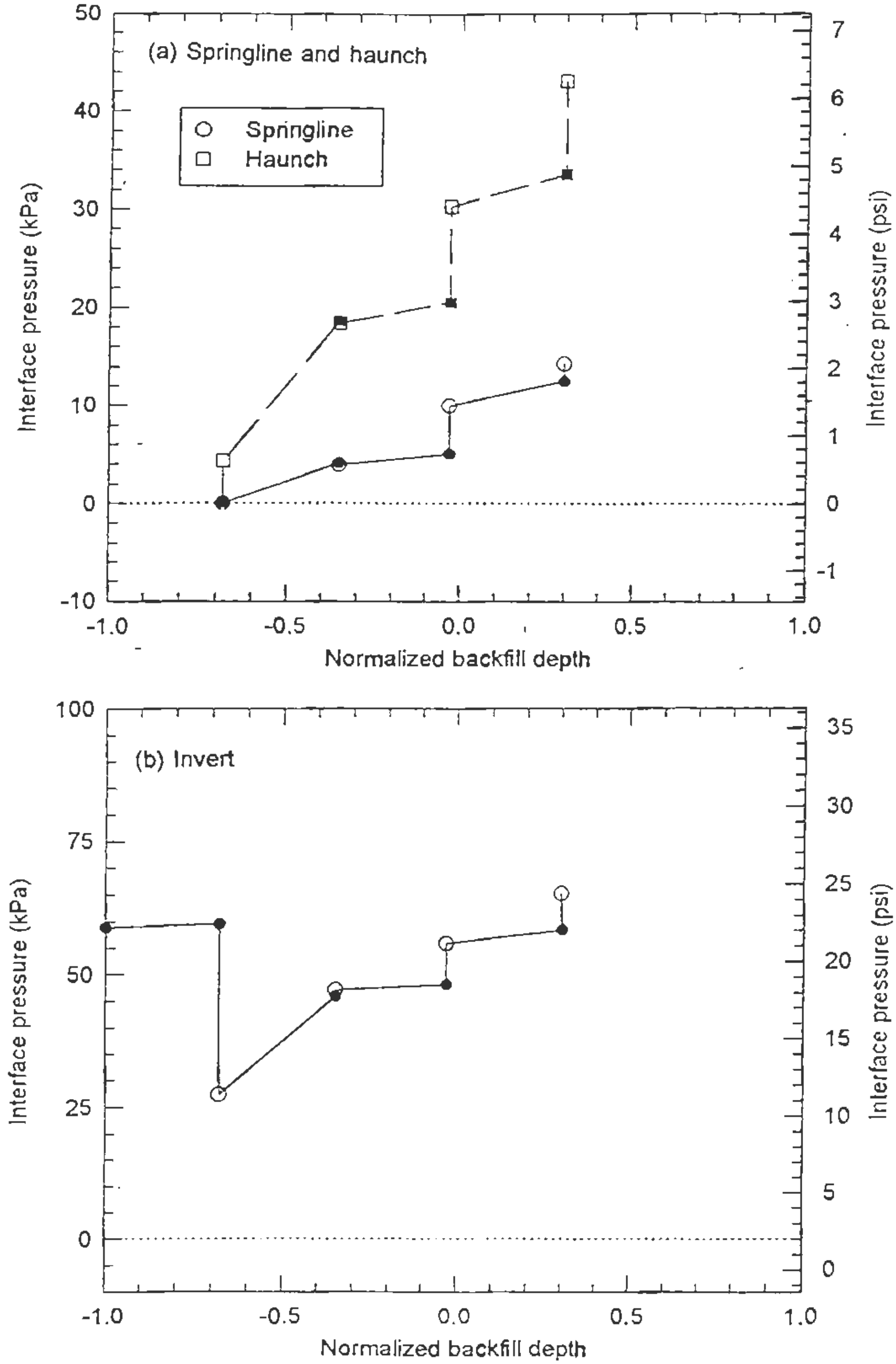

Figure 4.8 Concrete Pipe-Soil Interface Pressures (Lab Test 11)

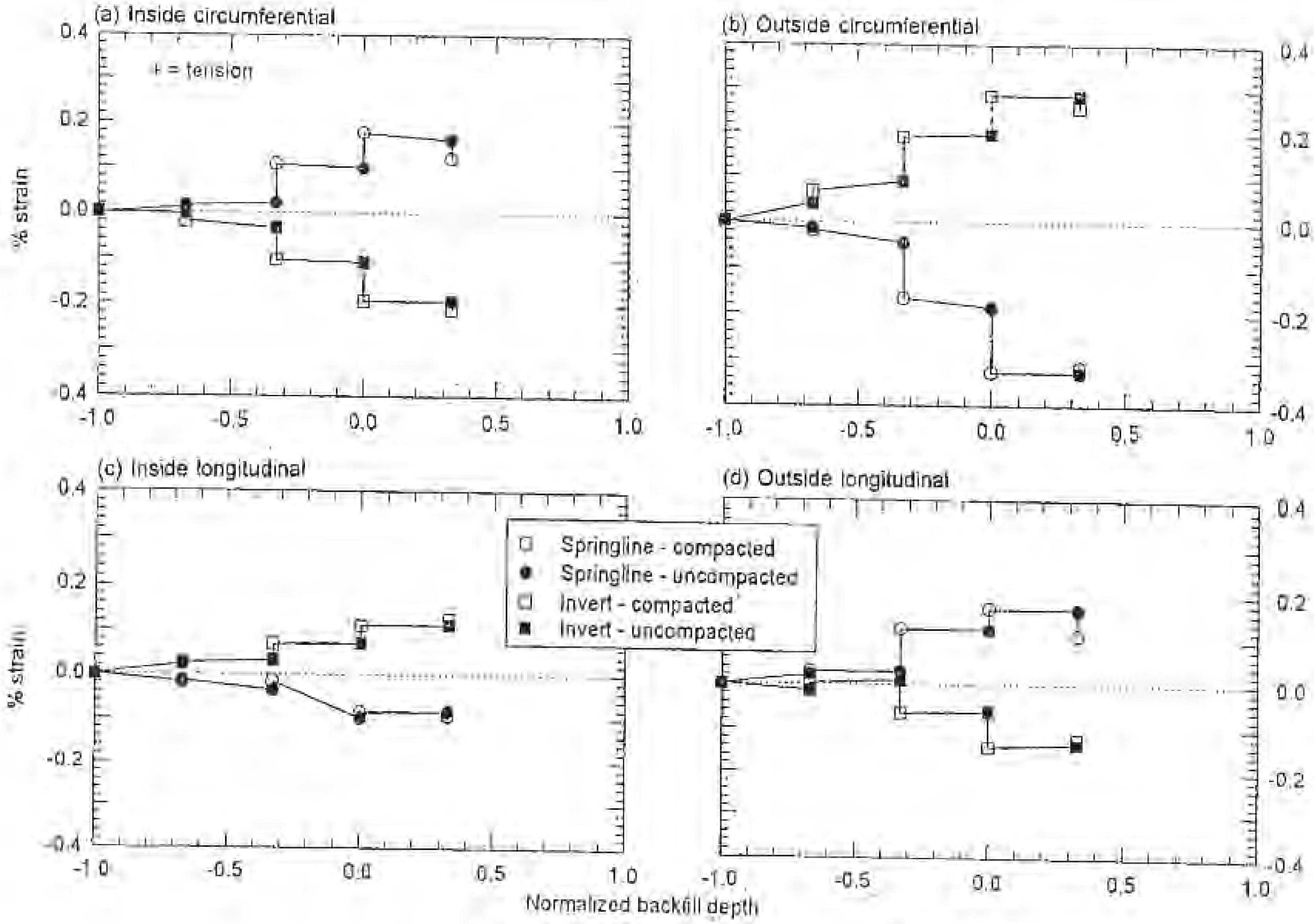

Figure 4.9 Plastic Pipe Strains (Test 15)

Proctor Penetration Resistance – Fig. 4.10 presents the results of penetrometer testing taken from test 21, performed with the metal pipe in a wide trench with intermediate stiffness walls, silty sand backfill, compacted with the vibratory plate, and the haunches compacted with the rod tamper. Data are presented for penetration depth of 25 mm (1 in.) and 50 mm (2 in.). The bedding soil was compacted for this test, and the invert showed the highest resistance. The penetration resistance at 30 and 60 degrees was similar, suggesting that the rod tamping used in the haunch zone was effective.

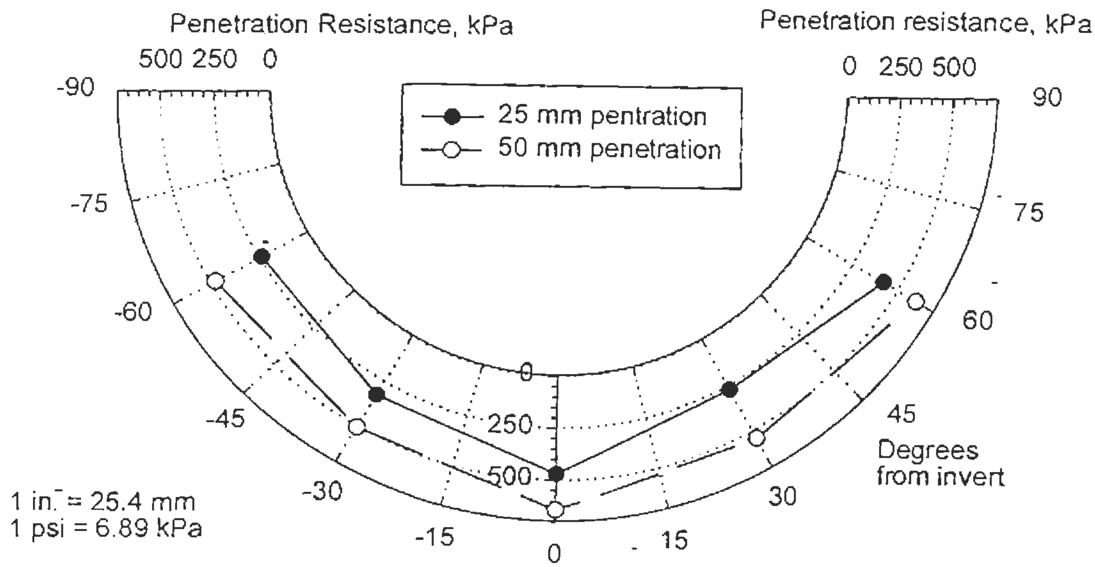

Figure 4.10 Penetration Resistance of Bedding After Lab Test 21 in Silty Sand Metal Pipe, Vibratory Plate, Compaction, and Rod Tamping

Trench Wall Displacements – Soft wall displacements for test 13 which was conducted with the concrete pipe placed in a narrow trench with soft walls, pea gravel backfill compacted with the rammer, and no haunching effort are presented in fig. 4.11. Most of the displacement in the wall occurred after the first layer was compacted near the inductance coils. As can be seen in fig. 4.11, as the first layer (NBD = -0.67) was compacted the walls at the haunch elevation compressed. As the second backfill layer (NBD = -0.33) was compacted, the walls at the springline elevation showed displacement and the walls in the haunch elevation continued to compress. This trend continued as the backfilling proceeded.

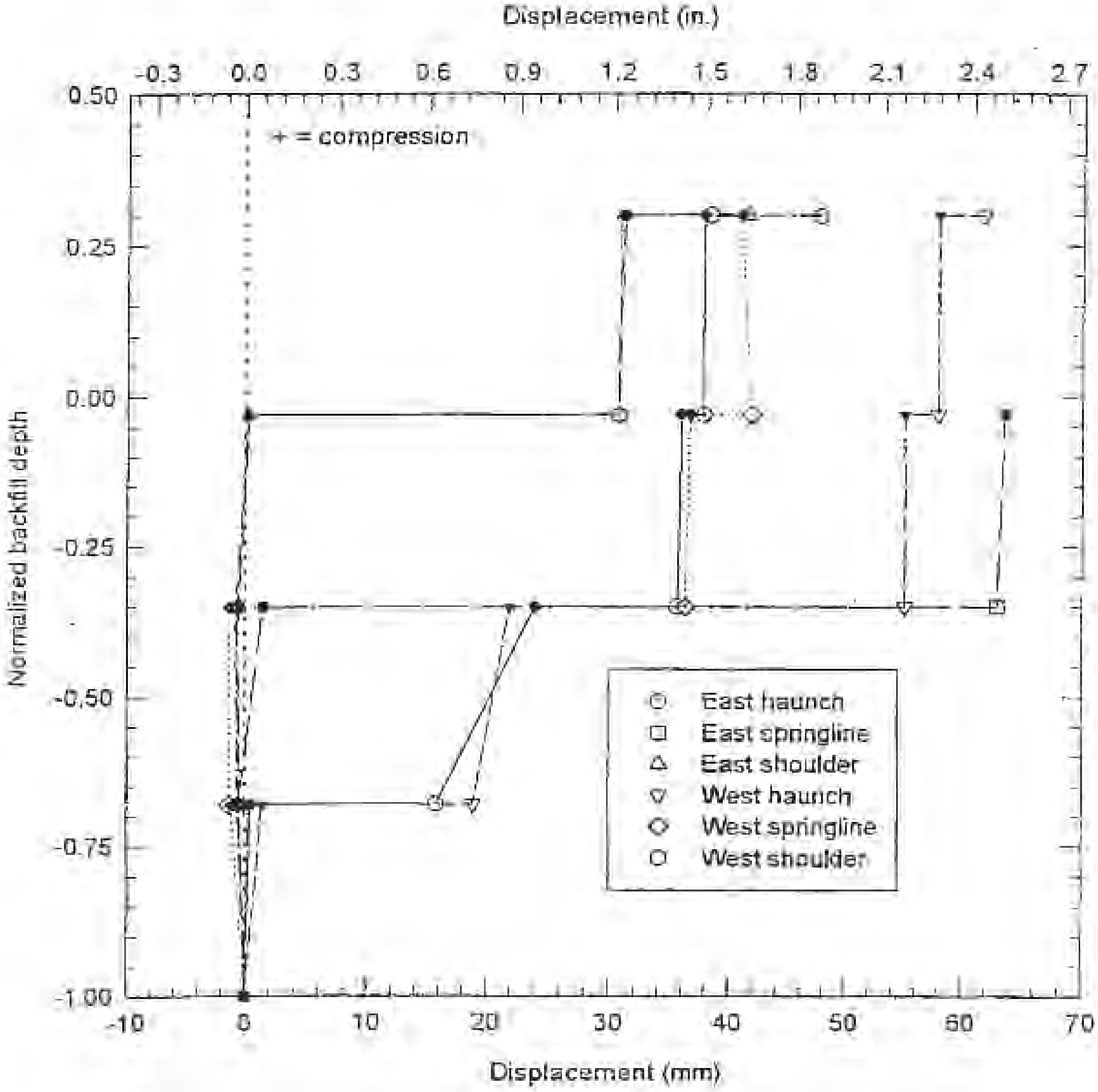

Note: Filled symbols represent readings taken prior to compaction

Figure 4.11 Soft Trench Wall Displacements (Lab Test 13)

4.1.6.2 Vertical Pipe Movement

The data on vertical pipe movement show that the plastic and metal pipe lifted up from 15 to 25 mm (0.6 to 1.0 in.) when compacted with the rammer and from 0 to 12 mm (0.0 to 0.5 in.) when compacted with the vibratory plate. As noted above, this difference further emphasizes the significant difference in the applied stresses under the two types of compaction equipment. Only a small percentage of the uplift was recovered as fill was placed above the springline. The uplift is greater in silty sand than in pea gravel. When no compaction was applied the pipe dropped during placement of the sidefill. Uplift was significantly reduced when the trench walls were soft.

The values reported here should not be taken as indicative of actual field uplift values because the test lengths of pipe were short. In the field, the uplift would be resisted by the weight of pipe adjacent to the section being compacted (see section 4.2 for actual field data). However, the tests do suggest that compaction of the sidefill below the springline has the beneficial effects of reducing the invert pressure under a pipe. The reduced uplift noted when trench walls are soft indicate that the compactive energy deforms the trench wall and is less effective in forcing backfill into the haunch zone.

Only limited data were collected for the concrete pipe, and no uplift was noted. The pipe had settled downward 1 to 2 mm (0.04 to 0.08 in.) when backfill was at the springline level and up to 5 mm when backfill was placed to 300 mm (12 in.) over the top of the pipe. When trench walls were soft, the settlements at the springline level and at the final level were about twice the settlements measured for similar conditions with hard trench walls.

4.1.6.3 Pipe Profiles and Deflections

The presentation of pipe profile and deflection data is limited to the tests with the plastic and metal pipes as the concrete pipe did not measurably deflect. The general trend of the deflections versus depth of fill is shown in fig. 4.12. The figure indicates the following:

- Most upward deflection occurs during compaction of backfill between the springline and crown level.

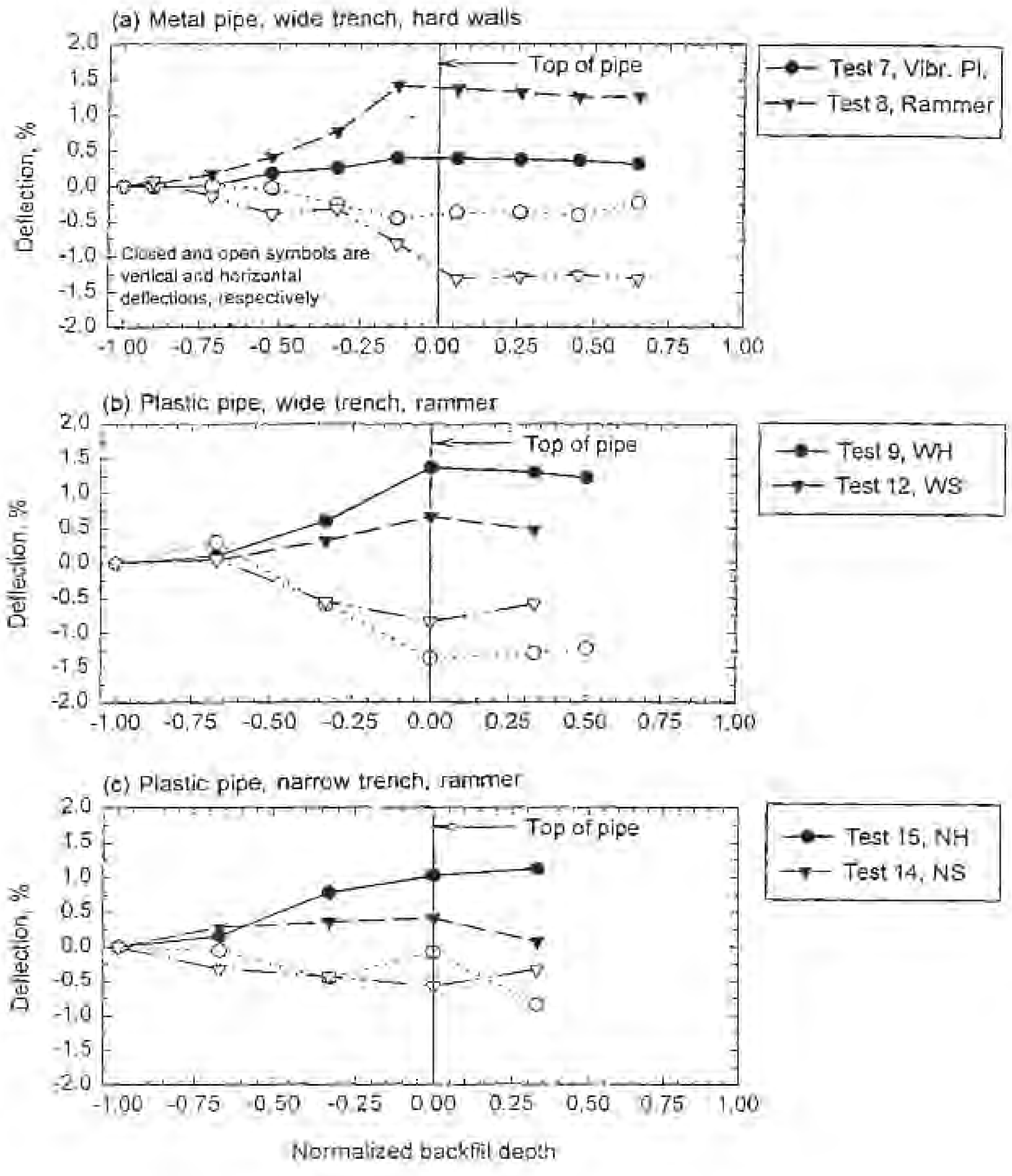

Figure 4.12 Pipe Deflections in Laboratory Tests

- The rammer creates much more upward deflection during compaction than the vibratory plate (fig. 4.12(a)); and

- Much more upward peaking occurs with the hard trench walls than with the soft trench walls, suggesting that some compaction energy is deforming the trench walls rather than densifying the soil.

Deflection data for a wider range of variables are presented in fig. 4.13 which shows the deflection magnitude when the backfill was at a level 150 mm (6 in.) above the springline. This figure also shows trends similar to those in fig. 4.12, and shows that pipe backfilled with silty sand deflects more during compaction than pipe backfilled with pea gravel.

Deflections when backfill is at the springline, the top of pipe, and at the end of the test, 300 mm (12 in.) or more over the top of the pipe for tests with pea gravel backfill are presented in fig. 4.14. The figure again shows the significant difference in peaking between the rammer and the vibratory plate, less peaking for installations with soft trench walls and increased downward deflection for tests with soft trench walls, even with only about 300 mm (12 in.) of backfill over the pipe. This indicates that compaction against soft trench walls is far less effective than against hard trench walls.

Profilometer and deflection data are shown in figs. 4.15 and 4.16 also demonstrate the effect of compaction method and trench wall stiffness respectively. Fig 4.15 shows that the rammer compactor produces more upward peaking than the vibratory plate. This suggests that the energy delivered by the rammer compactor is more concentrated than that delivered by the vibratory plate, which is consistent with the compactor calibrations that showed compaction to a specific density is achieved with fewer passers of the rammer relative to the vibratory plate. Fig. 4.16 shows that compaction when trench walls are soft results in substantially less peaking than when the walls are hard. This suggests that in the field contractors installing pipe in soft native soils will need to pay extra attention to the compaction procedures.

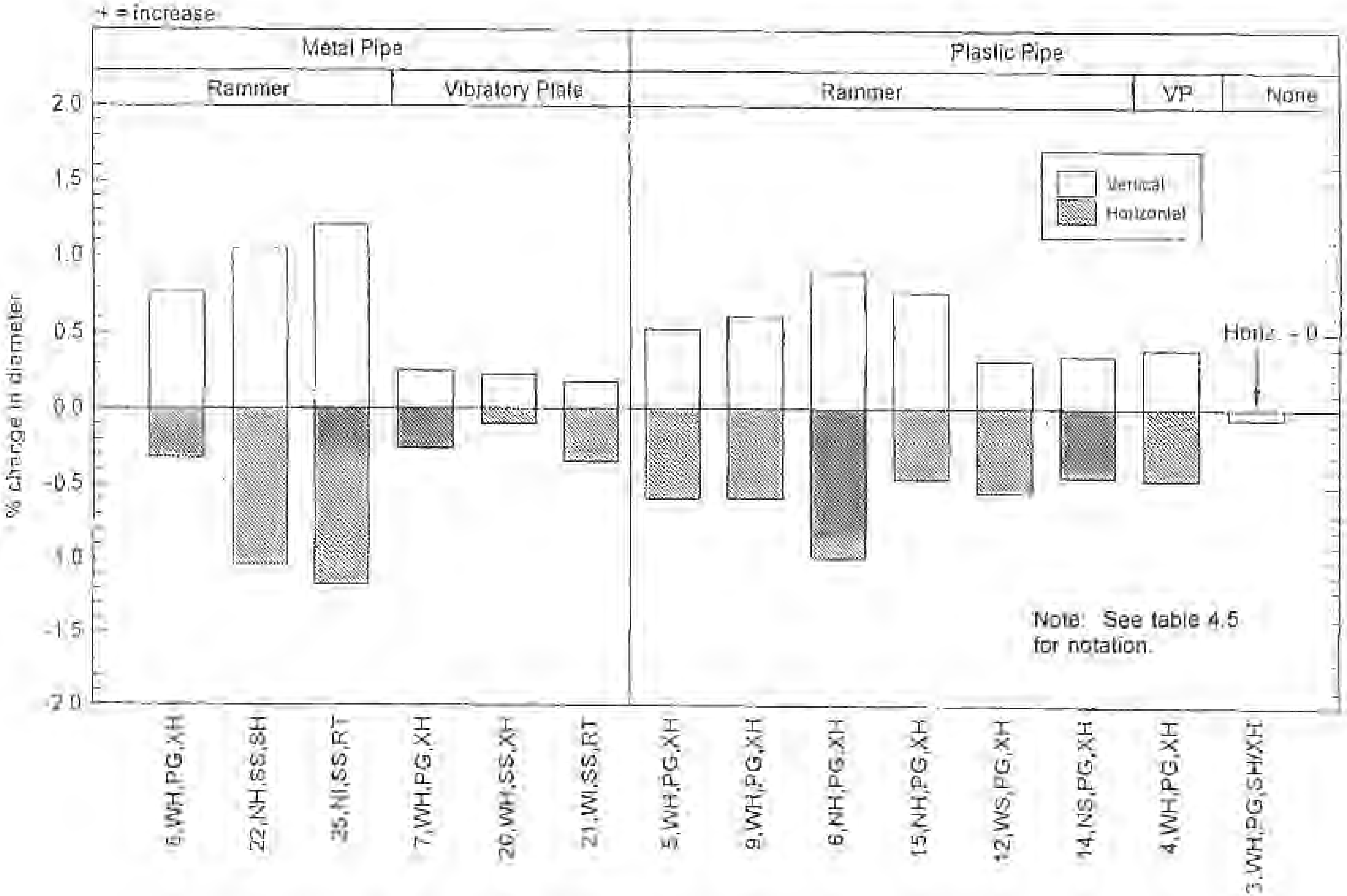

Figure 4.13 Pipe Deflections, Backfill Placed, and Compacted to the Springline Lift

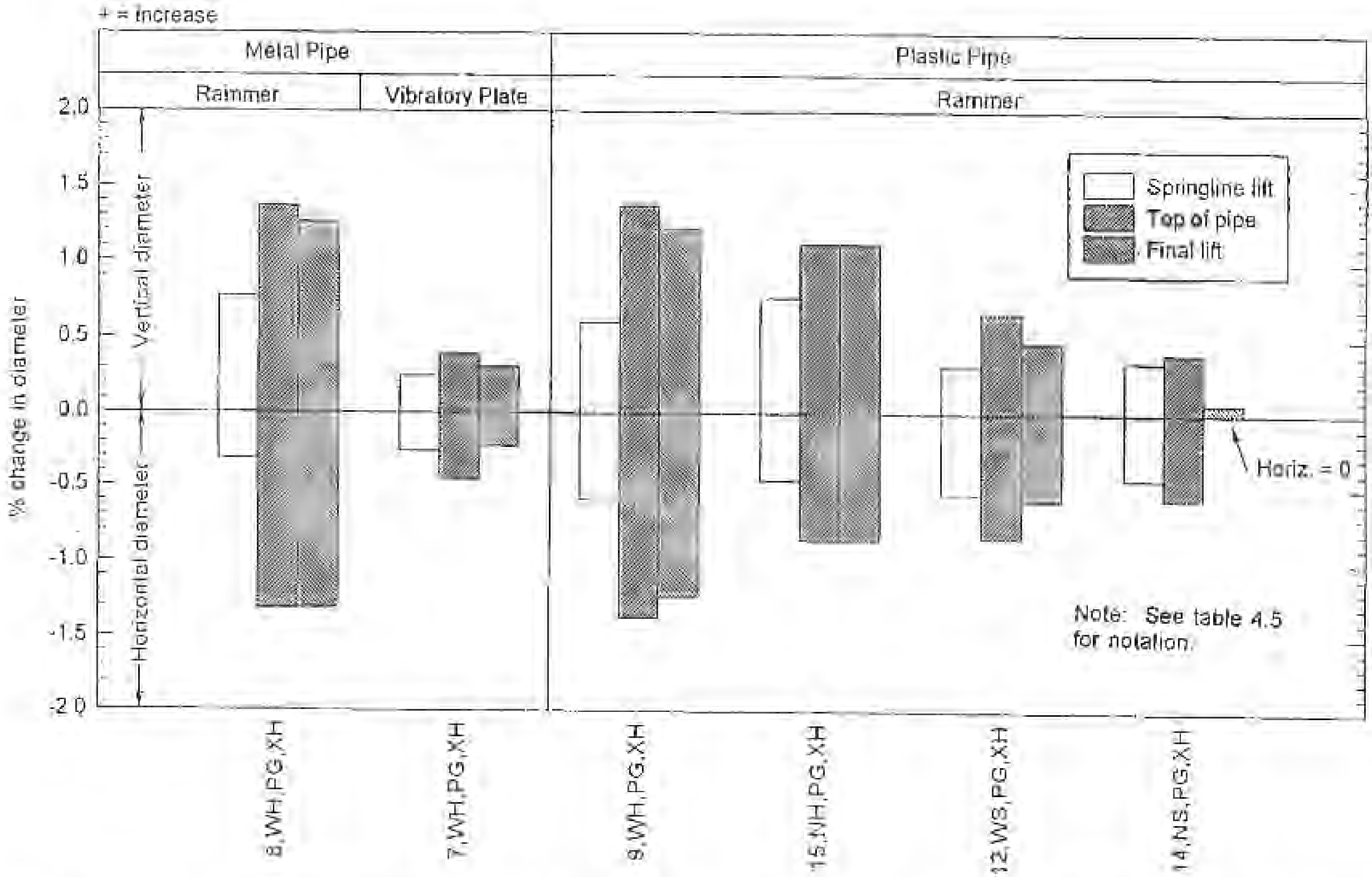

Figure 4.14 Pipe Deflections, Backfill Placed and Compacted to the Springline Lift, the Top of the Pipe, and the Final Lift

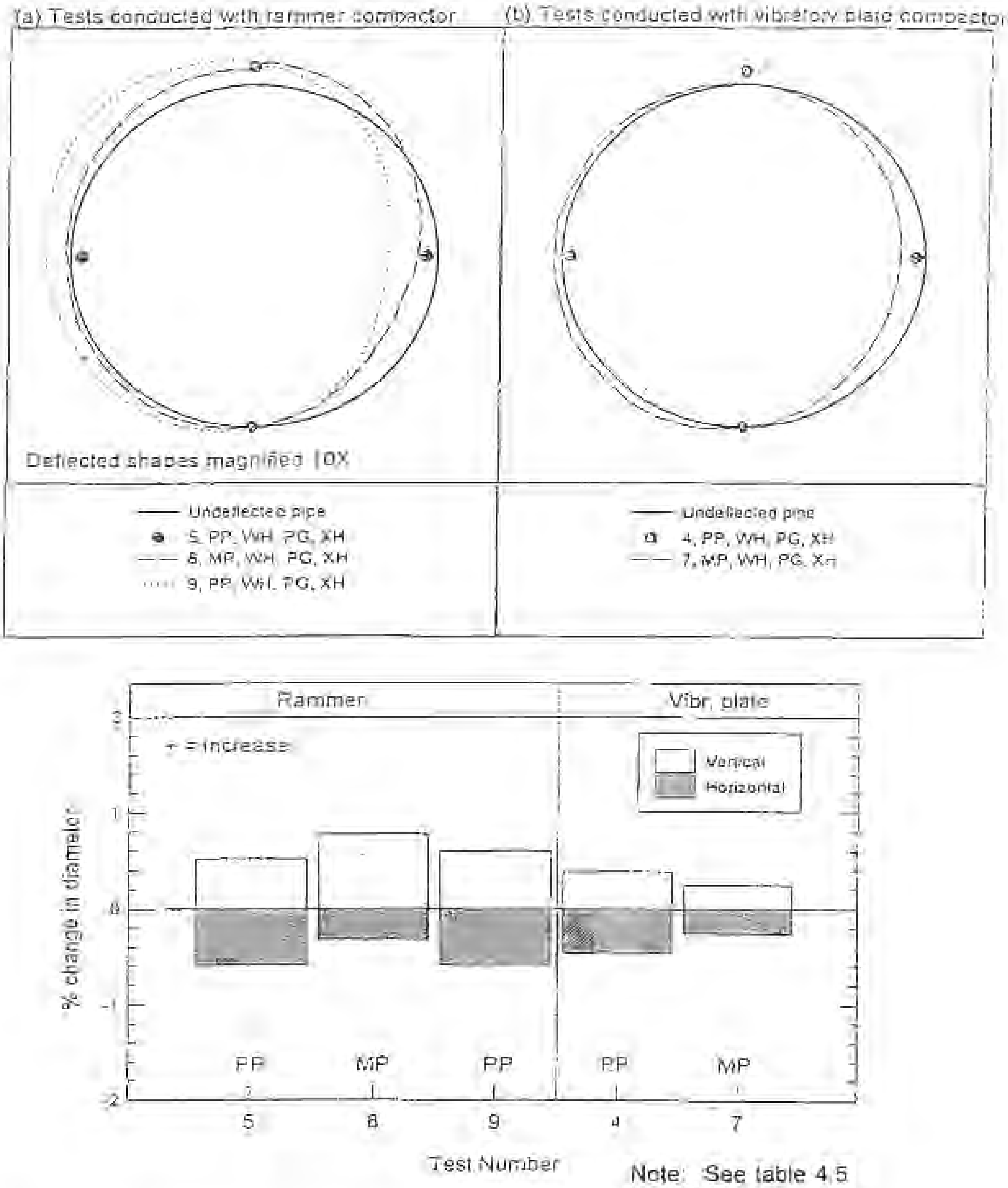

Note: See table 4.5 for notation.

Figure 4.15 Comparison of Pipe Deflections with Pipe Type and Method of Compaction, Backfill Compacted to the Springline Lift

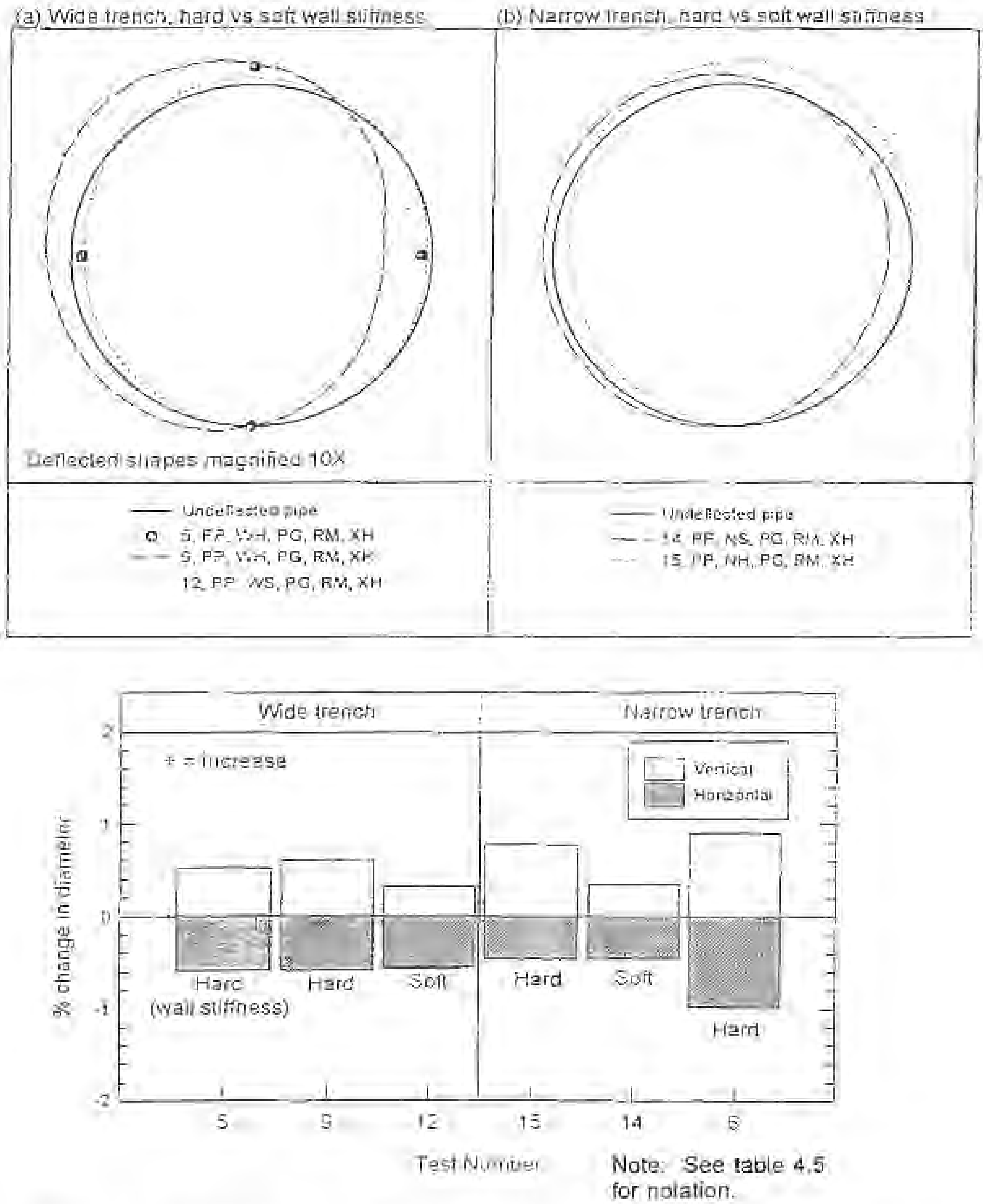

Figure 4.16 Comparison of Pipe Deflections with Trench Wall Stiffness, Backfill Compacted to the Springline Lift

4.1.6.4 Haunch Zone Pipe Support

Haunch zone pipe support is evaluated by both the pipe-soil interface pressures and the penetration resistance. Interface pressure readings were made for the concrete and metal pipe with both backfill materials while the penetration resistance was only measured for tests backfilled with the silty sand.

The initial invert pressure, i.e., when the pipe is first placed on the bedding, is somewhat random as it is very sensitive to small deviations in the grade along the length of the pipe. Changes in the invert interface pressure during backfilling, however, indicate the change in pipe support that results from compaction and haunching effort below the springline. Fig. 4.17 shows the invert pressure under the concrete pipe for two tests backfilled with pea gravel and compacted with the rammer. Test 10 was conducted with compacted bedding and soft trench walls while test 11 was conducted with the central third of the bedding uncompacted and hard trench walls. Neither test incorporated any effort at compacting material in the haunch zone. Pressures before and after compacting each lift of backfill are shown. Both figures show significant reduction in invert pressure when the first lift, below the springline, is compacted. This confirms observations made in other tests that the rounded pea gravel backfill readily flows under compaction and no specific effort is required to compact it in the haunch zone (see below). However, when backfill is placed above the springline, the pipe with soft trench walls and hard bedding shows large increases in invert pressure while the invert pressure under the pipe with soft bedding and hard trench walls returns to the pretest pressure. Both the trench wall and bedding stiffness are thought to contribute to the reduced invert pressure. Fig. 4.18 shows a similar trend in the invert pressure under the metal pipe.

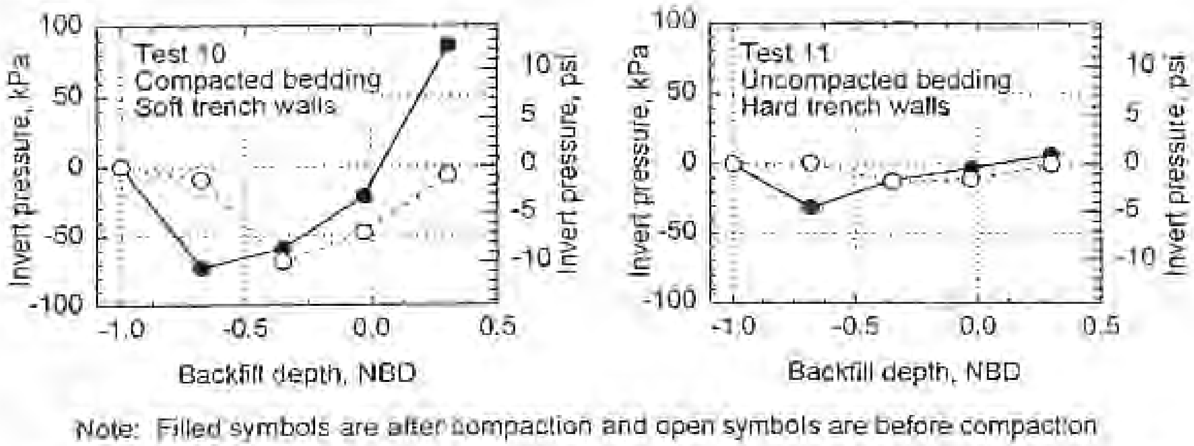

Figure 4.17 Invert Interface Pressure, Concrete Pipe with Pea Gravel Backfill

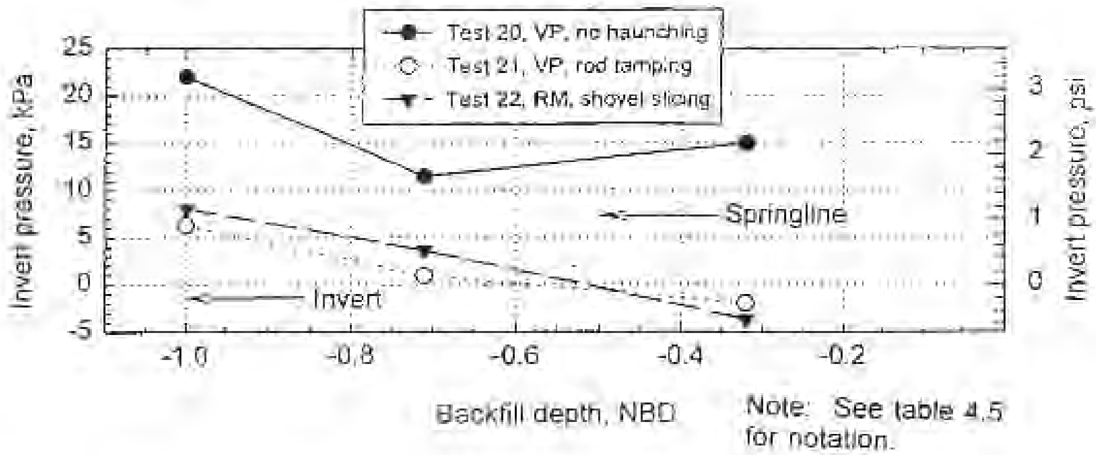

Figure 4.18 Invert Interface Pressure, Metal Pipe with Silty Sand Backfill

The radial pressures around the concrete pipe for Tests 23 and 24, backfilled with silty sand and compacted with the rammer when backfill was at a level 150 mm (6 in.) above the springline are presented in Fig. 4.19. For Tests 23 and 24 the backfill was worked into the haunch zone by shovel slicing and rod tamping respectively. These tests show the following:

- Neither type of haunching effort produces significant radial pressure on the pipe at an angle 22.5 degrees from the invert.
- The two types of haunching effort appear to provide equivalent pipe support at angles of 45 degrees and more from the invert.
- Both tests showed essentially zero invert pressure after placing backfill; however, the pressure for both tests was quite low when the pipe was placed, thus, the low pressures are not a result of the haunch effort or compaction.

The interface pressures with backfill compacted up to the springline lift for a metal and concrete pipe under similar installation conditions are presented in fig. 4.20. The figure suggests that the metal pipe develops lower interface pressures at 45 degrees from the invert, this seem consistent with the low weight and stiffness of the metal pipe.

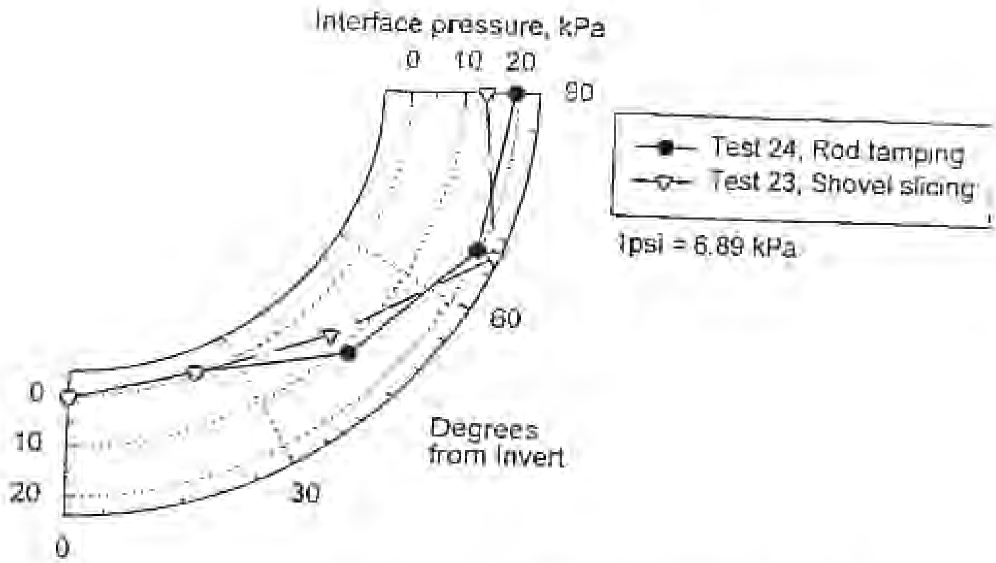

Figure 4.19 Radial Pressure Against Concrete Pipe

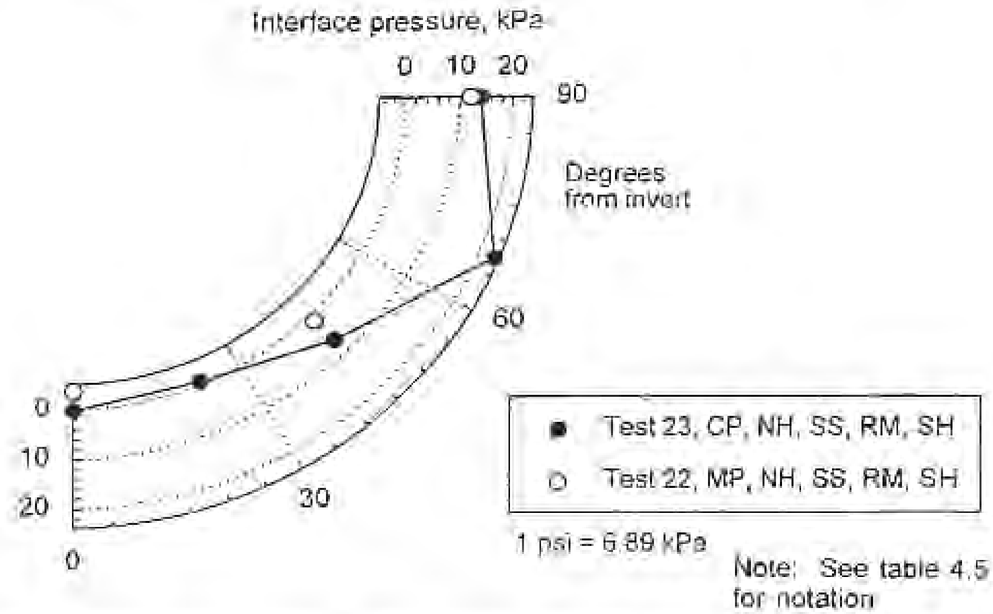

Figure 4.20 Comparison of Radial Pressure Against Concrete and Metal Pipe

Proctor penetration tests were conducted only in the silty sand backfill because the penetrometer is used only in fine-grained materials (ASTM D 1558). Penetration tests for tests 20 to 25 were conducted after testing with the pipe removed. Measurements were conducted at the invert and 30 and 60 degrees from the invert. Tests 20 and 21 were measured with a 640 mm^2 (1 $in.^2$) tip, and tests 22 through 25 were conducted with a 480 mm^2 (0.75 $in.^2$) tip.

The penetration resistance for tests 20 and 21, both conducted with the metal pipe are compared in fig. 4.21. Test 20 was conducted without haunch effort while in test 21 the haunch was compacted using rod tamping. The lower strength of the soil in the haunch region is evident, which is consistent with the interface pressure data. The soil strength under the concrete pipe for tests 23 and 24, which had soft bedding and compacted bedding, respectively are compared in fig. 4.22. The data is consistent with the interface pressures for the same conditions and shows that the soil strength is lower when the backfill is left uncompacted. This is significant because it shows that the soft bedding remains relatively soft even after pipe and backfill are placed.

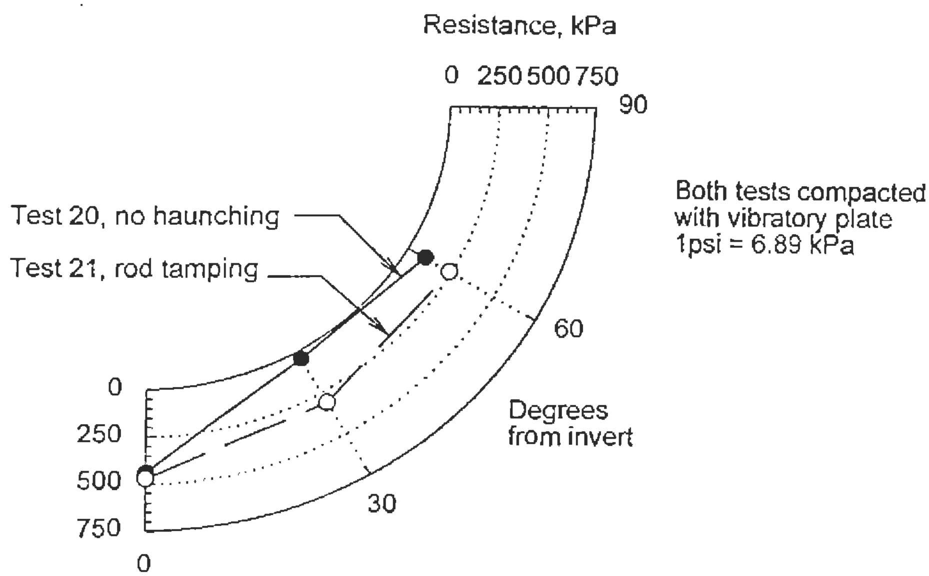

Figure 4.21 Penetration Resistance of Backfill Under Metal Pipe

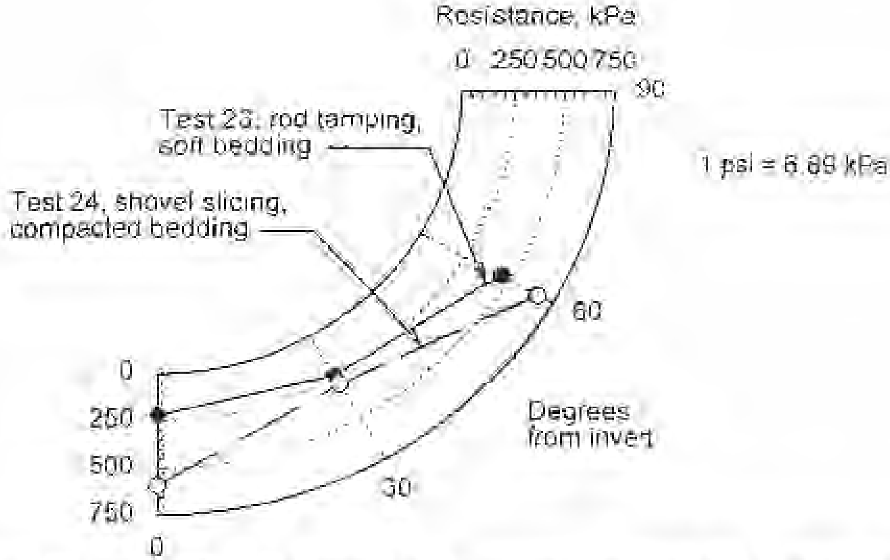

Figure 4.22 After Test Penetration Resistance of Backfill Under Concrete Pipe

4.1.6.5 Horizontal Soil Stresses at the Trench Wall

Horizontal backfill stresses were measured on both sides of the trench at the pipe springline and haunch elevations. Horizontal soil stresses when the backfill is placed and compacted to the springline lift for specific test variables are presented in figs. 4.23 to 4.25. The horizontal stresses at the haunch elevation are greater than the stresses at the springline elevation, which is consistent with the depth of fill. The horizontal soil stresses are generally lower for the concrete pipe than for the plastic pipe, and the stresses were higher with the hard and intermediate trench wall stiffness than with the soft wall stiffness. In both the wide and narrow trench conditions, the horizontal soil stresses were, on average, four times greater with the hard wall. The silty sand resulted in higher horizontal stresses than the pea gravel. Horizontal stresses were, on average, 35 percent higher with the silty sand material.

The horizontal stresses at the springline and haunch level for tests where backfill was brought over the top of the pipe are shown in fig. 4.26. This figure also shows the geostatic lateral pressure, assuming a K_o value of 0.4, when the backfill was at the final elevation. This figure demonstrates the significant loss of lateral support when the trench walls are soft.

Trench wall displacement measurements show that large compression occurred in the soft trench wall, on the order of 30 to 50 mm. Compression of the intermediate trench wall was on the order of 0.5 mm to 1.0 mm (0.02 in. to 0.04 in.).

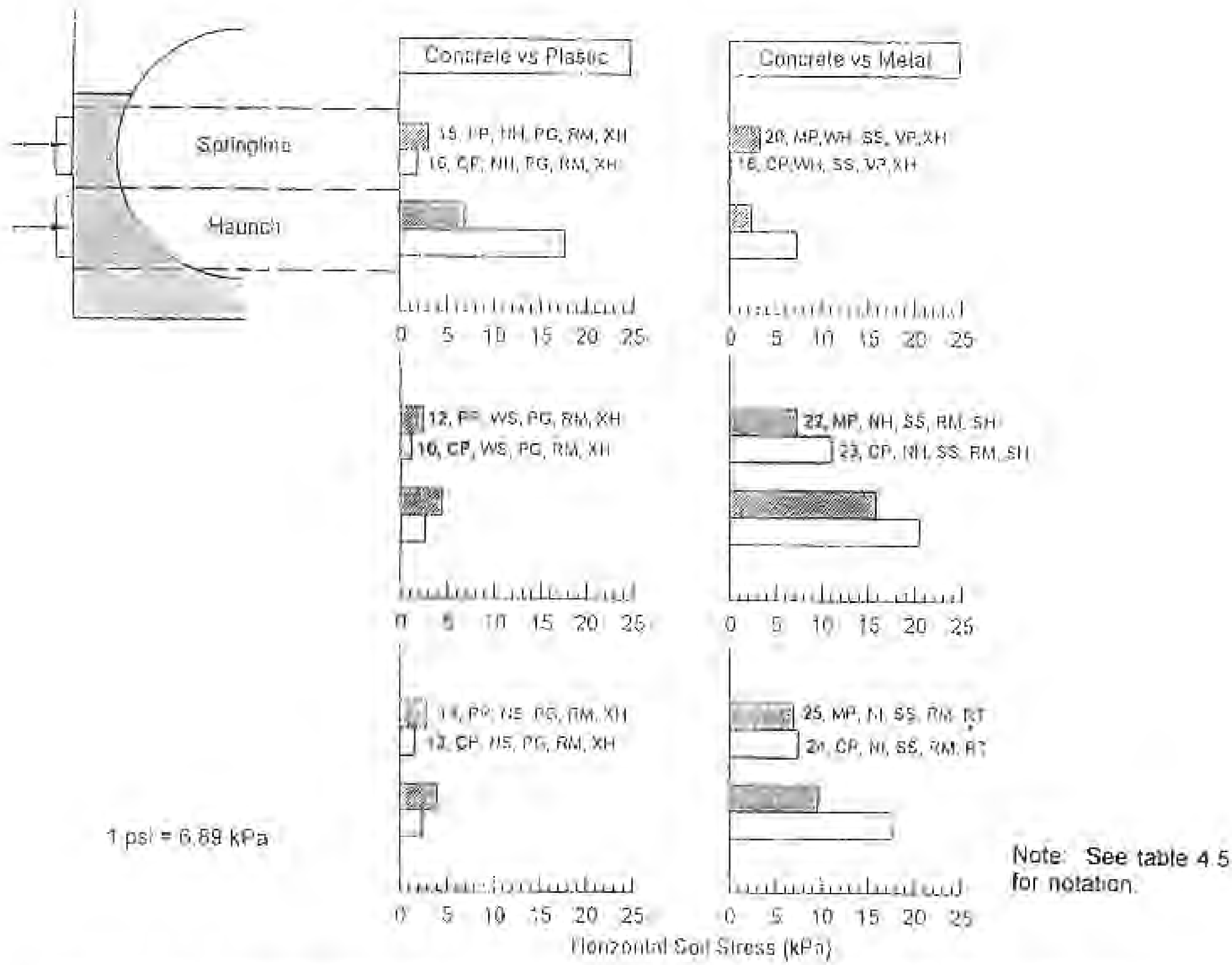

Figure 4.23 Comparison of Horizontal Soil Stresses at the Trench Wall Due to Pipe Type, Backfill Placed and Compacted to the Springline Lift

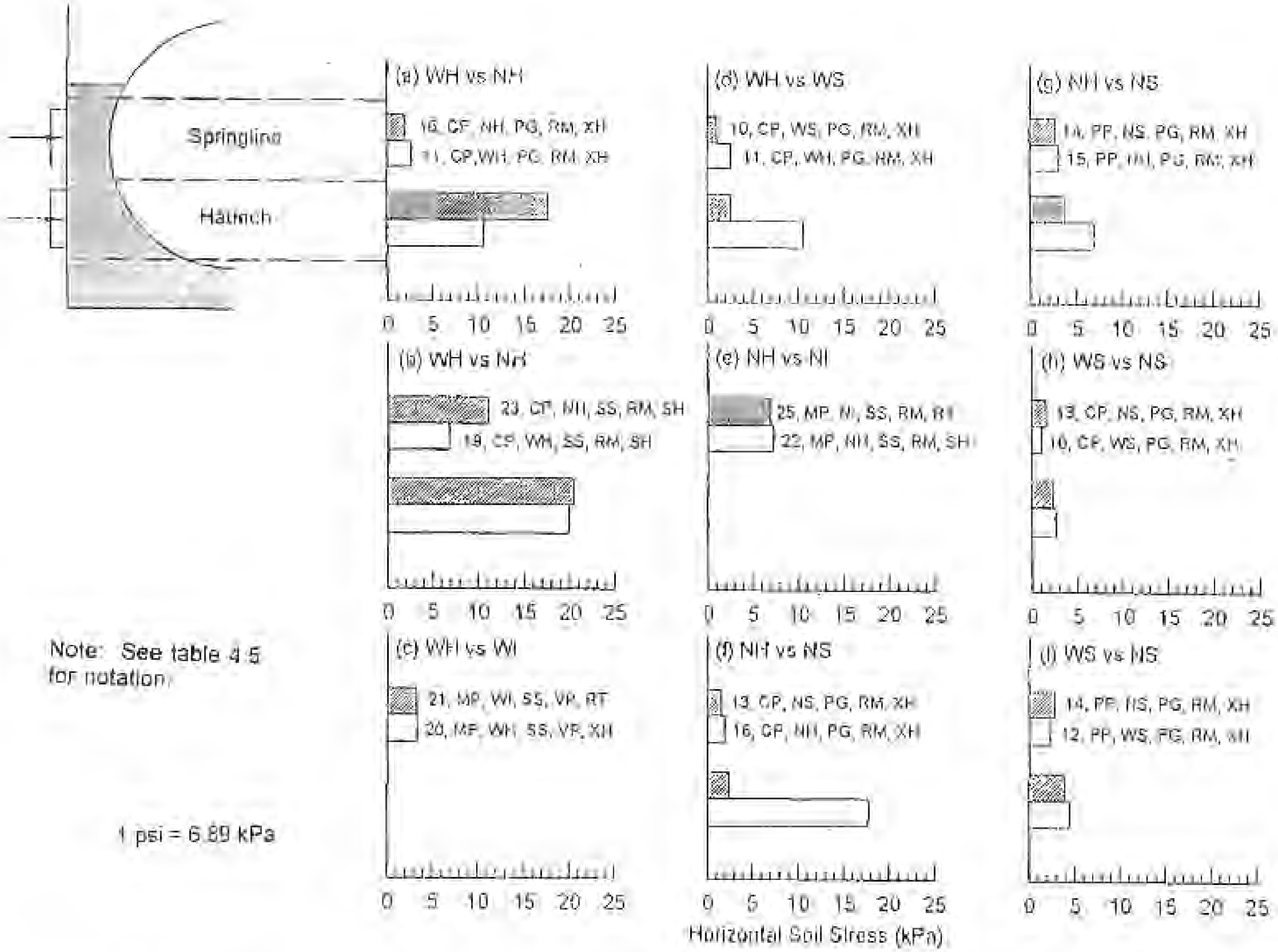

Figure 4.24 Comparison of Horizontal Soil Stresses at the Trench Wall Due toTrench Condition, Backfill Placed and Compacted to the Springline Lift

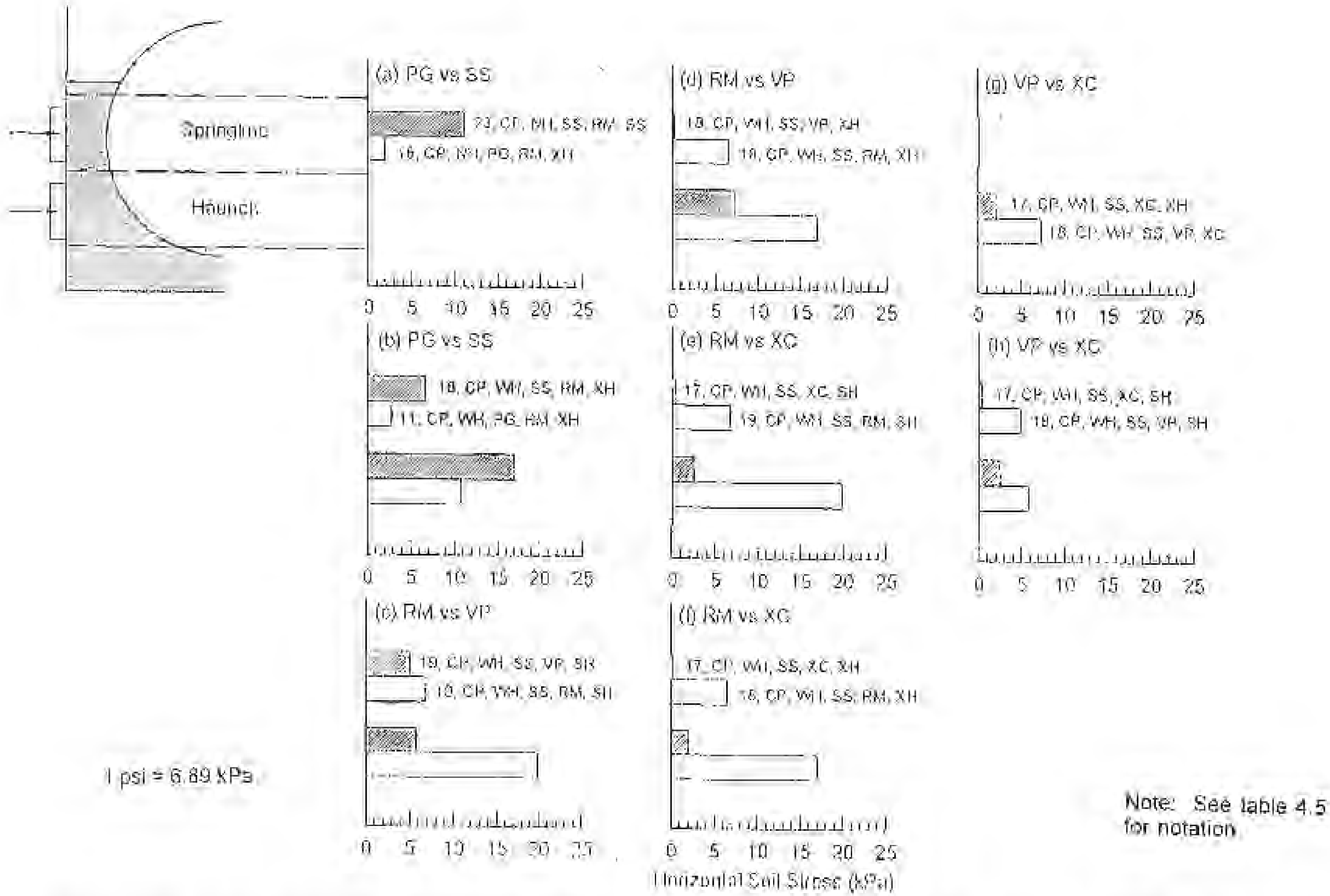

Figure 4.25 Comparison of Horizontal Soil Stresses at the Trench Wall Due to Backfill Material and Method of Compaction, Backfill Placed and Compacted to the Springline Lift

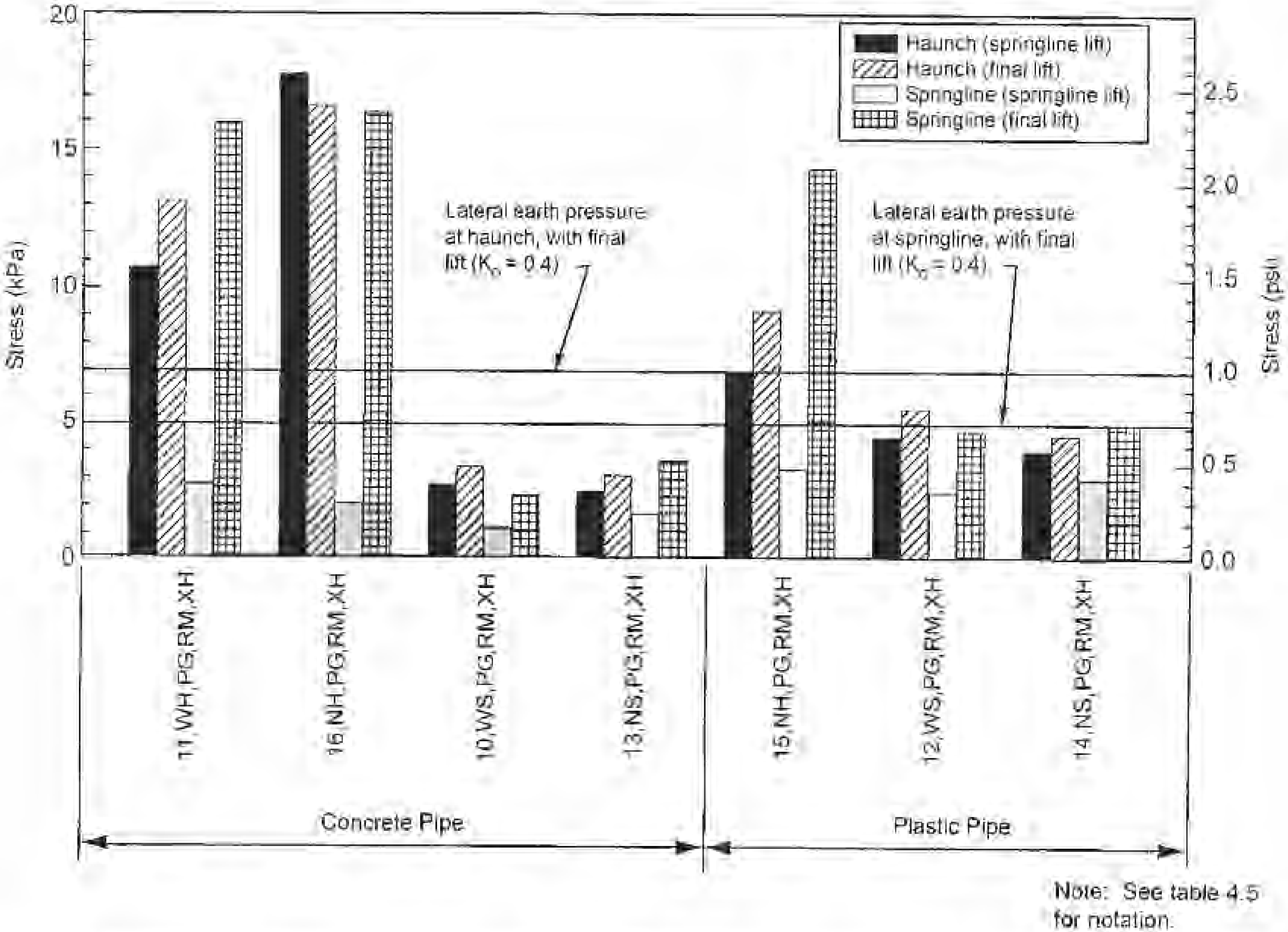

Figure 4.26 Horizontal Soil Stresses at the Trench Wall, Backfill Placed and Compacted to the Springline and the Final Lift

4.1.6.6 Pipe Strains

Strains were measured for only three tests conducted with the plastic pipe and the results are presented as strain versus normalized depth of fill in fig. 4.27. Gages were located at the springline and invert both on the inner and outer walls of the pipe. Positive readings indicate tension. Note that for all of these tests the backfill was compacted with the rammer. The circumferential strains (fig. 4.27(a) and (b)) are consistent with the deflection and other data collected, i.e., upward peaking of the pipe during compaction but reduced in magnitude when the trench walls are soft. The outside wall strains were larger than strains in the inside wall, which is consistent with the location of the centroidal axis. The longitudinal strains are of opposite sign from the circumferential strains at the same location.

Plots of strain versus deflection at every depth of fill, with the best fit regression curve and correlation coefficient, r, and slope, m, are presented in fig. 4.28. The data are relatively linear, with coefficients of correlation always greater than 0.74 except for the longitudinal strain at the springline. The best fit curves generally pass through the origin of the plot. The ratios of the slopes, presented in table 4.7, indicate the relative magnitude of the longitudinal strain compared to the circumferential strain. The ratio is higher at the invert than at the springline.

Table 4.7

Strain Versus Deflection in Plastic Pipe

Location	Circumferential strain	Longitudinal strain	Ratio: long./circumf.
	(% strain/%defl.)	(% strain/%defl.)	
Springline, inside	0.16	-0.07	-0.44
Springline, outside	-0.31	0.14	-0.45
Invert, inside	-0.18	0.11	-0.61
Invert, outside	0.21	-0.14	-0.67

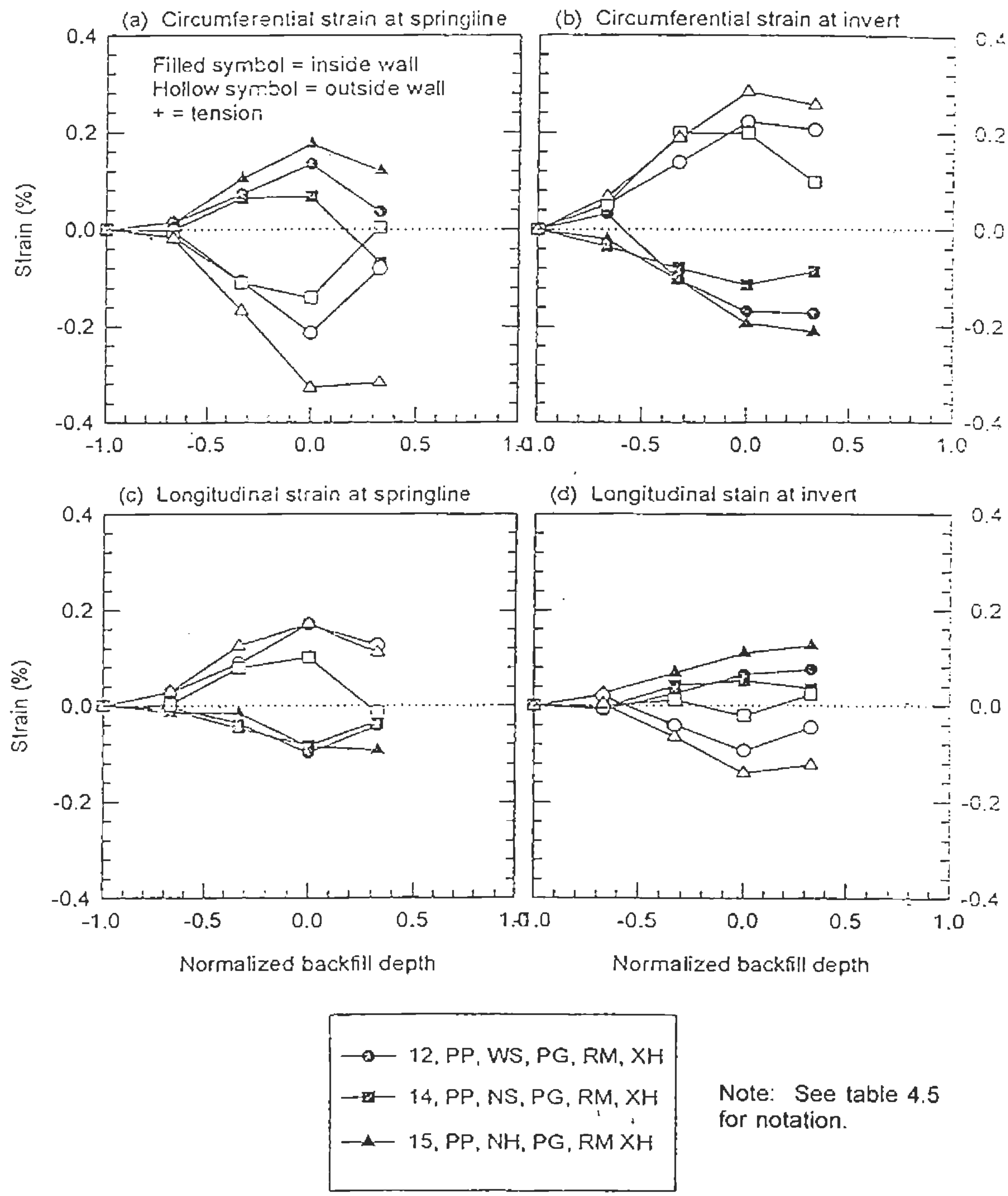

Note: See table 4.5 for notation.

Figure 4.27 Plastic Pipe Strains

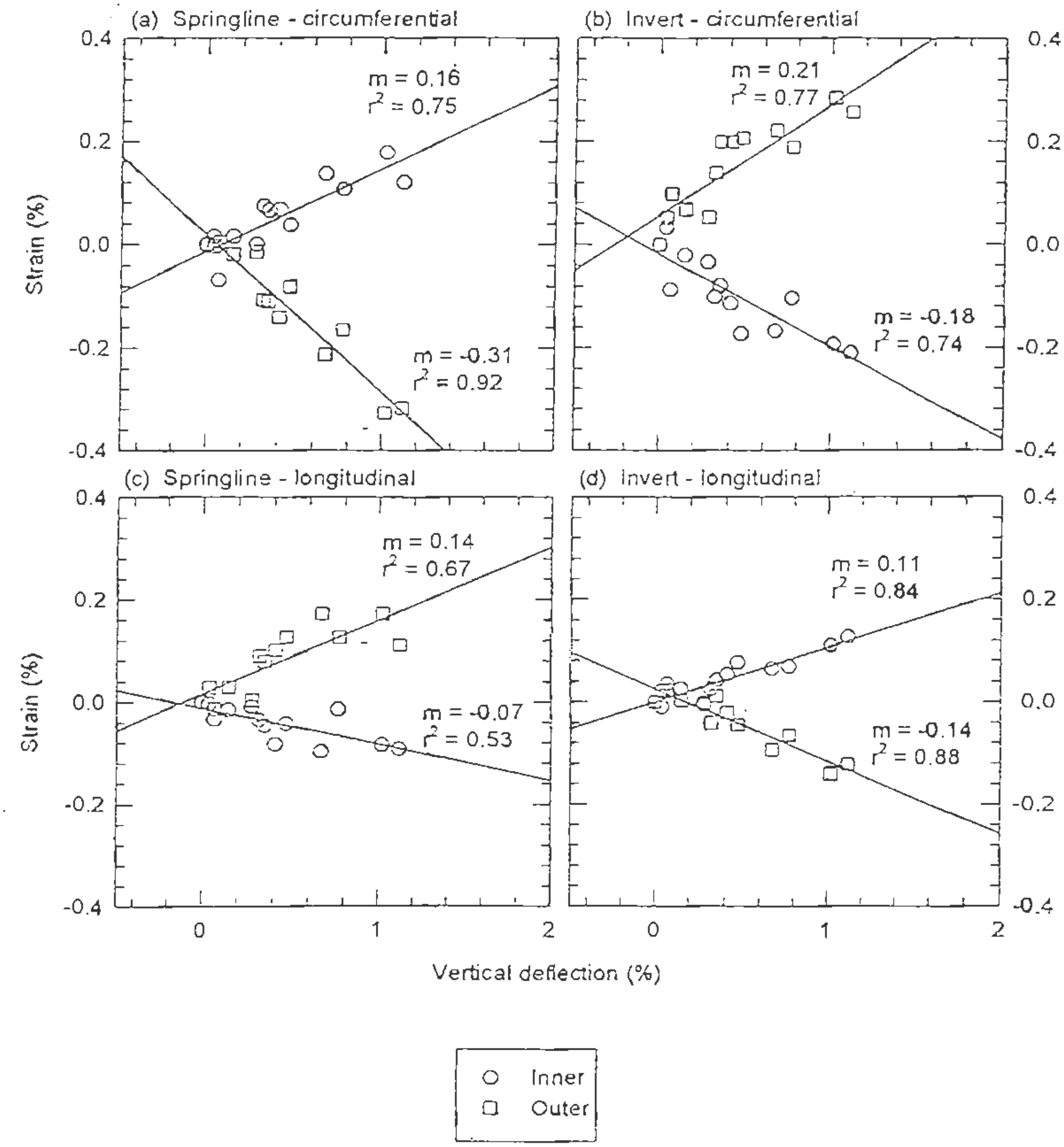

Figure 4.28 Strain Correlated with Deflection After Compaction of Backfill

4.2 Field Tests

Full-scale field tests were conducted to gather data on the stresses, strains, and deformations in pipe and the surrounding soil embedment as the pipe-soil system is being constructed. The test program was developed to provide information that could improve our understanding of the response of a pipe and the surrounding soil to installation variables. The test program has been reported in detail in Webb (1995). Tables and figures of all of the raw data are reported in Webb et al.(1995) and Zoladz et al. (1995).

A total of 14 tests were conducted. Each test included a reinforced concrete, corrugated or profile wall polyethylene, and a corrugated steel pipe. Tests variables for each test are described in table 4.8. Because of the number of variables involved, it was not possible to test every possible combination of parameters. The specific combinations selected were based on the judgement of the research team.

The general configuration for each test consisted of one length each of concrete, plastic, and metal pipe installed end to end as shown in fig. 4.29 for the 900 mm (36 in.) diameter pipe. The configuration for the 1,500 mm (60 in.) diameter pipe was similar. All the pipes were backfilled to a depth of 1.2 m (4 ft) over the top of the pipe.

More detailed information on pipe, backfill, test sites, and other variables is provided in the following sections.

Table 4.8
Summary of Variables for Field Tests

Test No.	Trench Width (1)	In situ soil	Pipe diameter mm (in.)	Backfill material	Sidefill compaction	Haunch (2)	Bedding compaction (3)
1	N	Sand	900 (36)	Stone	Rammer	SS	Fully compacted
2	N	Sand	900 (36)	Stone	None	N	Fully compacted
3	W	Sand	900 (36)	Stone	Rammer	SS	Sides compacted
4	W	Sand	900 (36)	Stone		N	Sides compacted
5	N	Sand	900 (36)	Silty sand	None	N	Fully compacted
6	N	Sand	900 (36)	Silty sand	Rammer	SS	Fully compacted
7	W	Sand	900 (36)	Silty sand	Vibr. plate	N	Sides compacted
8	W	Sand	900 (36)	Silty sand	Rammer	SS	Sides compacted
9	N	Clay	900 (36)	Stone	Rammer	SS	Fully compacted
10	N	Clay	900 (36)	CLSM	Rammer	--	Fully compacted
11	W	Clay	900 (36)	Stone	Vibr. plate	N	Sides compacted
12	N	Clay	1,500 (60)	Stone	None	RT	Fully compacted
13	W	Clay	1,500 (60)	Stone	Vibr. plate	RT	Sides compacted
14	I	Clay	1,500 (60)	Silty sand	Vibr. plate	RT	Sides compacted

Notes: 1. N = narrow (O.D. -0.6 m), W = wide (O.D. plus 1.8 m), and I = intermediate (O.D. plus 0.9 m).
2. SS = shovel slicing, RT = rod tamping and N = none.
3. Bedding was compacted with the vibratory plate. Fully compacted means the bedding was compacted over the full trench width. Sides compacted means that a strip directly under the pipe, one third of the pipe outside diameter in width, was left uncompacted.

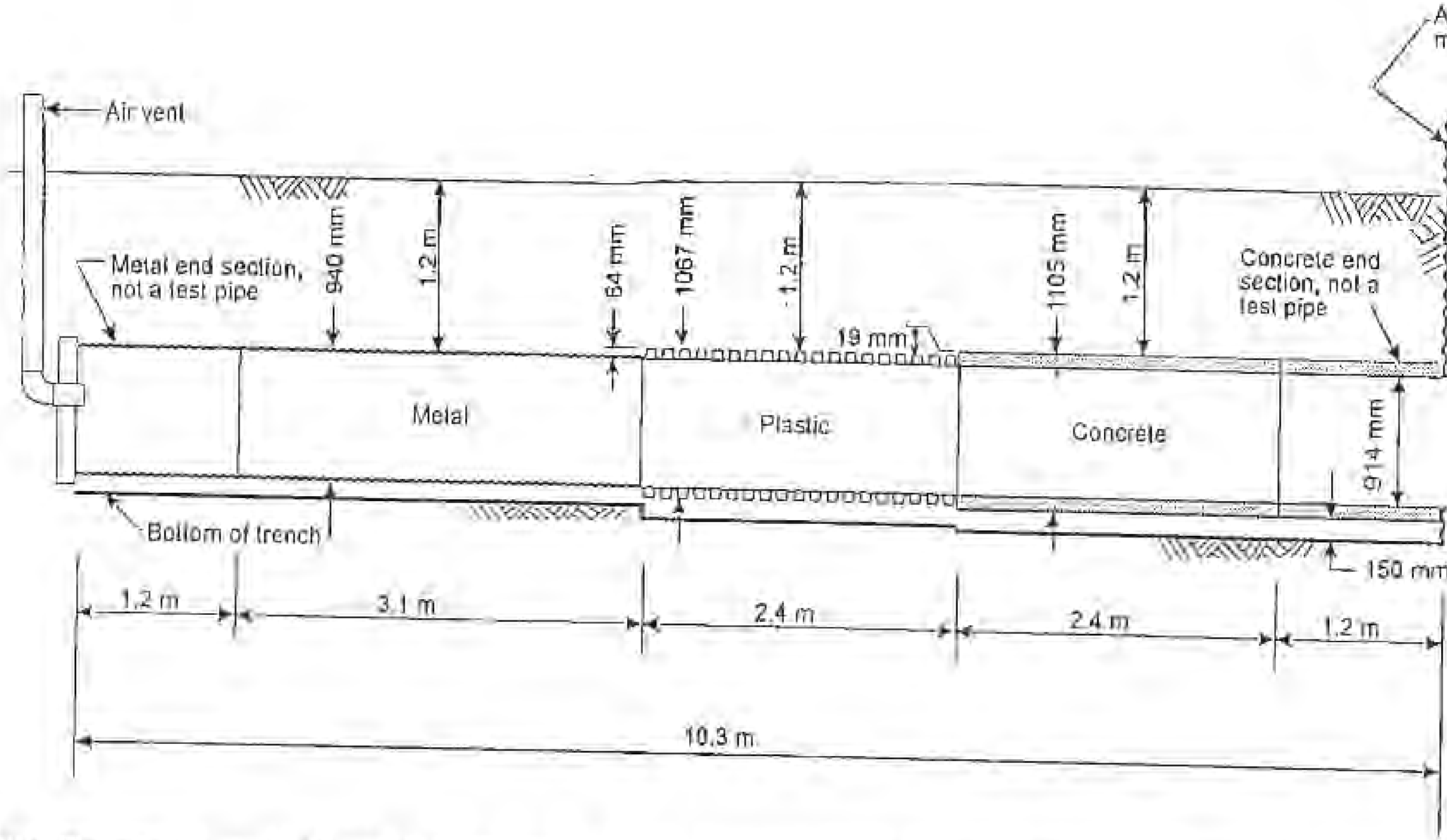

Note: Dimensions shown for 914 mm (36 in.) diameter pipe; some dimensions change for the 1524 mm (60 in.) diameter pipe.
1 in. = 25.4 mm
1 ft = 0.305 m

Figure 4.29 Schematic of Layout of Test Trenches for 900 mm Diameter Pipe

4.2.1 Test Pipe

Eleven tests were conducted with 900 mm (36 in.) nominal inside diameter pipe, and three tests were conducted with 1,500 mm (60 in.) nominal inside diameter pipe. The 900 mm diameter plastic pipe had a corrugated pipe wall with a liner to provide a smooth inside surface. The 1,500 mm plastic pipe had a smooth pipe wall with a spiral rib on the outside. The test pipe are referred to herein as the concrete, metal, and plastic pipes, respectively. Pipe were supplied with no joints, allowing them to be laid end to end in the test trenches. These pipes were selected to provide a range of pipe bending and hoop stiffnesses that is typical in actual culvert applications.

The geometric, material, and stiffness parameters of the test pipe are summarized in table 4.9. In this table, the nominal short term modulus of the polyethylene is reported and used to calculate the pipe stiffnesses. Depending on the duration of an applied load, other values of the modulus may be appropriate; however, since the tests discussed in this paper are all of relatively short duration, the short-term modulus was deemed most appropriate. The pipe stiffnesses are calculated values, rather than test values. Test values for plastic and metal pipes are often lower than the calculated values.

Table 4.9
Summary of Properties of Test Pipe

Pipe type	Diameter mm	E GPa	A mm^2/mm	I mm^4/mm	PS_H kN/m^2	PS_B kN/m/m
Concrete	900	25	119	140,000	$5{,}800\text{x}10^3$	170,000
	1,500		169	402,000	$5{,}000\text{x}10^3$	111,000
Plastic	900 corrugated	0.8	10.2	8,470	$16\text{x}10^3$	390
	1,500 profile		11.3	3,180	$11\text{x}10^3$	36
Metal	900	205	1.64	31	$720\text{x}10^3$	410
	1,500		1.88	142	$500\text{x}10^3$	420

1 mm = .039 in., 1 GPa = $145\text{x}10^3$ psi, 1 kN/m^2 = 0.15 psi

Table 4.9 shows that the concrete pipe has high hoop and bending stiffness relative to both the metal and plastic pipe, while the plastic pipe has low flexural and hoop stiffnesses. However, the metal pipe has a low bending stiffness, which is consistent with its traditional treatment as a flexible pipe but an intermediate hoop stiffness. Thus, each of the three pipes represents a different regime of pipe stiffnesses. Low hoop stiffness has been shown to cause significant reductions in load on buried pipe (Hashash and Selig, 1990).

4.2.2 Test Sites

Tests were conducted at two sites. At the first site, called here the "sand" site, the soils were glacial deposits of coarse to medium sand (SP, SW-SM). Samples of these soils were incorporated into the backfill test program reported in chapter 3 as Soils Nos. 11 and 12. In its natural condition, this sand was compact and partially cemented, providing a stiff stable material to excavate trenches in and compact soil against. The ground water table was near the bottom of the excavations for some of the tests and pumps were used to keep the excavation reasonably dry. Seepage from the trench walls also affected some of the tests.

The second site consisted principally of a sedimentary varved clay deposit (CL). Samples of these soils were incorporated into the backfill test program reported in chapter 3 as Soils No. 9 and 10. This formation is generally quite soft and was selected to represent a poor in situ soil condition, unfortunately the specific area selected proved to be stiffer than anticipated. Penetrometer readings suggest unconfined compression strength values between 190 kPa and 380 kPa (2 tsf and 4 tsf), with values as low as 100 kPa (1 tsf) in some areas. Some water seeped into the trenches during the tests; however, the rate was low enough that positive action to control the water was not required.

4.2.3 Backfill

Thirteen of the fourteen tests were completed with either of two soil backfill materials, in a 19 mm (3/4 in.), broadly graded crushed stone, called stone herein and characterized as Soil No. 3 in chapter 3, and a poorly graded silty sand characterized as Soil No. 6 in chapter 3.

One test was backfilled to the pipe springline with CLSM. The batch design of the flowable fill, shown in table 4.10, was selected based on the material study reported in chapter 3. The target strength for the mix was 690 kPa (100 psi) at 28 days. The material was delivered in two batches, and although the ready mix supplier reported that both batches were identical, the strengths and stiffnesses of the two batches varied significantly, as shown in table 4.11. This backfill above the springline was the in situ clay material which is discussed in a subsequent section.

Table 4.10
CLSM Backfill Mix Design

Material	Mass kg/m^3 (lb/yd^3)
Concrete sand	1606 (2707)
Cement	46 (78)
Class F fly ash	247 (416)
Water	274 (462)

Table 4.11
CLSM Strength Test Results

Batch No.	Strength, kPa (psi)		Modulus of elasticity, MPa (psi)	
	7 day	28 day	7 day	28 day
1	420 (61)	779 (113)	165 (24,000)	234 (34,000)
2	248 (36)	434 (63)	70 (10,000)	145 (21,000)

4.2.4 Instrumentation

Extensive instrumentation was used to monitor the behavior of the test pipe and surrounding soil as the backfill was placed and compacted at the sides of the pipe. The instrumentation was largely the same as used in the laboratory tests and described in detail in McGrath and Selig (1996). The instruments included a profilometer to monitor pipe deflections and overall changes in the pipe shape, strain gages mounted on the metal and plastic pipe, interface pressure cells on the concrete and metal pipe, and earth pressure cells to monitor horizontal soil stresses at the trench wall-backfill interface and vertical soil stresses in a plane 150 mm (6 in.) over the top of the pipe. In addition, inductance coil soil strain gages that were not used in the laboratory tests were installed to monitor horizontal soil displacements between the springline of the pipe and the trench wall. Instrument layouts for each type of pipe are shown in figures 4.30 to 4.35.

Strain gages were mounted on the springlines, crown, and invert of the plastic and metal pipes. At each position gages were mounted on the inside and outside surfaces in both the circumferential and longitudinal directions.

Soil stresses were monitored with 230 mm (9 in.) diameter, fluid filled, earth pressure cells with vibrating wire transducers. The cells mounted in the trench wall at the springline (see figures 4.30, 4.32, and 4.34) had heavy backplates to minimize the effect of non-uniform support against the trench wall. The cells over the top of the pipe were sensitive to pressure on both faces.

In addition to the above instruments, standard survey equipment was used to monitor pipe and backfill elevations. Observations were used to supplement measurements whenever appropriate. Most instruments were read electronically using a computerized data acquisition system.

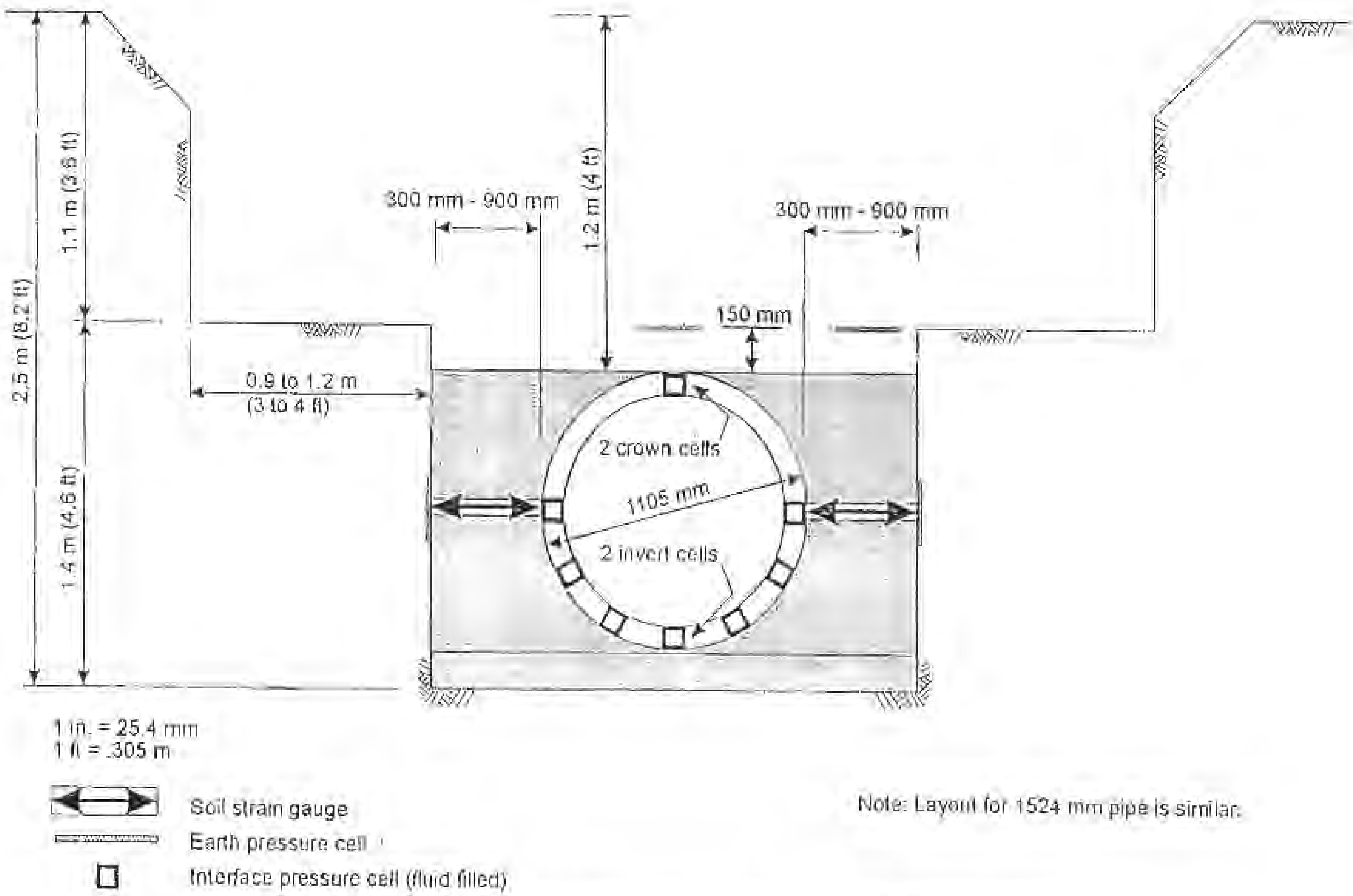

Figure 4.30 Cross-Section of Concrete Pipe in Trench with Instrumentation

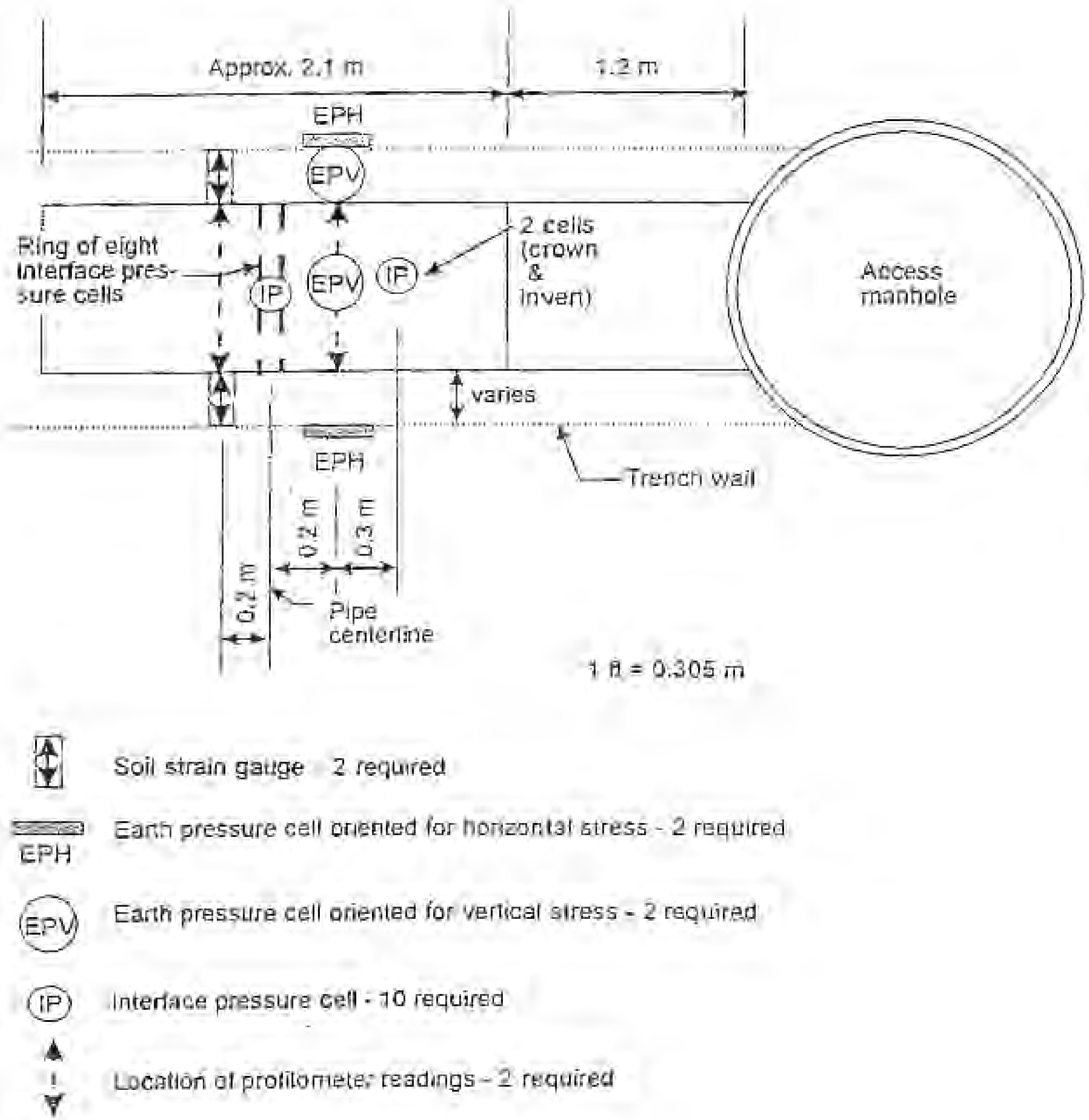

Figure 4.31 Longitudinal Instrumentation Layout for the Concrete Pipe

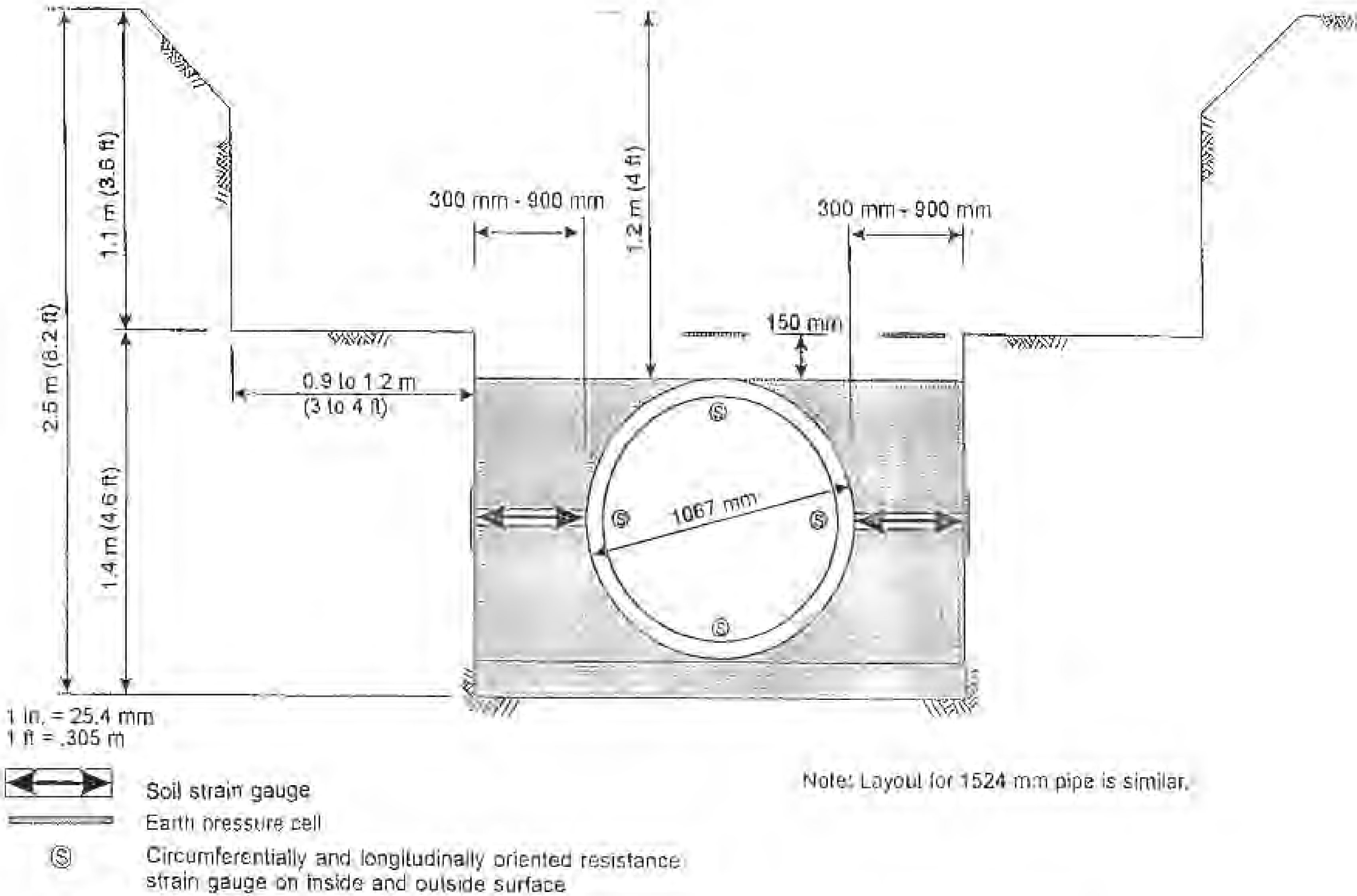

Figure 4.32 Cross-Section of Plastic Pipe in Trench with Instrumentation

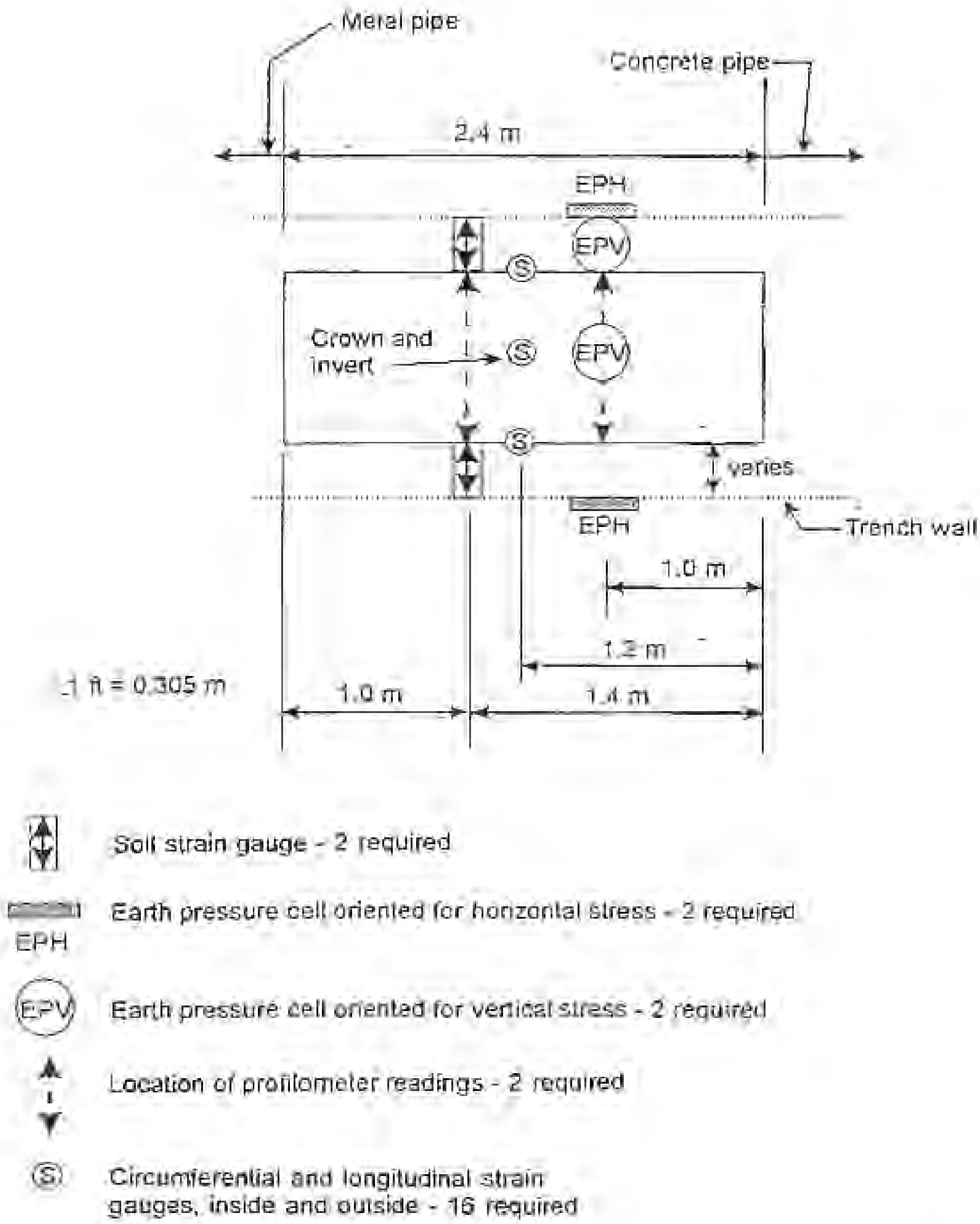

Figure 4.33 Longitudinal Instrumentation Layout for the Plastic Pipe

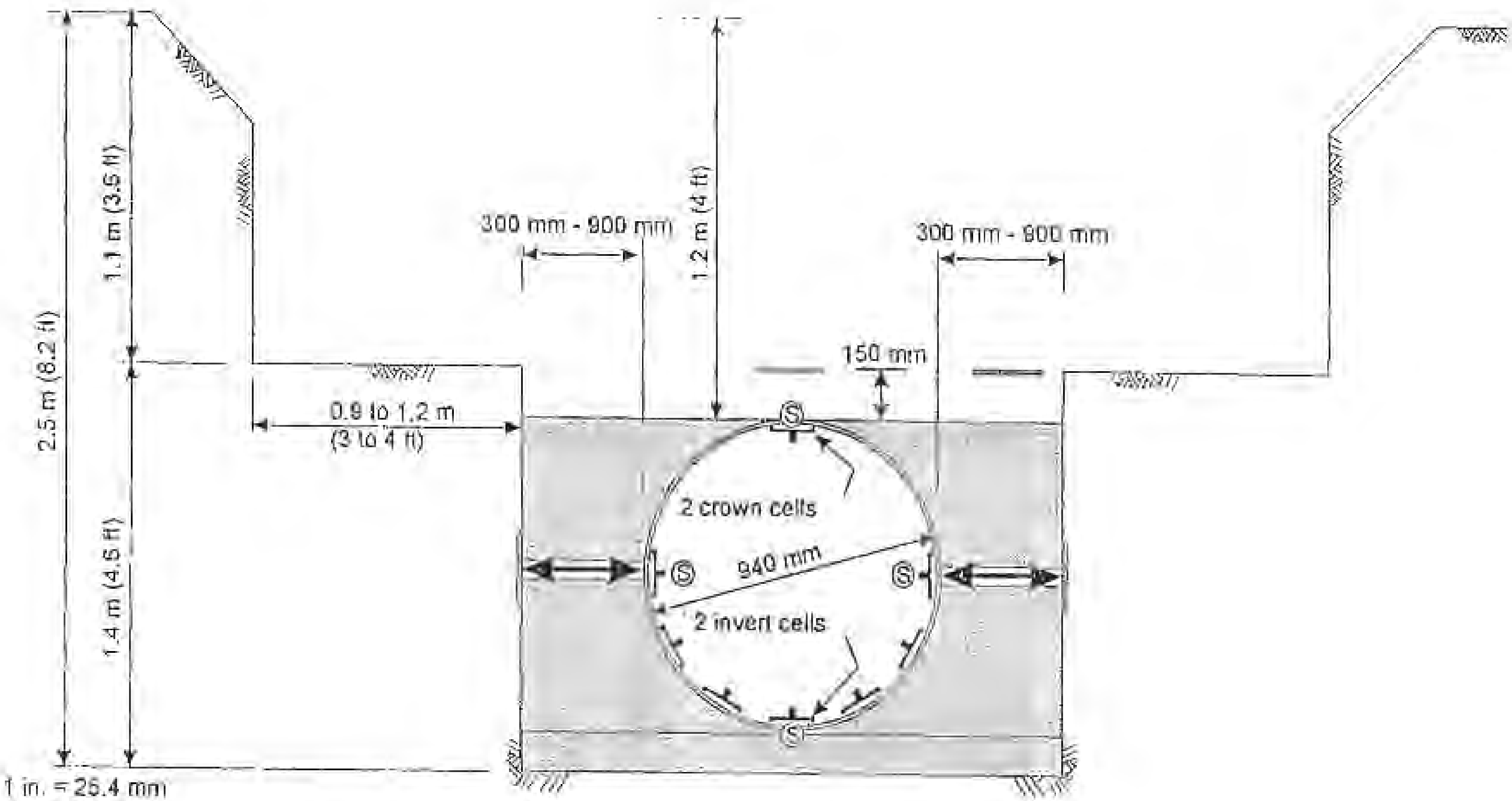

1 in. = 25.4 mm
1 ft = .305 m

Soil strain gauge
Earth pressure cell
Interface pressure cell (beam bending type)
Ⓢ - Circumferentially and longitudinally oriented resistance strain gauge on inside and outside surface

Layout for 1524 mm pipe is similar.

Figure 4.34 Cross-Section of Metal Pipe in Trench with Instrumentation

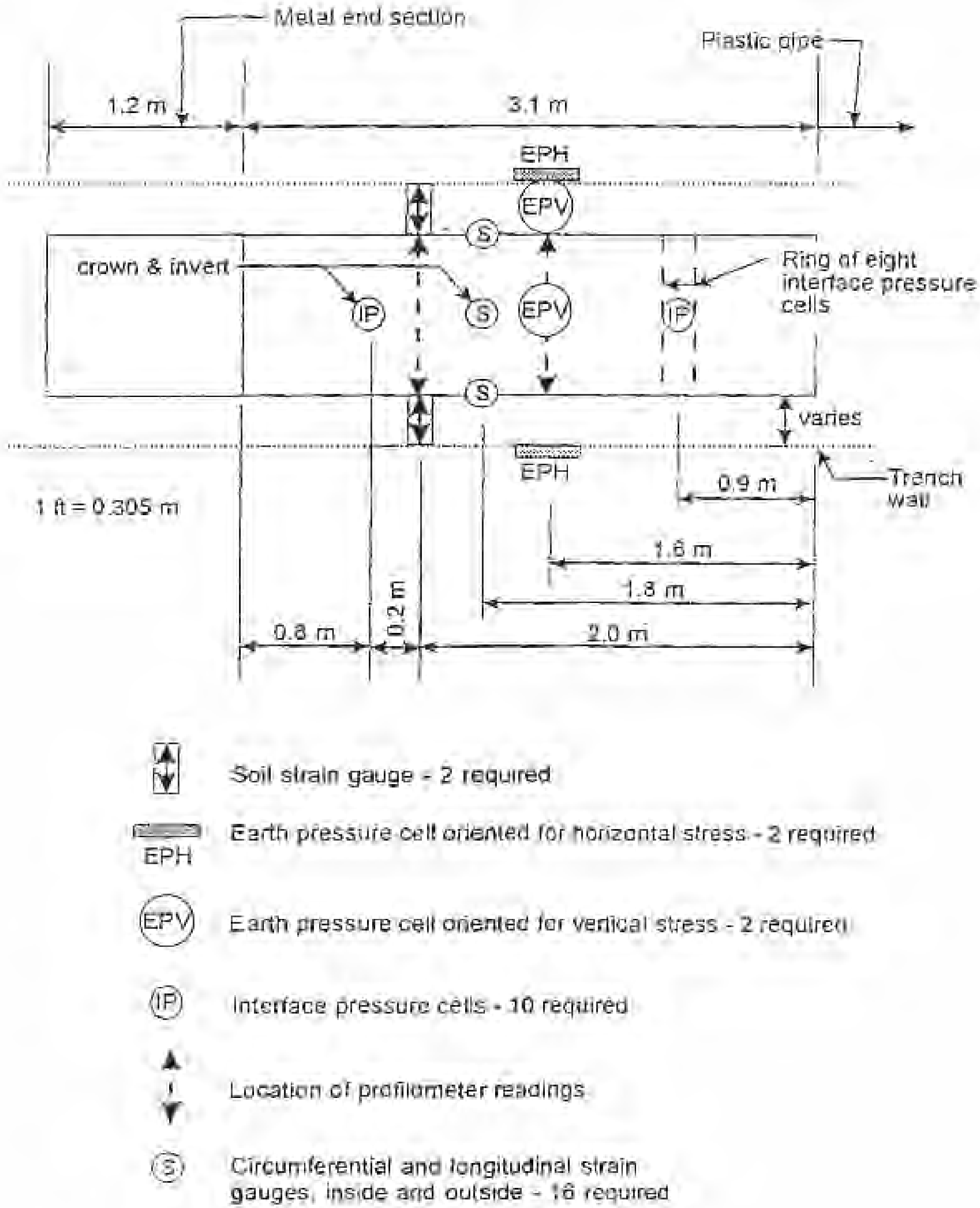

Figure 4.35 Longitudinal Instrumentation Layout for the Metal Pipe

4.2.5 Test Procedures

The principal purpose of the test was to closely monitor the pipe and soil behavior that take place during the installation and backfilling process. This was accomplished by taking measurements after nearly every layer of backfill was placed at the sides of the pipe. Backfill was placed to a depth of 1.2 m (4 ft) over the pipe for all tests. At the end of a test, the site was immediately re-excavated to retrieve instruments and pipe and to inspect the condition of the bedding.

If the protocol for a test called for compacting the bedding, then this was done with the vibratory plate. Compaction of the backfill was accomplished with the same vibratory plate and rammer compactors that were used for the laboratory tests (see section 4.1.4). If the test plan called for compaction, then two coverages were always used. Backfill over the top of the pipe was compacted with a Bomag, double drum, walk behind, and vibratory roller. The soil unit weights for each type of material and compaction equipment was quite consistent. The data are summarized in table 4.12 for the stone and silty sand materials, expressed as a percentage of maximum dry density (AASHTO T-99), and in table 4.13 for the CLSM and the in situ materials over the pipe, expressed as wet unit weight.

Table 4.12
Soil Compaction Test Results and Moisture Contents

Soil type	Compactor	Test Nos.	Compaction Test Results		Average Moisture Content
			Ave. % of Max. Unit Weight (AASHTO T99)	Stand. Dev. kN/m^3 (No. of measurements)	
Stone	Rammer	1,3,9	92	0.5 (26)	2
	Vibr. plate	4,11,13	85	0.5 (14)	3
	None	2,12	79	0.4(8)	4
Silty sand	Rammer	6,8	95	0.2 (11)	8
	Vibr. plate	7,14	89	0.2 (13)	7
	None	5	82	0.5 (6)	5

1 kN/m^3 = 6.4 lb/ft^3

Table 4.13
Compaction Test and Moisture Content Results for In Situ Soils

Soil type	Compactor	Test Nos.	Ave. Wet Unit Weight kN/m^3	Stand. Dev. kN/m^3 (No. of test measurements)
In situ sand	Bomag	1,3,4,6-8	20.1	0.6 (48)
	None	2,5	17	0.5 (6)
In situ clay	Bomag	9-14	18.7	0.8 (28)
CLSM	–	10	20.9	0.2 (2)

1 kN/m^3 = 6.4 lb/ft^3

In general water contents during compaction were below optimum. Only a minimal effort was made to introduce moisture to improve compactibility, as this was deemed more closely related to actual practice. Moisture was added only when the material became dusty and difficult to work with.

Note that although the vibratory plate compactor has a greater mass, the rammer compactor produces substantially higher soil stresses during compaction because of the smaller plate area and impact type of compaction. Table 4.12 shows that the rammer produced significantly higher soil unit weights than the vibratory plate when the same number of coverages were applied.

4.2.5.1 Trench Layout

As noted for each test, the concrete, plastic, and metal pipes were laid end to end as shown in fig. 4.29. Most trenches were excavated twice, the first test was conducted in a trench as wide as the pipe outside diameter plus 0.6 m (24 in.), called the narrow condition, and then, while retrieving the pipe from the first test, the trench was widened to equal the pipe outside diameter plus 1.8 m (6 ft) for the second test. For test 14, an intermediate width of the pipe outside diameter plus 0.3 m (3 ft) was used. This trench was only excavated once. Test 10, with CLSM backfill was conducted in a narrow trench that was also excavated only once.

At each trench location, a custom fabricated manhole was set to provide access to the test pipe. Test trenches were excavated in both directions, allowing a total of four tests to be conducted without resetting the manhole. This arrangement allowed excavation to be ongoing in one trench while readings were being taken during backfilling of the trench on the other side of the manhole, thus optimizing the use of the construction equipment.

All trenches were benched, as shown in figs. 4.36, 4.37, and 4.38. The benching resulted in a negative projection ratio of about 0.15 for the 900 mm (36 in.) pipe and a positive projection ratio of about 0.36 for the 1,500 mm (60 in.) diameter pipe.

The concrete pipe was backfilled to the springline with the selected material for a given test (see table 4.8). Excavated in situ material, compacted in the same fashion as the select backfill was used above this level. The selected backfill material was placed to 150 mm (6 in.) above the top of the plastic and metal pipe. For all pipe, the excavated in situ material was used as final backfill from a level 150 mm (6 in.) above the top of the pipe to the ground surface.

4.2.5.2 Typical Test Sequence

Tests were typically conducted in the following steps. Trench configurations and lifts are shown in figs. 4.37 to 4.38. Deviations from these procedures for specific tests are noted in the following subsections.

1. Trenches were excavated to 150 mm (6 in.) below the bottom of the test pipe. The same backfill to be used for the test was placed as bedding and compacted according to the requirements of that particular test. Pipes were set in place, and all instrumentation that was in place was read.

2. Backfill was placed in layers approximately 300 mm (12 in.) thick after compaction. Some adjustments were made to the thickness to allow layers to come to certain target elevations and to accommodate the different outside diameters of the test pipe. After compaction, all in-place instrumentation was read.

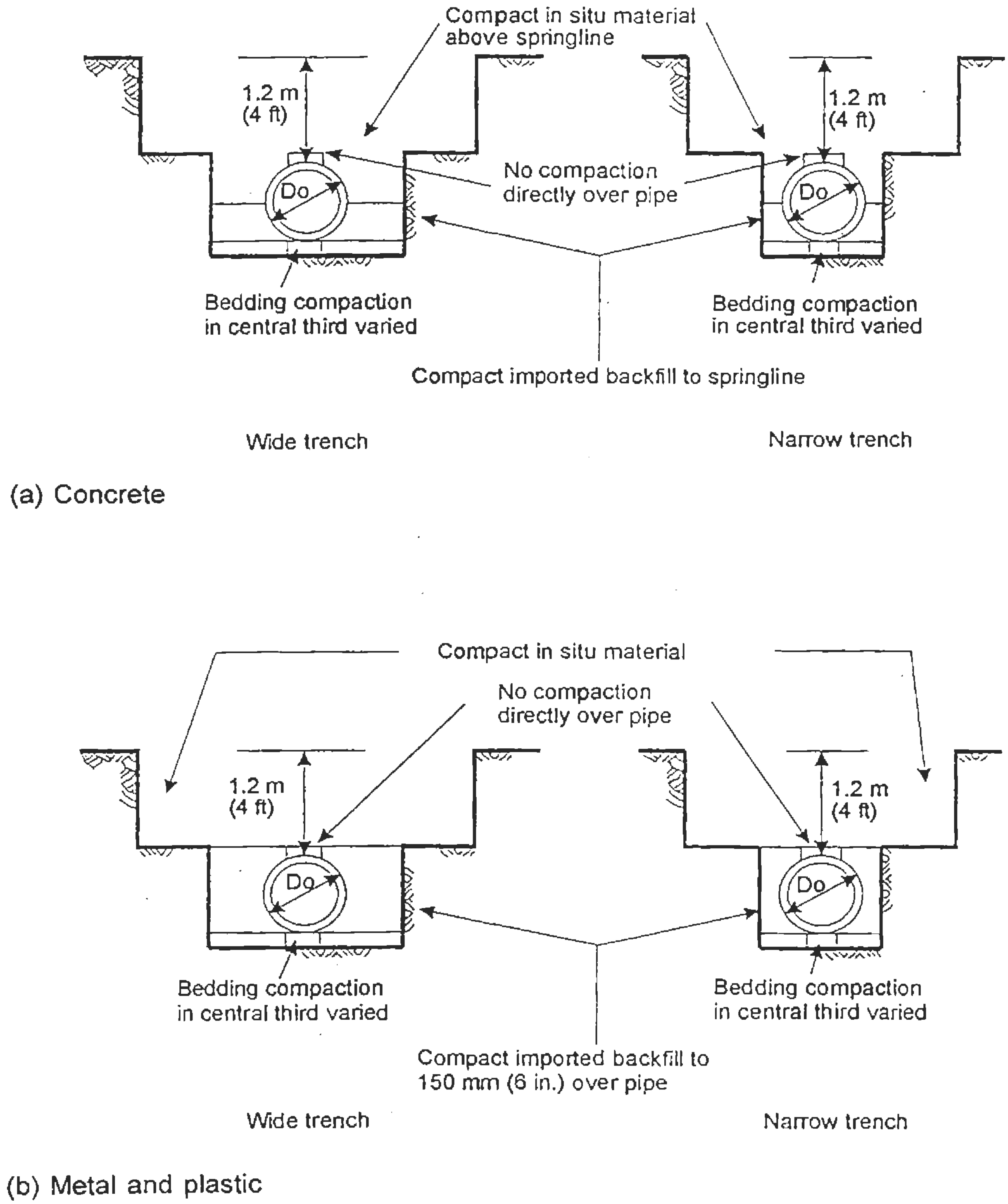

Figure 4.36 Backfill Configurations for Rigid and Flexible Pipes

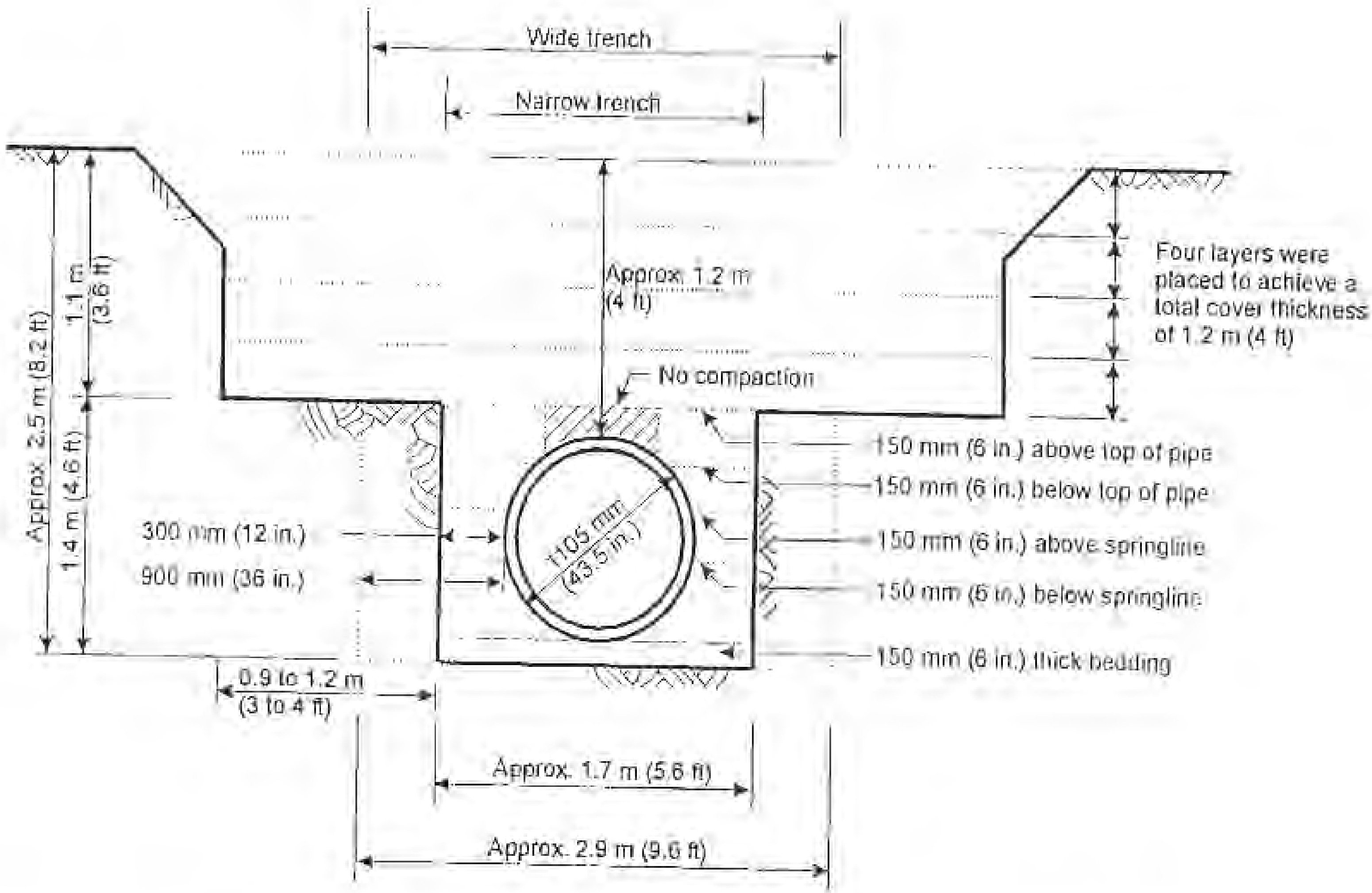

Figure 4.37 Typical Trench Cross-Section and Backfill Layer Thicknesses for 900 mm (36 in.) Diameter Concrete Pipes (Section for Plastic and Metal Pipes Similar)

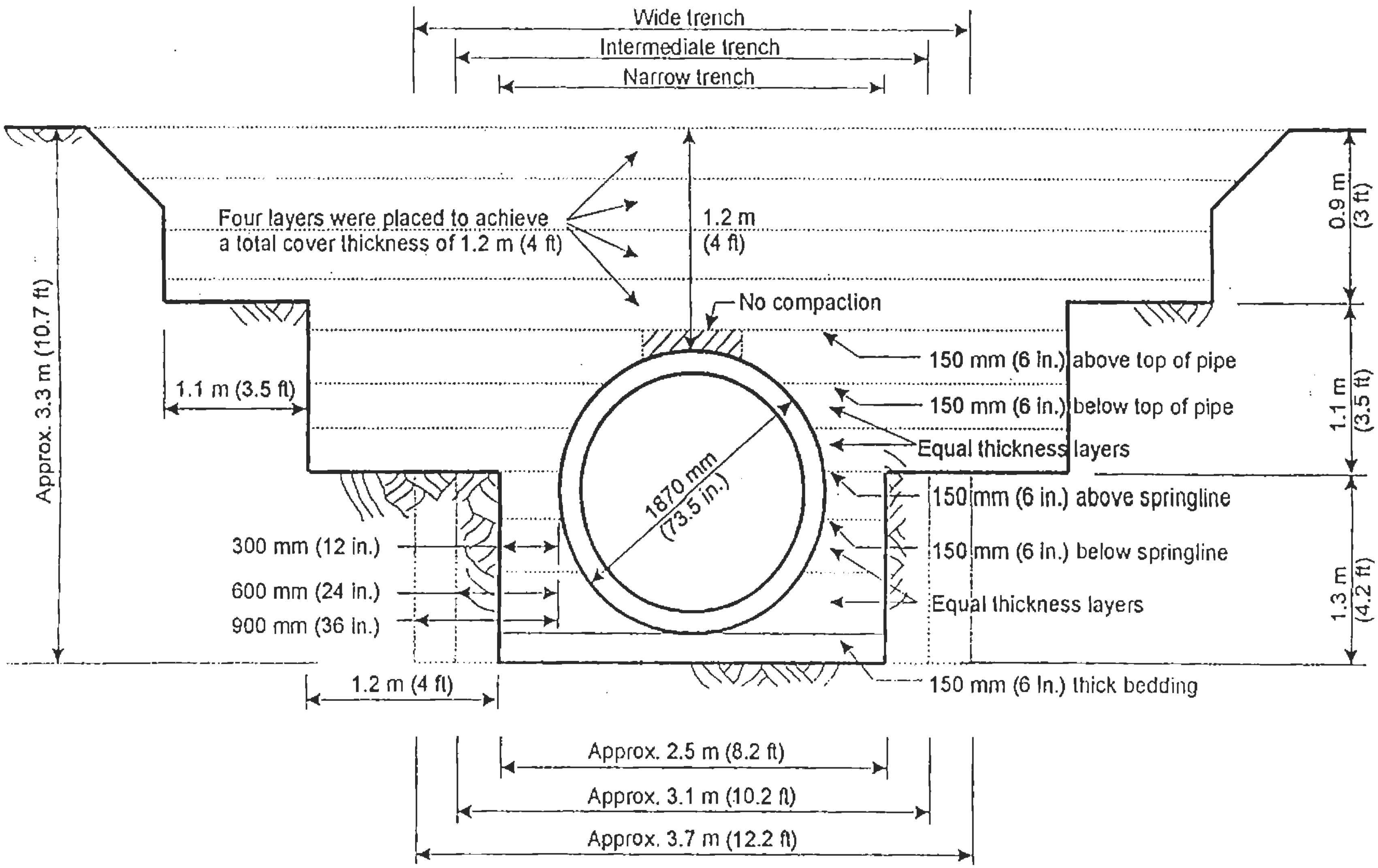

Figure 4.38 Typical Trench Cross-Section and Backfill Layer Thicknesses for 1,500 mm (60 in.) Diameter Concrete Pipe (Section for Plastic and Metal Pipe Similar)

3. The trench wall earth pressure cells and the soil strain gages were installed after placing, but before compacting, the backfill layer that came to 150 mm above the springline. The instruments were installed by digging small holes in the backfill. The trench wall was smoothed as much as possible prior to placing instruments up against it. Sand was tamped into any space that was left behind the instrument. After placing the instruments the holes were refilled, initial readings were taken, then the layer was compacted according to the requirements of the plan.

4. The backfill layer that came to 150 mm (6 in.) above the top of the pipe was left uncompacted for a width of 0.45 m (18 in.) centered over the test pipe. After the rest of this layer was compacted, the earth pressure cells used to measure vertical soil stresses were installed, and initial readings were taken.

5. Backfilling was completed with four approximately equal layers of in situ material, of approximately equal thickness, until the total cover over the pipe was about 1.2 m (4 ft). Most instruments were read after compacting each layer; however profilometer readings were taken only after the second and fourth layers.

6. When the fourth layer of in situ material was compacted the test was complete. The pipe were re-excavated to examine the bedding and haunching and to retrieve the test pipe and instruments for use on the next test.

4.2.5.3 Deviations from Typical Test Procedures

The vagaries of the weather, the need to complete all of the tests in a short period of time, and a desire to maximize the information obtained from the tests resulted in deviations from the standard procedures. These deviations are summarized below.

Test 4 – While excavating to remove the test pipe after completion of the test, a thunderstorm flooded the trench and prevented inspection of the bedding under the plastic and metal pipe.

Tests 5, 6, 7, 8, and 14 – After placing and compacting the bedding for test 5, the trench was left overnight. During this time, groundwater seepage saturated the silty sand creating a running soil condition. The soft soil was excavated and replaced in the worst areas. To avoid this problem, the bedding material was changed to a concrete sand.

Test 11 – After placing and compacting the first layer of in situ material over the top of the pipe, heavy rains occurred for several days, flooding the trench and filling the test pipe with water. The water was pumped out and the instruments dried. Work was restarted after a delay of 7 days.

Test 10 – CLSM backfill was used for test 10. For this test, imported bedding was not used. The pipe were set on bags of gravel to hold them off of the trench bottom and allow the CLSM to flow underneath. Bags of gravel were also placed on top of the plastic and metal pipe to minimize the risk of flotation. The CLSM was produced at a concrete batching plant and delivered to the site in a concrete truck. The flowability of the mix was checked using a 75 mm (3 in.) diameter, 150 mm (6 in.) long tube. CLSM was placed and leveled in the tube which was then raised. The CLSM had to spread to a diameter of at least 225 mm (9 in.) to indicate proper flow characteristics. CLSM was received in two deliveries. The first delivery was used to bring the fill to about 150 mm (6 in.) above the invert. About 2 hours later, the second lift was placed to just above the pipe springline. While the second lift was being placed, the metal pipe came free and raised up about 40 mm (1.6 in.). The plastic pipe, even though it was lighter, did not lift. Apparently the deep corrugations allowed the plastic pipe to develop an anchorage to the first pour that prevented flotation. The morning after the CLSM was placed, the trench backfilling was completed. For all pipe, the in situ clay material was placed and compacted with the rammer compactor to a level 150 mm (6 in.) above the crown. Backfill above this point followed the standard test procedures. Because of the nature of the test and the plan to leave the pipe in the ground for a period of time, the soil strain gages and earth pressure cells were not installed for this test. The CLSM test pipe were left in the ground for 22 days before excavation.

4.2.6 Results

Measurements taken during the field test program covered a wide range of behavior. Complete data are presented in Webb (1995), Webb et al. (1995), and Zoladz et al. (1995).

4.2.6.1 Pipe Deflections

Plots of deflection versus depth of fill are presented in fig. 4.39 for 9 of the 14 tests. The deflections generally reflect the effects of the compaction method used and the soil unit weights that were achieved. Tests compacted with the rammer, which creates the highest soil stresses during compaction, showed the most peaking (upward deflection when the backfill is at the top of the pipe, (depth of fill equal to 0.0 m), and the least downward deflection as backfill was placed over the crown. The final deflected shape for pipe with rammer compacted backfill was always ovalled upward at the end of the test. The vibratory plate compactor produced less peaking and more downward deflection as backfill was placed over the top of the pipe. This is consistent with the lower density produced by the vibratory plate. Most pipe in tests where the vibratory plate was used for compaction were deflected downward at the end of the test. Tests with no compaction applied to the backfill showed about the same peaking as tests compacted with the vibratory plate; however, these tests with no compaction showed more downward deflection due to backfilling over the pipe. One exception to the above trends is test 7 (Fig. 4.39c and 4.39d). Even though backfill was compacted with the vibratory plate, the deflection profile appears to follow that of test 5 which had no compaction. The backfill material for test 7 was the silty sand, and no haunching effort was applied. As noted above, this material is very sensitive to moisture. When this test was backfilled to a level 150 mm (6 in.) over the pipe, it was left overnight. On the following morning, several instruments showed that the backfill had softened overnight. The earth pressure and several pipe-soil interface pressure cells showed drops in stress levels, and the invert interface pressure cell showed an increase. It is believed that the silty sand took up moisture from the surrounding native material and flowed into the voids in the haunch zone, causing the drop in pressure and the increased deflections. Also, the deep corrugations of the plastic pipe, which are not filled with backfill in the lower region of the pipe may have provided a larger void, relative to the metal pipe, which could explain part of the increased deflection in the plastic pipe for this test.

The metal pipe showed less peaking than the plastic pipe. This is expected because of the higher metal pipe bending stiffness. Peaking behavior is affected more by this pipe stiffness than is downward deflection due to backfilling over the pipe. Downward deflection is controlled more by soil stiffness. This is also reflected in the higher peaking deflections in the 1,500 mm (60 in.) diameter plastic pipe than in equivalent tests in the 900 mm (36 in.) diameter plastic pipe. The 1,500 mm (60 in.) plastic pipe had the lowest pipe bending stiffness of all of the pipe tested.

The smaller deflection change during the last backfill increment for the tests with no compaction of the backfill indicates a reduction in the rate of deflection. This could suggest that the pipe deflected sufficiently to mobilize support from the trench walls, which were much stiffer than the backfill or that the low compactive effort left voids in the backfill around the pipe which closed up, resulting in a higher rate of deflection during the first increments of backfill.

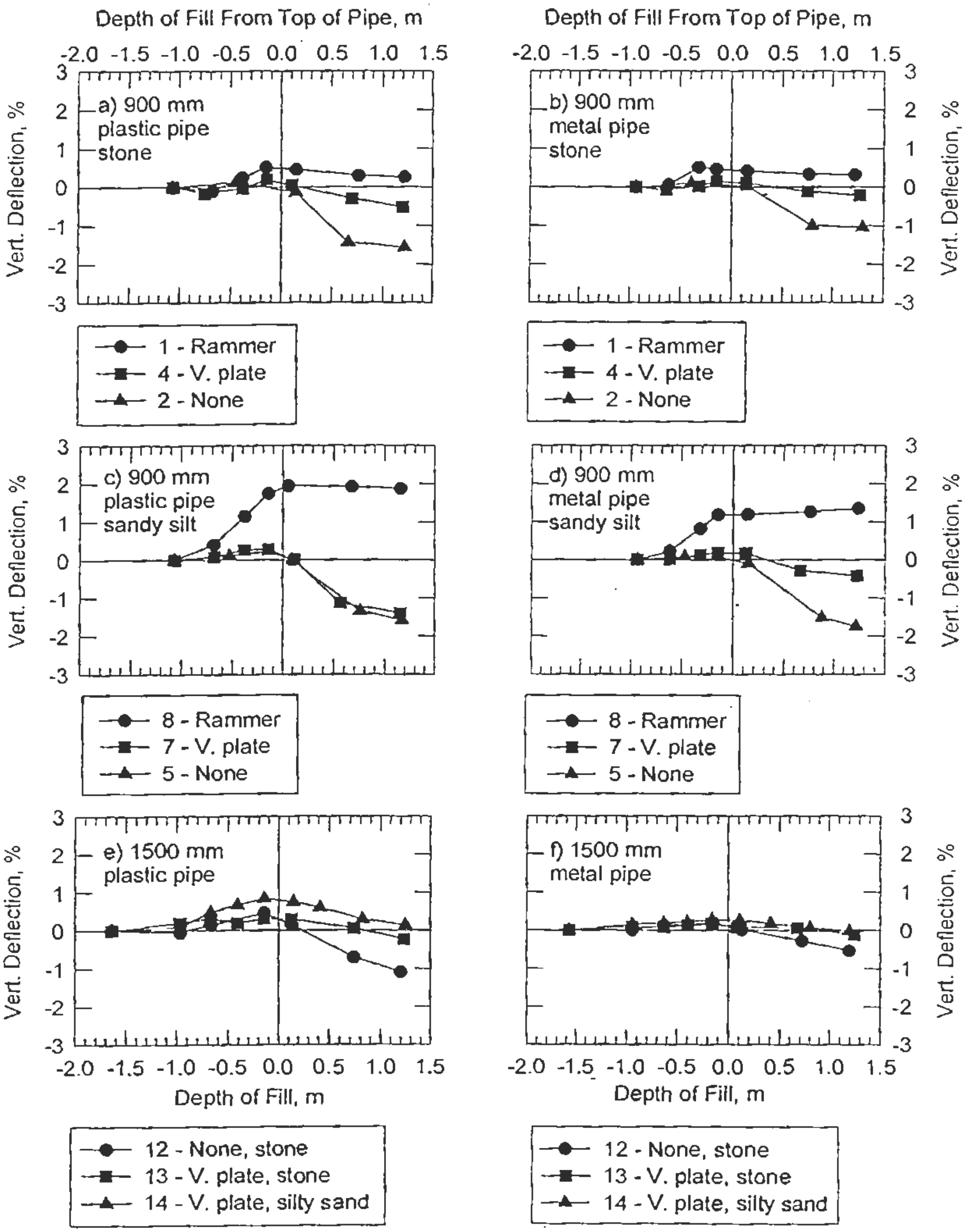

Figure 4.39 Typical Plots of Vertical Deflection Versus Depth of Fill

Vertical deflections for all tests are summarized in figs. 4.40a and 4.40b which show the peaking deflection, the change in deflection during backfilling over the top of the pipe, and the final deflection at the end of the test. Fig. 4.40(c) shows the ratio of change in vertical deflection to change in horizontal deflection caused by backfilling over the crown. Together, Figs. 4.39 and 4.40 show:

- Significantly more peaking occurred with the silty sand backfill than the stone backfill. This is probably because of the higher lateral pressures generally exerted by the lower strength of finer grained soils and the reduced pressures due to the higher strength from the interlocking of the stone particles.
- The downward deflection in test 11 was higher than expected based on other results. This was particularly true of the plastic pipe. Test ll was flooded during the backfilling process, and the flooding apparently softened the backfill and the trench walls. This was the only test where the soil strain gages showed significant outward movement of the trench walls during backfilling over the top of the pipe.
- Tests with wide trenches show slightly more peaking during backfilling to the top and slightly less downward deflection due to backfilling over the top of the pipe than equivalent tests in narrow trenches. Tests 1 and 3 and tests 6 and 8 are used for this comparison.
- The ratio of the vertical to horizontal deflection due to backfilling over the crown is generally larger in absolute magnitude for the plastic pipe than for the metal pipe, particularly when backfill was compacted with the rammer, where the ratios were substantially larger than 1.0. This is thought to be due, at least in part, to the lower hoop stiffness of the plastic pipe. This type of pipe has been shown to undergo substantial circumferential shortening relative to traditional flexible pipe, when subjected to earth load. This shortening is seen as a decrease in vertical and horizontal diameter, hence the higher ratios of vertical to horizontal deflections.

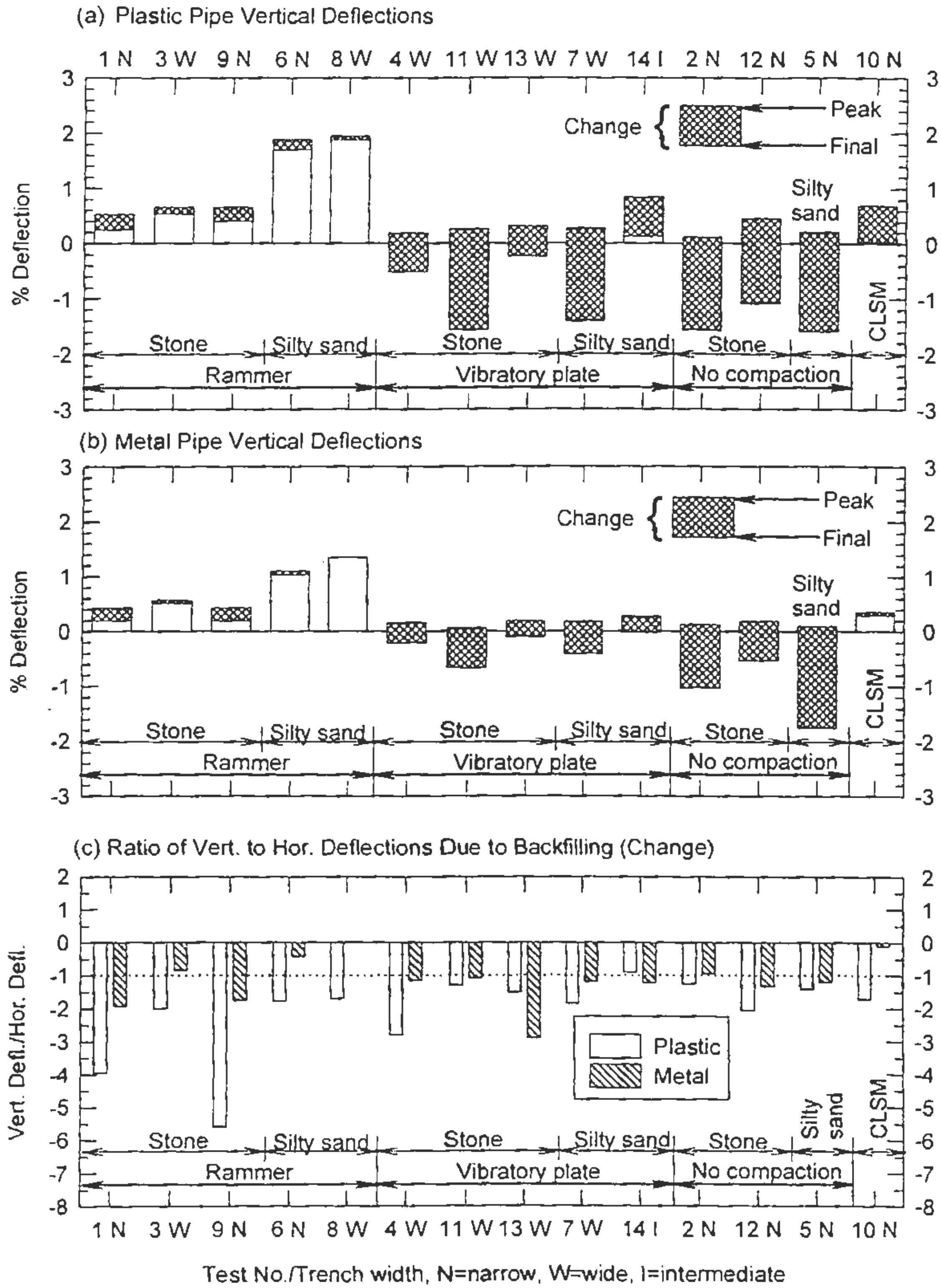

Figure 4.40 Summary of Field Test Deflections

4.2.6.2 Pipe-Soil Interface Pressures

The development of interface pressure on the concrete pipe for tests 1 to 4, with stone backfill, and partial data for tests 5 to 8, with silty sand backfill are presented in fig. 4.41. The end of test interface pressures for tests 1 to 4 in a radial plot are presented in fig. 4.42. In both figures, the invert interface pressures are the changes after the pipe was set in place, thus the weight of the pipe is not reflected.

The highest invert pressure occurs for test 2 where no haunching or compactive effort was provided. Test 1, compacted with the rammer and haunched, shows a decrease in invert pressure as the sidefill was placed and compacted, suggesting that the compactive effort actually lifted the pipe off the bedding. Tests 3 and 4 show intermediate results.

Interface pressures at thirty degrees from the invert are low regardless of compactive effort or haunching effort. This suggests that design should always consider a region of the haunch as unsupported after backfilling.

The benefit of higher compactive effort is clearly seen in the interface pressures at 60 degrees from the invert. The two tests where the backfill was compacted with the rammer show high pressures. This is beneficial for pipe performance as it indicates more uniform support for the pipe. Interface pressures at this location for test 4, compacted with the vibratory plate, showed very little difference from the pressures in test 2, where no compactive effort was applied.

For tests 5 to 8, with silty sand backfill, the data is similar to that for the tests with stone backfill. The tests where the rammer compactor was used show higher interface pressures. Of interest are the drops that occur for tests 6 and 8 at a backfill depth of about 0.1 m (4 in.) over the top of the pipe. This drop occurred overnight. As discussed previously for the deflections of test 7, the silty sand is sensitive to moisture and the overnight delay in backfilling may have allowed the material to take up water and soften. For tests 6 and 8, the drop in the radial pressure does not appear to be paralleled with an increase in deflection for the plastic and metal pipe, as was the case with test 7. This is likely because tests 6 and 8 had backfill with higher unit weights, from the rammer compaction and haunching during backfilling.

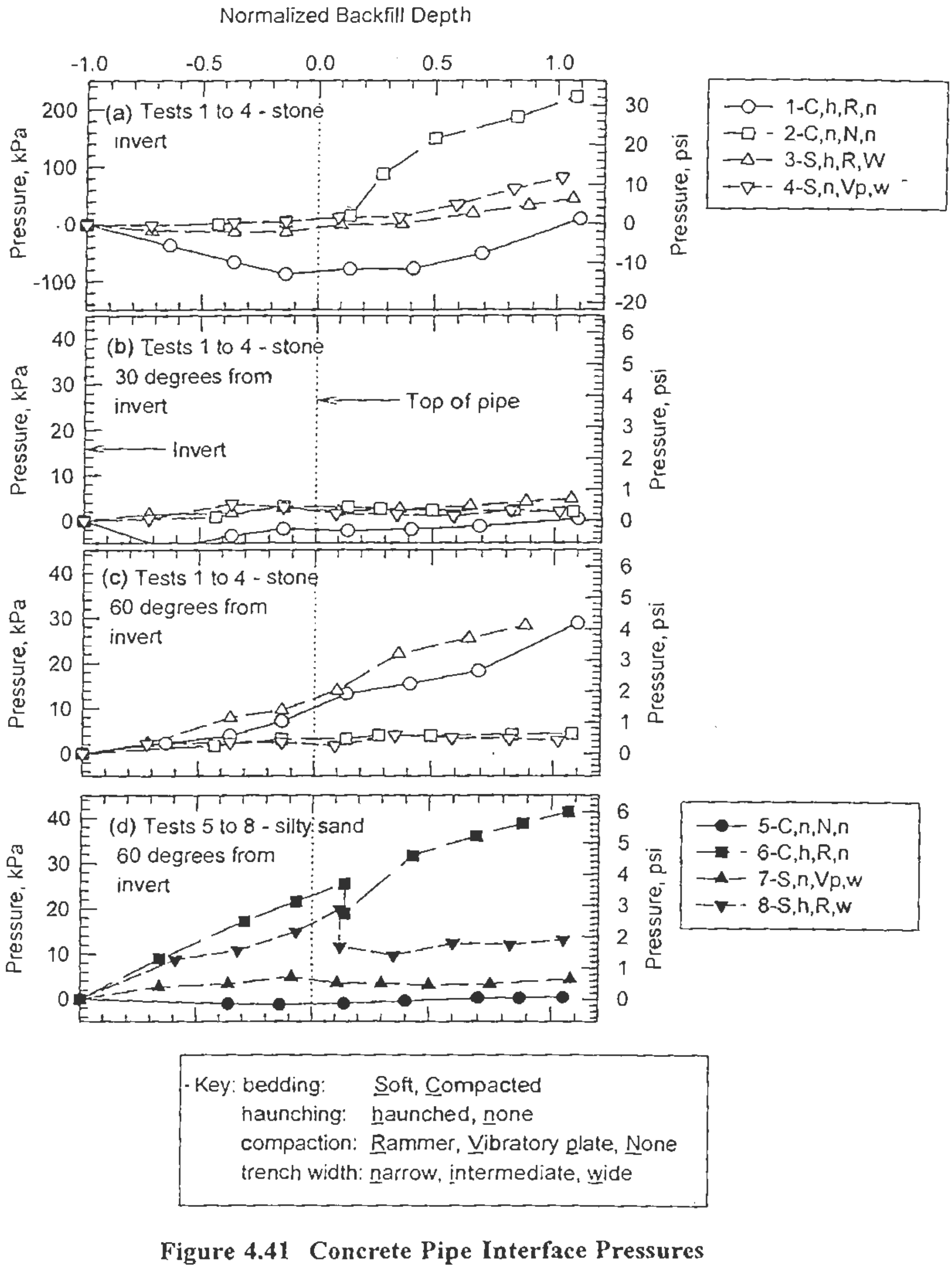

Figure 4.41 Concrete Pipe Interface Pressures

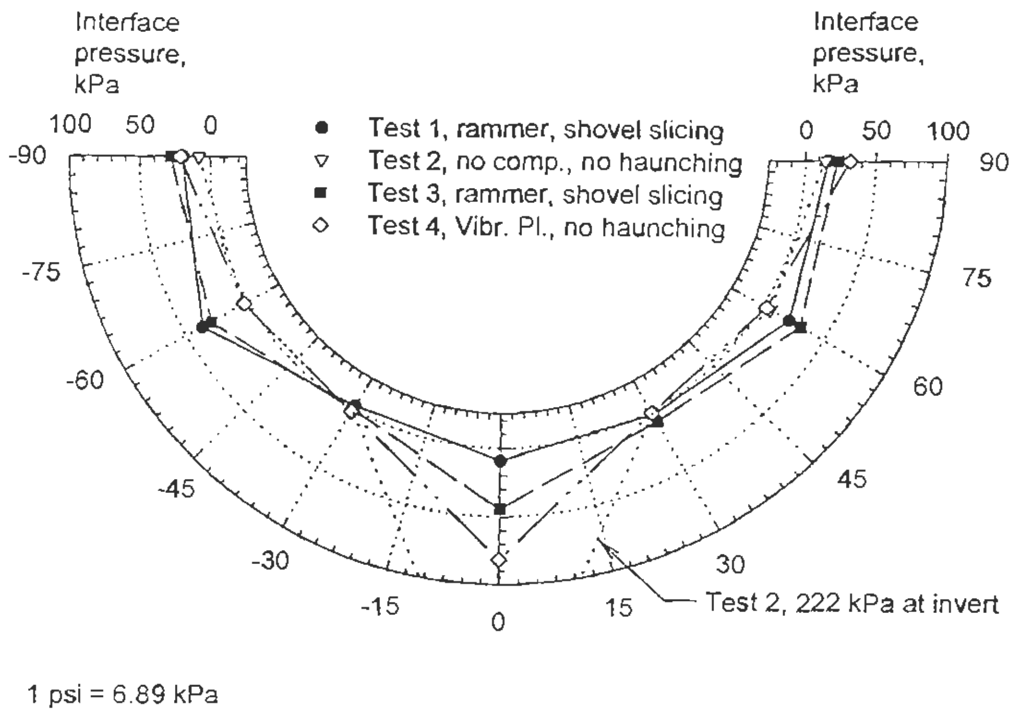

Figure 4.42 Radial Pressures, 900 mm (36 in.) Diameter Concrete Pipe, Stone Backfill

Interface pressure data for the other tests was similar. The end-of-test invert interface pressures under the 1,500 mm (60 in.) pipe (tests 12 to 14, all with haunching) were between 100 and 200 kPa (14.5 and 29 psi), which were all less than the pressure under the concrete pipe in test 2 without haunching.

4.2.6.3 Trench Wall Soil Stresses

Earth pressure cells were installed at the trench wall at the springline level to monitor the soil stress at this location as backfill was placed. Fig. 4.43 presents the data from tests 5, 6, and 7 in the form of stress versus depth of fill. Figure 4.44 is a bar chart showing, for all tests where data was taken, the trench wall stress when the backfill was at the top of the pipe, and at the end of the test. Typical trends, as displayed by the figures include:

- In tests with no compaction, lateral stresses do not develop at the springline level of any type of pipe until the backfill level rises over the top of the pipe. During backfilling above the crown, trench wall interface stresses develop beside the plastic and metal pipe, but stresses next to the concrete pipe are never greater than about 5 kPa. The trench wall stress beside the flexible pipe develops because the pipe is deflecting outward into the soil.

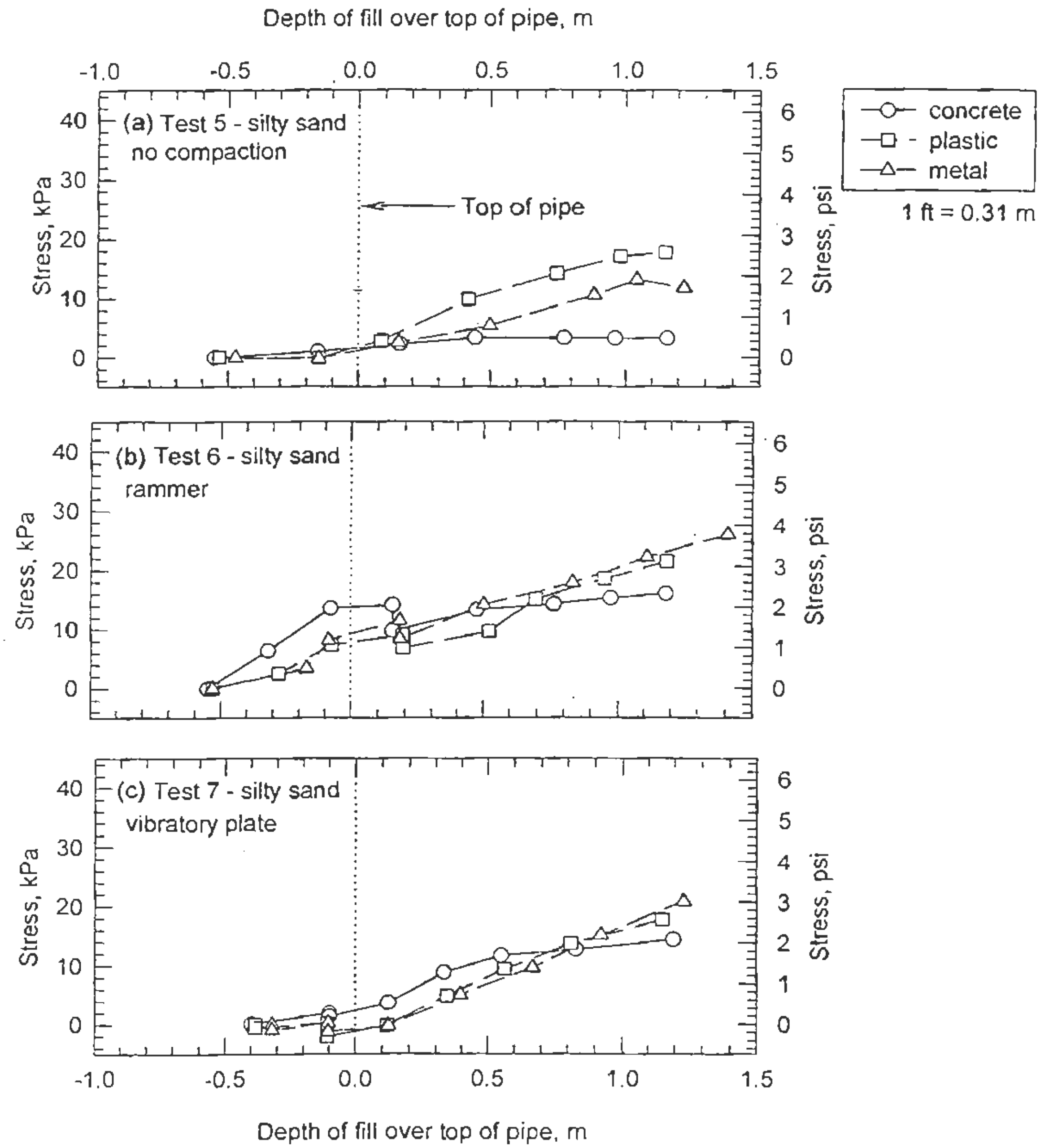

Figure 4.43 Horizontal Soil Stresses at Springline at Trench Wall-Backfill Interface

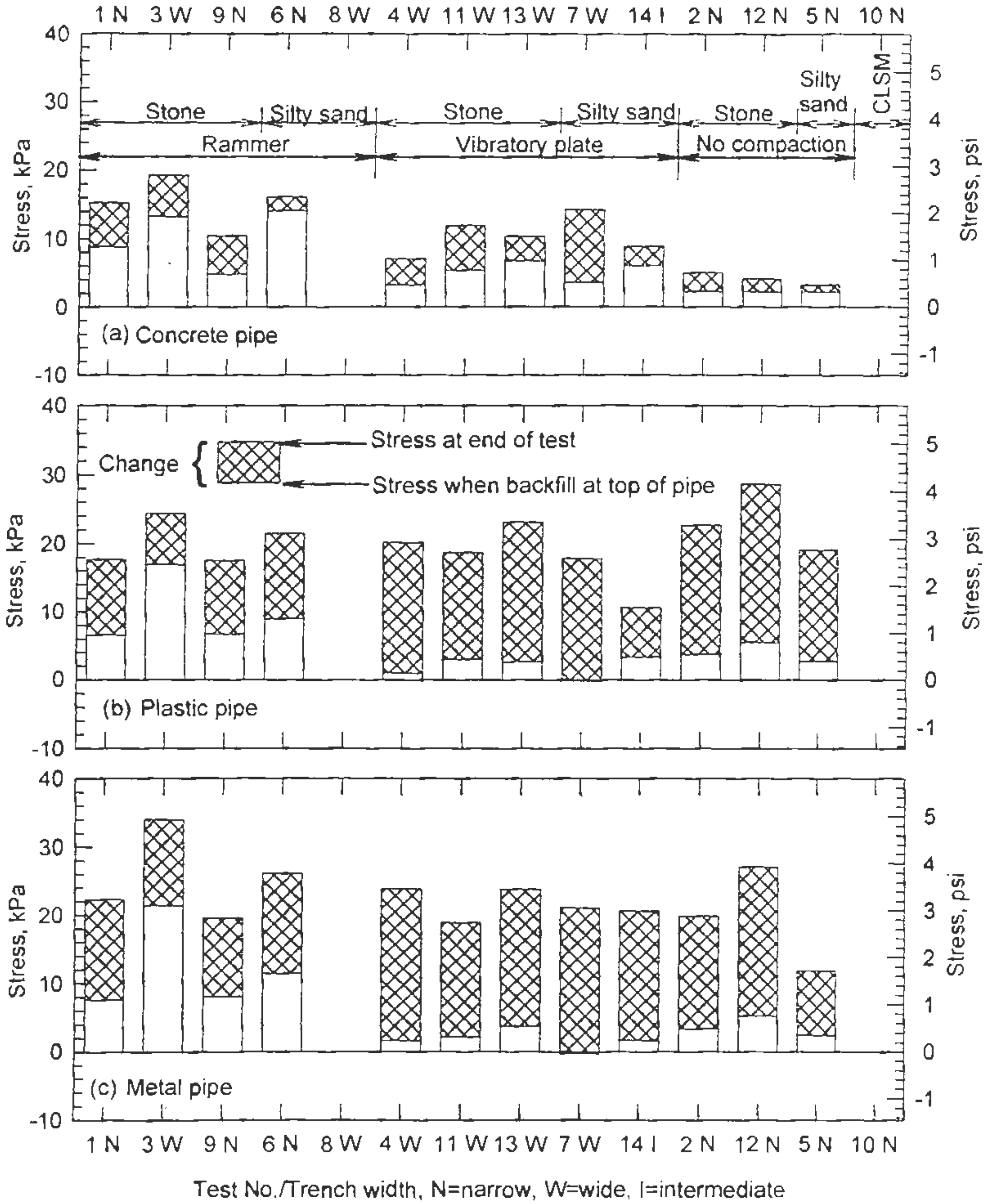

Figure 4.44 Summary of Horizontal Stresses at Trench Wall

- For concrete pipe in tests with compactive effort applied, horizontal stresses develop during compaction; however, as backfill is placed over the pipe the rate of increase in lateral stress at the trench wall is reduced.

- While the sidefill is placed, the plastic and metal pipe only develop lateral pressure when the sidefill is compacted with the rammer. When the sidefill is compacted with the vibratory plate only small trench wall stresses develop. These observations are consistent with the development of peaking deflections as the sidefill is compacted with the rammer, but not with the vibratory plate.

- The only direct comparison to evaluate trench wall stresses developed in narrow and wide trenches are tests 1 and 3. For all three pipe the trench wall stress developed while placing the sidefill was greater for test 3, the wide trench. The change in horizontal stress as the backfill was placed over the pipe was the same in test 3 as in test 1. The net effect was that all three pipe developed more lateral stress when installed in the wide trench.

- For the tests with no compaction, less trench wall stress developed in test 5, with silty sand backfill, than in tests 2 and 12 with stone backfill.

- The only instances in which no trench wall stresses developed while placing sidefill was with the flexible pipe in test 7. Actually, as shown in fig. 4.43, a small stress developed during placement of the sidefill, but it dissipated overnight. This is consistent with the previous hypothesis that the sandy silt backfill in this case softened while testing was stopped for the night.

- For test 11, during which the backfill became flooded, trench wall stresses developed to about the same magnitude as during tests 4 and 13, even though higher deflections developed during those tests.

- For the plastic and metal pipe the final trench wall pressures are generally the same at the end of all tests, regardless of type of compaction, backfill type or trench width, even though as noted above, the deflections varied widely.

4.2.6.4 Vertical Soil Stresses Over Pipe

Vertical soil stresses directly over the pipe and sidefill are summarized in table 4.14. The stresses are normalized by the geostatic soil stresses at the elevation of the gages based on the soil unit weights in table 4.12. The ratio of the crown to sidefill stress is not the arching factor but is indicative of the arching of load onto, or off of, the pipe. No trend was noted based on diameter or trench width, thus the data is presented by type of compaction.

Table 4.14
Normalized Vertical Soil Stresses Over the Test Pipes

Location	Concrete		Plastic		Metal	
	Mean	Std. Dev.	Mean	Std. Dev.	Mean	Std. Dev.
a. Rammer compactor (Tests 1, 3, 6, 8, 9)						
Crown Sidefill	0.96 1.03	0.10 0.26	0.91 1.19	0.21 0.19	1.06 1.21	0.08 0.17
Crown /sidefill (%)	94		77		88	
b. Vibratory plate compactor (Tests 4, 7, 11, 13, 14)						
Crown Sidefill	1.04 1.11	0.08 0.14	0.96 1.15	0.22 0.11	0.98 1.05	0.24 0.09
Crown /sidefill (%)	94		83		93	
c. No compaction (Test 2, 5, 12)						
Crown Sidefill	1.28 0.87	0.23 0.21	0.94 1.10	0.20 0.20	0.99 1.11	0.17 0.22
Crown /sidefill (%)	147		85		89	

Table 4.14 suggests the following:

- With one exception, the crown vertical pressure is highest over the concrete pipe, lowest over the plastic pipe and intermediate over the metal pipe. This is consistent with traditional load theory. The one exception, the metal and concrete pipes with the rammer used for compaction, is thought to be anomalous.

- For the plastic and metal pipes, the vertical soil stress over the sidefill is always greater than over the crown. This is also true for the concrete pipe with compaction. However, for the concrete pipe with no backfill compaction, the crown stress is greater than the sidefill soil stress.

4.2.6.5 Pipe Wall Strain

The development of strains in the pipe wall during backfilling paralleled the development of deflections. As an example, figs. 4.45 to 4.47 present the invert and right springline strain versus depth of fill for tests 8, 12, and 2, respectively. These tests represent the three types of compaction, two pipe sizes, and two backfill types used in the tests. Peaking develops in test 8 during placing and compaction of the sidefill and stabilizes or partially reverses as fill is placed over the pipe. In test 2, with no compaction, there is very little peaking strain, but notable strain as backfill is placed over the crown. The plastic pipe strains in test 12, with the 1,500 mm (60 in.) diameter pipe, are quite small because the profile depth of the 1,500 mm (60 in.) plastic pipe is less than that of the 900 mm (36 in.) diameter pipe, thus there is far less bending response. Strains in the metal pipe follow the same trend as the plastic pipe but are much smaller, which is consistent with the relative depth of the pipe walls. Longitudinal strains in the plastic pipe are significant relative to the circumferential strains, while longitudinal strains in the metal pipe are small at all locations.

Figs. 4.48 and 4.49 show the total strain versus deflection at the end of each test for the plastic and metal pipes, respectively. Also shown on the figures is a linear regression curve for the data. For both pipe there is a reasonable linear correlation between the two parameters, but the slopes and intercepts of the regression curves differ significantly. Observations include:

- The left and right sides of each pipe show approximately the same trend, thus reasonable symmetry was achieved in the tests;
- The reversed slopes for the regression lines of the inside and outside circumferential gages suggest that strains are dominated by bending effects. (The one exception to this is the crown gages in the metal pipe, where the outside gages show a negative slope. The relatively parallel slopes suggests that hoop forces are significant. The reason for this is not clear at this time.);
- The longitudinal strains in the metal pipe are small and do not appear to be related to deflection; and
- The longitudinal strains in the plastic pipe are significant (of equivalent magnitude to the circumferential strains) at all locations except at the inside gages at the springline.

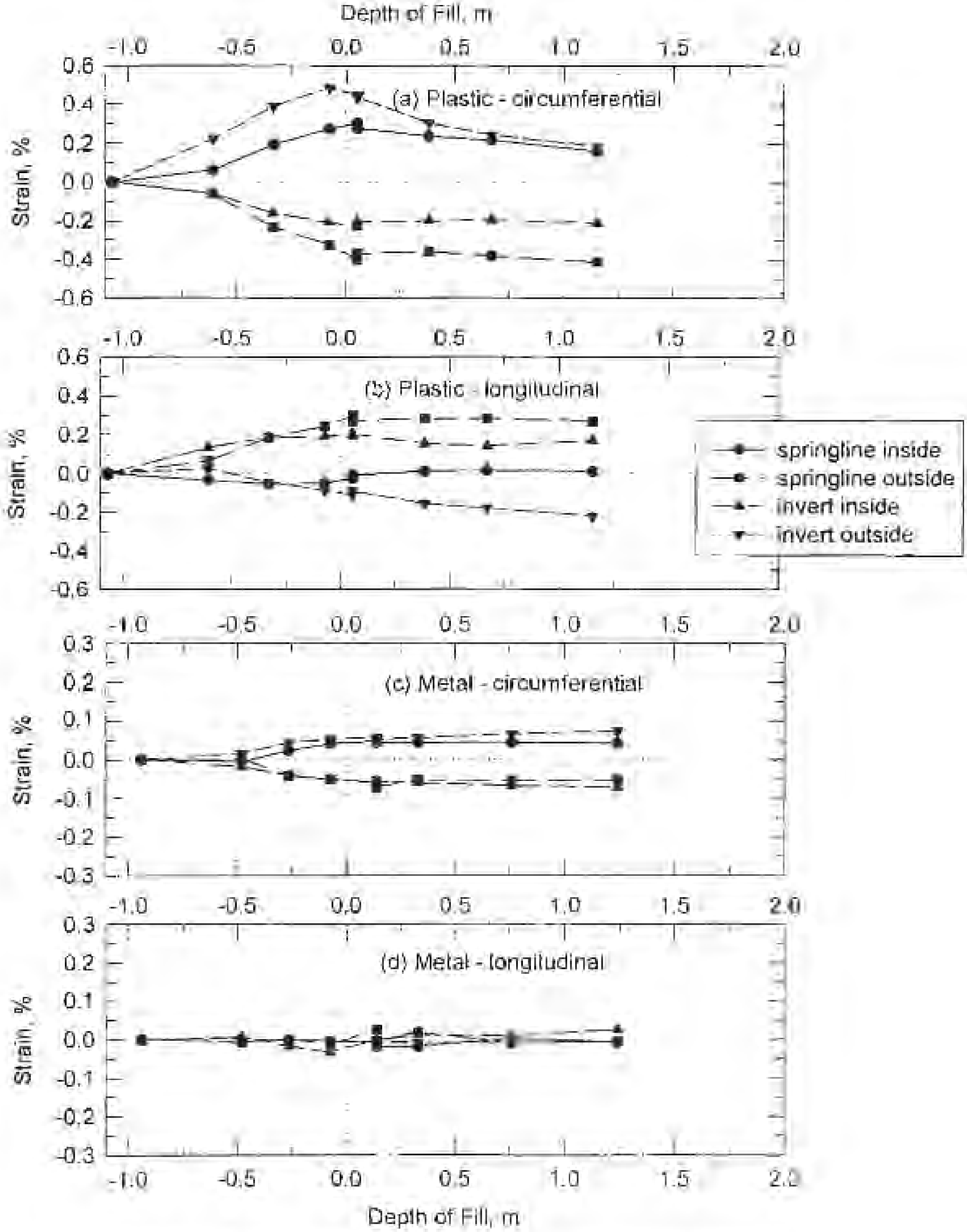

Note: Test 8 was conducted in a wide trench with silty sand backfill and was compacted with the rammer.
1 ft = 0.31 m

Figure 4-45 Pipe Wall Strains From Test 8

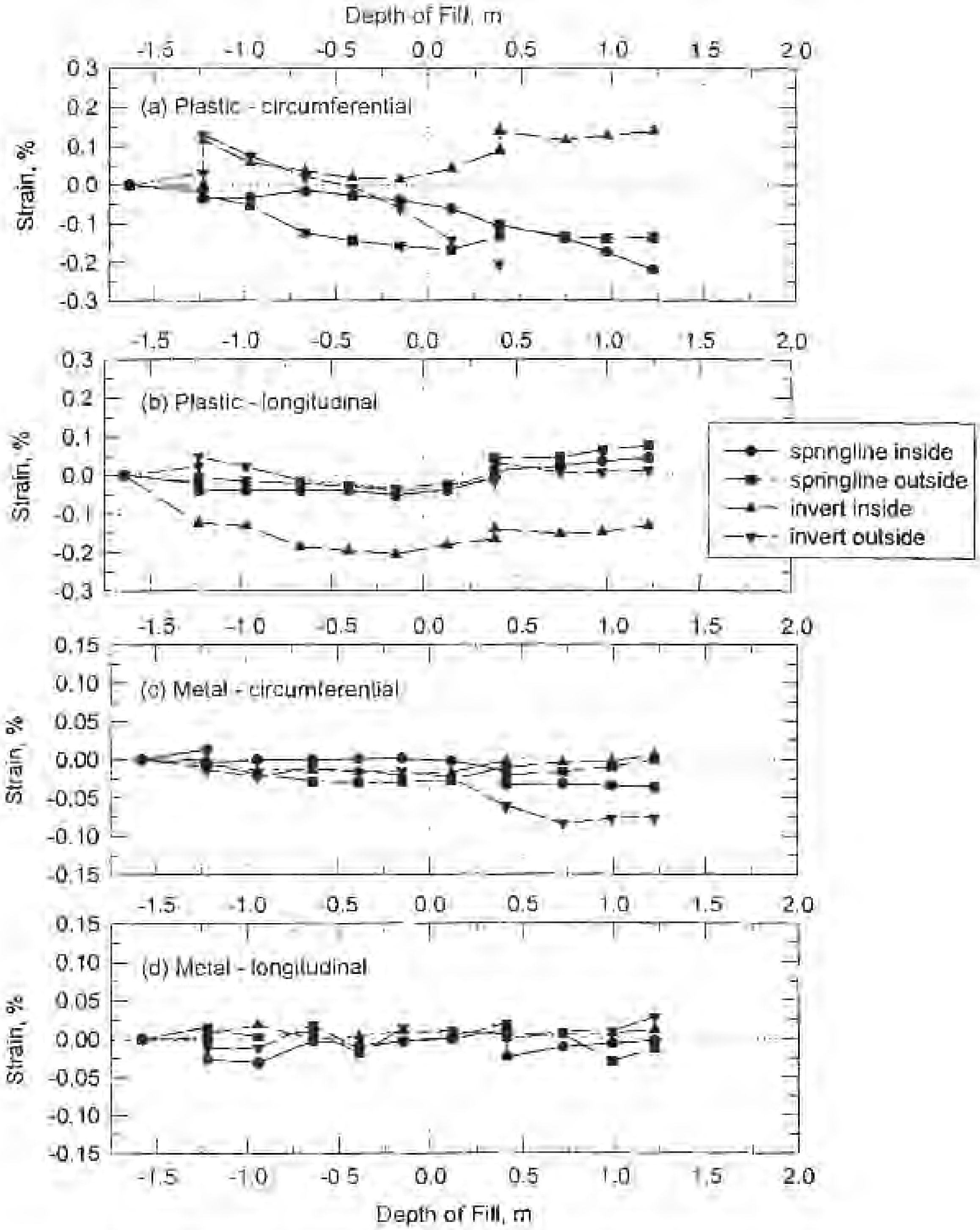

Note: Test 12 was conducted in a narrow trench with stone backfill and was not compacted.

1 ft = 0.31 m

Figure 4-46 Pipe Wall Strains From Test 12

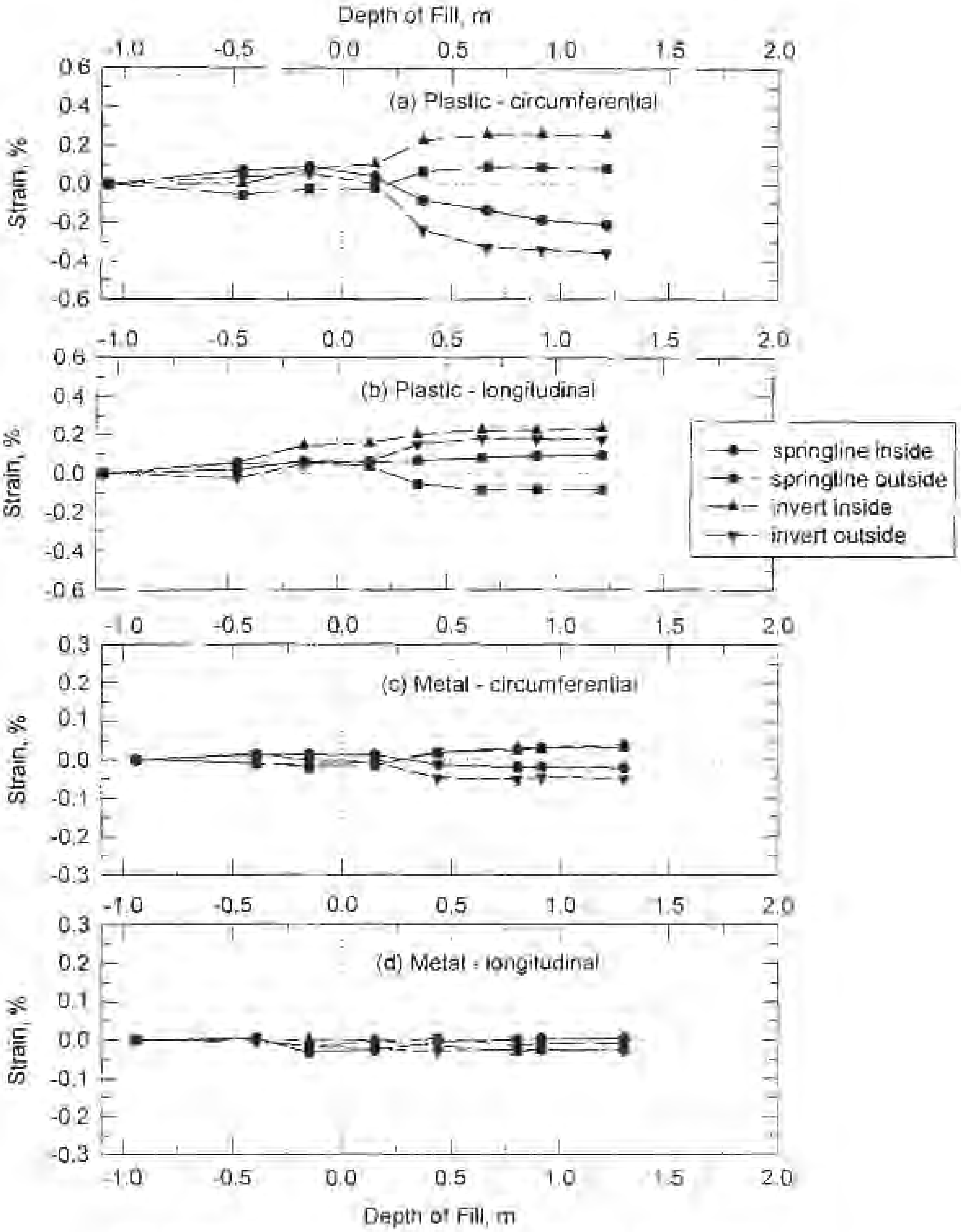

Note: Test 2 was conducted in a narrow trench with stone backfill and was not compacted.

1 ft = 0.31 m

Figure 4-47 Pipe Wall Strains From Test 2

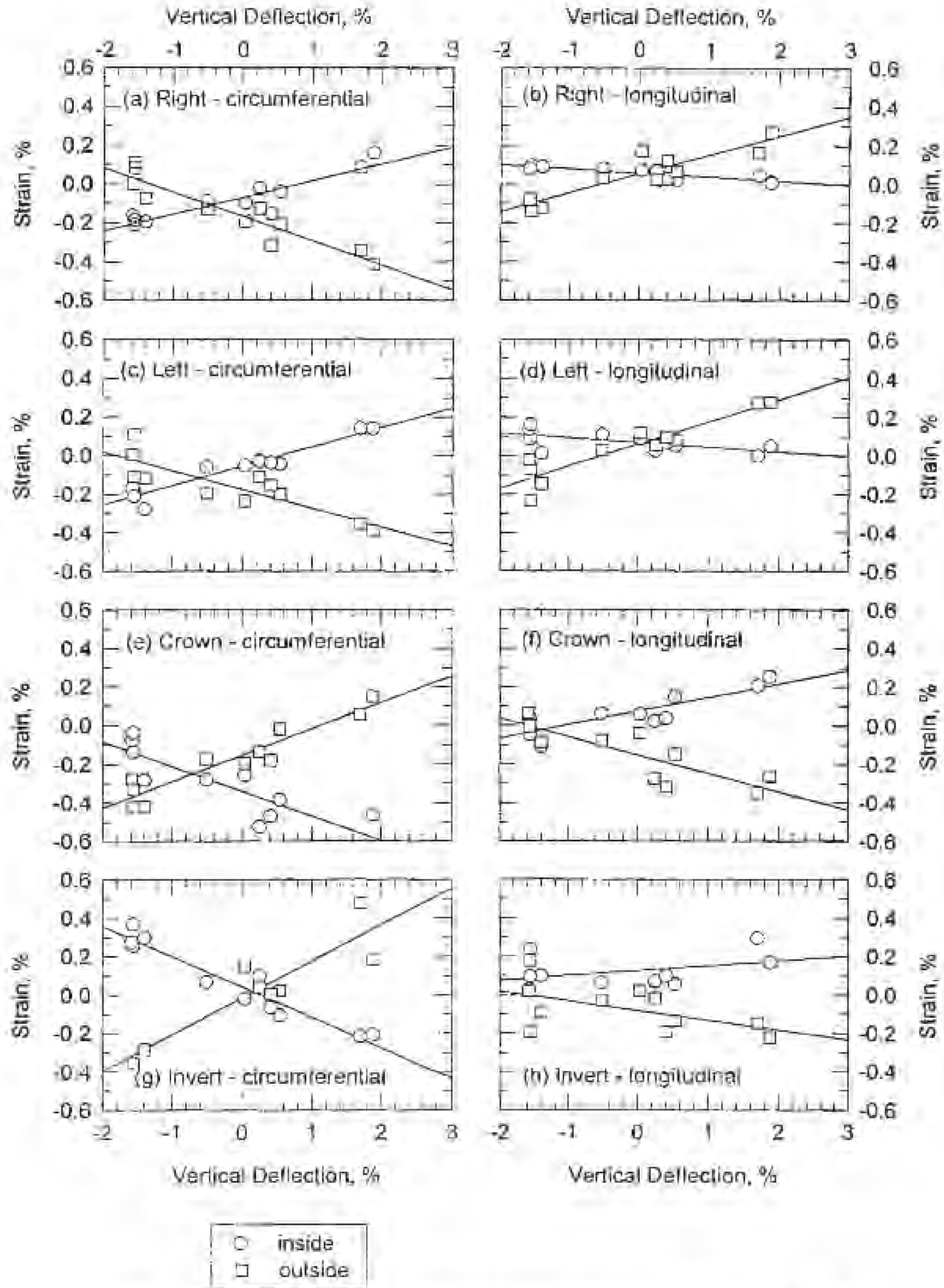

Figure 4-48 Strain and Deflection at End of Backfilling for 900 mm (36 in.) Plastic Pipe

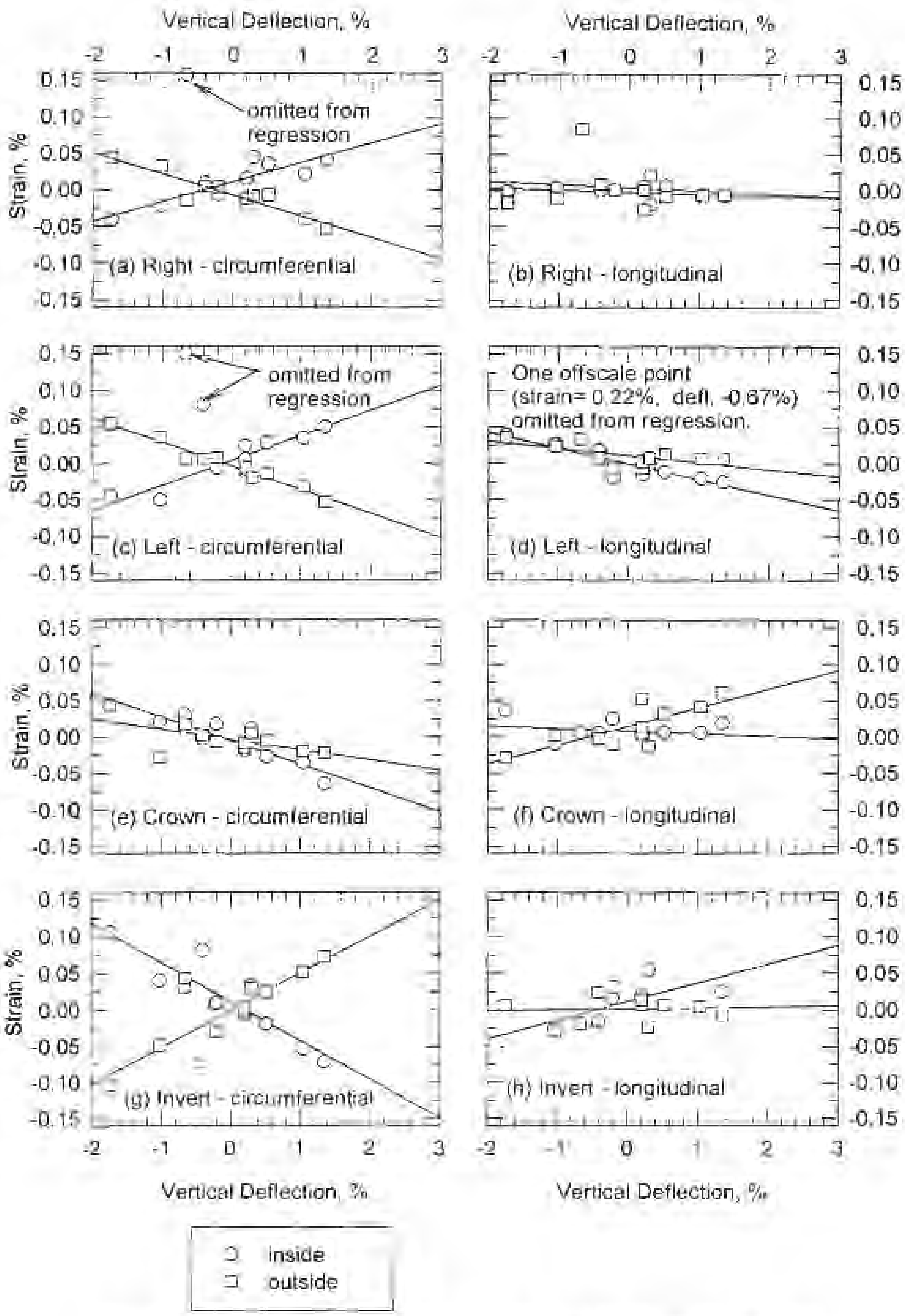

Figure 4-49 Strain and Deflection at End of Backfilling 900 mm (36 in.) Metal Pipe

The total strains can be separated into bending and hoop components. The Poisson effect circumferential strains are removed by using the measured longitudinal (ϵ_{l-m}) and circumferential (ϵ_{c-m}) strains at the same location and the relationships:

$$\epsilon_{c-d} = \frac{\epsilon_{c-m} + \epsilon_{l-m} \nu}{1 - \nu^2} , \tag{4.1}$$

and

$$\epsilon_{l-d} = \frac{\epsilon_{l-m} + \epsilon_{c-m} \nu}{1 - \nu^2} . \tag{4.2}$$

where

ϵ_{c-d}	=	circumferential strain due to direct stress,
ϵ_{c-m}	=	measured circumferential strain,
ν	=	Poisson's ratio,
ϵ_{l-m}	=	measured longitudinal strain, and
ϵ_{l-d}	=	longitudinal strain due to direct stress.

Assuming a linear distribution of strain across the wall, these direct strains can then be separated into the components due to hoop thrust and bending moment using the expressions:

$$\epsilon_h = \epsilon_{c-d-out} - \left(\frac{\epsilon_{c-d-out} - \epsilon_{c-d-in}}{c_{in} - c_{out}} \right) c_{out} , \tag{4.3}$$

$$\epsilon_{b-in} = \epsilon_{c-d-in} - \epsilon_h , \tag{4.4}$$

and

$$\epsilon_{b-out} = \epsilon_{c-d-out} - \epsilon_h , \tag{4.5}$$

where

ϵ_h	=	strain duc to hoop compression forces.

$\epsilon_{c\text{-}d\text{-}out}$ = outside strain caused by direct stress,

$\epsilon_{c\text{-}d\text{-}in}$ = inside strain caused by direct stress, and

c_{in} = distance from centroidal axis to inside surface, mm, in.,

c_{out} = distance from centroidal axis to outside surface, mm, in.,

$\epsilon_{b\text{-}out}$ = strain on outside surface caused by bending forces, and

$\epsilon_{b\text{-}in}$ = strain on inside surface caused by bending forces.

Figs. 4.50 and 4.51 show the hoop and bending strains for the plastic and metal pipe versus depth for tests 6 and 2, respectively. The bending strains, as expected, parallel the deflection plots. The magnitude of the hoop strain in the metal pipe is very small and the data does not appear to be meaningful. The hoop strains in the plastic pipe show a trend of increasing with the depth of fill, at approximately the same rate at the invert, crown and springlines, however the peak occurs at the crown. This higher value at the crown is mostly caused by thrust developed during placement of the sidefill, and thus is not indicative that the crown develops thrust at a higher rate than the springlines because of soil placed over the top of the pipe.

Springline hoop strain, and crown, invert, and springline bending strains for the plastic pipe are presented in table 4.15. Table 4.16 presents similar data for the metal pipe, except that, as noted, the hoop strains are not presented because the data did not appear meaningful. This data will be discussed in more detail in chapter 5.

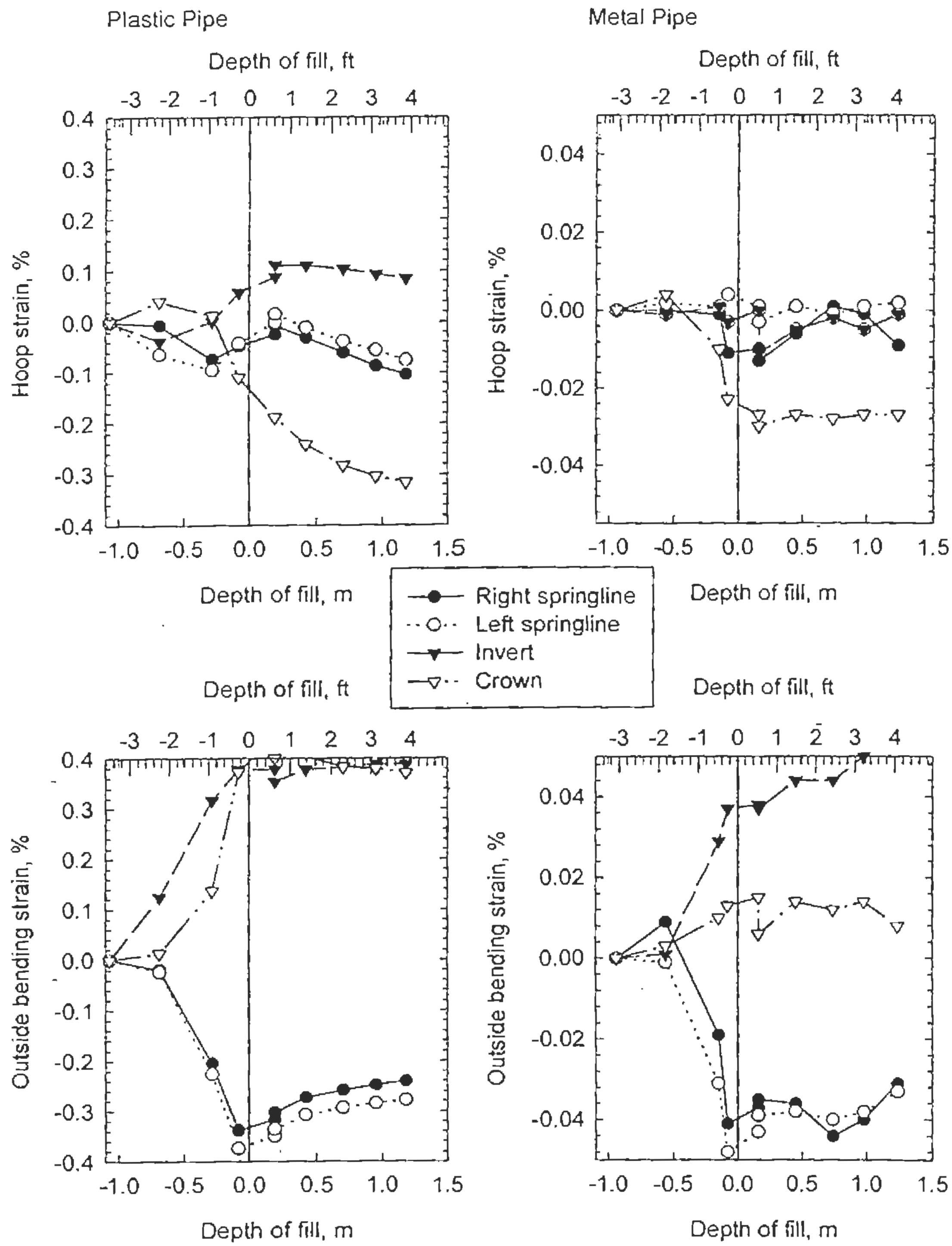

Note: Test 6 was installed with silty sand backfill in a narrow trench and compacted with the rammer.

Figure 4.50 Hoop and Bending Strains for Field Test 6

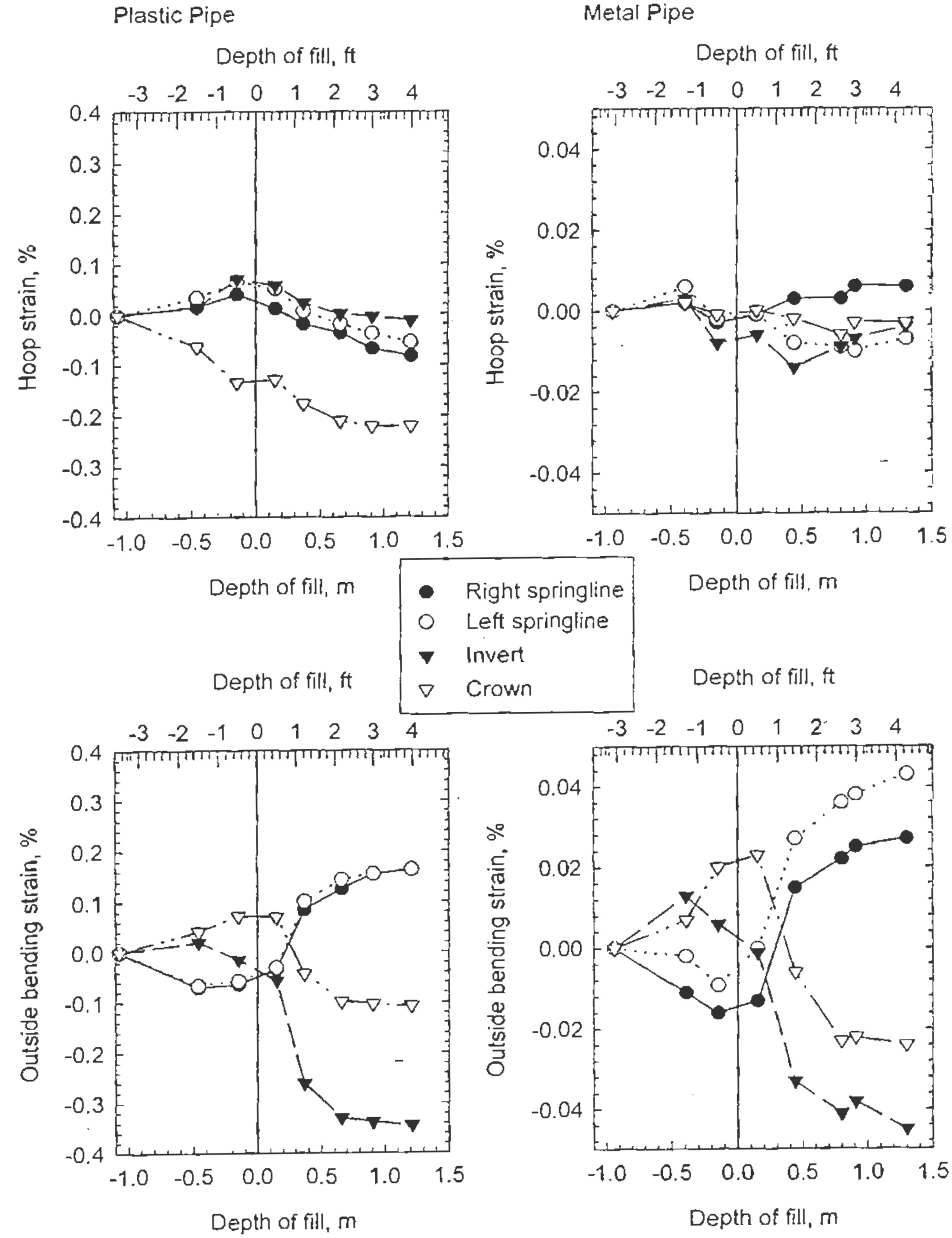

Note: Test 2 was installed with silty sand backfill in a narrow trench with no compaction.

Figure 4.51 Hoop and Bending Strains for Field Test 2

Table 4.15
End of Test Strains – Plastic Pipe

Test No.	Compaction and Backfill	Pipe strains, %			
		Springline Hoop compression	Bending, outside surface (2)		
			Springline	Invert	Crown
a. 900 mm (36 in.) Diameter Pipe					
1	Rammer/Stone	-0.058	-0.060	-0.050	0.184
3	Rammer/stone	-0.107	-0.095	0.042	0.170
9	Rammer/stone	-0.147	-0.075	-0.012	0.112
6	Rammer/silty sand	-0.062	-0.248	0.345	0.305
8	Rammer/silty sand	-0.055	-0.296	0.172	0.285
4	V. plate/stone	-0.102	-0.067	ND	0.041
11	V. plate/stone	-0.186	-0.009	ND	ND
7	V. plate/silty sand	-0.202	0.053	-0.396	-0.080
2	None/stone	-0.069	0.148	-0.390	-0.111
5	None/silty sand	-0.089	0.076	ND	-0.117
10	CLSM	-0.113	-0.073	ND	0.020
b. 1,500 mm (60 in.) Diameter Pipe					
12	None/stone	-0.155	0.084	ND	-0.013
13	V. plate/stone	-0.117	0.033	ND	0.228
14	V.plate/silty sand	-0.116	0.006	ND	0.248

Notes:
1. ND indicates no data, one of the gages did not function properly.
2. Inside bending strain is directly proportional to the outside bending strain, based on the distance from the centroidal axis and is not shown.

Table 4.16
End of Test Strains – Metal Pipe

Test No.	Compaction and Backfill	Circumferential bending strain, %		
		Springline	Invert	Crown
a. 900 mm (36 in.) Diameter Pipe				
1	Rammer/Stone	ND	0.0034	0.0075
3	Rammer/stone	-0.0258	0.0249	0.0161
9	Rammer/stone	-0.0179	0.0016	0.0110
6	Rammer/silty sand	-0.0333	0.0582	0.0144
8	Rammer/silty sand	-0.0515	0.0740	0.0302
4	V. plate/stone	0.0078	-0.0186	-0.0192
11	V. plate/stone	-0.1107	0.0041	ND
7	V. plate/silty sand	-0.0220	-0.0780	0.0015
2	None/stone	0.0373	-0.0492	-0.0246
5	None/silty sand	0.0444	-0.1143	-0.0113
10	CLSM	-0.0161	ND	-0.0029
b. 1,500 mm (60 in.) Diameter Pipe				
12	None/stone	0.003	-0.042	-0.024
13	V. plate/stone	0.004	-0.008	-0.003
14	V.plate/silty sand	-0.003	-0.028	0.007

Notes:
1. ND indicates no data, one of the four gages did not function properly.

4.2.6.6 Sidefill Soil Strain

Soil strain gages were installed to measure the change in distance between the springline of the test pipe and the trench wall. Data from these gages for test 3, with rammer compacted stone backfill, and test 5, with uncompacted silty sand backfill, is shown in fig. 4.52, which presents the average displacement from both sides of the pipe. These figures show the following characteristic trends:

- A substantial part of the extension of the gages occurs during compaction of the first backfill layer after the gages are installed (some of which may be a seating effect as the fill around the gages is compacted);

- For tests with compacted backfill very little displacement occurred thereafter (fig. 4.51(a)); and

- For tests with uncompacted backfill a notable compression occurred as backfill was placed over the crown (fig. 4.51(b)).

Data for the change in width of the soil sidefill during backfilling over the top of the pipe are presented in table 4.17.

Table 4.17
Change in Soil Sidefill Width During Backfilling Over Top of the Pipes

Test	In situ soil	Concrete	Plastic	Metal
		mm	mm	mm
1	sand	0.1	0.2	0.0
3	sand	0.4	0.2	0.2
9	clay	0.5	0.5	0.5
6	sand	-0.5	-1.4	-1.0
8	sand	gages not installed		
4	sand	2.0	1.1	0.1
11	clay	1.7	-0.5	0.9
13	clay	0.5	-0.4	-0.3
7	sand	-1.1	-2.2	-1.3
14	clay	data erratic		
2	sand	data erratic		
12	clay	1.1	-2.9	-3.0
5	sand	-0.8	-5.1	-4.5
10	clay	gages not installed		

1 mm = 0.04 in

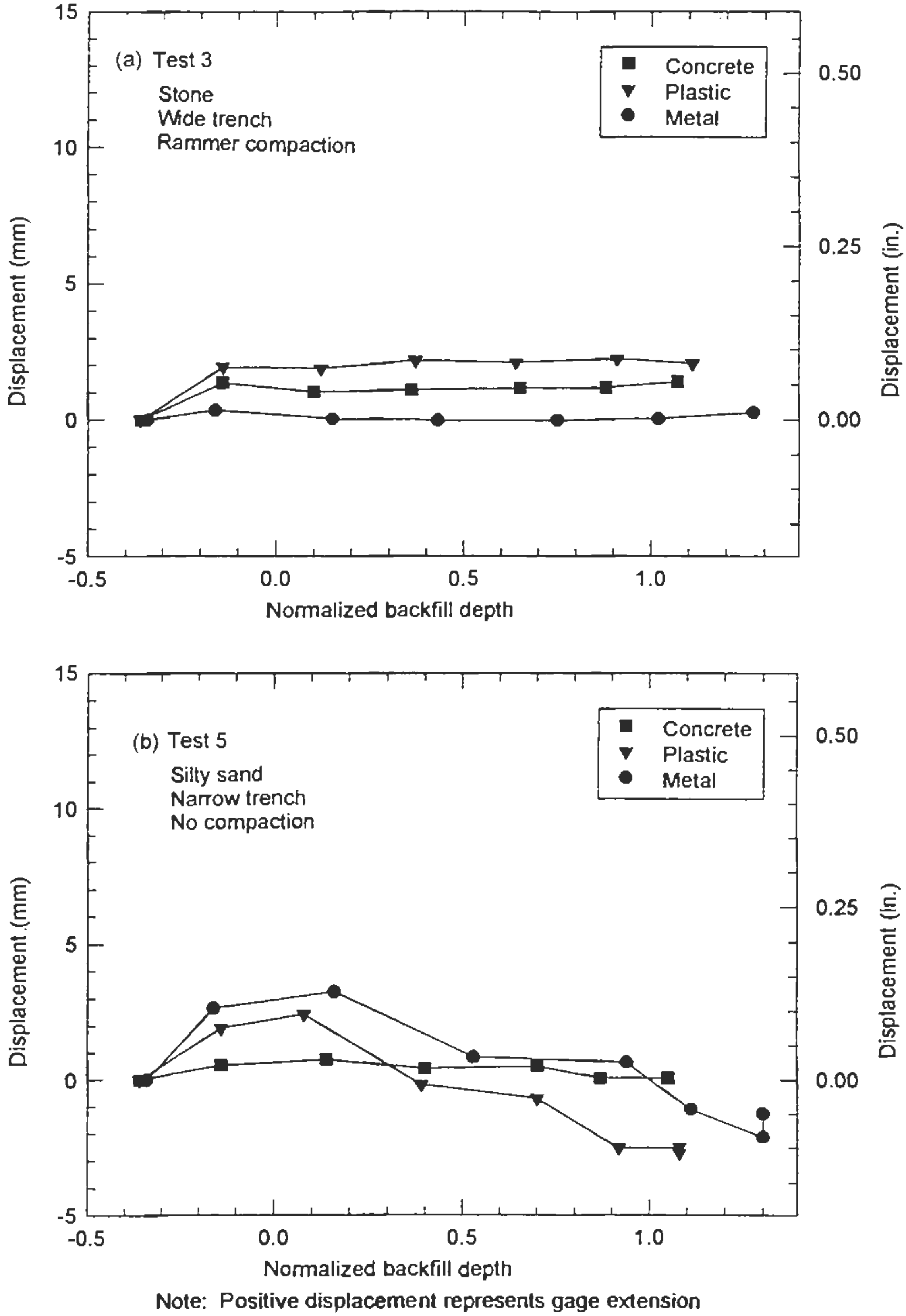

Figure 4.52 Sidefill Soil Displacement During Backfilling

In general the data from these gages were variable; but when several like conditions were averaged together, trends emerge. Several variables are evaluated in table 4.18.

Table 4.18
Change in Soil Sidefill Width – Grouped by Test Variable

Variable		Concrete	Plastic	Metal	Tests included
Type	Condition	mm	mm	mm	
In situ soil	sand	0.0	-1.2	-1.1	1,3,4,5,6,7
	clay	0.9	-0.8	-0.5	9,11,12,13
Backfill	stone	0.9	-0.3	-0.2	1,3,4,9,11,12,13
	silt	-0.8	-2.9	-2.3	5,6,7
Compaction	R	0.1	-0.1	-0.1	1,3,9,6
	VP	0.8	-0.5	-0.1	4,7,11,13
	N	0.2	-4.0	-3.8	12,5
Pipe diameter	900 mm	0.3	-0.9	-0.6	1,3,4,5,6,7,9,11
	1,500 mm	0.8	-1.6	-1.7	12,13
Trench width	Narrow	0.1	-1.7	-1.6	1,5,6,9,12
	Wd & Int.	0.7	-0.4	-0.1	3,4,7,11,13
All data		0.4	-1.0	-0.8	

1 mm = 0.04 in.

The data in table 4.17 can also be combined with the deflection data to evaluate movement of the trench wall. This evaluation was made and indicates that test 11, which was inundated with rain, showed outward trench wall movement of 4 to 6 mm (0.15 to 0.25 in.). This movement undoubtedly resulted from the inundation and explains the higher deflections in test 11 relative to other tests with similar variables. In general, tests where the native soil was sand showed less than 2 mm (0.08 in.) of outward trench wall movement and tests where clay was the native soil showed 1 to 3 mm (0.04 to 0.12 in.) of outward movement. These small movements are unimportant.

CHAPTER 5
ANALYSIS OF TEST RESULTS

Analytical models of buried pipes were evaluated against the field data to investigate the accuracy of the models and then to improve understanding of the physical processes that take place during installation.

5.1 Elasticity Model

The Burns and Richard (1964) elasticity solution was discussed in chapter 2. As noted it is idealized in that it models an elastic ring embedded in an isotropic elastic medium. In some respects this makes it particularly ill-suited to model the field tests because of the use of a trench installation, the shallow cover, and the variable haunch control; however, the model still shows trends that match the data, and are informative to examine.

Analyses were conducted for the field tests using the three 900 mm (36 in.) diameter pipes and the three 1500 mm (60 in.) diameter pipes, with soil properties representing the stone backfill with densities of 95 percent of maximum standard Proctor density (rammer compaction) and 85 percent (no compaction) of maximum standard Proctor density. Based on table 3.6, for an SW material with a vertical soil stress at the springline of about 4 psi, one-dimensional soil moduli, M_s, of 16 MPa (2300 psi) and 3.5 MPa (500 psi) were selected for the compacted and uncompacted conditions respectively. The Burns and Richard model is not capable of evaluating the stresses and deformations that occur while placing backfill at the sides of the pipe, thus the results of the analysis are compared to the changes in deflection, stress and strain that occurred while placing backfill over the top of the pipe. The applied vertical soil stress was 23 kPa (3.3 psi), representing the free field stress at the crown of the pipe at the end of backfilling. Considering the generally warm weather and test durations of several days, the plastic pipe data was converted to thrusts and moments using a modulus of elasticity of 500 MPa (72,500 psi).

Table 5.1 compares the results of the analysis with the Burns and Richard method using the equations for a full-slip pipe-soil interface with field data from Test Nos. 1, 2, 3, and 9.

Table 5.1

Comparison of Burns and Richard Full-Slip Predictions with Field Data for 900 mm (36 in.) Diameter Pipe

a. Deflections and Interface Pressures

Pipe Type	M_s	S_B	S_H	Burns and Richard				Field Data			
				ΔV	ΔH	p-cr	p-sp	ΔV	ΔH	p-cr	p-sp
	(MPa)	Eq. 2.14	Eq. 2.13	(%)	(%)	(kPa)	(kPa)	(%)	(%)	(kPa)	(kPa)
Concrete	3.5	0.1	0.001	-0.008	0.007	40	5.9	---	---	30	0.5
	16	0.6	0.003	-0.008	0.007	40	6.3	---	---	25	0.5
Plastic	3.5	98	0.34	-0.97	0.60	22	17	-1.3	1.3	21	21
	16	450	1.54	-0.31	0.07	13	12	-0.2	0.1	18	12
Metal	3.5	57	0.005	-0.71	0.71	27	19	-1.5	1.3	24	18
	16	260	0.022	-0.19	0.19	24	22	-0.2	0.1	23	15

Notes

1. Field data is change caused by backfilling over top of the pipe for tests backfilled with stone. Field data for M_s = 3.5 MPa is taken from test 2. Field data for M_s = 16 MPa is taken from test 1 (Narrow trench, haunched, sand site), test 3 (Wide trench, haunched, sand site), and test 9 (Narrow trench haunched, clay site).
2. All plastic pipe calculations assume a modulus of elasticity of 500 MPa to account for the temperature and test duration.
3. Plastic and metal pipe interface pressure data taken from soil pressure cells 150 mm over crown and at trench wall.
4. ΔV = change in vertical diameter, ΔH = change in horizontal diameter, p-cr = interface pressure at crown and p-sp = interface pressure at springline.
5. 1 kPa = 6.89 psi, 1 MPa = 145 psi

Table 5.1 (Cont.)

Comparison of Burns and Richard Full-Slip Predictions with Field Data for 900 mm (36 in.) Diameter Pipe

b. Moments, Thrusts, and VAF

Pipe Type	M_s	S_B	S_H	Burns and Richard				Field Data			
	(MPa)	Eq. 2.14	Eq. 2.13	N-sp (kN/m)	M-cr (kN-m/m)	M-sp (kN-m/m)	VAF	N-sp (kN/m)	M-cr M-inv (kN-m/m)	M-sp (kN-m/m)	VAF
Concrete	3.5	0.1	0.001	14.82	-1.55	1.49	1.25	--	--	--	--
	16	0.6	0.003	14.72	-1.51	1.45	1.24	--	--	--	--
Plastic	3.5	98	0.337	9.88	-0.219	0.187	0.87	3.5	0.112 0.257	0.154	0.25
	16	447	1.540	6.11	-0.060	0.040	0.54	3.0(T1) 5.5(T3) 7.6(T9)	0.012 0.067	0.057	0.21(T1) 0.39(T3) 0.57(T9)
Metal	3.5	57	0.005	11.39	-0.289	0.288	1.05	--	0.146 --	0.162 0.171	--
	16	261	0.022	10.84	-0.077	0.076	1.00	--	0.016 0.081	--	--

Note
1. All plastic pipe calculations assume a modulus of elasticity of 500 MPa to account for the temperature and test duration.
2. Field data for M_s = 3.5 MPa is taken from test 2. Field data for M_s = 16 MPa is taken from test 1 (Narrow trench, haunched, sand site, called T1), test 3 (Wide trench, haunched, sand site, called T3), and test 9 (Narrow trench haunched, clay site, called T9).
3. Due to symmetry in Burns and Richard solution, M-cr = M-inv
4. 1 kN/m = 5.71 lb/in., 1 kN-m/m = 225 ft-lb/ft

Results from the field tests are only differentiated when significant differences are present. The table indicates that the predictions are in general agreement with the trends shown in the field data. The main observations are:

- The Burns and Richard analysis shows almost no change of bending moment, thrust, or deflection in the concrete pipe as a result of the change in soil stiffness. This is anticipated as the concrete pipe is so stiff, both in bending and in hoop compression that the soil stiffness change from 3.5 to 16 MPa (500 to 2400 psi) is not significant.

- For the concrete pipe, the measured interface pressures are lower than the Burns and Richard predictions. This is believed to be the result of the trench installation, which would reduce the vertical load on the pipe and greatly reduce the lateral pressure.

- The measured interface pressures for the metal pipe and plastic pipe are in reasonable agreement with the predicted pressures.

- Predicted vertical soil pressure near the top of on the plastic pipe are relatively uniform for both soil conditions. The measured data is uniform for the loose soil condition but less so for the dense soil condition. The vertical pressure measurement for the plastic pipe was taken at 150 mm over the top of the pipe, which could have resulted in a more nearly geostatic stress than would exist closer to the pipe.

- The predicted deflections for the metal and plastic pipe embedded in compacted soil are in good agreement with the measured deflections.

- The predictions for deflection in loose soil underestimate the measured values for both the metal and the plastic pipe. This may represent the result of the lack of haunching, which Burns and Richard cannot model, or indicate that the dumped backfill leaves voids that allow greater deformation when the first lifts of backfill are placed. Data on deeper installations would be required to evaluate this.

- The field data for thrust in the plastic pipe, appears to be affected by several factors. Lowest thrust was measured in the dense stone in a narrow trench in the sand in situ soil (test 1). Only slightly higher thrusts were measured in the loose stone in a narrow trench in sand in situ soil (test 2). Much higher thrust was measured in the dense stone in the wide trench in sand in situ soil (test 3) and still higher values were measured for the dense stone in a narrow trench but in the clay in situ soil (test 9). In all cases, the field vertical arching factors are less than the Burns and Richard predictions. As noted in Section 4.2.6.5, the metal thrust strains were not analyzed.

- Measured bending moments are variable relative to the Burns and Richard solution. The crown moments are substantially lower than the invert moments, which is expected because of the haunching effect. Invert moments are on approximately the same order of magnitude as the Burns and Richard for the plastic and metal pipe. Measured springline moments for the metal pipe are much lower than predicted, while for the plastic pipe the measured moments at the springline are somewhat lower than predicted in the loose soil and higher than predicted in dense soil. The low springline moments may be the due the influence of the trench walls. The overall match of measured to predicted moments is actually a little surprising for the loose soil, since the deflections were under predicted.

Overall, the match between the Burns and Richard predictions and the measured data is quite good considering the idealized model and the uncertain approximations, such as the estimated modulus of elasticity; however, the predictions pertain only to the changes in behavior due to backfilling over the top of the pipe.

5.2 Computer Analysis of Field Test Results

Analysis of the field tests was undertaken with CANDE, Level 3. Complete finite element meshes were developed to represent the installation conditions of the tests.

The finite element meshes for analysis of the 900 mm diameter and 1,500 mm diameter pipe installations are shown in figures 5.1 and 5.2, respectively, which also show the boundaries of the trench and various soil zones. Descriptions of the soil zones are provided in table 5.2. The same mesh was used for both the narrow and wide trench installations by changing element assignments from in situ soil to backfill as shown in the figures. Symmetry was assumed about the vertical centerline of the pipe. The pipe was divided into 20 segments, each segment extending for an arc length of nine degrees.

Undisturbed in situ soils were modeled with estimated linear elastic properties while placed soils were modeled with non-linear behavior using the Duncan (1970) hyperbolic Young's modulus with the Selig (1985) hydrostatic hyperbolic bulk modulus. The *CANDE User Manual*, Appendix A, (CANDE, 1989) contains two sets of Selig bulk modulus properties, called the "modified," which are the defaults, and the "hydrostatic," which must be input manually. Based on the evaluation in chapter 3, the hydrostatic properties were used for the analyses reported here. Soil properties and compaction levels used to model the various soil zones are summarized in table 5.3. Although the field tests were conducted to a depth of 1.2 m (4 ft) over the test pipe, the analyses were continued to a depth of 6.1 m (20 ft) to investigate implications of the various installation conditions under more demanding loading conditions.

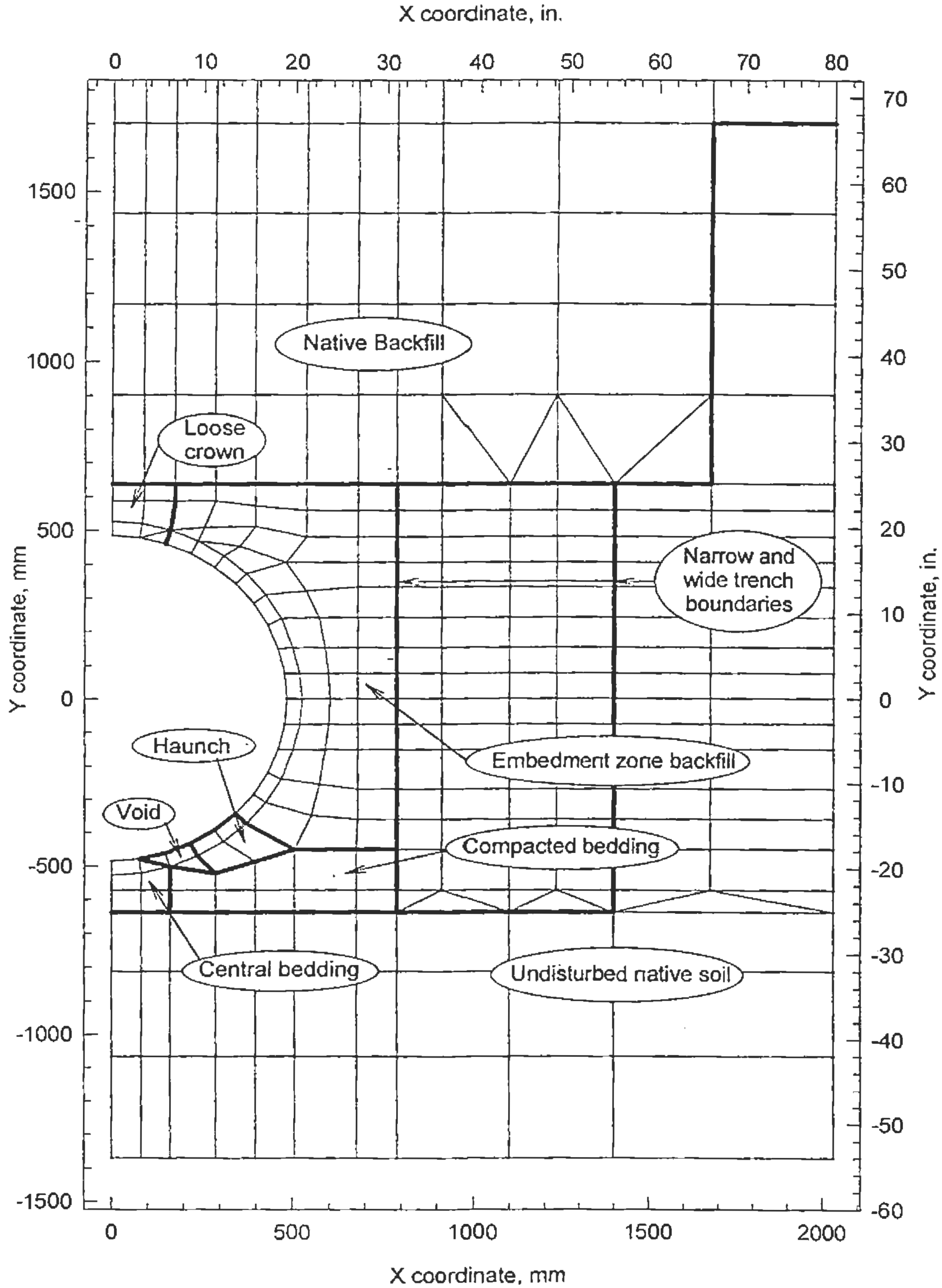

Figure 5.1 Soil Zones for 900 mm (36 in.) Diameter Plastic Pipe

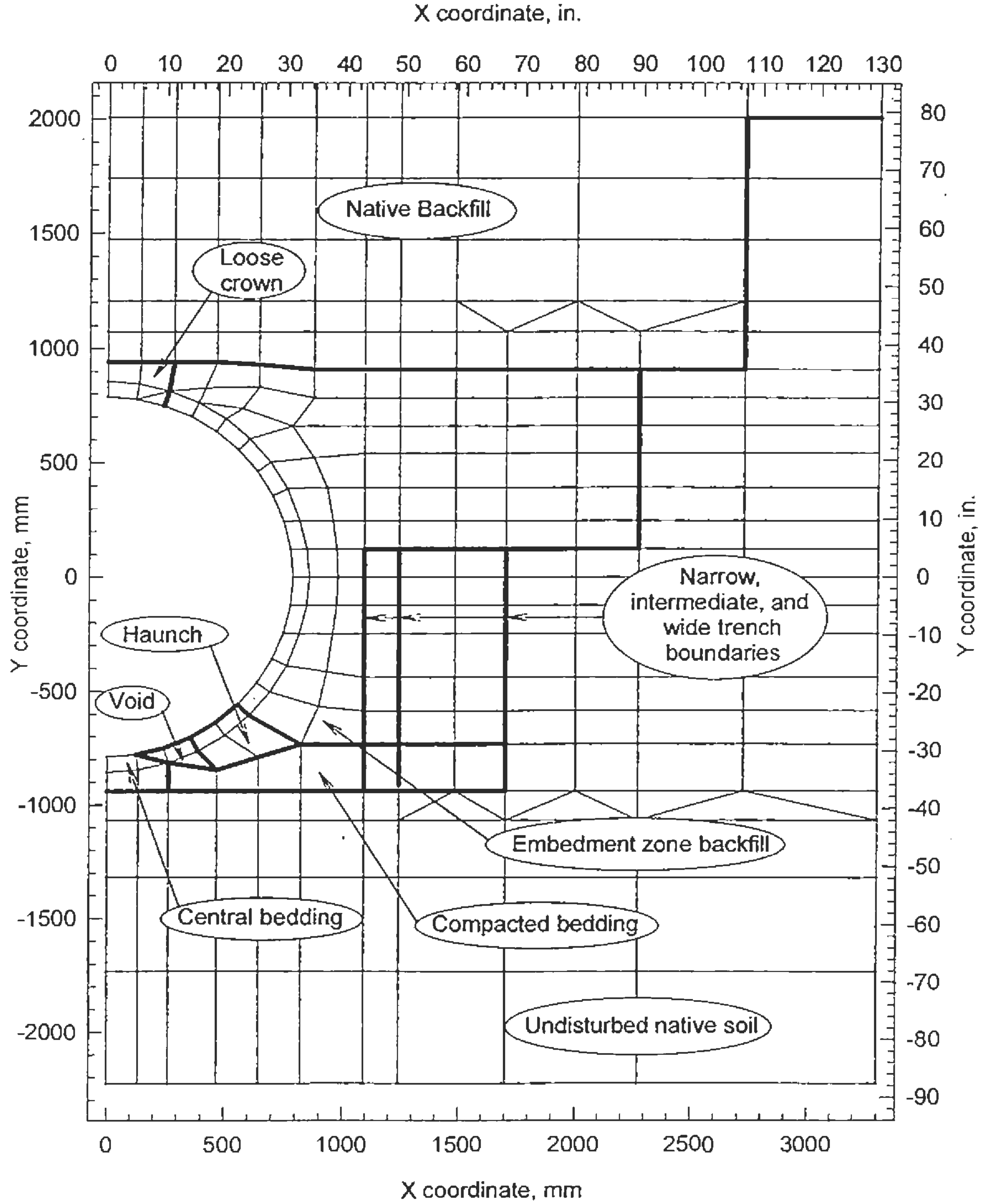

Figure 5.2 Soil Zones for 1500 mm (60 in.) Diameter Pipe

Table 5.2
Soil Zones Used in FEM Analysis of Field Installations

Soil Zone Label in Figures 5.1 and 5.2	Zone Description
Undisturbed native soil	Natural soil formation, sand or clay
Compacted bedding	150 mm deep layer of compacted backfill
Central bedding	150 mm deep, 300 mm wide layer of backfill, loose or compacted as required for specific tests
Void	Loose soil (ML49) under all conditions, even when haunching was specified
Haunch	Compacted backfill material if haunching was specified, otherwise loose backfill material
Embedment zone fill	Backfill material with properties based on achieved density
Loose crown	Backfill material with properties of loose soil
Native backfill	Compacted native backfill material

Table 5.3
Soil Properties Used in FEM Analysis

Common Name		Compacted Density (1)		Soil Model	CANDE Designation or Young's Modulus (MPa) (2)
		%	kN/m^3		
Undisturbed native sand		–	–	linear elastic	28
Undisturbed native clay		–	–	linear elastic	7
Compacted native soil	sand	96	20.1	hyperbolic	SW95
	clay	90	18.7	hyperbolic	CL90
Loose stone		79	17.9	hyperbolic	SW80
Stone compacted with vibratory plate		85	19.3	hyperbolic	SW85
Stone compacted with rammer		92	20.7	hyperbolic	SW90
Loose silty sand		82	13.0	hyperbolic	ML80
Silty sand compacted with vibratory plate		89	14.3	hyperbolic	ML90
Silty sand compacted with rammer		95	15.4	hyperbolic	ML95

Notes:
1. The compacted density is reported as the average percentage of maximum dry density, per AASHTO T 99, measured in the field, and as the wet density measured in the field.
2. Selig soil properties include the hydrostatic bulk modulus values.
3. 1 MPa = 145 psi, 1 kN/m^3 = 6.4 pcf

5.2.1 Modeling of Construction Effects During Sidefill

Modeling pipe-soil interaction while placing the sidefill requires a method to introduce compaction effects. Compaction effects are the pipe deformations and interface pressures that result from the process of bringing backfill soil from the loose state at which it is placed to its final density. The soil-culvert interaction that takes place during this stage of construction can be significant; however, the hyperbolic soil models available in CANDE were not developed to address this load condition. CANDE was tested to evaluate several methods of modeling compaction effects, without program technical changes, and to provide guidance to pipe designers who must use available software packages. Three approaches were taken in this effort:

1. Applying vertical loads to the surface of the just placed layer of backfill;

2. Squeezing the most recently placed layer of backfill between vertical upward and vertical downward forces; and

3. Applying horizontal nodal forces directly to the pipe.

Methods 1 and 2 have the advantage of creating pipe distortion and movements as a result of the pipe-soil interaction that takes place as a consequence of forces applied by a compactor. However, when using an elastic soil model, removing the compaction force results in a rebound of the pipe. Also, to correctly model the compaction problem, the model should start with the properties of a loose soil, having a low strength and stiffness, and finish with the properties of a compacted soil. Yet, again, the hyperbolic soil model was not developed to provide this transition from significantly different states of soil density, nor can it simulate the cumulative deformations that result from successive passes of the compactor. Efforts at using Methods 1 and 2 were unsuccessful in creating deformations representative of those in the field, and in general were unsuccessful in creating any significant peaking effects.

Method 3 is the least sophisticated of the three techniques in that it requires a separate algorithm or chart to provide guidance on the magnitude of the forces to be applied. Key variables in this are the soil friction angle, the size and type of compactor, and the size of the pipe. Nodal forces were applied to represent the placement of layers of backfill, as they were in the actual field tests. The distribution of the nodal forces assumed that the compaction pressures were of uniform magnitude for a depth of 300 mm (12 in.) below the soil surface. This is demonstrated in figs. 5.3 and 5.4 for both pipe sizes.

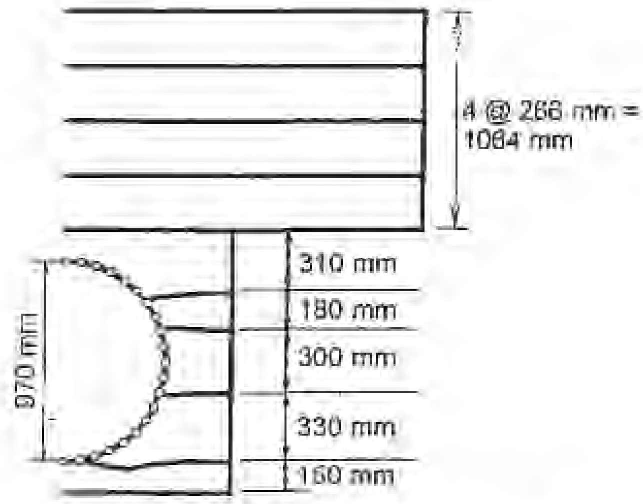

a. 900 mm Diameter Pipe in Narrow Trench
(Increments for the wide trench were at the same elevations)

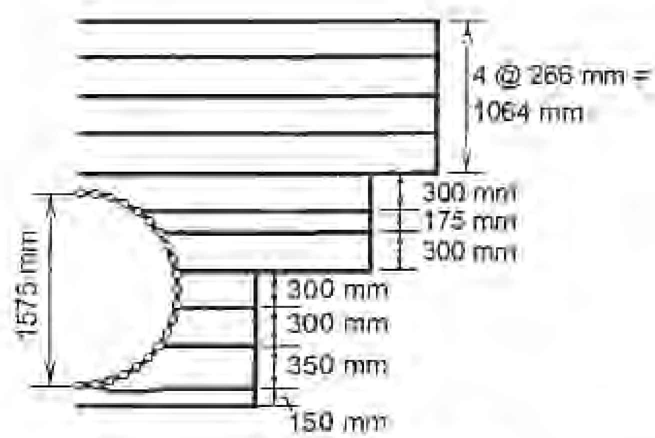

b. 1500 mm Pipe in Narrow Trench
(Increments for intermediate and wide trench were at the same elevation)

1 in. = 25.4 mm

Figure 5.3 Construction Increment Thicknesses for Field Tests

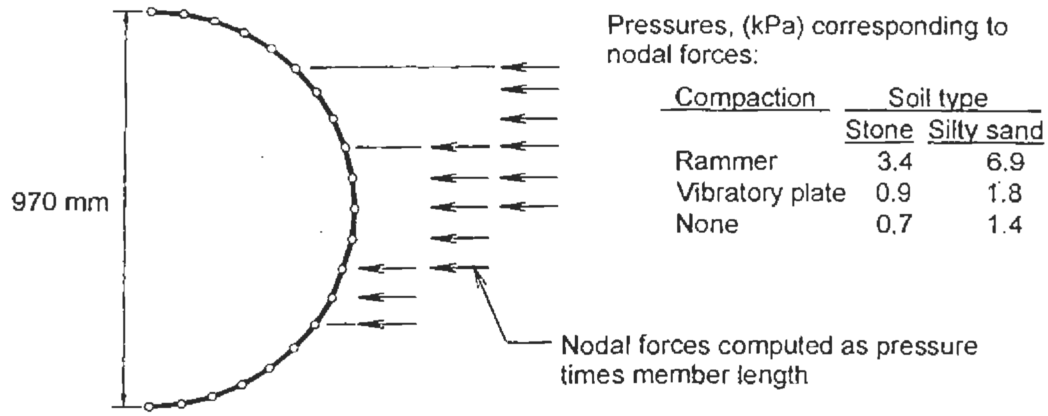

Pressures, (kPa) corresponding to nodal forces:

Compaction	Soil type	
	Stone	Silty sand
Rammer	3.4	6.9
Vibratory plate	0.9	1.8
None	0.7	1.4

a. 900 mm Diameter Pipe

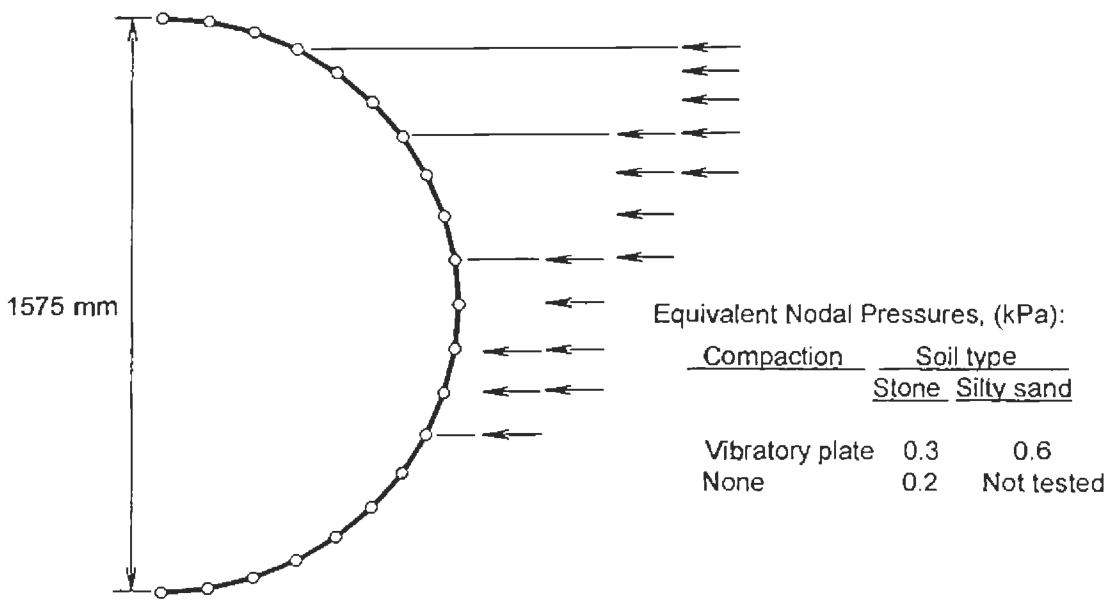

Equivalent Nodal Pressures, (kPa):

Compaction	Soil type	
	Stone	Silty sand
Vibratory plate	0.3	0.6
None	0.2	Not tested

b. 1500 mm Diameter Pipe

Note: 1psi = 6.89 kPa

Figure 5.4 Application of Nodal Forces to Model Compaction Effects

For the metal and plastic pipe, the analysis showed that, for a given type of soil, compaction, and pipe size, the forces required to match the field deflections were consistent. Although the modeling was completed using concentrated nodal forces, equivalent pressures were calculated to assist in comparison of the two pipe sizes. The pressures that best matched the field deflections for each combination of parameters are presented in table 5.4.

Table 5.4
Applied Pressures (kPa) to Represent Compaction Effects

Soil Type	Compaction Type/ Pipe Diameter (mm)				
	Rammer	Vibratory Plate		None	
	900	900	1500	900	1500
Stone	3.4	0.9	0.3	0.7	0.2
Silty sand	6.9	1.8	0.6	1.4	--

1.0 psi = 6.89 kPa

Table 5.4 shows that the compaction pressures are twice as great for the silty sand as for the stone, and substantially smaller for the 1,500 mm (60 in.) pipe than for the same type of compaction for 900 mm (36 in.) pipe. Pressures that model the vibratory plate are only slightly larger than those for no compaction.

It is interesting to note the relatively small pressures required in the CANDE model to produce the observed field peaking effects. Part of this is because CANDE is a two-dimensional model, thus the model represents compaction forces applied to an infinite length of the pipe, all at the same time. In the real three-dimensional world, the compaction forces spread longitudinally away from the compactor location and a length of pipe greater than the loaded portion resists the applied load, thus, the concentrated load to cause the observed peaking would be greater than the force in the two-dimensional model.

A simple expression was developed based on the above pressures to predict the compaction pressures under other conditions. The expression assumes that the lateral pressures on the pipe are related to the at-rest lateral pressure of the soil, which is computed as the vertical stress times 1-sin ϕ, where ϕ is the friction angle of the soil in a loose condition. Values of ϕ were selected from the CANDE User Manual, Appendix A, from the Selig "hydrostatic" soil properties. The resulting expression (which is only developed in SI units) is:

$$np = 1.3P(1-\sin\phi)^3\left(\frac{970}{dc-250}\right)^2 \tag{5.1}$$

where

np	=	nodal pressure used in CANDE model, kPa,
P	=	total compactor force, kN (not less than 4 kN to account for gravity effects of backfill),
ϕ	=	friction angle of soil in loose condition, degrees, and
dc	=	centroidal diameter of pipe, mm.

Table 5.5 compares the nodal pressures predicted by the Eq. 5.1 with the pressures actually used in the CANDE analyses.

The equation was developed based on limited data but suggests several items to consider when selecting compaction equipment and backfill:

- The lateral force applied to a pipe is sensitive to the friction angle as indicated by the fact that the compaction of the silty sand, with a loose friction angle 8 degrees lower than that of the stone, resulted in twice the compaction effect;
- Required compaction pressure drops significantly with increasing diameter; and
- The vibratory plate, which densifies soil by vibration, rather than by impact like the rammer, produces only slightly more compaction deflection than the gravity weight of the soil (remember, however, that the rammer produced about 5 percent greater density, per AASHTO T-99 for the same number of passes).

Table 5.5
Computed and Applied Nodal Pressures

Compactor		Diam. (mm)	Soil		Nodal pressure (kPa)	
Type	Force (kN)		Type	ϕ (degrees)	Eq. 5.1	CANDE analysis
Rammer	20.5	900	stone	36	3.4	3.4
			silty sand	28	7.2	6.9
Vibratory plate	5.2	900	stone	36	0.9	0.9
			silty sand	28	1.8	1.8
		1,500	stone	36	0.3	0.3
			silty sand	28	0.5	0.6
None	4.0	900	stone	36	0.7	0.7
			silty sand	28	1.4	1.4
		1,500	stone	28	0.2	0.2

Note: 1 lb = 0.454 kg, 1 in. = 25.4 mm, 1 psi = 6.9 kPa.

5.2.2 Results

The CANDE analyses predicted behavior during backfilling that is in substantial agreement with the results of the field tests. There are some notable exceptions that will be discussed below. The deflections, moments, thrusts, and shears in the pipe wall, and interface pressures for each analysis are presented in appendix A. Summary plots are presented here.

5.2.2.1 Deflections

The match between the field test data and the CANDE analyses can best be investigated by comparing the plots of deflection versus depth of fill. This comparison is presented in figs. 5.5, 5.6 and 5.7 for tests with (1) the 900 mm (36 in.) diameter plastic pipe with soil backfill; (2) the 900 mm (36 in.) diameter metal pipe with soil backfill, and (3) the 900 mm (36 in.) diameter pipe with CLSM backfill and all 1500 mm diameter pipe, respectively. These figures generally show that the peaking deflection during sidefilling and the deflection due to overfill are modeled quite well with the CANDE analyses.

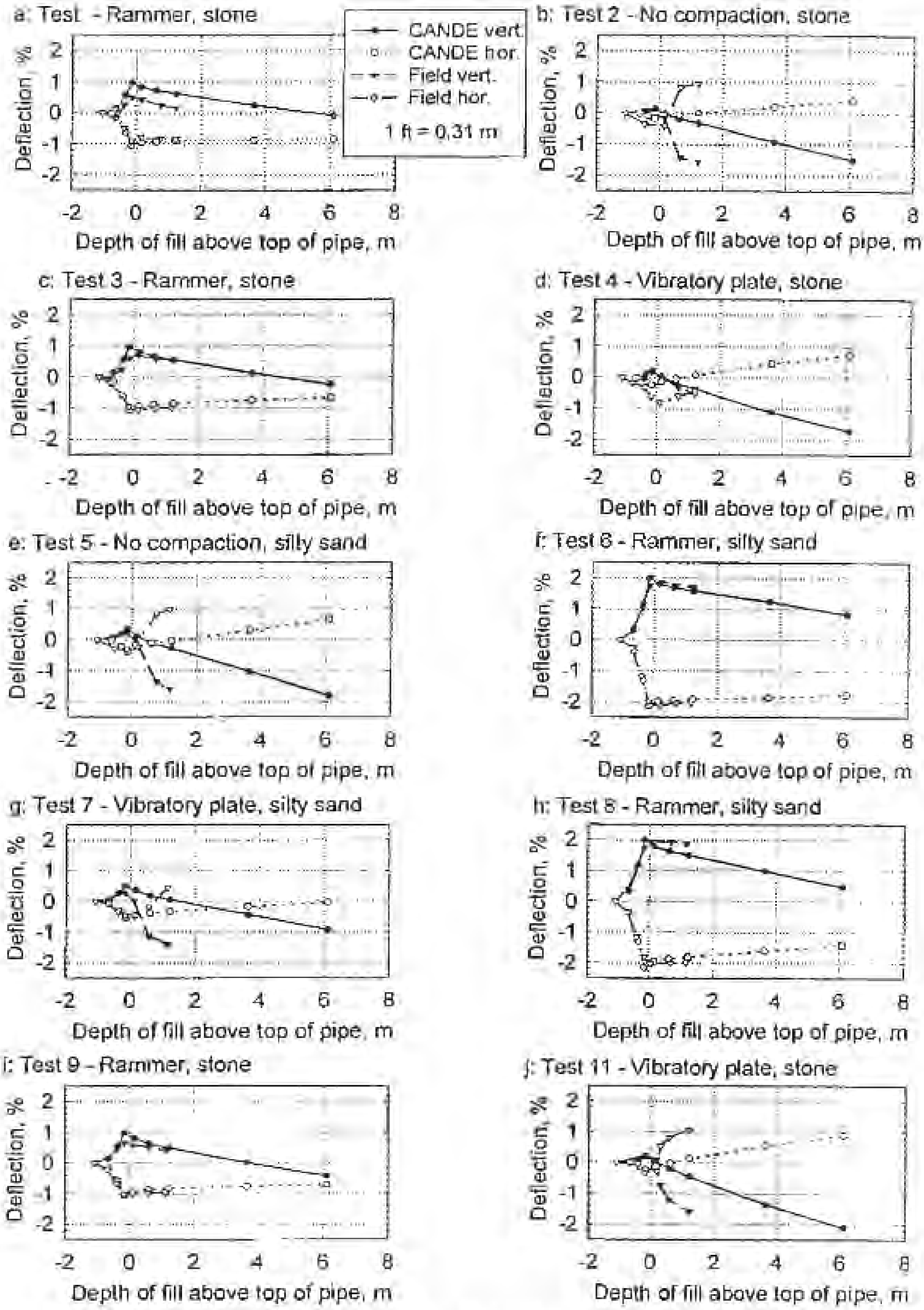

Figure 5.5 CANDE Deflection Compared to field Deflection for 900 mm (36 in.) Diameter Plastic Pipe (except CLSM)

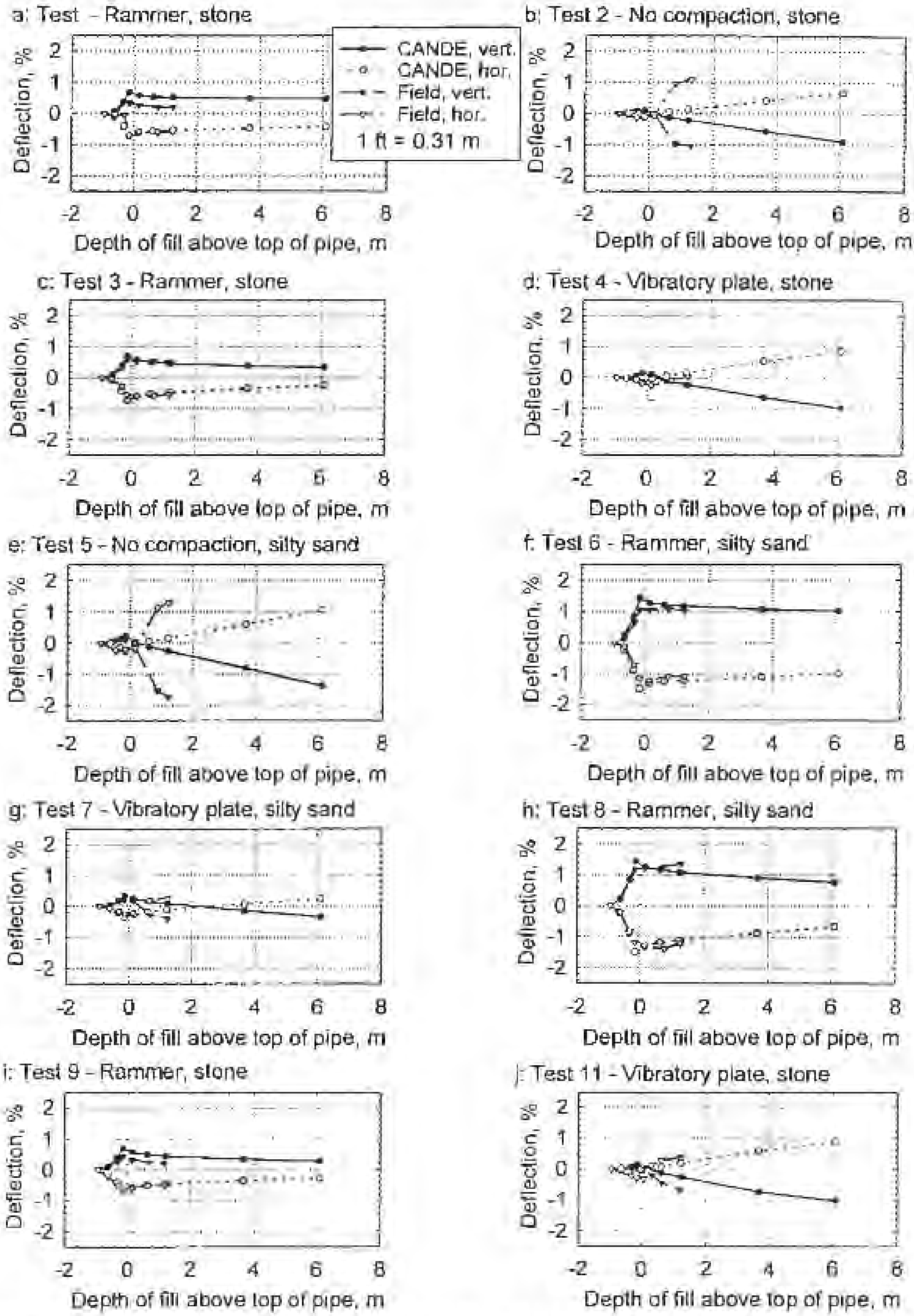

Figure 5.6 CANDE Deflection Compared to Field Deflection for 900 mm (36 in.) Diameter Metal Pipe (except CLSM)

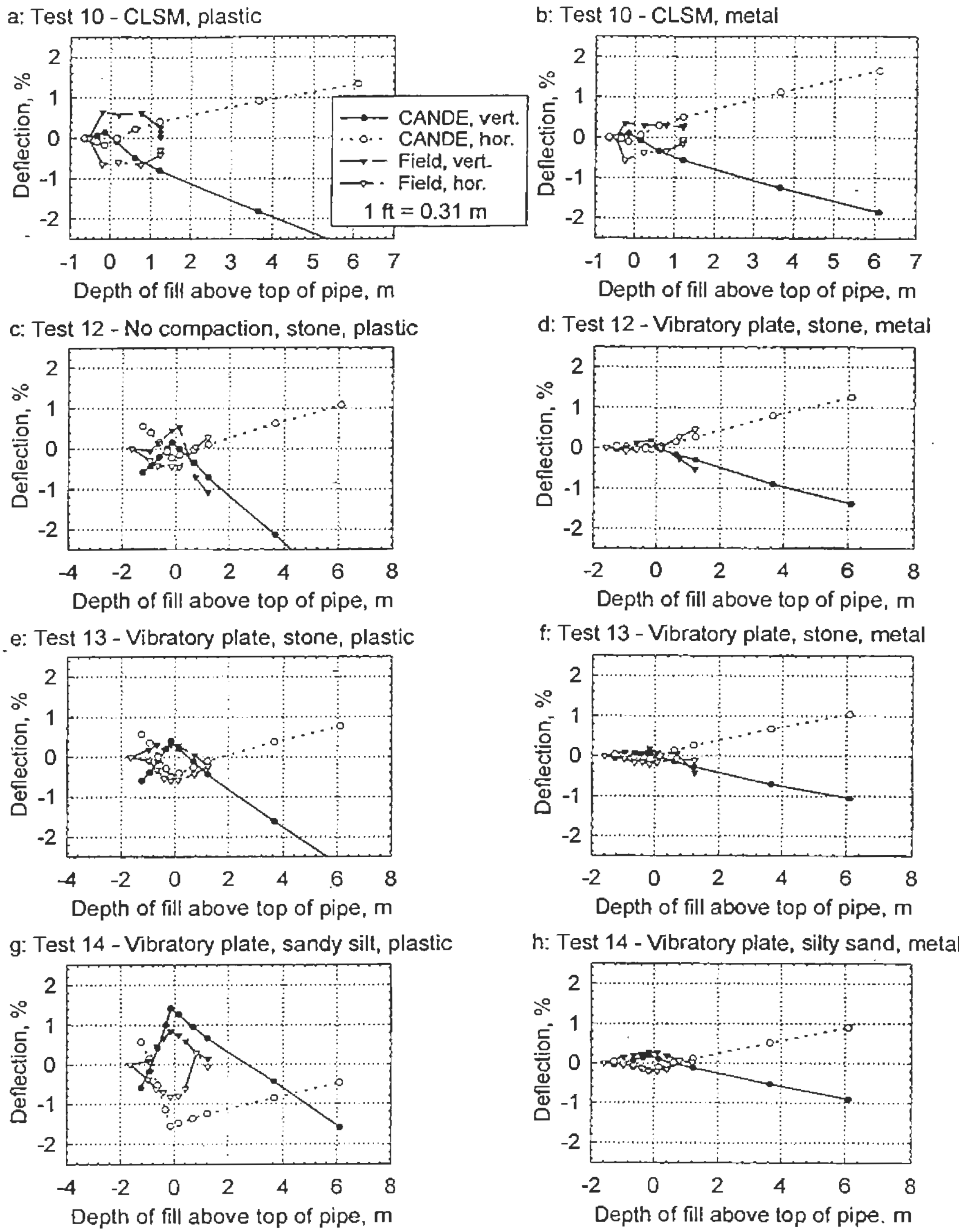

Figure 5.7 CANDE Deflections Compared to Field Deflections for CLSM Test with 900 mm (36 in.) Diameter Pipe and All Tests with 1500 mm (60 in.) Diameter Pipe

For tests 2 and 5 on 900 mm diameter pipe with uncompacted backfill, the field data show an increase in deflection of about 1 percent for the first lifts of backfill over the pipe, up to about 600 mm (24 in.) over the pipe, as shown in figs. 5.5b, 5.5e, 5.6b, and 5.6e. For the last two lifts, from 600 mm to 1,200 mm over the top of the pipe, the rate of change of deflection is closer to that predicted by the CANDE analyses. The effect, evident with both stone and silty sand backfill, is thought to be the result of the large void resulting from a lack of haunching effort and smaller voids that remain from backfill placement and do not get collapsed because no compactive effort is applied. This could be considered a seating effect. When backfill is compacted, it is pushed into intimate contact with the pipe and the trench wall, and voids in the backfill are eliminated. If the backfill is not compacted, then these voids are eliminated during overfilling and result in a significant deflection increment. This effect is apparent for the plastic pipe in test 12 (1,500 mm, fig. 5.7c) but not for the metal pipe. Test 12 was haunched, and the effect may also be less apparent because the trench is relatively narrow (pipe diameter to trench width ratio of 0.7 for test 12 versus 0.6 for tests 2 and 5) and the stiff trench walls may have a greater effect.

In test 7, the plastic pipe deflections, fig. 5.5g, also increased more during placement of fill over the top of the pipe. Test 7 was backfilled with silty sand, compacted with the vibratory plate to 90 percent of maximum standard Proctor density, but no haunching effort was applied. Test 4 (figs. 5.5d), with the same test variables except that the backfill was stone did not show this effect. The silty sand is uniform, relatively fine grained and very sensitive to moisture content, as evidenced by the saturation and loss of bedding compaction in test 5 (see section 4.2.5.3) that was remedied by introducing a bedding layer of coarser sand. The sensitivity to moisture and the presence of voids due to lack of haunching may have permitted the backfill to deform, and drop in average density as fill was placed over the top of the pipe. The stone backfill of test 4 would be more stable under moist conditions. This effect was readily evident in the plastic pipe, which has deep corrugations that do not get filled near the invert. The metal pipe, which has less prominent corrugations, shows the same effect but with a lower magnitude.

The plastic pipe in test 11, fig. 5-5j, showed a higher deflection trend than predicted by the CANDE analysis or as seen in the metal pipe, Fig. 5-6j. This test was inundated during construction when the backfill was at a level about 450 mm over the top of the pipe, and construction was halted for about 1 week. Even though the clay in situ soil was relatively stiff during excavation in the dry it became soft when wet and could and have deformed during the delay. This is the test where the most trench wall movement was recorded by the soil strain gages (see section 4.2.6.6). The same trend was not noted in the metal pipe. This may be because the metal pipe is substantially stiffer under long term loads than the plastic pipe.

The pipe in test 10, figs. 5-7a and 5-7b, showed peaking effect during the placement of the CLSM which was not modeled well by the assumptions used in the CANDE analysis. The hydrostatic nature of the loading is somewhat different from the horizontal loads applied. Undoubtedly, with additional data, a method of modeling this peaking could be developed.

Other observations related to the deflection comparison include:

- The CANDE predictions of deflection due to backfill over the top of the pipe generally match the field deflection quite well. This suggests that the Selig hydrostatic properties are an appropriate design choice.
- For the plastic pipe, the vertical deflection decreases with increasing depth of fill over the pipe at a greater rate than the horizontal diameter increases, while for the metal pipe the vertical and horizontal diameter change at approximately the same rate. This trend, apparent in both the field data and the CANDE analyses, suggests that the plastic pipe is shortening circumferentially due to the low hoop stiffness.
- The CANDE analysis indicates that the 1500 mm diameter plastic pipe deflects about 0.5 percent under its own weight. This was not evident in any of the other tests, but the 1,500 mm plastic pipe was about 10 times less stiff than the 900 mm diameter plastic pipe or either of the steel pipe. Field data were not taken to monitor this effect.
- Related to the previous observation, while the peak deflection that developed in the CANDE model for this pipe reasonably matched the measured peak deflection, the CANDE model actually produced far too much peaking effect that is partially obscured because of the initial downward deflection caused by self weight. The Spirolite type of profile wall may mobilize a greater length of pipe than the corrugated profiles.

5.2.2.2 Interface Pressures

The CANDE vertical and horizontal pressure distribution against the concrete pipe for tests 1 and 2 are shown in figs. 5.8 and 5.9, respectively. These figures show the principal characteristics of all of the figures in appendix A.

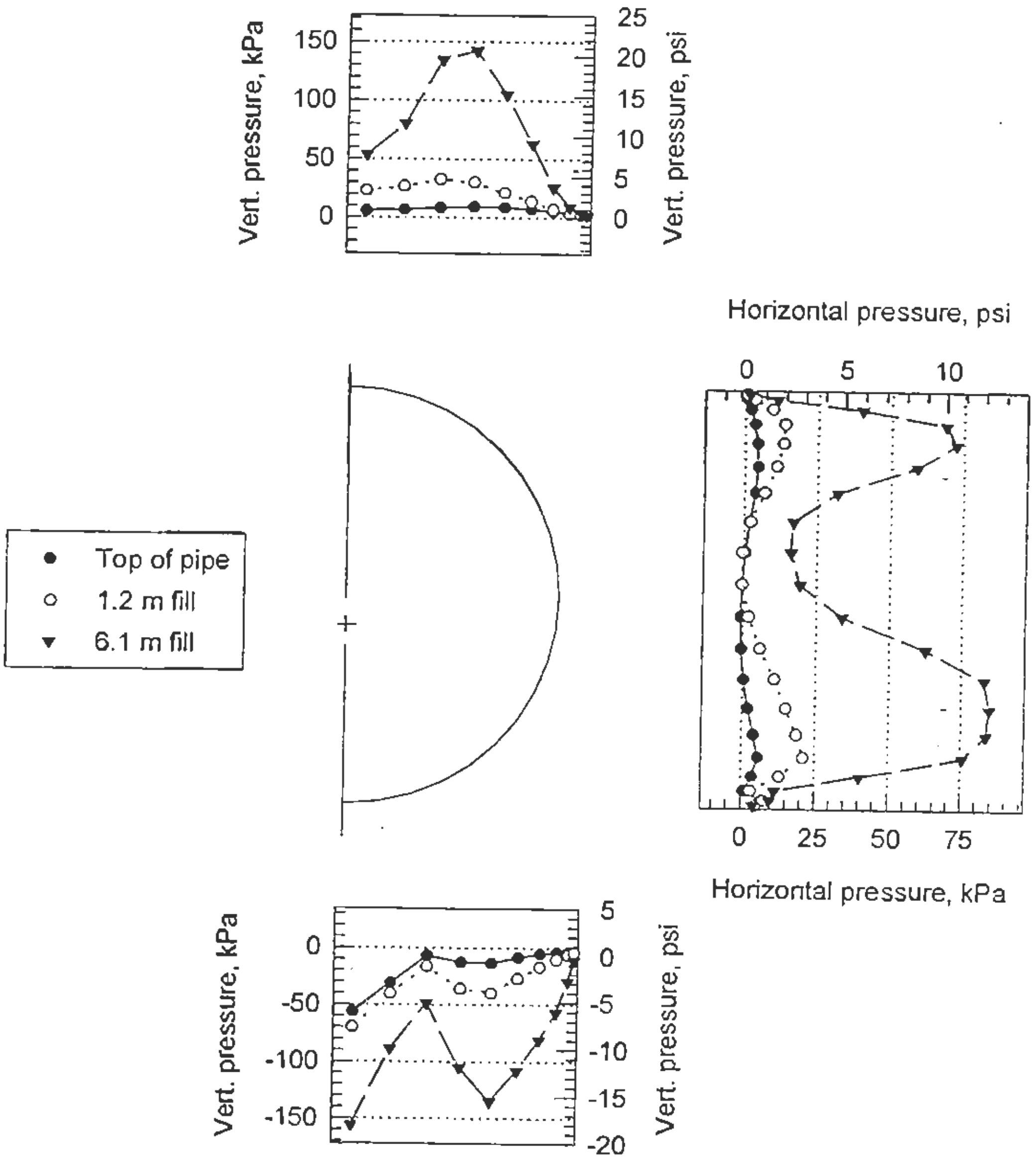

Figure 5.8 Vertical and Horizontal Pressures on Concrete Pipe, CANDE Analysis Test 1 – Rammer Compaction, Compacted Bedding, Haunching, Stone Backfill

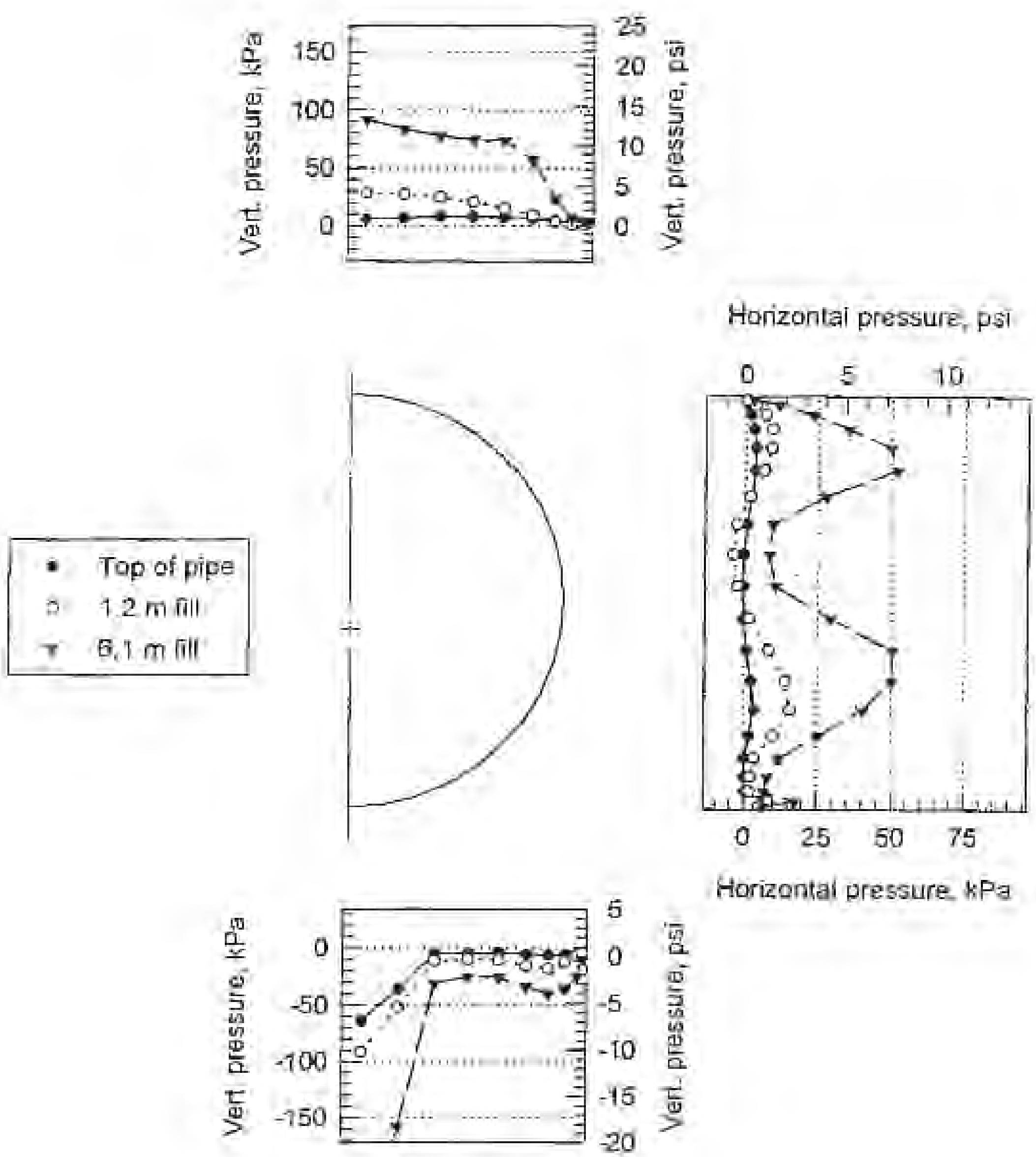

Figure 5.9 Vertical and Horizontal Pressures on Concrete Pipe, CANDE Analysis Test 2 – No Compaction, Compacted Bedding, No Haunching, Stone Backfill

Results for test 1, which was backfilled with stone, compacted with the rammer, and haunched are shown in fig. 5.8. The vertical upward pressure distribution at the bottom results from the assumption of a void, even though haunched. This was borne out in the field tests by the low interface pressures measured at thirty degrees from the invert and the low penetration resistance measured after removal of the pipe. The vertical pressure distribution at the top of the pipe is relatively uniform at 1.3 m of cover, but shows a significant drop at 6.1 m of cover. This is apparently the result of not compacting directly over the pipe. The side pressure at the invert is low at all stages of backfilling; however significant pressures develop just above and below the springline. These are only changes in pressure caused by fill over the crown, because the CANDE analysis did not model compaction pressures.

Results for test 2, which was backfilled with stone, without compaction and without haunching are presented in fig. 5.9. The upward vertical pressure distribution at the bottom of the pipe is peaked at the invert and does not develop the secondary pressure at the side of the pipe. This results from the lack of side support and haunching effort. At the top, the vertical downward pressure distribution is uniform at all depths. For test 2 without compaction, all of the backfill over the pipe is of uniform density and this is reflected in the pressure distribution. The lateral pressure distribution at the side of the pipe is similar to that in test 1, but lower in magnitude.

Measured interface pressures and soil stresses at the trench wall and 150 mm over the crown for the concrete pipe are compared to the CANDE predictions in fig. 5.10. The data presented are the changes in interface pressure as the backfill was placed and compacted from an elevation 150 mm (6 in.) above the pipe, called the top of the pipe, to 1.2 m (4 ft) above the pipe, called the end of test.

The CANDE predictions for invert interface pressure against the concrete pipe are consistently low relative to the field measured values, and the disparity increased as the compactive effort decreased (rammer, vibratory plate, none). The highest field change in invert pressure occurred in tests 2 and 12 which had compacted stone bedding, no haunching, and no compaction. Pressures were closer to the field values as the installation quality improved.

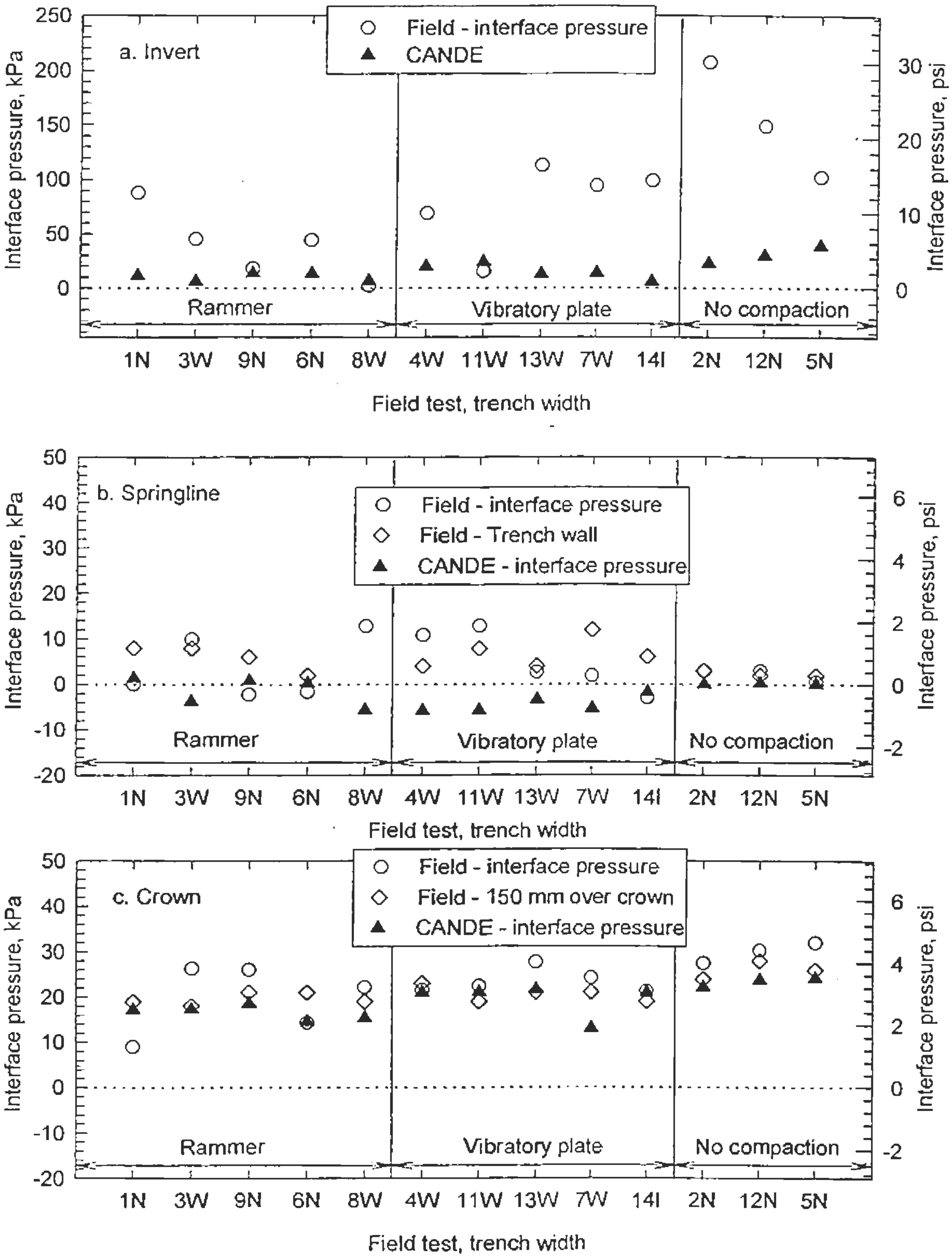

Figure 5.10 CANDE Interface Pressures Compared to Field Pressures for Concrete Pipe

Interface pressures at the springline were quite low in both the CANDE analyses and the field data. The larger pressures developing above and below the springline, as shown in figs. 5.8 and 5.9 indicate that the backfill is arching between the pipe and the trench wall, and little load travels directly through the backfill at the springline.

Measured interface pressures at the crown of the concrete pipe were similar to those predicted by CANDE.

The interface pressures calculated with CANDE for the plastic and metal pipe for test 5 with sandy silt backfill, no compaction, no haunching and compacted bedding (the saturation of the silty sand bedding may have resulted in a softening of the bedding) are presented in fig. 5.11. The pressures for the metal pipe were similar and, for clarity, are only shown at a depth of 6.1 m (20 ft). The trends are similar to the those for the concrete pipe for the vertical pressures at the top and bottom; however, at the side, substantially more pressure develops for the flexible plastic and metal pipe than did for the rigid concrete pipe. The pressure is greatest below the springline. The same information for test 8, with sandy silt backfill, rammer compaction, haunching and soft bedding, is presented in fig. 5.12. The effect of the soft bedding in reducing the invert pressure and increasing the vertical pressure at the side of the pipe is significant. Also of note is that the lateral pressure for test 8 is of a higher magnitude and more centered on the springline than was the case for test 5. Similar plots for all the metal and plastic pipe tests are included in appendix A. The appendix figures plot actual data against the CANDE predictions.

Interface pressure predictions for all flexible pipe tests are compared with CANDE predictions in fig. 5.13. The field data are slightly higher than the predicted data, but the trends with test variables are quite consistent. In fig. 5.13 the field test data are actually taken from the gages installed 150 mm (6 in.) over the crown and at the backfill-trench wall interface. This difference in location from the predictions of pressure at the actual interface by CANDE could account for some of the mismatch between the data and the predictions. In general the lateral pressures are of relatively constant magnitude, even though the deflection varied considerably, upward in some cases and downward in others. This shows that the lateral pressures required to carry a given load is about constant and the pipe will deflect until that pressure develops. This emphasizes the importance of compaction to provide stiff soil and control deflection levels.

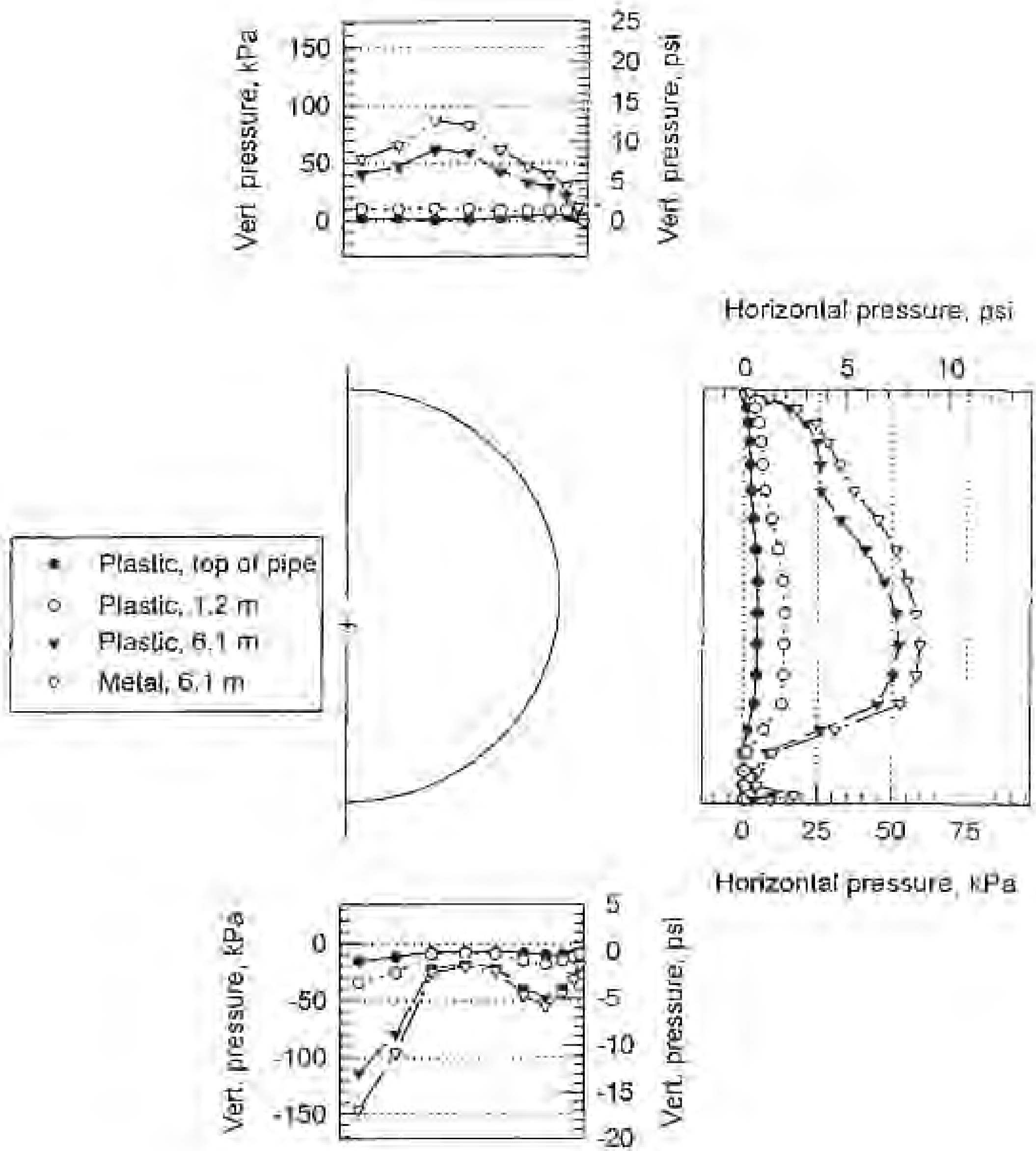

Figure 5.11 Vertical and Horizontal Pressures on Plastic and Metal Pipe, CANDE Analysis, Test 5 – Rammer Compaction, Soft Bedding, No Haunching, Sandy Silt Backfill

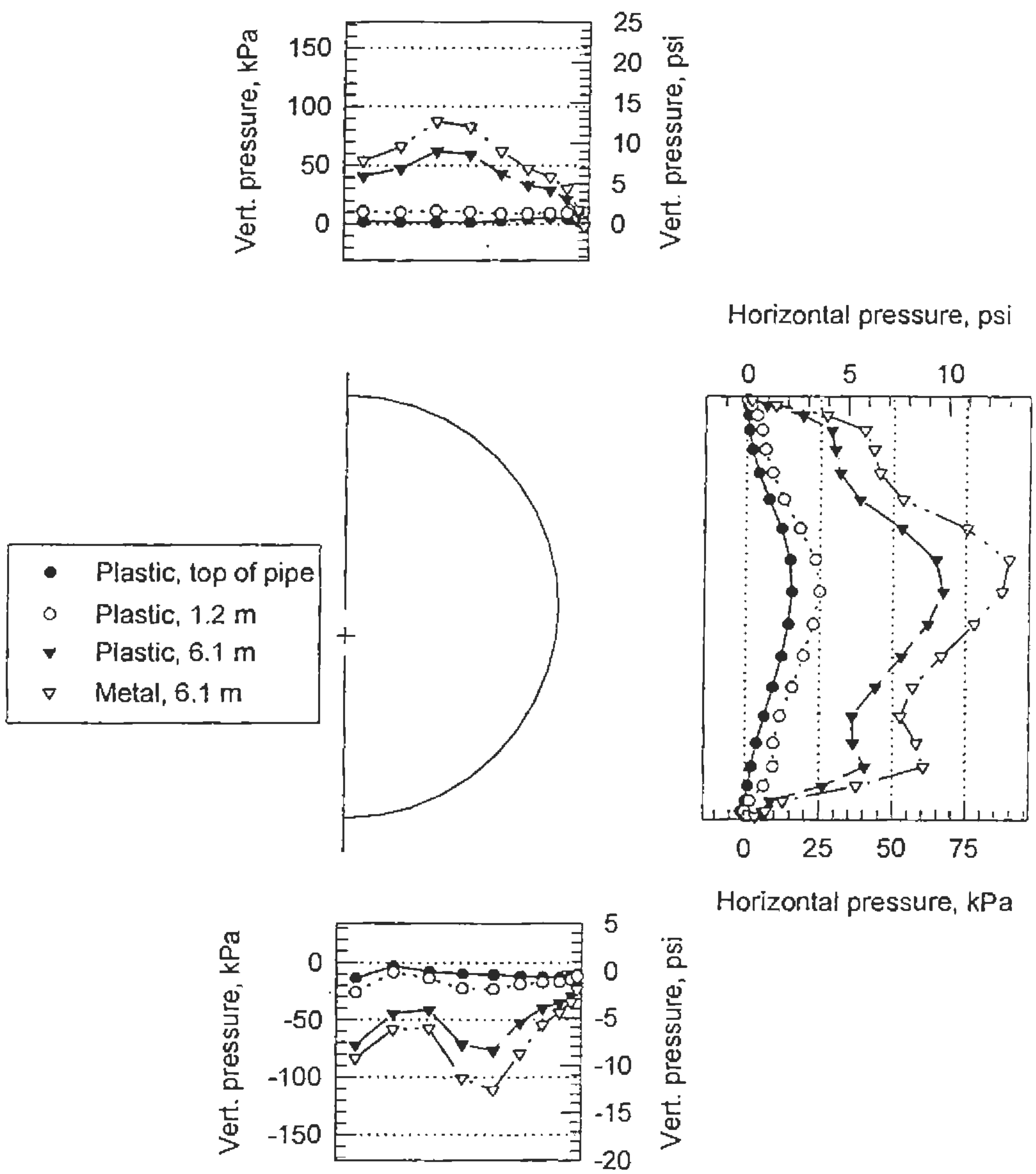

Figure 5.12 Vertical and Horizontal Pressures on Plastic and Metal Pipe, CANDE Analysis, Test 8 – Rammer Compaction, Soft Bedding, Haunching, Sandy Silt Backfill

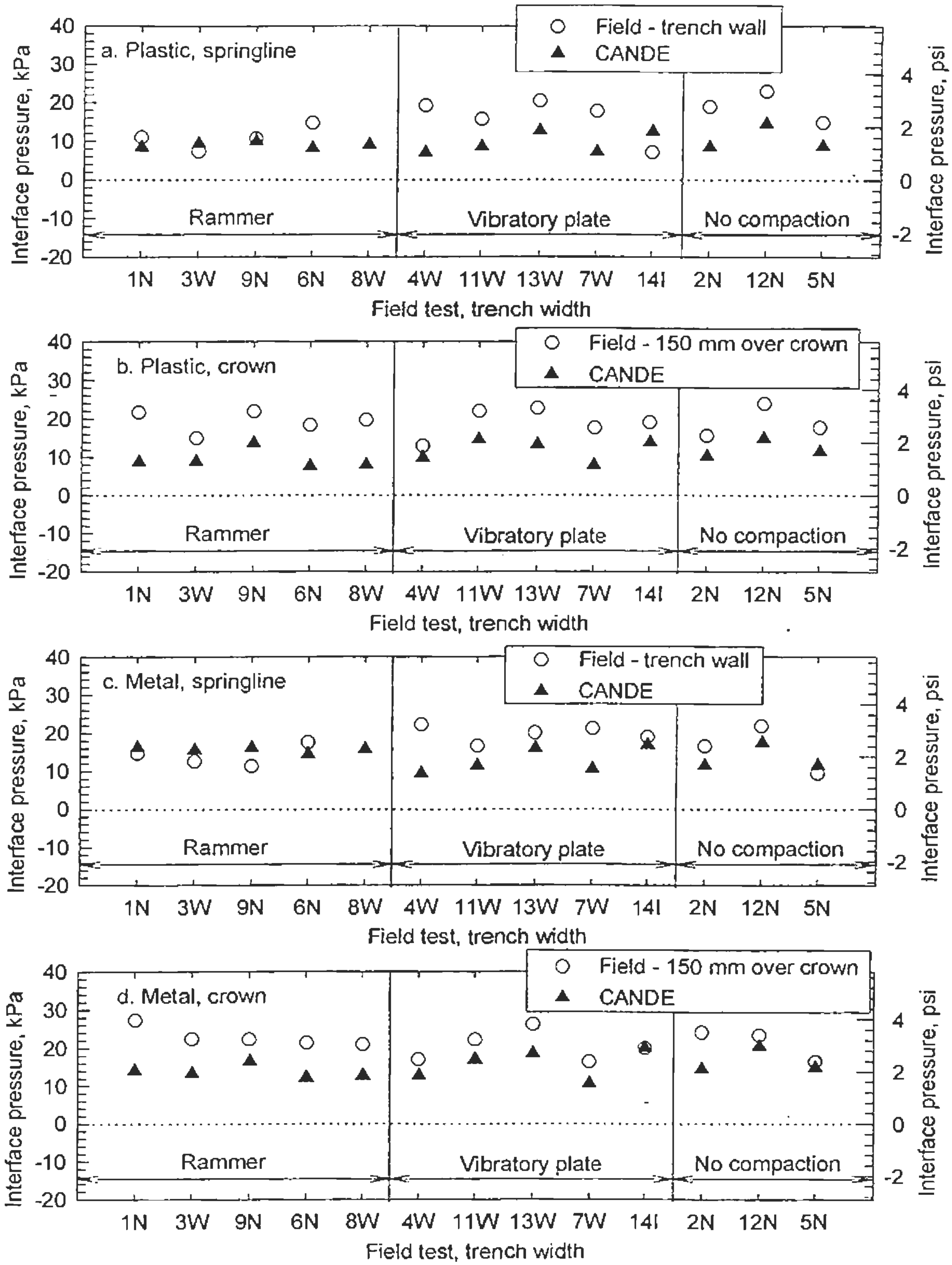

Figure 5.13 CANDE Interface Pressures Compared to Field Pressures on Plastic and Metal

5.2.2.3 Strains

The thrust and bending moment predictions from CANDE were converted to strains by dividing by the modulus of elasticity of 205 GPa (29,000,000 psi) for steel and 500 MPa (72,500 psi) for plastic and comparing to the field data in figs. 5.14 and 5.15 for the plastic and metal pipe respectively. The modulus of plastic is an estimated value, as noted earlier in this chapter. As noted in section 4.2.6.5, the strain levels for the metal pipe were small and are not reported. The match between analysis and data is generally good, which is expected since the deflection predictions matched well.

The comparison of thrust strains in fig. 5.14a suggest that CANDE predicts the thrust reasonably well for the 900 mm (36 in.) diameter pipe and modestly overestimates the thrust for the tests with 1,500 mm (60 in.) pipe. The strain predictions at the invert, springline, and crown of the plastic pipe are also in general agreement with the field data.

The same comparison for the metal pipe in fig. 5.15 also shows that the data are in general agreement with the CANDE predictions.

5.3 Summary

In general, both the Burns and Richard elasticity solution and the CANDE finite element program provide reasonable estimates of pipe response to earth load. The Burns and Richard solution is somewhat idealized and does not have the ability to treat special design conditions such as soft haunching, trench installations, or differing embedment material; however with some empirical adjustments, it is likely that this method could be developed into a simplified design method. The CANDE finite element program provided quite good estimates of behavior and is quite powerful in its ability to address special design situations; however, the complexity of the program and the uncertainty of actual installation conditions for most pipes, will probably result in CANDE being used only for special design situations.

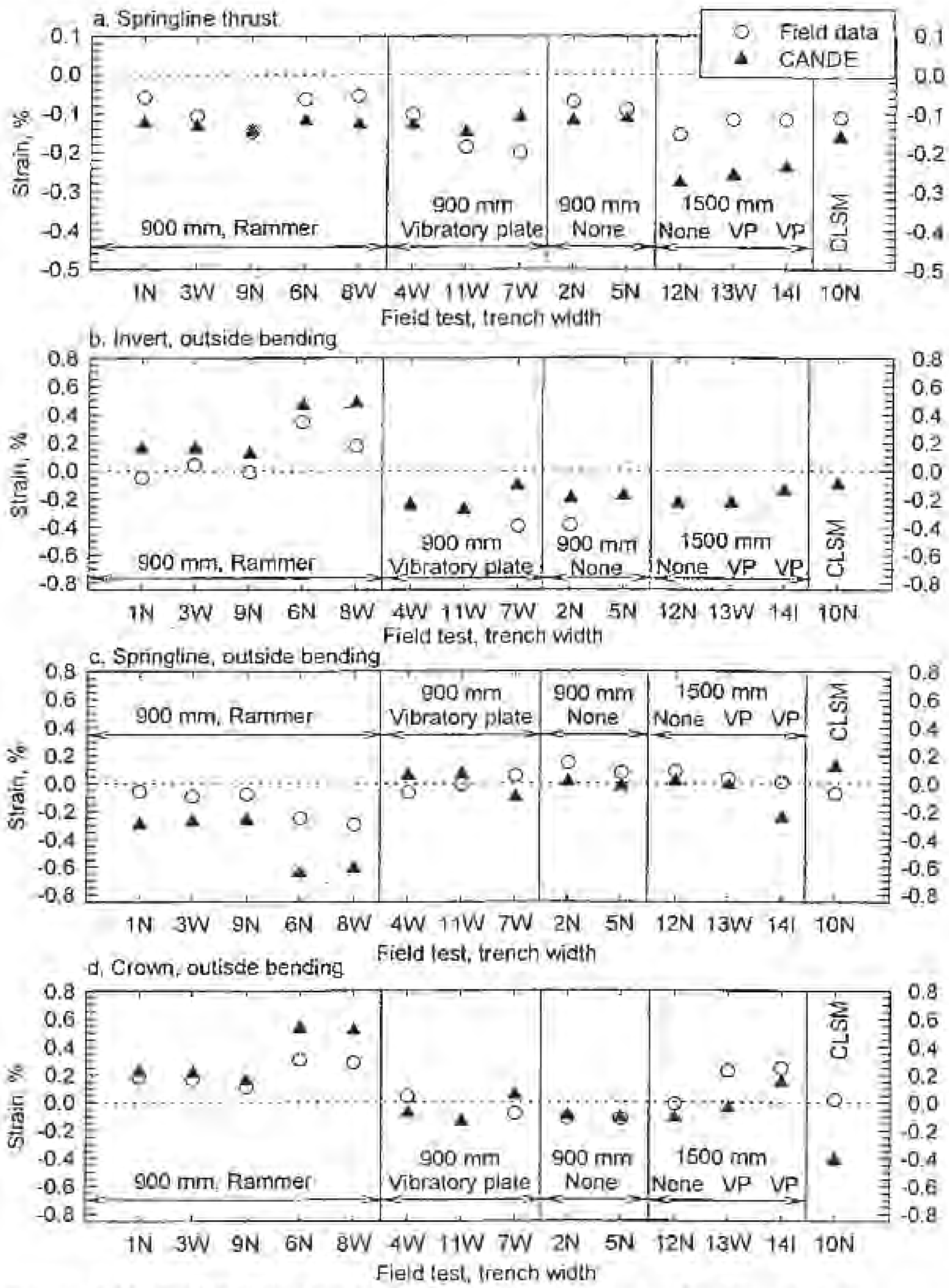

Figure 5.14 CANDE Strains Compared to Field Strains for Plastic Pipe

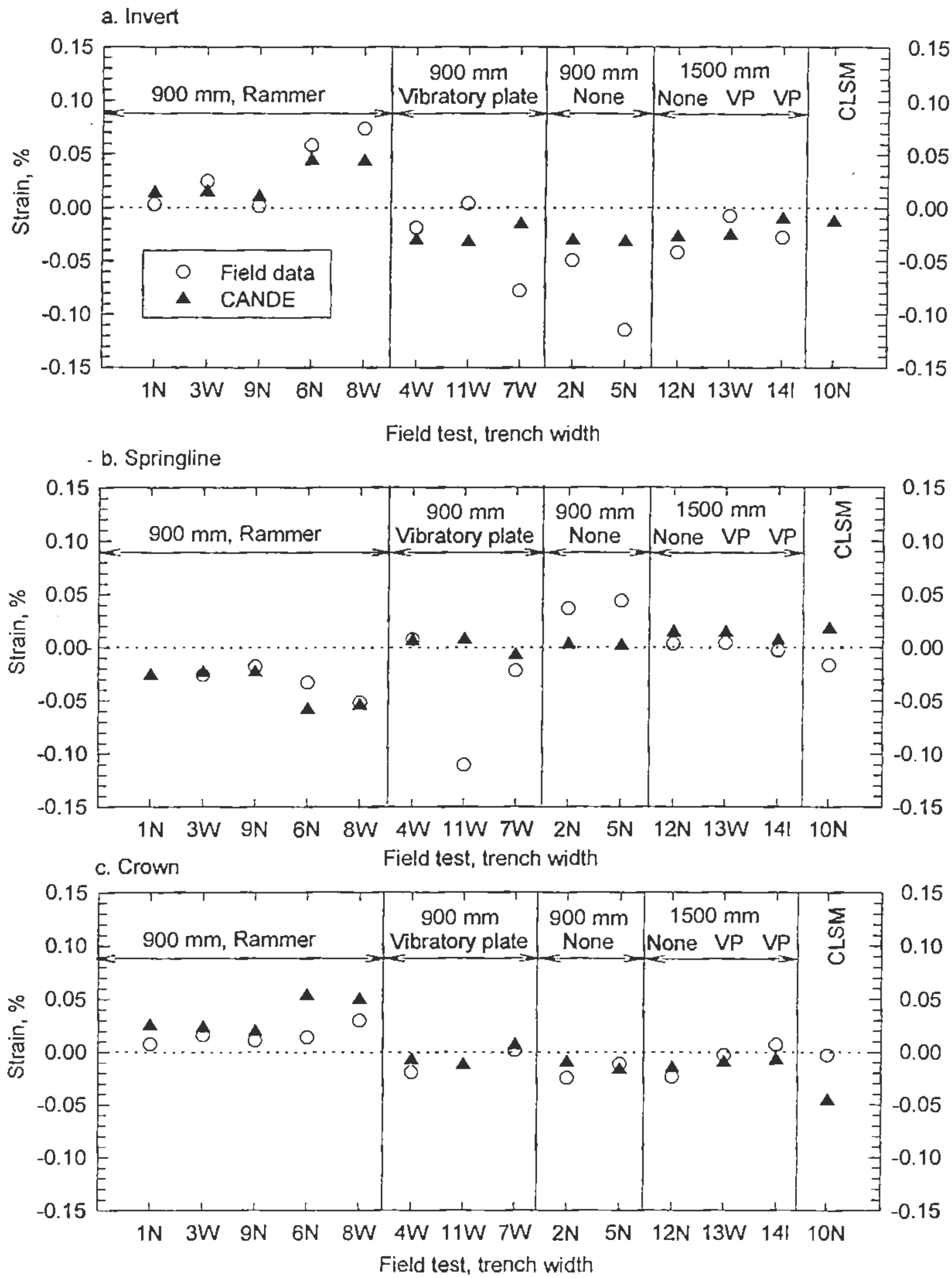

Figure 5.15 CANDE Strains Compared to Field Strains for Metal Pipe

CHAPTER 6
CONSIDERATIONS FOR INSTALLATION PRACTICE

Prior chapters have presented information on the following important issues related to installation practice for buried pipe:

- Characterization of in situ soils.
- Classification and characterization of backfill materials.
- Guidelines for installation practice.
- Computer modeling of buried pipe behavior.
- Use of CLSM as backfill for buried pipe installations.
- General behavior of buried pipe.

The nature of the pipe soil system makes it difficult to separate installation practice from design practice and almost any decision regarding one will affect the other. While the focus of this project is to understand the process of pipe installation, i.e., what happens as backfill is placed at the side of the pipe, some of the findings are applicable to the design process. In the following sections, each of the above items is discussed with a primary focus on installation practice. Design practice is discussed where appropriate.

6.1 In Situ Soils

Installation of a pipe requires stable in situ soil. This includes vertical support of the bedding and, for trench installations, lateral support by the trench walls. Provisions for achieving a stable foundation beneath a buried pipe are well defined in installation standards such as ASTM D 2321 and were not a subject of this study. Characterization of trench walls for lateral support provided to pipe, especially flexible pipe, is not as well defined. To address this issue, the designer needs to characterize the soil properties in terms of stiffness and strength and then assess the affect on the pipe's performance. The latter issue will be affected by the trench width relative to the pipe diameter and by the stiffness of the in situ soil relative to the backfill soil. These are largely matters considered in flexible pipe design, where a soil stiffness is required to evaluate lateral soil support to the pipe. In designing rigid pipes for trench installations, it is often assumed that the pipe receives no lateral soil support.

In Situ Soil Stiffness – The stiffness of in situ soils is vastly more variable than that of placed backfill materials. Placed materials must have a range of particle sizes that is suitable for handling and placing next to a pipe, and the potential for developing adequate support to the pipe when placed and compacted. Thus, formations with boulders and solid rock, aged deposits, such as some glacial tills that can be extremely hard when undisturbed, or excessively compressible materials, such as peats and soft clays, need not receive consideration as backfill materials. However, as in situ materials, all of these types of soils must be considered and evaluated.

A second issue in evaluating in situ materials is that pipelines are linear structures extending over great distances, and often through several soil formations. While complete evaluation of in situ properties could require many soil borings, few are generally taken because of the expense.

It is desirable therefore to provide simplified methods for evaluating in situ soils, such that the results of standard exploration techniques may be used. Perhaps the most common test conducted as part of soil exploration is the standard penetration test (ASTM D 1586), which evaluates soil by driving a sampler with a known effort. The result of this test is reported as the blows required to advance the sampler 300 mm (12 in.). Alternatively, either by the use of unconfined compression test (ASTM D 2166) or penetrometers, the strength of a fine-grained soil may be estimated relatively quickly. AWWA Manual M 45 (AWWA, 1996), *Fiberglass Pipe Design*, has published a table of E' values that are based on the results of the standard penetration test (SPT) or the unconfined compression strength of the soil (table 2.14). Given the work of chapter 3 (See section 3.4 and fig. 3.13, and section 6.2), which provides support for the use of the equality $E' = M_s$, this table can be used in empirical- or elasticity-based design methods, and should be a substantial aid to designers who have SPT or unconfined compression data available. The one-dimensional modulus may also be related to Young's modulus through Eq. 2.5, allowing the use of correlations between modulus and other soil properties.

A key consideration when evaluating in situ soil stiffness is that the condition of the soil at the time of testing may not be representative of the conditions at all times. Field tests 9 to 14, conducted at the clay site provide a good example of this. The undisturbed clay was relatively stiff, and for most of these tests, the soil strain gages indicate that lateral movement of the trench wall was inconsequential; however, during field test 11, there were heavy rains and the site became inundated. At the end of the test the trench, walls had moved outward 4 to 6 mm (0.15 to 0.25 in.). This is a relatively small movement, but it occurred over a period of a few days, and is indicative of ongoing movements that would continue in a permanent installation. Thus, the designer must consider potential changes in natural conditions.

Combined Pipe Support from Backfill and In Situ Soil – Also required for flexible pipe design is an evaluation of the affect of the in situ soils in providing support to a pipe. In a very narrow trench with little clearance between the trench walls and the pipe, the pipe deflection may be controlled mostly by the stiffness of the in situ soil; while in a very wide trench, the stiffness of the in situ soil will be inconsequential. Leonhardt (1979) developed Eq. 2.10 to address this issue and AWWA Manual M 45 (AWWA 1996) adopted a similar approach in the form of a table of influence factors for the in situ soil. The basis of both of these approaches is that the in situ soil is inconsequential for trench widths wider than about five pipe diameters. The field tests were consistent with this previous approach. In tests with wide trenches, with a width of about three pipe diameters for the 900 mm (36 in.) pipe, there was still an influence of the trench wall on the pipe behavior. The lateral soil stresses at the trench wall were of similar magnitude for the tests with this condition as for the narrow trench tests, with a width of about 1.6 pipe diameters (See fig. 4.44). While the assumption of needing a trench width of five pipe diameters would appear to be conservative, the cost of excavating wide trenches is expensive, especially with large diameter pipe. The method of Eq. 2.10, or AWWA Manual M 45 may be used in design for the time being, but better solutions are desired.

6.2 Backfill

Soil Groupings for Design – Many installation standards for buried pipe (ASTM D 2321, ASTM D 3839, AWWA Manual M 45, and AASHTO SIDD standard concrete pipe installations) identify three or four general soil groups within which the soils have similar characteristics as pipe backfill materials. This approach was also adopted by Howard in developing his table of values for the modulus of soil reaction. The typical groups, as discussed in section 2.2.1, generally include:

- Angular processed material, such as crushed stone (except for the SIDD soil groups),
- Gravels and sands with minimal fines content,
- Soils with fines but with a limit on total fines content and/or low plasticity, and
- Soils with unlimited fines content, but low plasticity.

Soils with high plasticity such as CH, and in some systems MH, while included in some soil design groupings, are generally considered unsuitable for pipe backfill material.

Overall, the approach of grouping soils into three or four broad categories has worked well, but it is desirable to adopt a single system of soil groups for pipe backfill that will apply to all types of pipe. The two soil groupings of most interest, since they are associated with stiffness properties that can be used in design, are the SIDD soil groups adopted by AASHTO for concrete pipe design and the Howard soil groups. The differences between these two groups in terms of gradation and plasticity were discussed in section 2.2.1, where it was shown that the SIDD soil groups tend to differentiate on the basis of clay versus silt (above or below the A-line, fig. 2.8), while the Howard soil groups tend to differentiate on the basis of fines content (more or less than 30 percent coarse grained material). There is not a clear choice for one group over the other; however, since the soil properties in the SIDD groups were developed for finite element analysis, and are the basis for the stiffness recommendations in this report (table 3.6), it is proposed that these groups be adopted for all types of pipes. The one shortcoming of this is that no hyperbolic properties have been developed for angular crushed stone materials. The properties of the SW soils could be used until more appropriate values become available. Although empirical in nature, the Howard recommendations of E' could also be used as a basis for extrapolating the SW values to values for crushed stone.

Also of interest is the approach of the Water Research Centre in the United Kingdom (table 2.9) which distinguishes between single size gravel and graded gravel. The single size gravel has the benefit of having a relatively high stiffness when placed loosely (note the relatively high values of loose density for soils 1 and 4 in fig. 3.3). The results of the laboratory soil box tests confirm this (see fig. 4.4 and individual test results). This high stiffness with minimal effort can be a significant aid when installing backfill in difficult situations or without inspection. The one concern with single size materials is that they have significant void space and thus are susceptible to migration of fine-grained soil from the adjacent in situ soils. Action must be taken to assess the likelihood of migration and, if necessary, take action to prevent it by using a geosynthetic filter fabric or control of the relative gradations of adjacent soils. ASTM D 2321 provides guidance on the latter subject.

Empirical and True Soil Properties: E' versus M_s – Preceding discussions have recommended the adoption of the constrained, or one-dimensional modulus, M_s, as a design soil modulus in lieu of the historically used modulus of soil reaction, E'. This is highly desirable as it allows testing for soil properties rather than back calculation from buried pipe tests to evaluate different types of soil. However, a large body of literature exists based on the modulus of soil reaction and some of this information is useful in characterizing soil stiffness for design even when using the constrained modulus. A comparison of the Howard values of E' with the Selig/SIDD hyperbolic soil properties was presented in fig. 3.13. This suggests that at low levels of applied stress the two sets of properties match reasonably well, and indeed, the data base from which Howard developed his recommended values of E' was based on pipe buried at modest depths of fill. While it is desirable to move away from E' as a design parameter and to take advantage of the available work related to it, the relationship E' = M_s is recommended for use until more work is completed for values of M_s.

Reliability – The reliability of buried pipe installations is a significant issue. This requires an honest assessment by a designer about the quality of installation practice that will be exercised in the field. Examination of table 3.6 shows that the modulus of a soil at a density of 90 percent of maximum standard Proctor is about one half the modulus of a soil at 95 percent of maximum density, and the modulus of a soil at 85 percent of maximum density is one half or less that of a soil at 90 percent of maximum density. These significant changes suggest that the designer must evaluate the sensitivity of the installation to achieving the design soil stiffness, and must consider the likelihood of actually achieving the design soil stiffness during construction. In future development of design procedures for flexible or rigid pipes, introduction of a strength reduction factor on the soil stiffness term to account for sensitivity should be considered.

The selection of the most economical backfill and treatment in design is related to reliability as well as cost and deserves considerable attention. Crushed rock and SW materials provide good support to a pipe, and at high percent compaction will allow the use of the least expensive pipe. In addition, these materials have good stiffness properties even at low percent compaction. However, coarse grained backfills are often processed materials and are extremely expensive in some locations (Louisiana and Florida for example). Thus it is often economically desirable to use finer grained processed backfills or in situ soils as pipe embedment. Finer grained materials, such as the silty sand used in the field tests, are sensitive to moisture, are inherently less stiff at the same percent compaction as a coarser grained soil, and produce more deformation in flexible pipe during backfill compaction. The field tests clearly demonstrate that these materials may be successfully used as pipe backfill; however, they also demonstrate some of the problems that are likely. The saturation of the silty sand bedding in test 5, and the increased deflection in test 7, in which the pipe was installed without haunching are indications of the types of problems that can occur. Field tests with the stone backfill was subjected to the same conditions without problems.

The above discussion raises the question: What is the most economical pipe installation? It is easy to think that a less expensive pipe will be more economical; however, the total installation cost, which includes the cost of purchasing, placing, and compacting backfill and the cost of inspection, should be considered. High-quality installations should always be inspected. As noted above, the design soil stiffness is very sensitive to just a 5 percent variation in level of compaction. The cost of this inspection should be balanced against the cost of a more expensive pipe with backfill compacted to a less stringent requirement, and perhaps with reduced inspection. It may be more economical to purchase a more expensive pipe and reduce the sensitivity of the installation to variations in construction practice.

6.3 Guidelines for Installation Practice

There are many important steps that must be taken to achieve a quality buried pipe installation. A few of these steps and the related findings of the study are discussed here.

Trench Width – The previous section discussed the effects of trench width in terms of soil support to the pipe. There are many other considerations that affect the design decision of trench width as well. Traditionally, designers specify that trench widths be kept as narrow as possible to minimize excavation cost and the load predicted by the Marston trench load theory. Specifications sometimes allow trench widths as narrow as the pipe outside diameter plus 300 mm (12 in.). The actual criteria for trench width should be based on constructability. Working material into the haunch and compacting fill at the sides of the pipe are far more critical than minimizing the trench load. While wider trenches cost more to excavate and backfill, they must be used if required to properly construct the embedment zone. The findings of the project regarding trench width were:

1. For the 900 mm pipe the working space in the narrow trench (pipe outside diameter plus 600 mm, 24 in.), the working space was the minimum acceptable but adequate only because the trench was benched near the top of the pipe (See figs. 4.37 and 4.38).
2. For the 1,500 mm pipe, the narrow trench condition (pipe outside diameter plus 600 mm, 24 in.) was clearly inadequate to allow room for joining the pipe, haunching, and compacting the backfill. the intermediate trench (pipe outside diameter plus 900 mm, 36 in.) was marginally acceptable.
3. For both sizes of the pipe, the wide trench (pipe outside diameter plus 1800 mm, 72 in.) provided good working space.

In addition to the findings of the field tests, the conditions of a particular installation need to be considered. If CLSM is used as backfill then the trench need only be wide enough to allow placing and joining the pipe, because haunching and compaction are not required. If rounded pea gravel, or similar single sized material that is relatively free flowing is used then trenches could also be narrowed. The space between the trench wall and the springline should be wider than the compaction equipment. The rammer used in the field tests could be used for compaction in spaces as narrow as 300 mm, while compaction with the vibratory plate required a space at least 450 mm.

Bedding – Traditionally bedding under a pipe has been compacted, primarily as a method of controlling the pipe grade by minimizing settlement after construction (and perhaps also because it is easy to compact the bedding since the pipe does not get in the way). The SIDD installations adopted by AASHTO have incorporated a recommendation to leave the middle bedding, directly under the bottom of the pipe (fig. 2.4) and uncompacted. The computer modeling indicates that this reduces the load on the pipe and the invert bending moments. It is important that the outer bedding still be compacted to provide support to the haunch area of the pipe and to provide an alternate vertical load path around the pipe bottom. The field tests suggest that leaving the bedding soft does reduce the interface pressures at the pipe bottom. The computer modeling (chapter 5) confirms this benefit. Even though the invert interface pressures that were measured in the field were consistently higher than predicted by the model, both field and computer model demonstrate lower invert pressures with uncompacted bedding.

Haunching – Some effort at haunching should always be specified. The bending moments in the field tests and the computer models are significantly greater in the unhaunched installations. In addition, the failure to provide haunching incorporates a significant void in the backfill that can lead to longer term soil movements and corresponding reduced support to the pipe. In the field and laboratory tests, slicing backfill into the haunch area with shovels was shown to be an effective method of providing haunch support. Tampers, such as used on field tests 12 to 14 were also very effective. A large-faced tamper, 75 by 150 mm (3 by 6 in.), was effective for the silty sand and a small-faced tamper, 25 by 75 mm (1 by 3 in.) was effective for the stone. A small faced tamper is imperative for angular materials to generate sufficient force to overcome the particle interlocking. A tamper attached to a long rod can allow a laborer to be out of the trench while tamping the haunch.

Haunching is best accomplished after the pipe is set in position, by placing part of the first lift of backfill, working it into the haunches and then placing the remainder of the lift. Haunching effort cannot be effectively applied if backfill is placed so high on the pipe that it blocks access to the haunch zone.

Compaction of Backfill – Some compactive effort is always desirable. Even though some coarse-grained backfill materials may achieve 85 percent to 90 percent of maximum Proctor density when placed with little effort, there are undoubtedly voids that develop around pipes and against trench walls when the material is first placed. This appears to be particularly true with the deep corrugations of the plastic pipe. A modest effort at compaction (perhaps a simple effort at shovel slicing, although this was not evaluated during the tests) would likely eliminate the 1 percent jump in deflections observed in tests 2 and 5.

Compaction induced deflections (peaking) clearly increase as the backfill materials become finer grained. In the field tests the peaking deflection with silty sand backfill was about three times the peaking deflection with the stone for the same number of coverages of the compactor. While the magnitudes of the peaking deflections (up to 2 percent change in diameter, see fig. 4.40) were not excessive, they were significant, and designers should be aware of this issue. Larger compaction equipment, such as walk behind or ride on rollers, or the use of lower stiffness pipe, could easily result in excessive peaking, or distortion of the pipe shape during compaction. Limits on upward peaking because of compaction effects should be lower than limits on downward deflection caused by earth load. This recommendation is made because peaking deflection is essentially the result of a point load and can result in higher local deflections and stresses than deflection caused by earth load.

Similar to leaving the bedding uncompacted under the pipe, there is merit in leaving the portion of the first backfill lift that covers the pipe uncompacted directly over the pipe as well. The computer model suggests that this drops the interface pressure on the top of the pipe, meaning that load is transferred into the pipe further out toward the sides of the pipe which should reduce the bending moments in the pipe.

6.4 Computer Modeling

The field tests were successfully modeled using the finite element computer program CANDE. A consistent approach was taken for all of the tests, and the field data matched the computer predictions quite well. A number of recommendations are made here:

1. Interface pressure readings and penetrometer testing indicate that with soil backfill, even with significant haunching effort, there is always a soft spot about 30 degrees

from the invert. This was modeled with the "void" zone shown in figs. 5.1 and 5.2. It is recommended that this zone be incorporated in all models of buried pipe installations unless the backfill is CLSM.

2. The use of concentrated forces has been shown to be an effective method to model compaction effects, and a simplified expression for computing these forces was developed; however, a soil model should be developed that would allow application of compaction forces directly to the soil. No practical method of accomplishing this has yet been incorporated into a generally available computer program such as CANDE.

3. When a soil layer is placed in the CANDE program, it is assigned the properties of the final compacted material. In actual construction, it is placed loosely and then compacted. This means that the weight of the soil is imposed on the pipe when the soil strength and stiffness are low, and it is then compacted to improve the properties. This type of modeling can have a significant effect on the loads imposed on a pipe, particularly in a trench installation. The apparent "arching" of load between the trench wall and the pipe noted for concrete pipes in section 5.2.2 (figs. 5.8 and 5.9) could be significantly reduced if the soil properties are those of loose soil when the weight of the soil is applied, and then increased to dense properties.

4. The behavior of the plastic pipe was best modeled using a lower modulus of elasticity than the specified short term value in AASHTO. This suggests that the viscoelastic nature of thermoplastics has an effect on pipe response during backfilling.

6.5 CLSM

The field tests show that CLSM can be an excellent backfill material. It placed easily and formed a stiff, uniform pipe support. Study of CLSM was not a key goal of this project; however, several recommendations and suggestions for further research can be made.

Mix Design – The ASTM flow test, Provisional Standard PS-28, is an excellent measure of the flowability of the mix. The study showed that flowability is derived largely from fly ash, not water. Mixes with high water contents tend to have the water segregate and do not flow well. The drawback to high fly ash content is that the pozzolanic nature of fly ash contributes to the long term strength gain and inhibits excavatability of the material. The mix design used in this study, which included 45 kg/m^3 (76 lb/yd^3) cement and 244 kg/m^3 (412 lb/yd^3) of fly ash had excellent flowability characteristics but its strength made it difficult to excavate. It may be appropriate to reduce the cement content.

Placing CLSM – Placing pipe up on blockings or bags as was done for the field tests in this study assures that the CLSM gets under the pipe and provides uniform support. The blocking should not be overly stiff, i.e., polystyrene foam would be desirable, wood would probably be acceptable, and concrete blocks would be unacceptable. If blocking the pipe is found too time consuming, it should be acceptable to place the pipe directly on the bedding as shown in fig. 2.5 taken from the clay pipe installation standard ASTM C 12; however, the CLSM will have to be delivered to both sides of the pipe. Installation with CLSM requires some control over when the pipe is backfilled. The pipe should not be further backfilled until the CLSM embedment has a greater stiffness than the bedding. Adding backfill when the CLSM is still soft, may actually produce a hard bedding situation and a line load at the invert of the pipe, since the CLSM in the haunch zone could be quite soft and not capable of providing good support. This should be an area of future study.

Controlling flotation is a key issue in the use of CLSM. In the field test, the pipe were weighted with gravel bags; however, this is not appropriate for an actual construction project. A quickly installed bracket that holds down the top of the pipe by bracing against the trench wall could be developed or, short sections culverts could be (carefully) held down with construction equipment. Because of the large magnitude of the flotation forces, placing the CLSM in multiple lifts will almost always be required. In the field tests, the plastic pipe, with deep corrugations developed a mechanical interlock with the first lift of CLSM that kept it from floating while placing the second lift. This suggests that studs could be welded to steel pipes, or could be strapped to plastic pipes to similarly form a mechanical bond to a first lift. This type of system could be developed to serve both the function of supporting the pipe off the bedding and providing anchorage from flotation.

The two deliveries of CLSM to the field tests for this project were quite different in strength and flowability and hence required mix adjustment in the field. Thus, checking the flow characteristics at the time of placement should be standard practice.

Quality Control – The use of test cylinders for strength testing may not be suitable as a quality control procedure. The low strength mixes, which are desirable for excavatability, were fragile and very difficult to test at an age of 7 days, and could not have been tested at earlier ages. At an age of 7 days, it is likely that a pipe or culvert has already been backfilled and the test results would serve as documentation of the material rather than a true quality control test. During the conduct of the field tests in this study, the density of the CLSM was checked with a nuclear density gage. This has merit as a field control procedure since the result of the test is known immediately.

It is necessary to decide what CLSM characteristics are important and require quality control. In structural design of buried pipe and culverts, a dense soil backfill is considered to be a high quality pipe support. In the field tests, the in place density of the CLSM was 2,130 kg/m^3 (133 pcf) which is representative of a broadly graded dense sand. This suggests that the flowable nature of the CLSM is actually a delivery system to place soil, rather than a cementitious material dependent on strength gain. This philosophy allows field testing to use geotechnical type tests that can be conducted quickly with results available right away.

During the field tests, the excess water hydrated out of the CLSM quickly and the material could be walked on within two hours. There were no problems in placing the second lift after 2 hours, and, had it not been the end of the work day, it is expected that there would have been no problems continuing normal backfilling after the second pour had set for 2 hours.

Air-Modified CLSM – Although not tested in this study, McGrath and Hoopes (1997) reported on the use of air-modified CLSM. This is CLSM with high air content, about 30 percent by volume, to produce flowable mixes without depending on fly ash. This has the benefit of reducing the long-term strength gain that results because of the pozzolanic reaction of the fly ash. The draw back to air-modified CLSM is that it depends on the strength gain caused by the curing of the cement to develop strength and stiffness. This material could not be backfilled after 2 hours.

6.6 General Behavior of Buried Pipe

The relatively high compaction deflections generated in the computer model of the 1,500 mm (60 in.) plastic pipe relative to the 900 mm (36 in.) plastic and metal pipe and the 1,500 mm (60 in.) diameter steel pipe, that were not observed in the field data, suggest that this profile design (a solid wall with a bonded tube as a rib) mobilizes a greater longitudinal length of pipes to resist compaction forces than does the corrugated pipe wall.

It may be appropriate to introduce design conditions based on how great a length of pipe is developed in resisting concentrated (i.e., compaction) loads.

The longitudinal strains in the 900 mm diameter plastic pipe were about 50 percent of the circumferential strains. This is a significant level which means that consideration of longitudinal stresses may be necessary for buried pipe.

CHAPTER 7
CONCLUSIONS

This report presents the results of an in depth evaluation of installation practice for buried pipe. The current practice of AASHTO member States was surveyed, as well as the current practice of pipe suppliers and standards organizations such as ASTM and AASHTO. Additional insight into backfill materials, and pipe behavior during installation was developed through laboratory backfill characterization tests, laboratory soil box tests, full-scale field tests, and computer modeling of test results. The main conclusions of the study are:

1. The soil properties used for the development of the SIDD concrete pipe installations are recommended as design properties for all types of pipes. These properties were developed for the hyperbolic model of soil behavior that is widely used for culvert analysis.

2. For simplified design use of the constrained modulus, M_s, is recommended, in lieu of the historical, but empirical modulus of soil reaction, E'. Design values for the constrained soil modulus are presented. The introduction of the table of soil values for M_s allows designers to assess the impact of using lower quality backfill materials than currently allowed by AASHTO specifications and to consider the effect of change in soil modulus with increasing confinement. Although it has been clearly demonstrated that fine grained soils have inherently lower stiffness, are sensitive to moisture, and require greater compactive effort to install, there are installation conditions where use of such materials may be economical provided proper installation controls are in place.

3. Pipe bedding should be left uncompacted under the middle third of the pipe diameter. This has been shown to be an effective method of reducing invert bending moments, particularly for rigid pipes.

4. Finite element modeling with the computer program CANDE has been shown to be an effective tool to understand pipe behavior during installation. It is important to model the actual installation conditions, such as the soft area in the lower haunch and compaction effects.

5. CANDE is the only generally available finite element computer program for culvert design at the present time. Technical improvements, such as the introduction of soil with loose soil properties and a later conversion to compacted properties, have been proposed and a better user interface would greatly increase the utility of the program. Of particular importance is access to the SIDD soil properties. Currently, use of these properties in CANDE requires manual input by the user. CANDE should be modified to make these properties available as defaults.

CHAPTER 7
CONCLUSIONS

This report presents the results of an in depth evaluation of installation practice for buried pipe. The current practice of AASHTO member States was surveyed, as well as the current practice of pipe suppliers and standards organizations such as ASTM and AASHTO. Additional insight into backfill materials, and pipe behavior during installation was developed through laboratory backfill characterization tests, laboratory soil box tests, full-scale field tests, and computer modeling of test results. The main conclusions of the study are:

1. The soil properties used for the development of the SIDD concrete pipe installations are recommended as design properties for all types of pipes. These properties were developed for the hyperbolic model of soil behavior that is widely used for culvert analysis.

2. For simplified design use of the constrained modulus, M_s, is recommended, in lieu of the historical, but empirical modulus of soil reaction, E'. Design values for the constrained soil modulus are presented. The introduction of the table of soil values for M_s allows designers to assess the impact of using lower quality backfill materials than currently allowed by AASHTO specifications and to consider the effect of change in soil modulus with increasing confinement. Although it has been clearly demonstrated that fine grained soils have inherently lower stiffness, are sensitive to moisture, and require greater compactive effort to install, there are installation conditions where use of such materials may be economical provided proper installation controls are in place.

3. Pipe bedding should be left uncompacted under the middle third of the pipe diameter. This has been shown to be an effective method of reducing invert bending moments, particularly for rigid pipes.

4. Finite element modeling with the computer program CANDE has been shown to be an effective tool to understand pipe behavior during installation. It is important to model the actual installation conditions, such as the soft area in the lower haunch and compaction effects.

5. CANDE is the only generally available finite element computer program for culvert design at the present time. Technical improvements, such as the introduction of soil with loose soil properties and a later conversion to compacted properties, have been proposed and a better user interface would greatly increase the utility of the program. Of particular importance is access to the SIDD soil properties. Currently, use of these properties in CANDE requires manual input by the user. CANDE should be modified to make these properties available as defaults.

APPENDIX

CANDE ANALYSES AND COMPARATIVE DATA FOR CONCRETE, PLASTIC, AND METAL PIPE – ALL FIELD TESTS

This appendix contains detailed results from the finite element model of each of the field tests using the computer program CANDE. One figure is presented with deflections, interface pressures, bending moments, thrusts, and shears for each type of pipe and each field test; a total of 42 analyses. Details of the procedures used for the analyses were presented in chapter 5. For comparison purposes, field data have been added whenever available. The keys and formatting of all figures is the same, even if no field data were available.

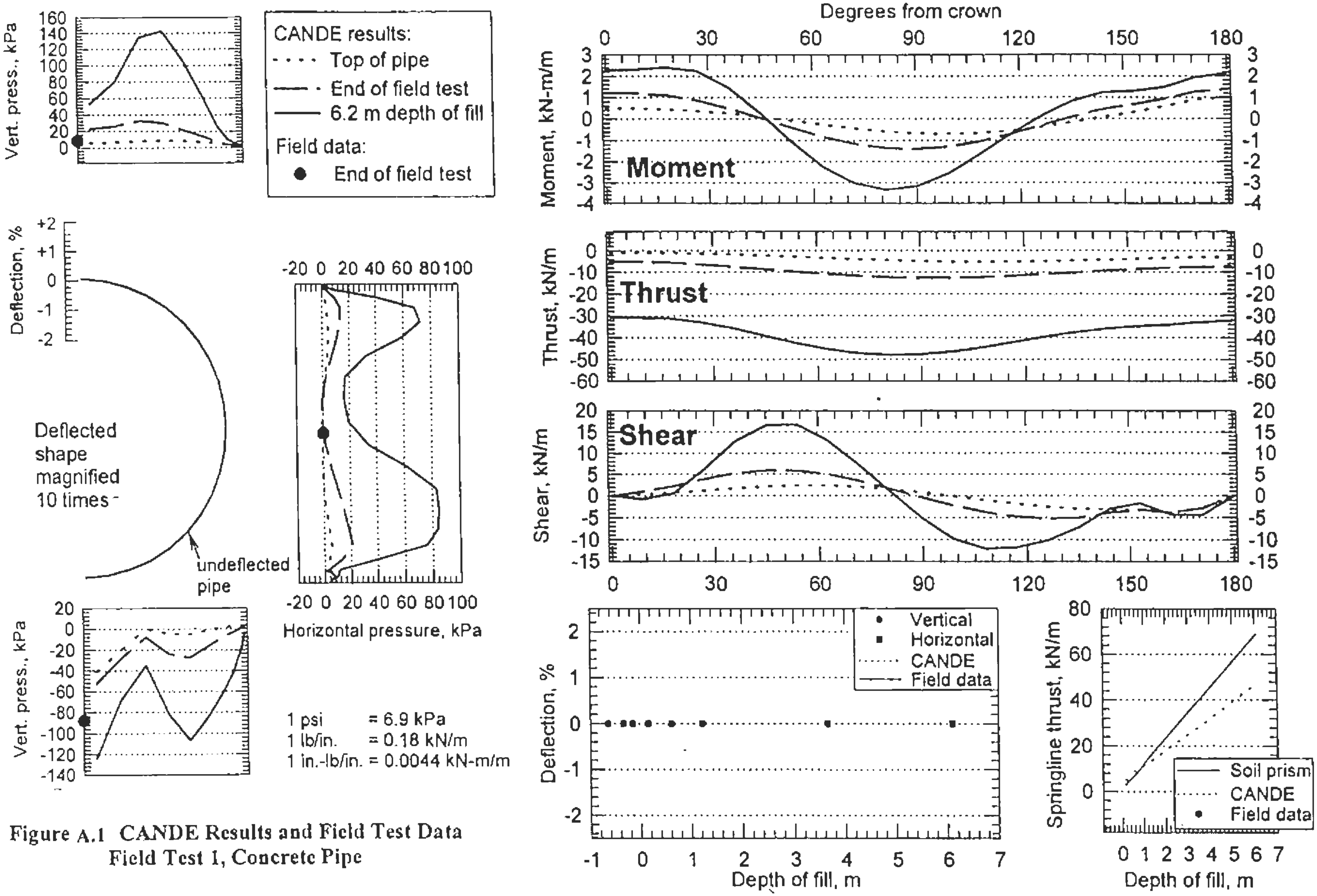

Figure A.1 CANDE Results and Field Test Data
Field Test 1, Concrete Pipe

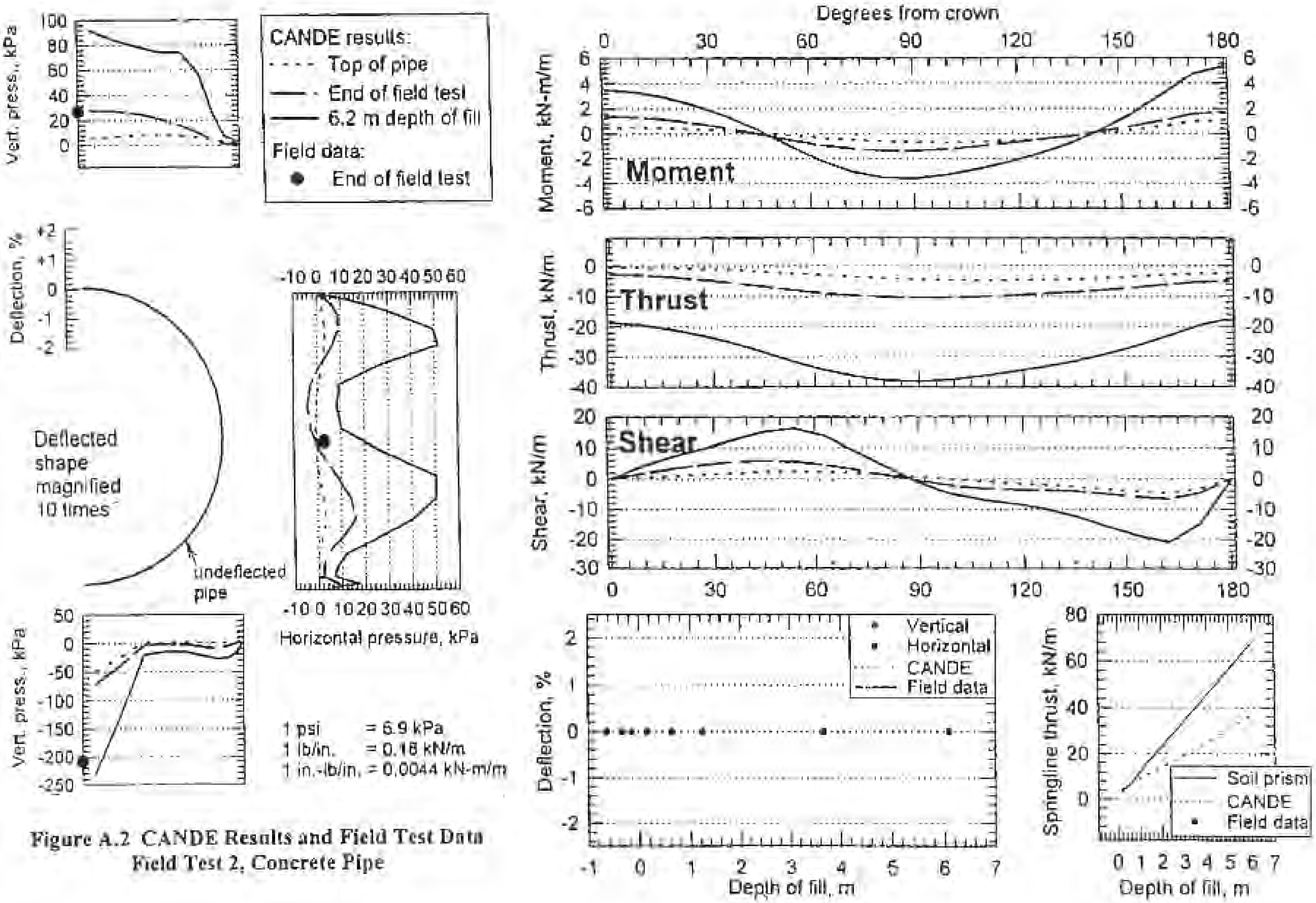

Figure A.2 CANDE Results and Field Test Data
Field Test 2, Concrete Pipe

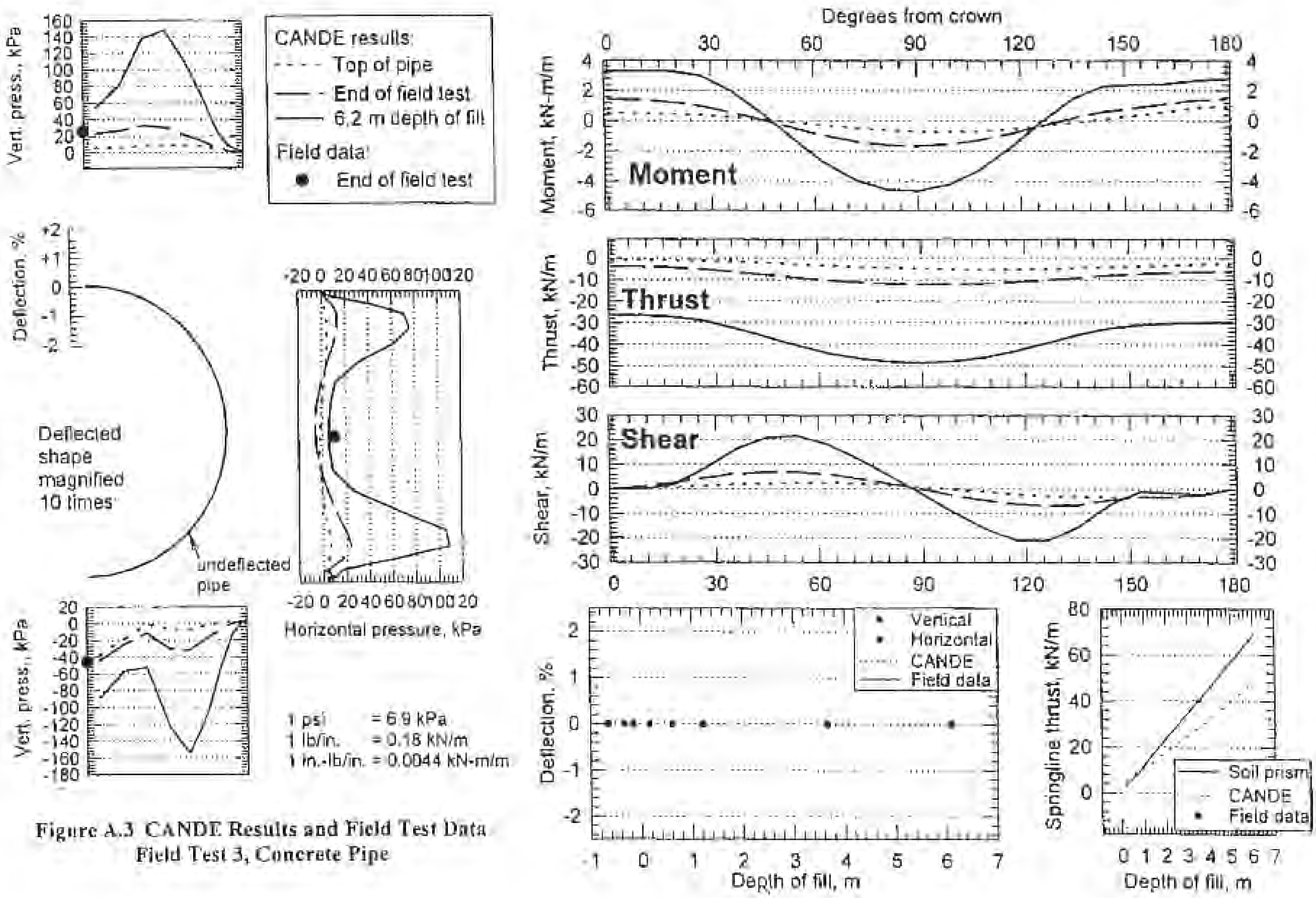

Figure A.3 CANDE Results and Field Test Data Field Test 3, Concrete Pipe

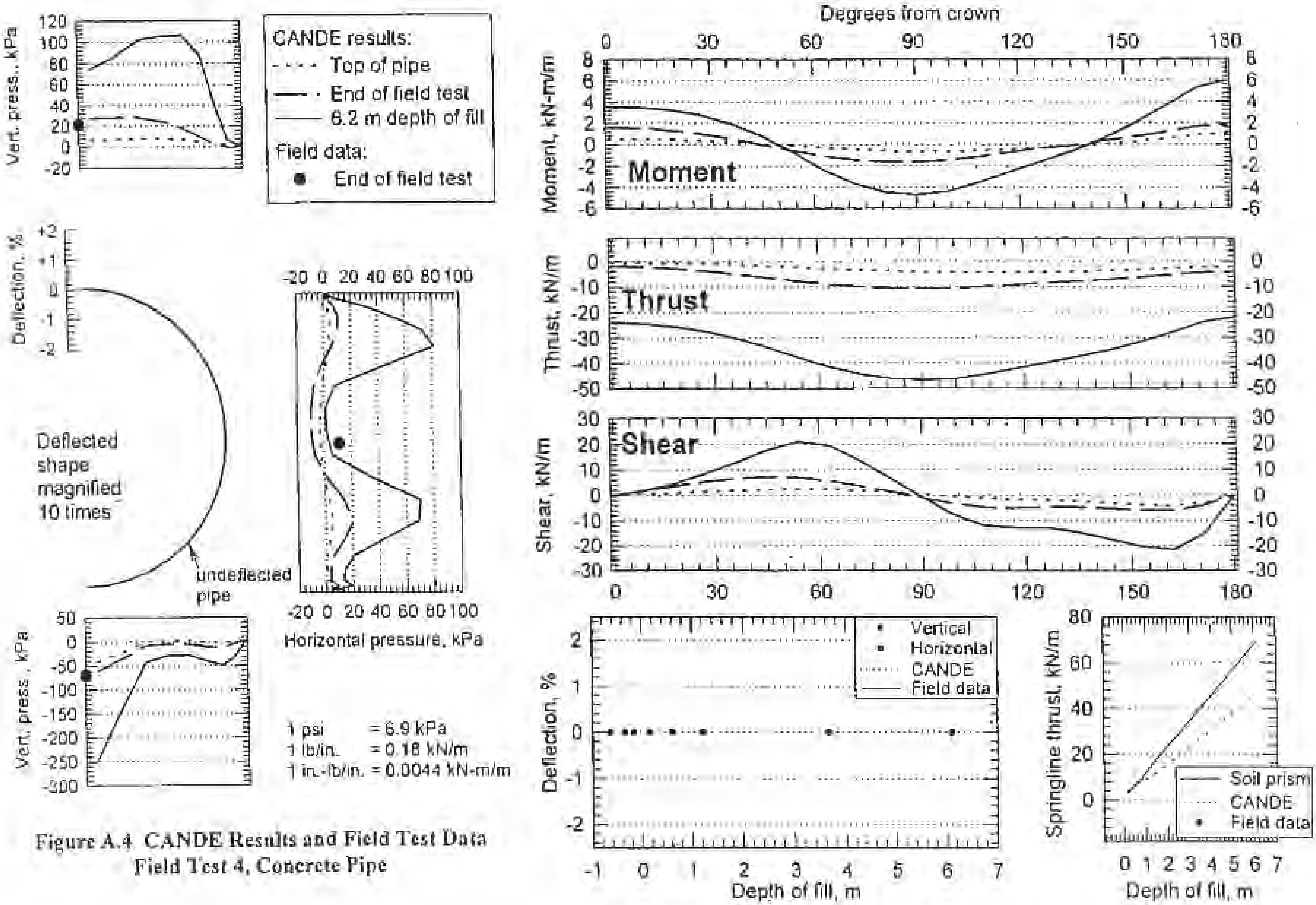

Figure A.4 CANDE Results and Field Test Data
Field Test 4, Concrete Pipe

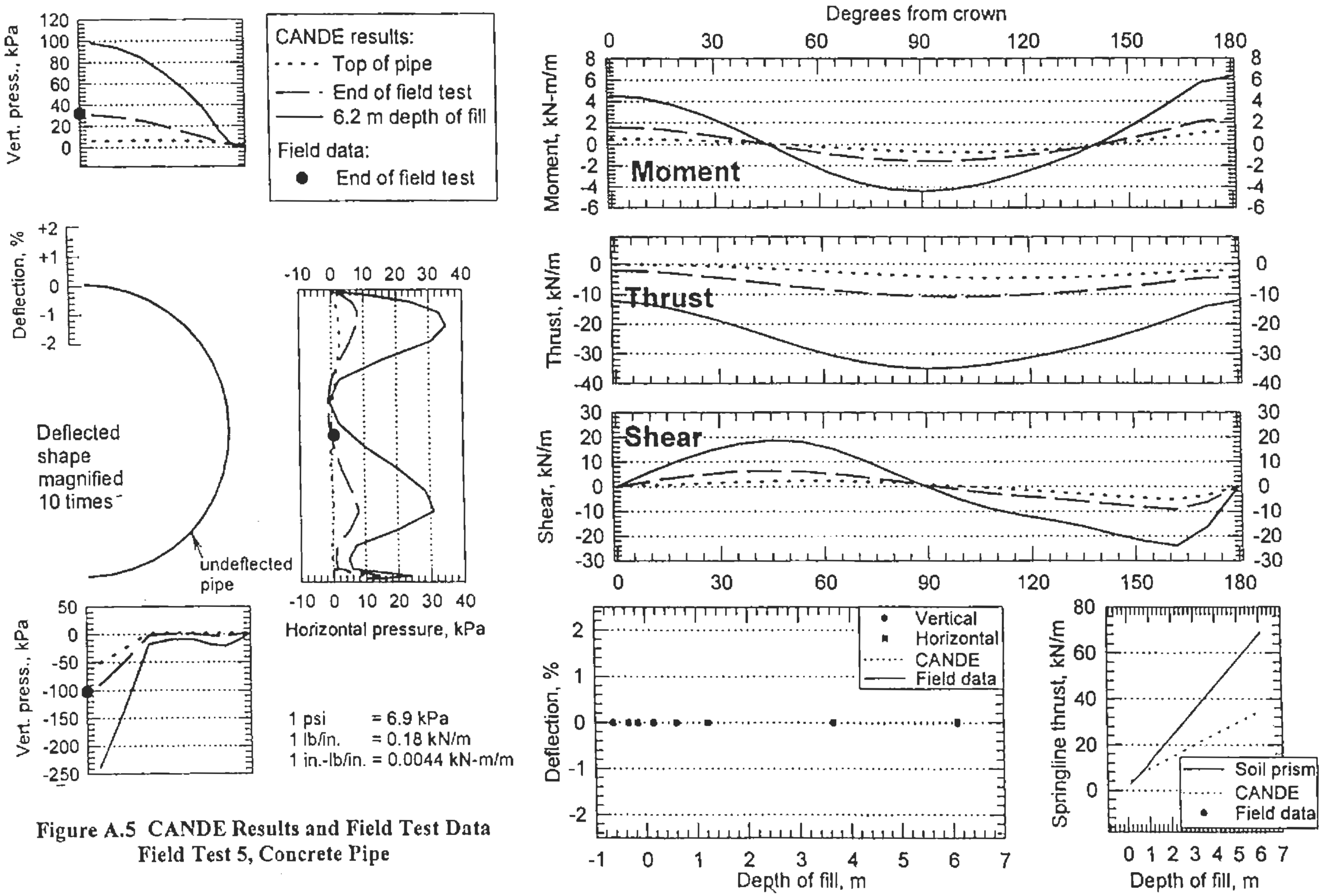

**Figure A.5 CANDE Results and Field Test Data
Field Test 5, Concrete Pipe**

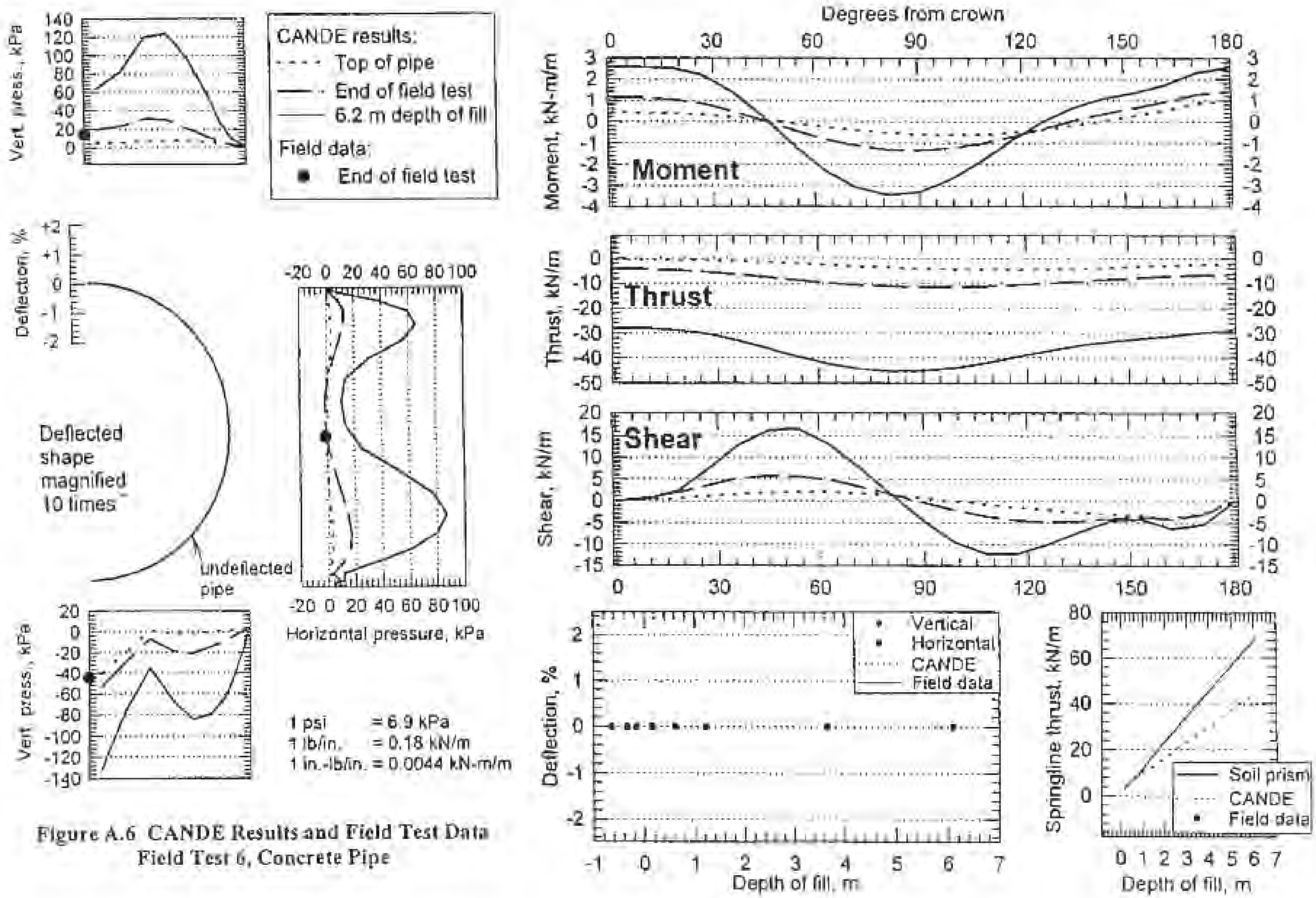

Figure A.6 CANDE Results and Field Test Data
Field Test 6, Concrete Pipe

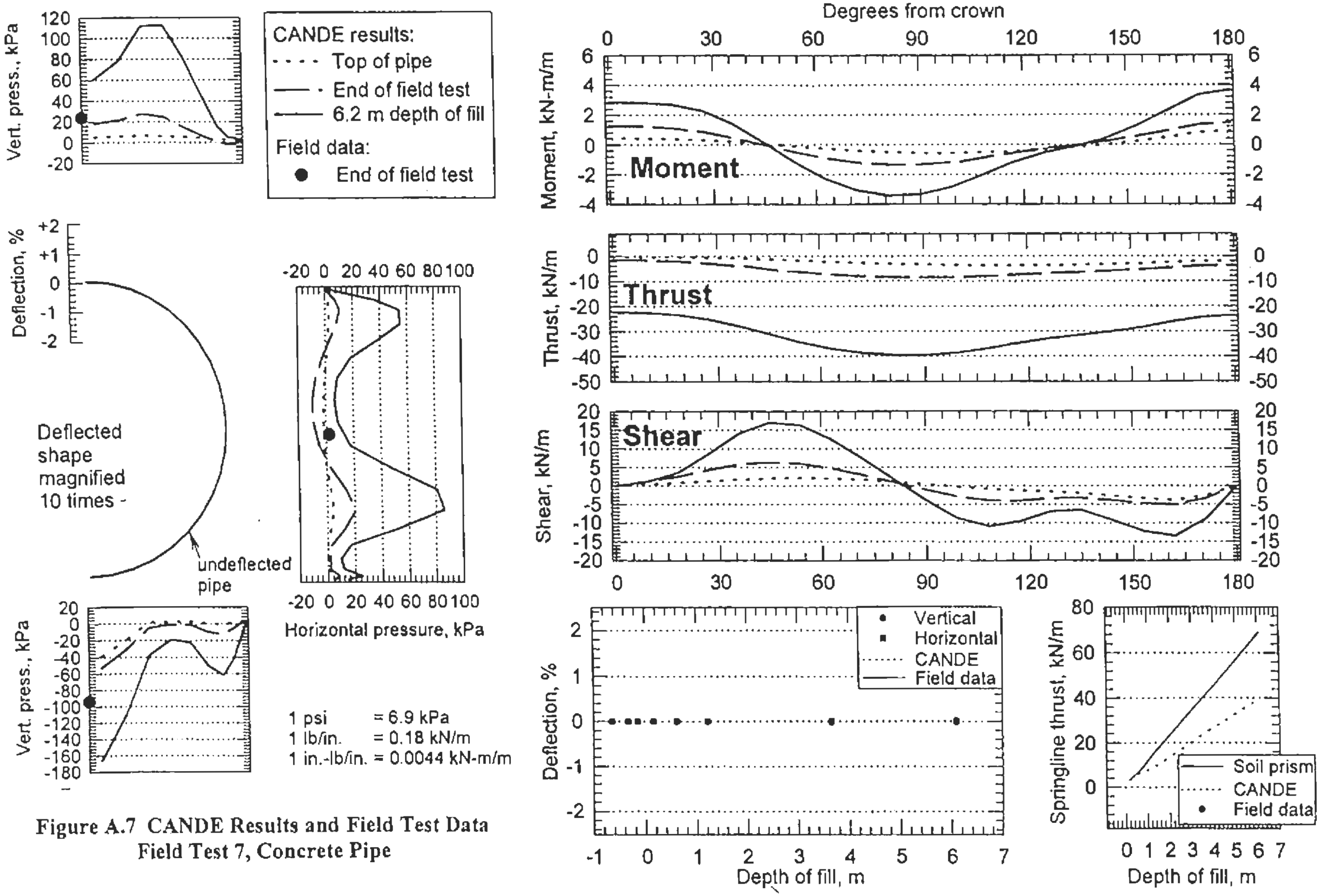

Figure A.7 CANDE Results and Field Test Data
Field Test 7, Concrete Pipe

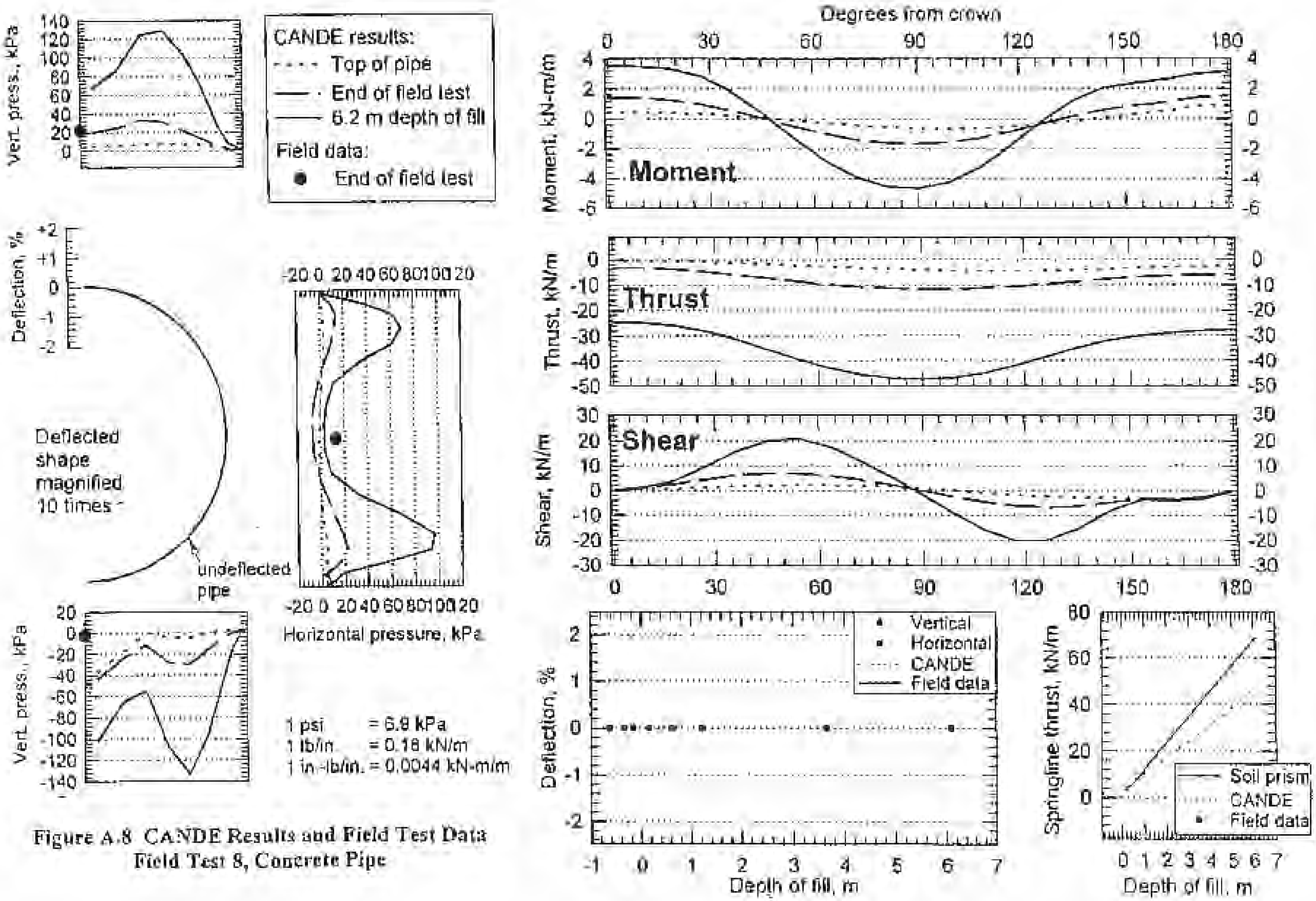

Figure A.8 CANDE Results and Field Test Data
Field Test 8, Concrete Pipe

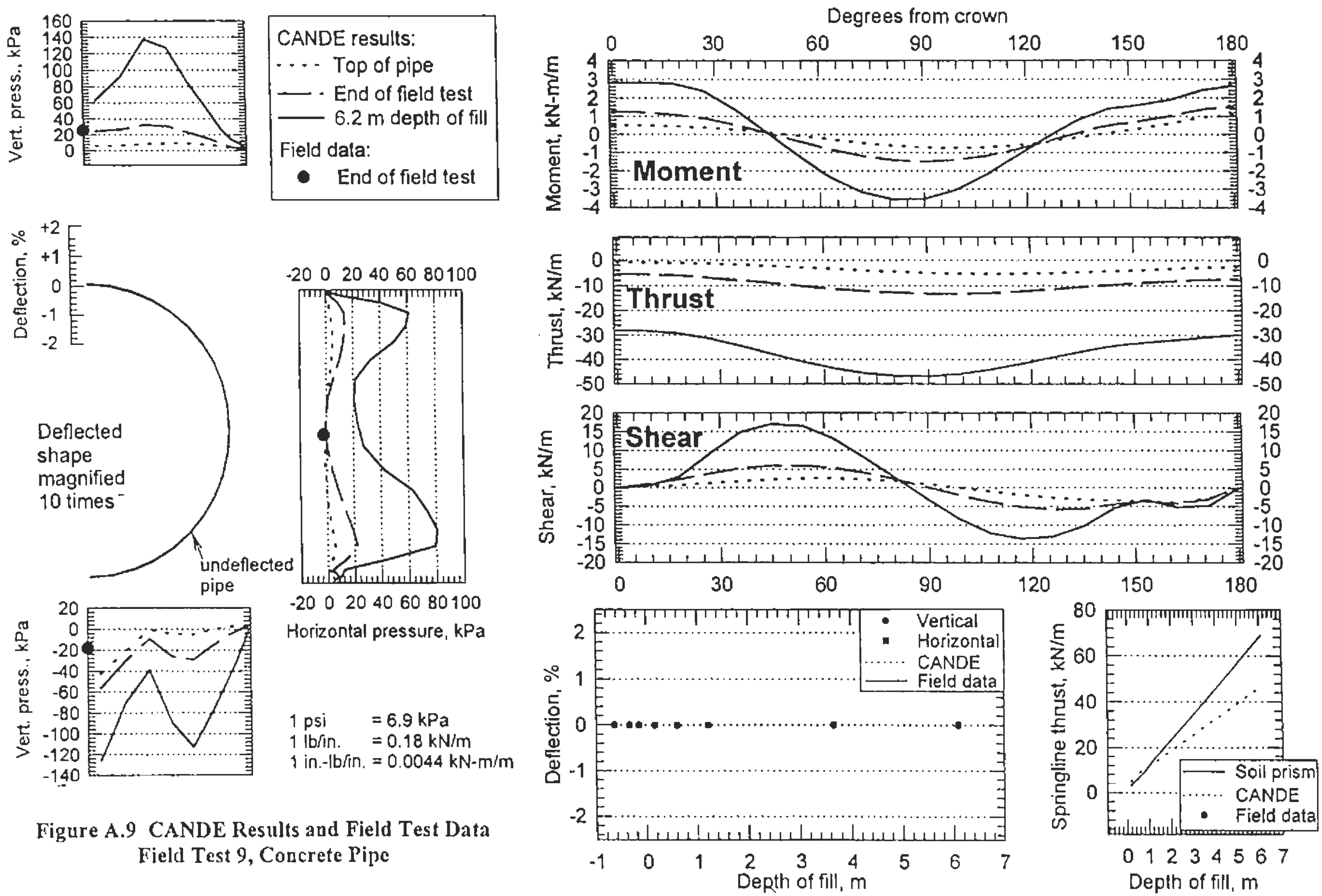

Figure A.9 CANDE Results and Field Test Data
Field Test 9, Concrete Pipe

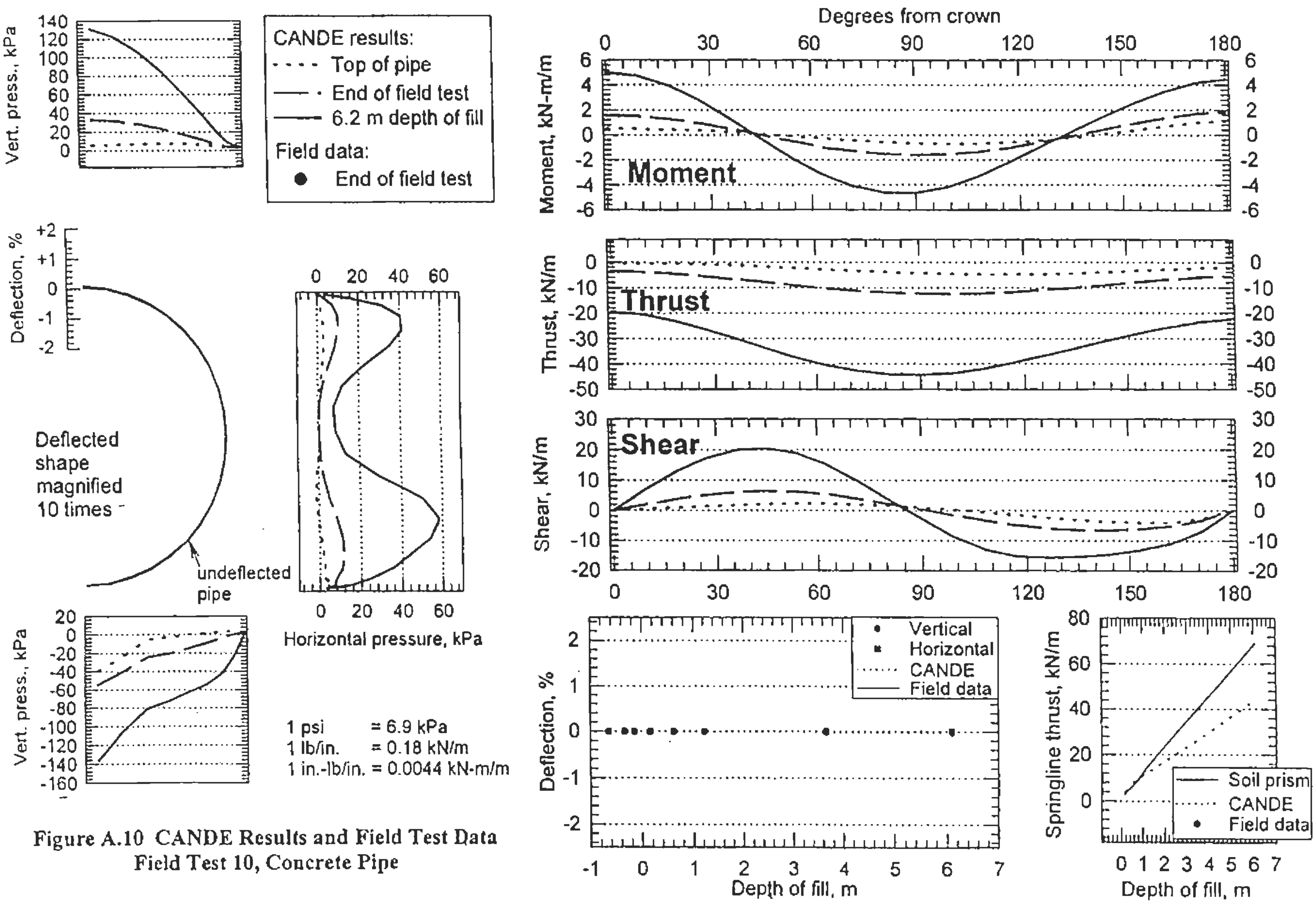

Figure A.10 CANDE Results and Field Test Data
Field Test 10, Concrete Pipe

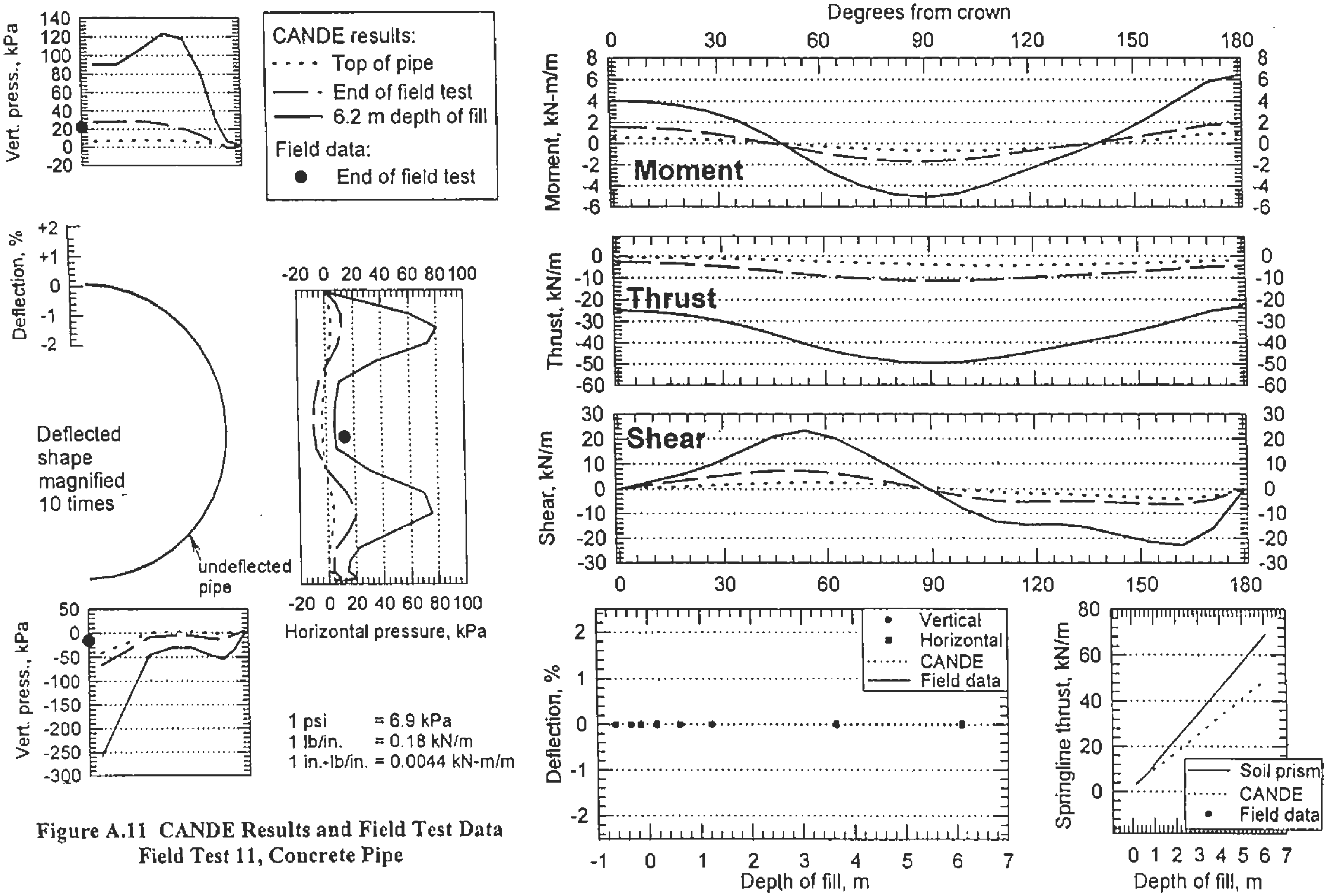

Figure A.11 CANDE Results and Field Test Data
Field Test 11, Concrete Pipe

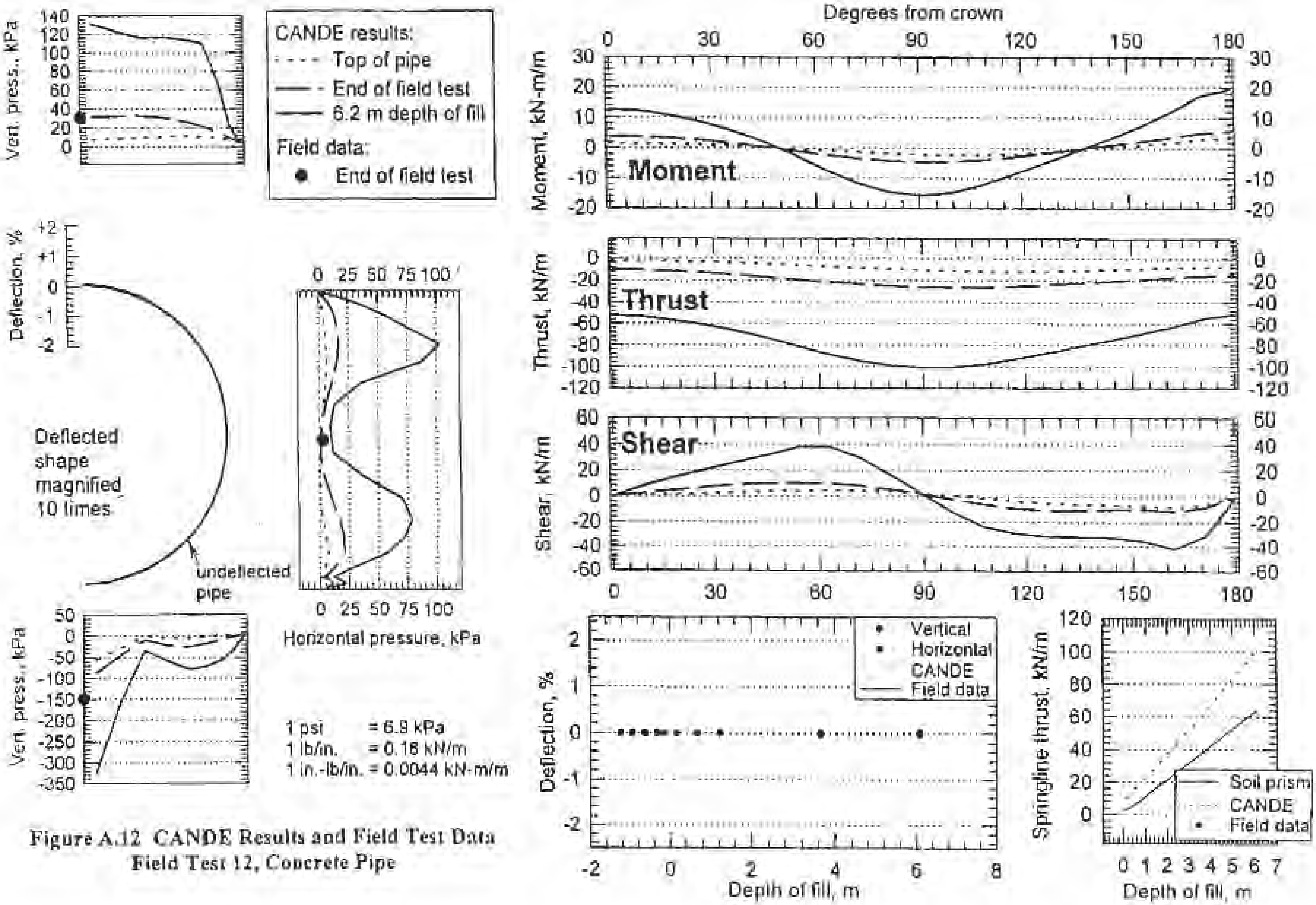

Figure A.12 CANDE Results and Field Test Data
Field Test 12, Concrete Pipe

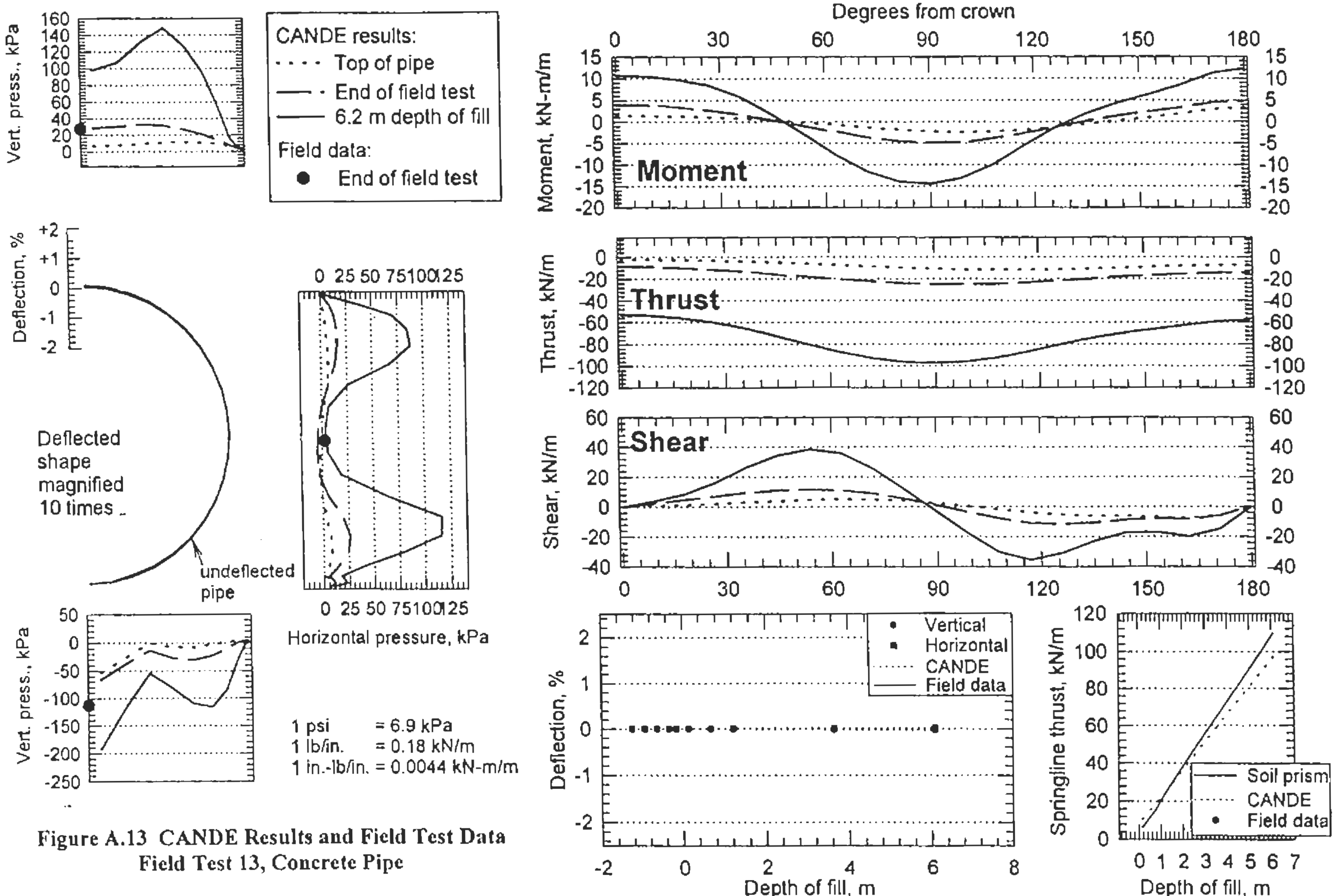

Figure A.13 CANDE Results and Field Test Data
Field Test 13, Concrete Pipe

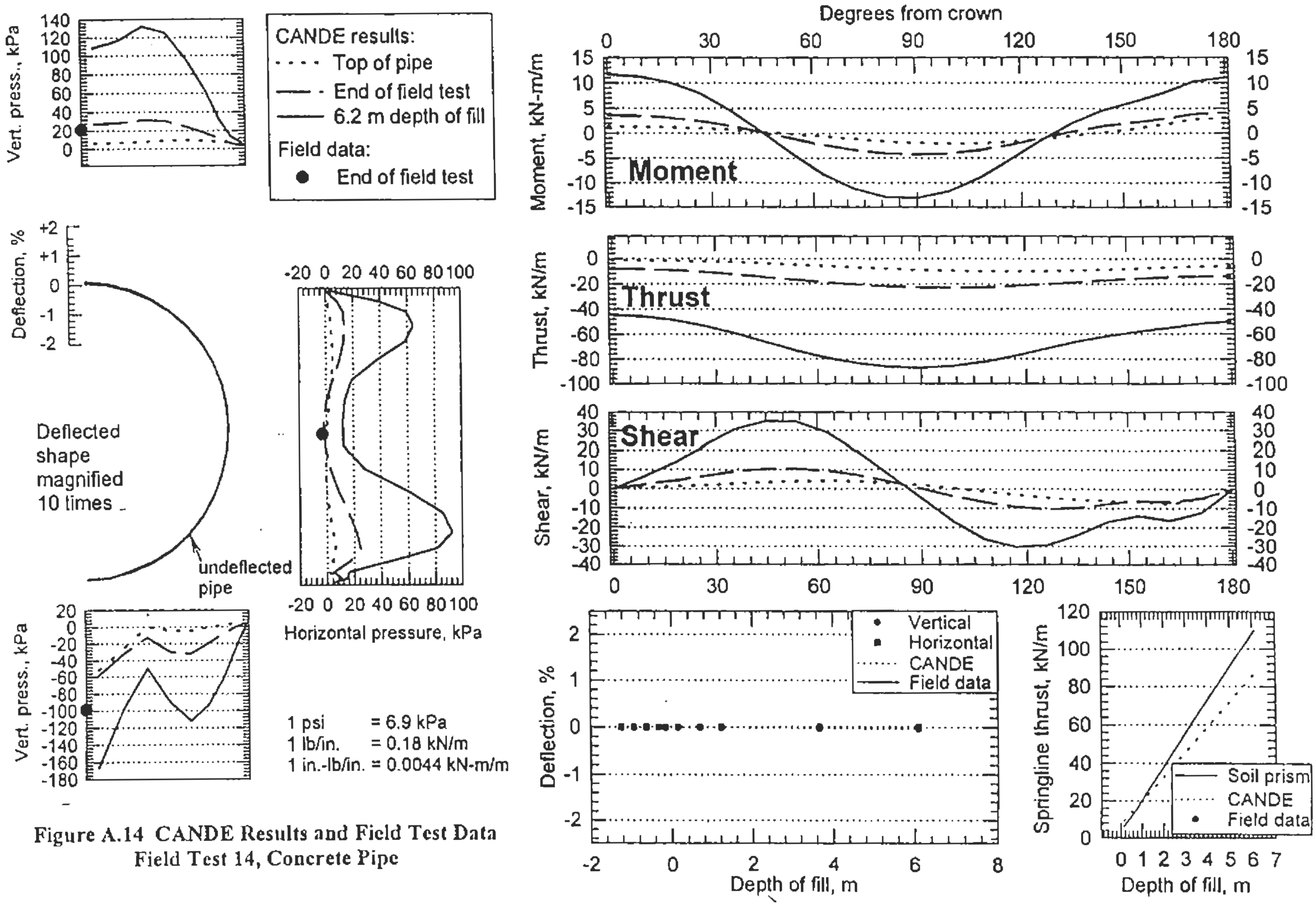

Figure A.14 CANDE Results and Field Test Data
Field Test 14, Concrete Pipe

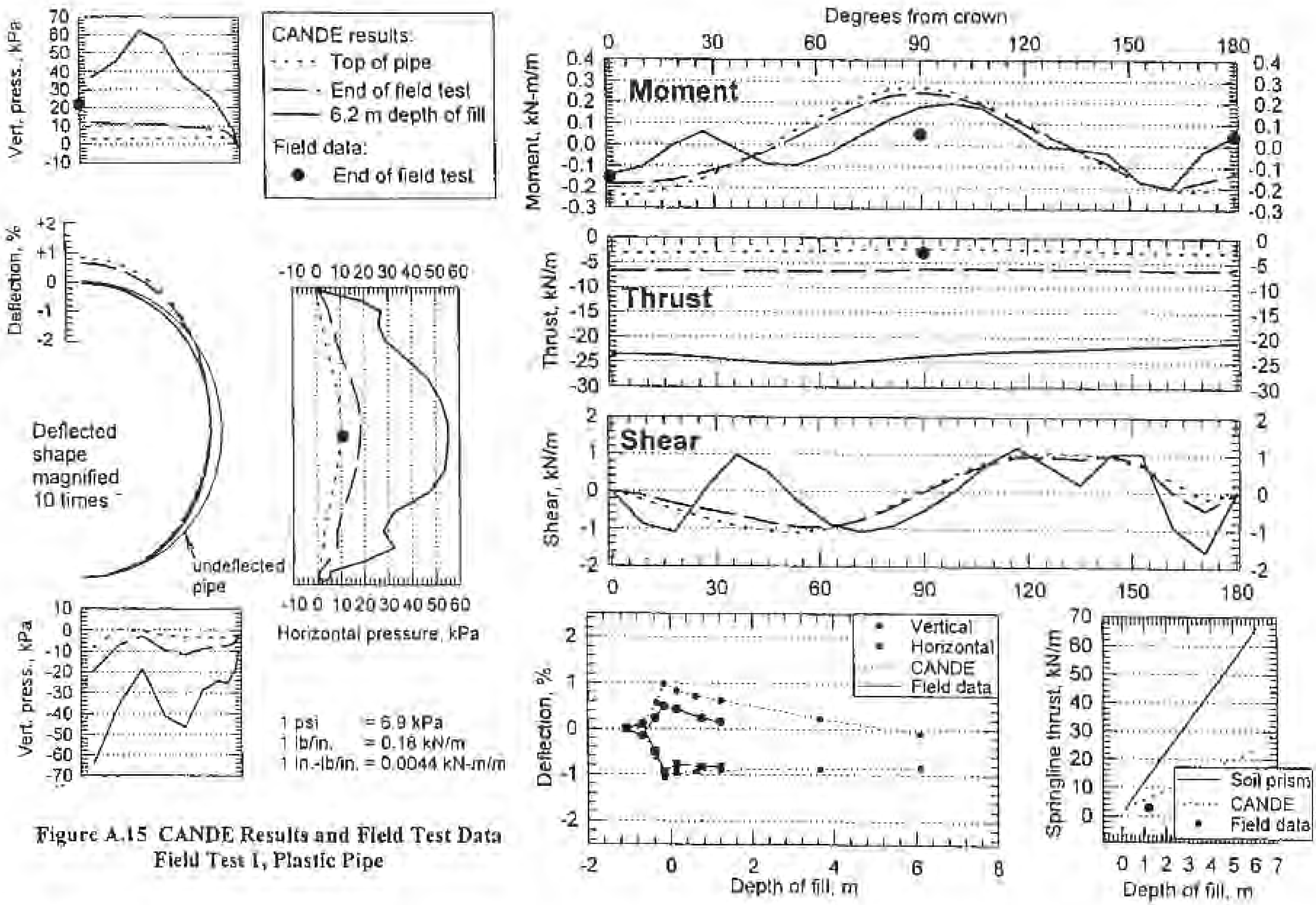

Figure A.15 CANDE Results and Field Test Data
Field Test 1, Plastic Pipe

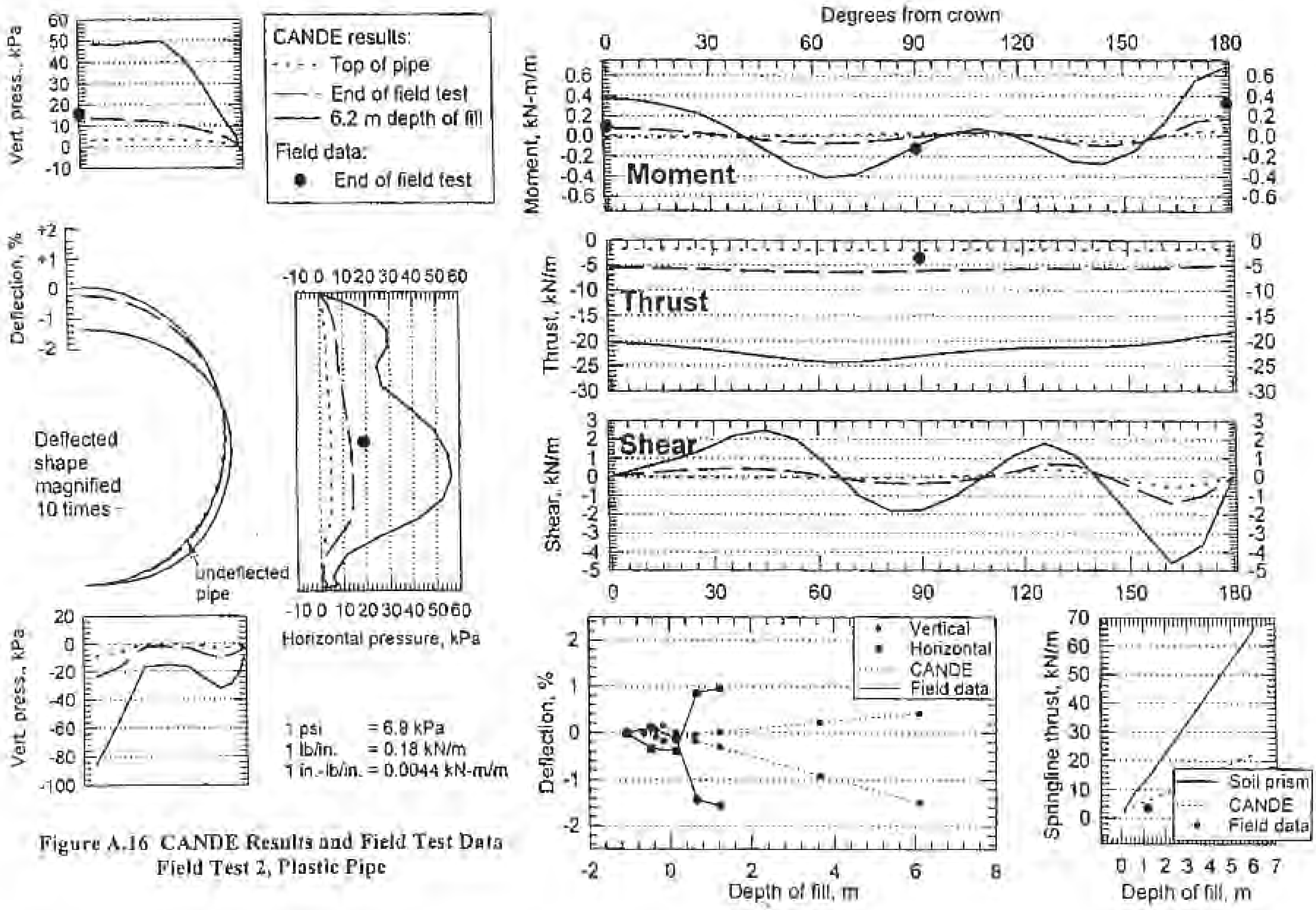

Figure A.16 CANDE Results and Field Test Data
Field Test 2, Plastic Pipe

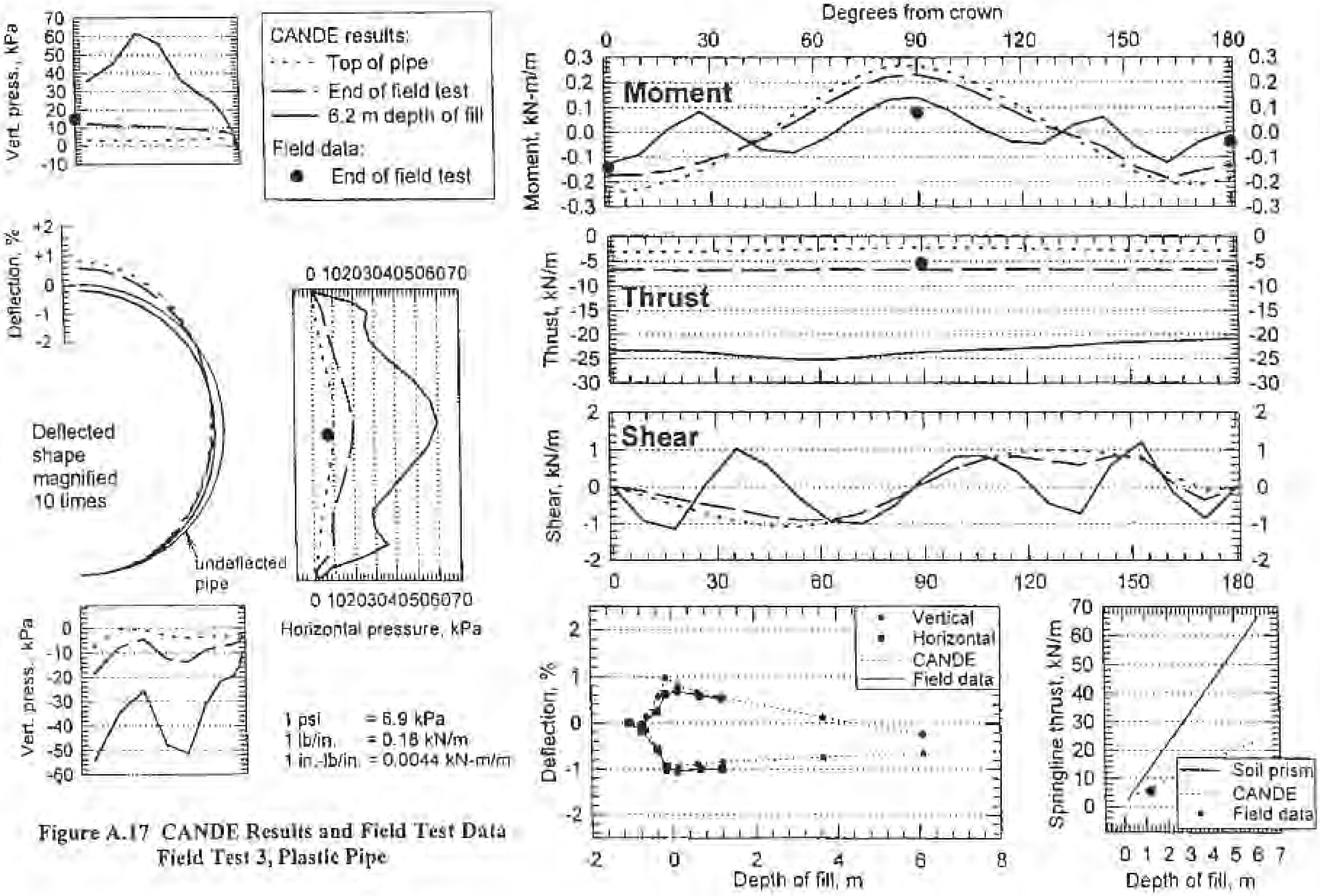

Figure A.17 CANDE Results and Field Test Data Field Test 3, Plastic Pipe

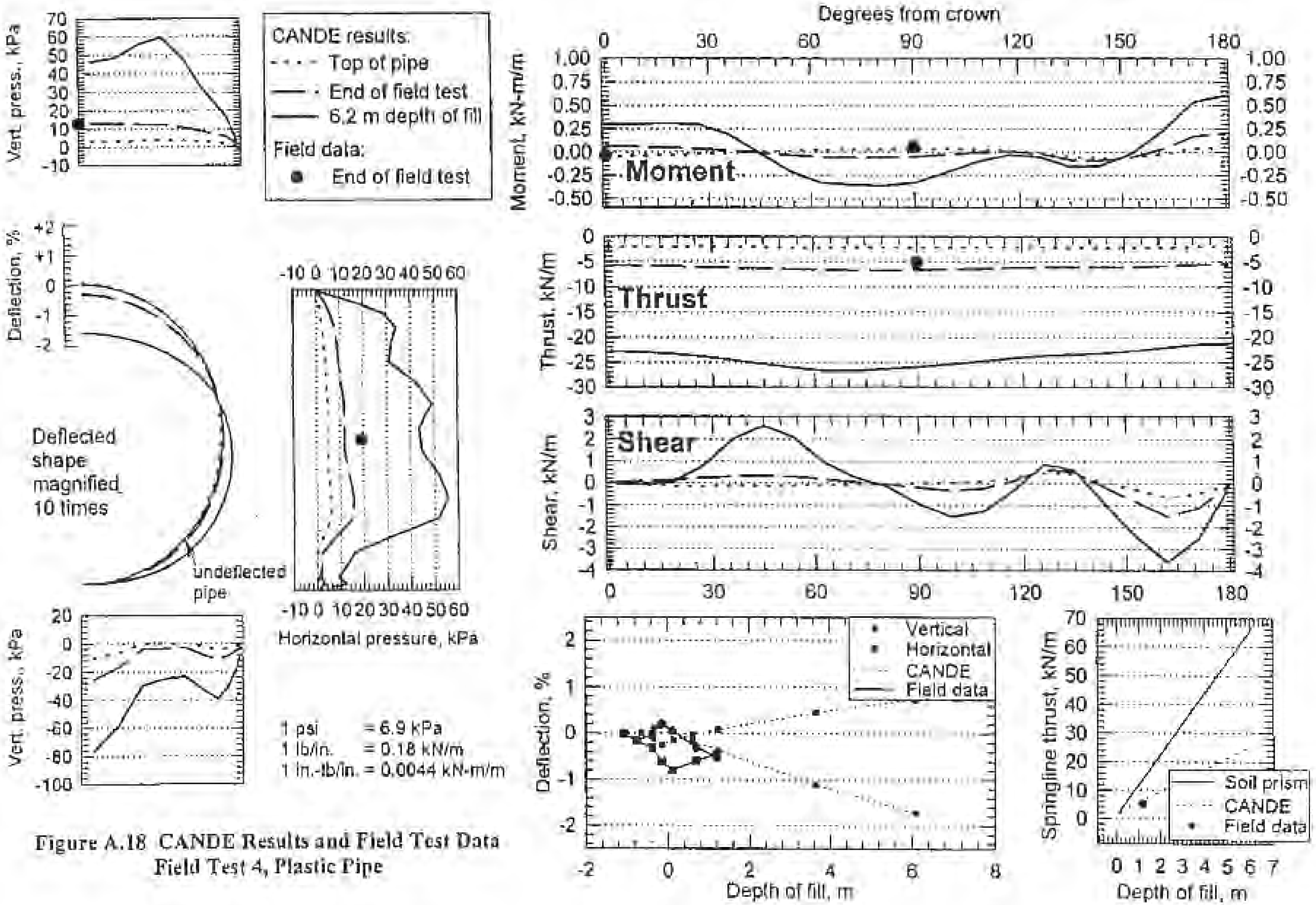

Figure A.18 CANDE Results and Field Test Data
Field Test 4, Plastic Pipe

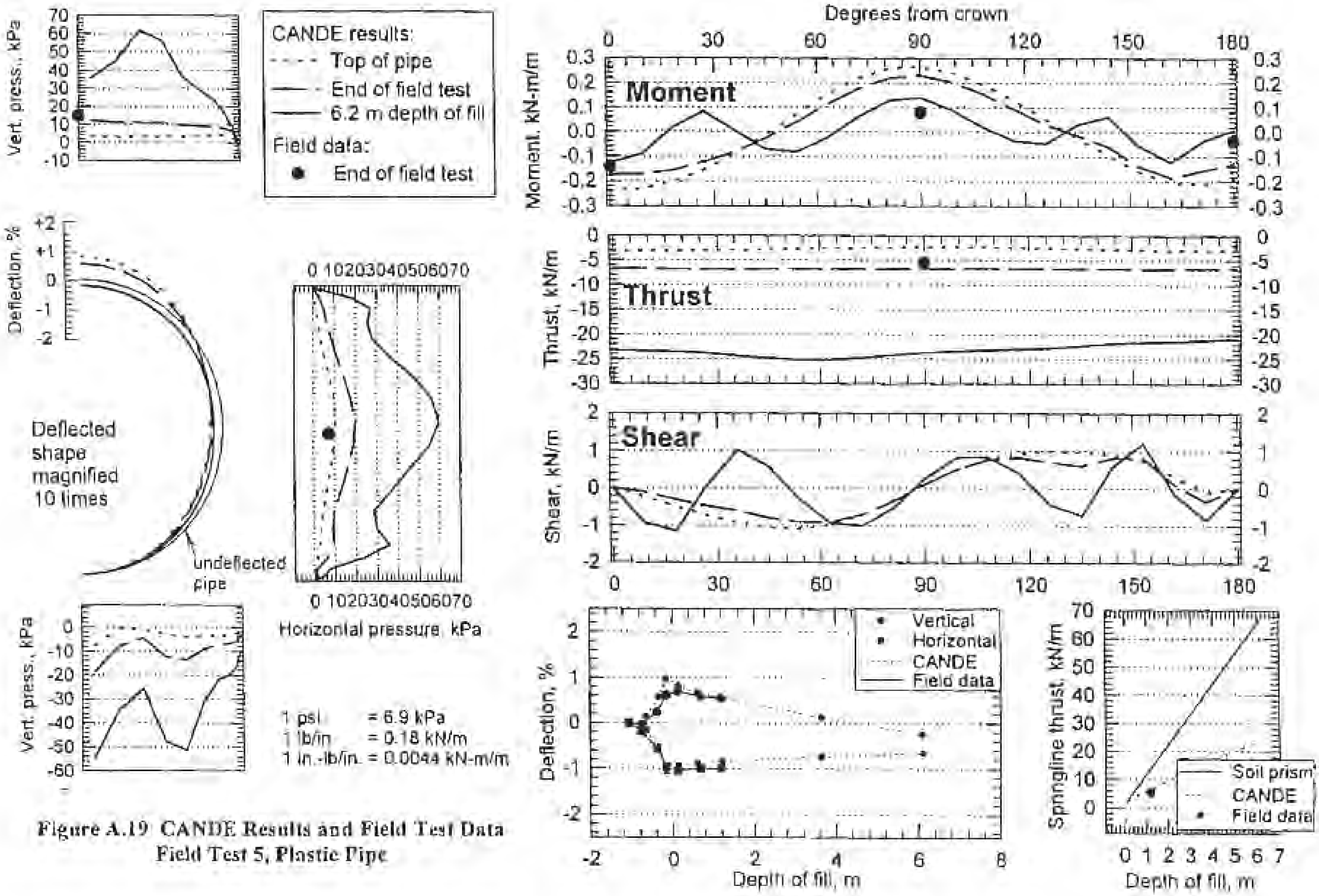

Figure A.19 CANDE Results and Field Test Data
Field Test 5, Plastic Pipe

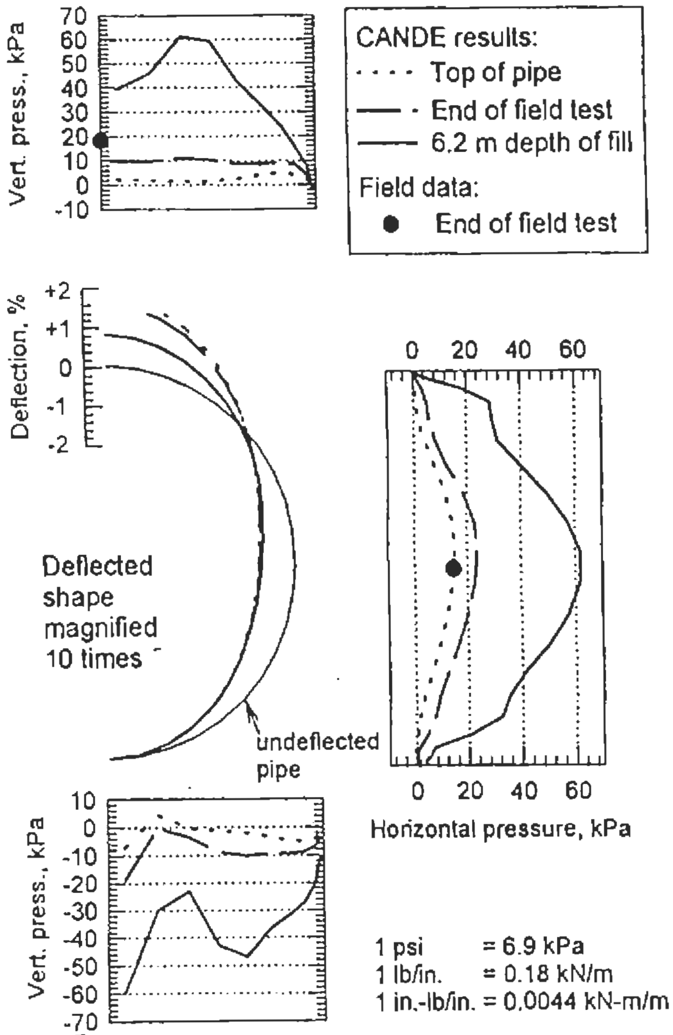

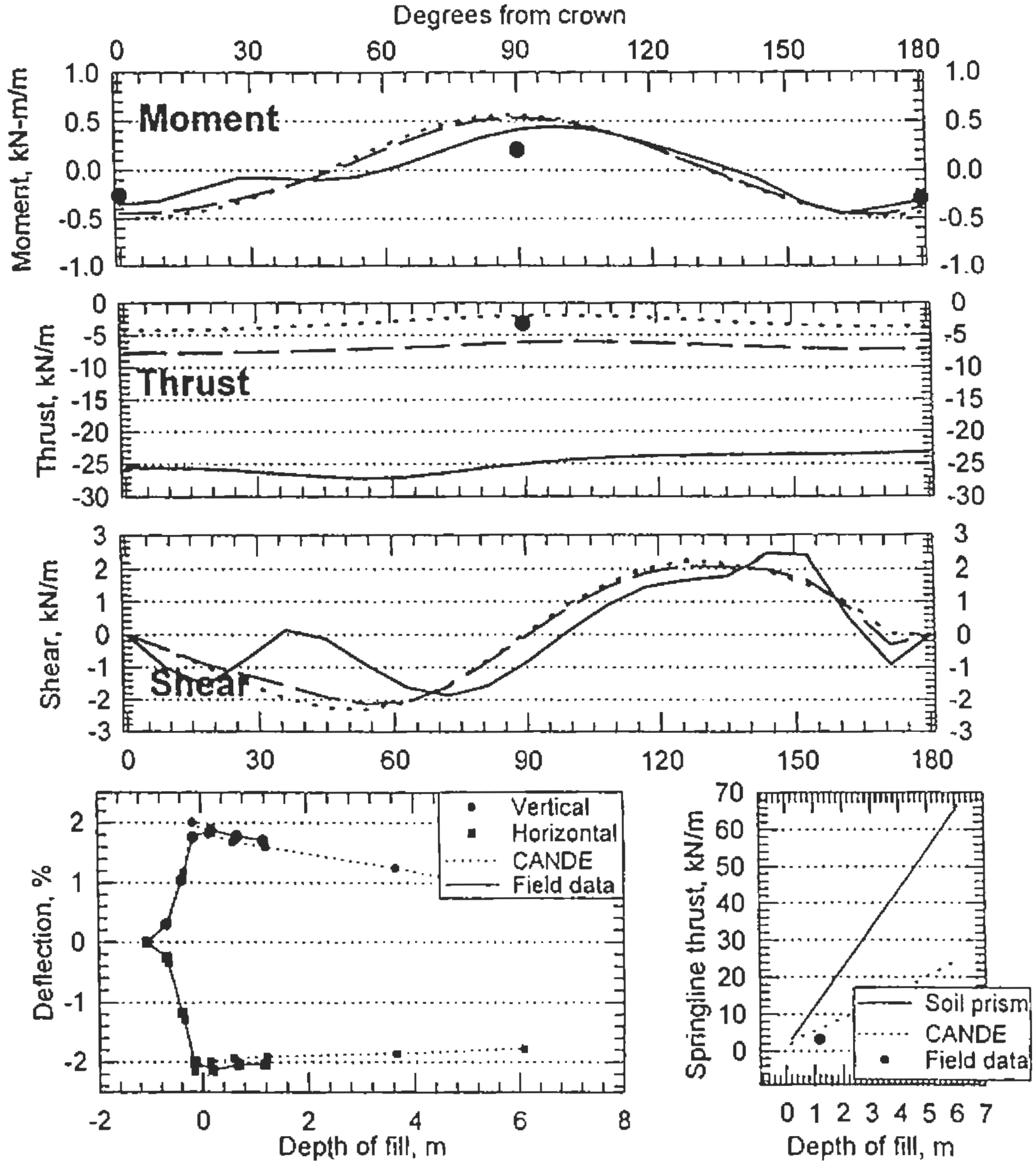

Figure A.20 CANDE Results and Field Test Data
Field Test 6, Plastic Pipe

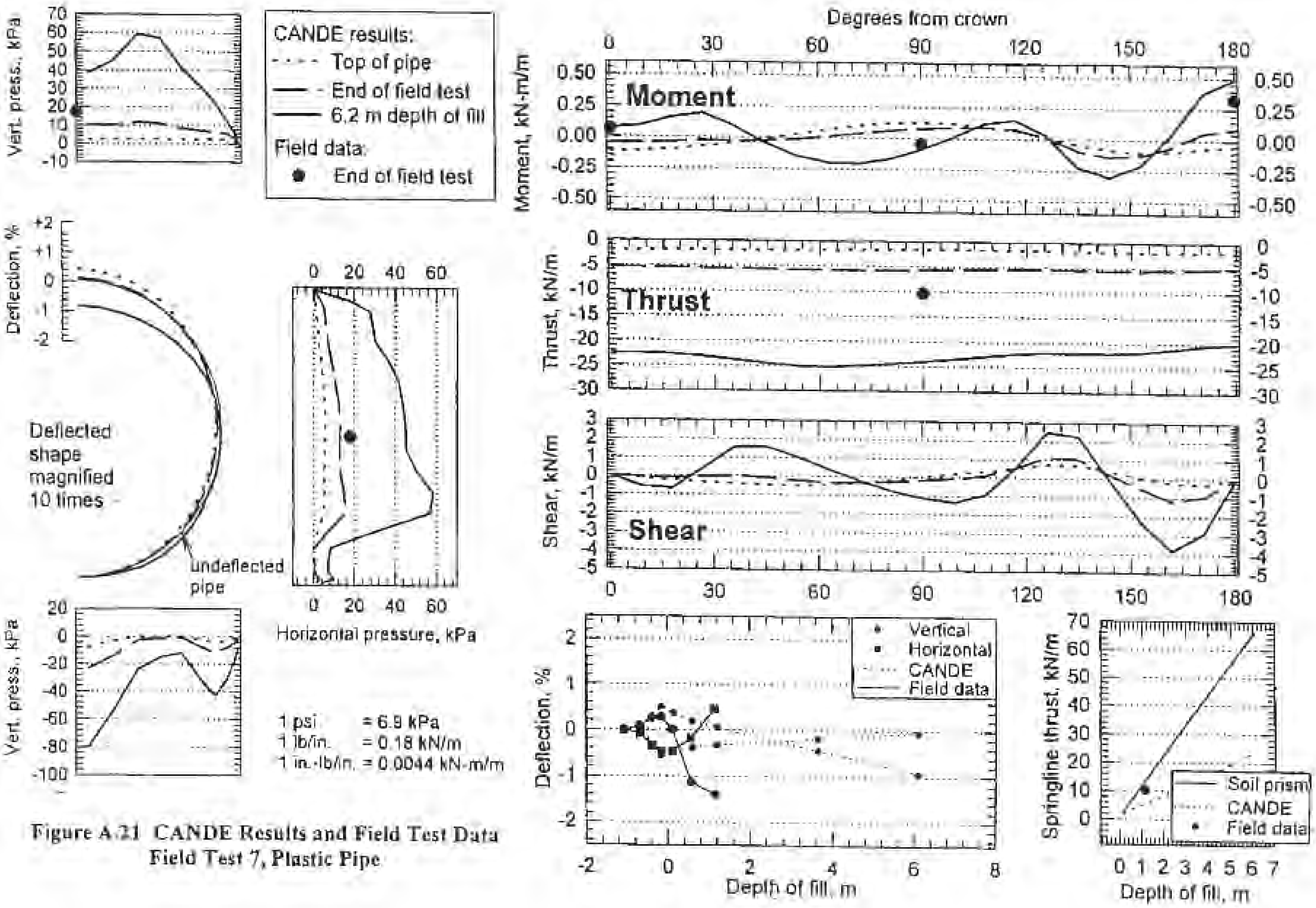

Figure A.21 CANDE Results and Field Test Data
Field Test 7, Plastic Pipe

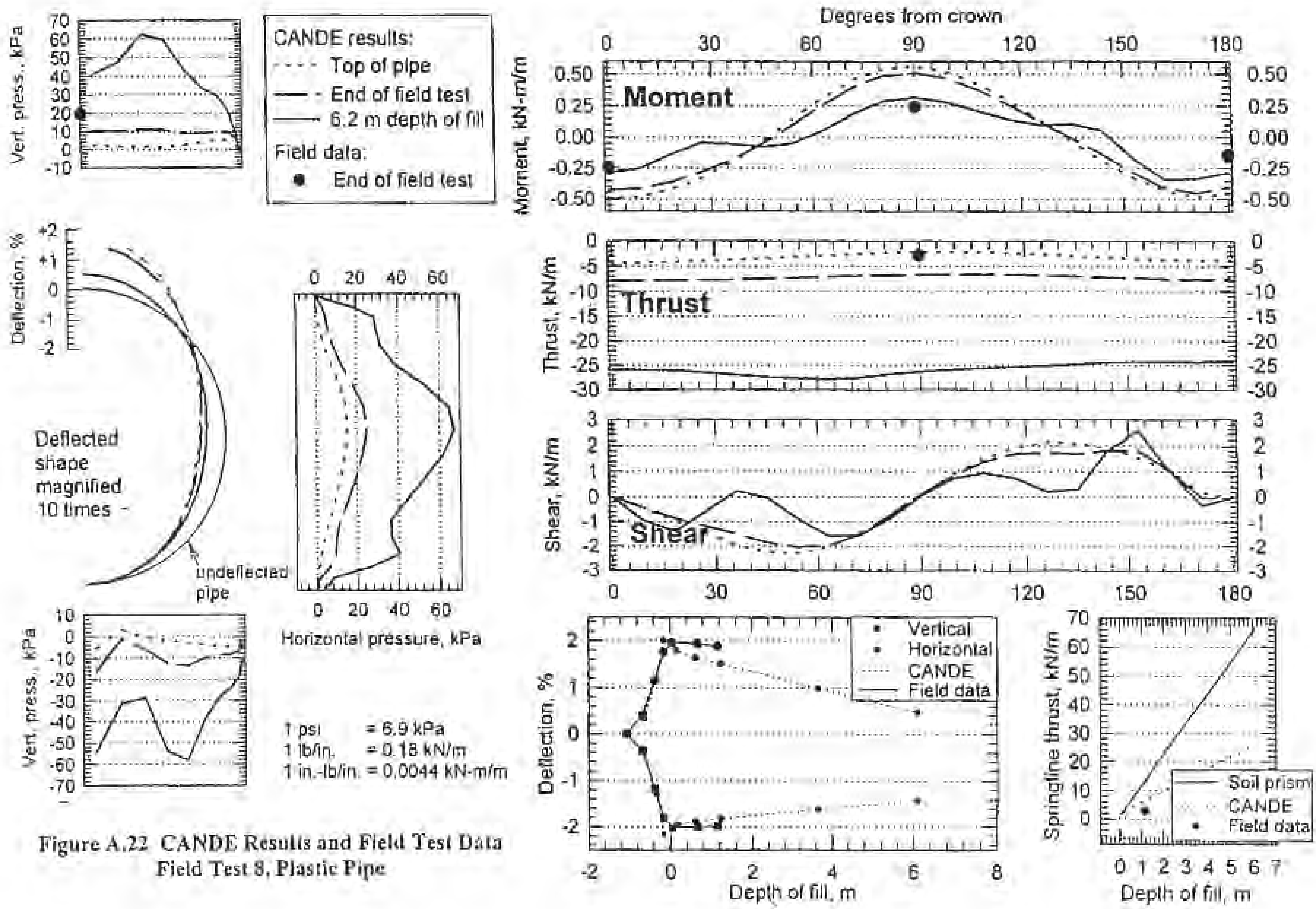

Figure A.22 CANDE Results and Field Test Data Field Test 8, Plastic Pipe

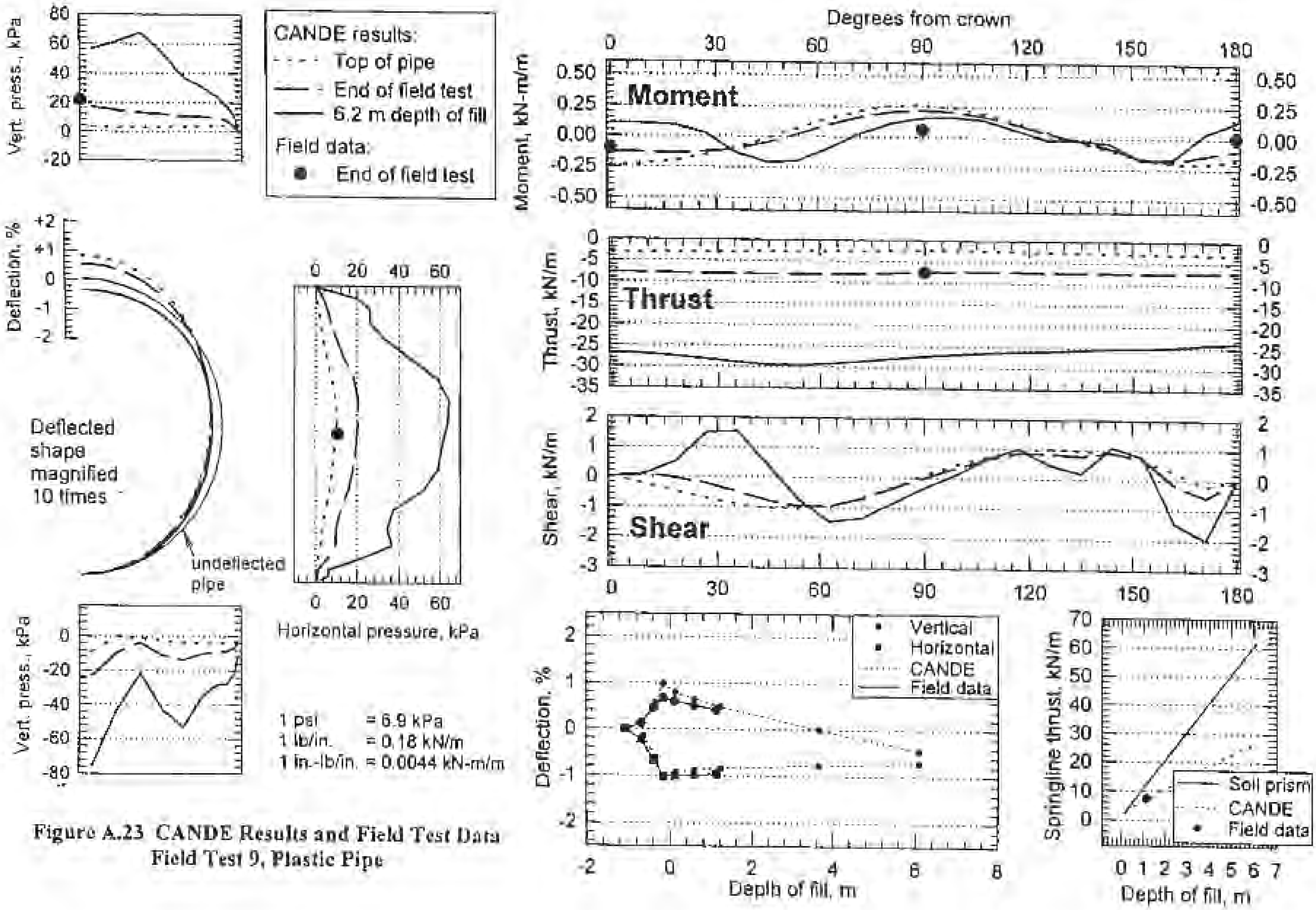

Figure A.23 CANDE Results and Field Test Data Field Test 9, Plastic Pipe

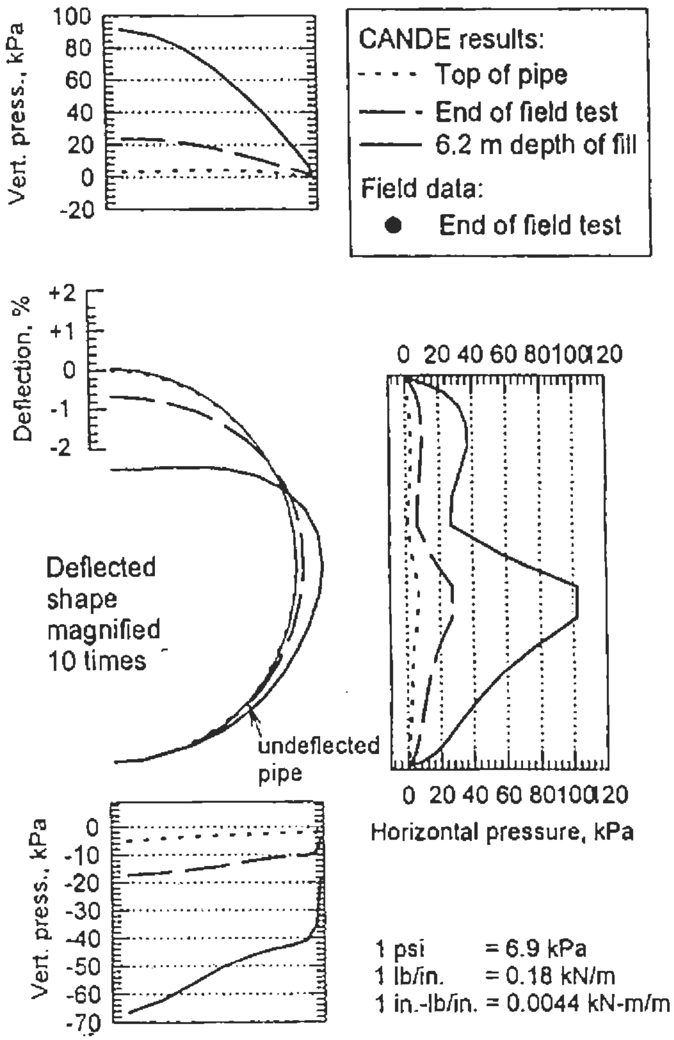

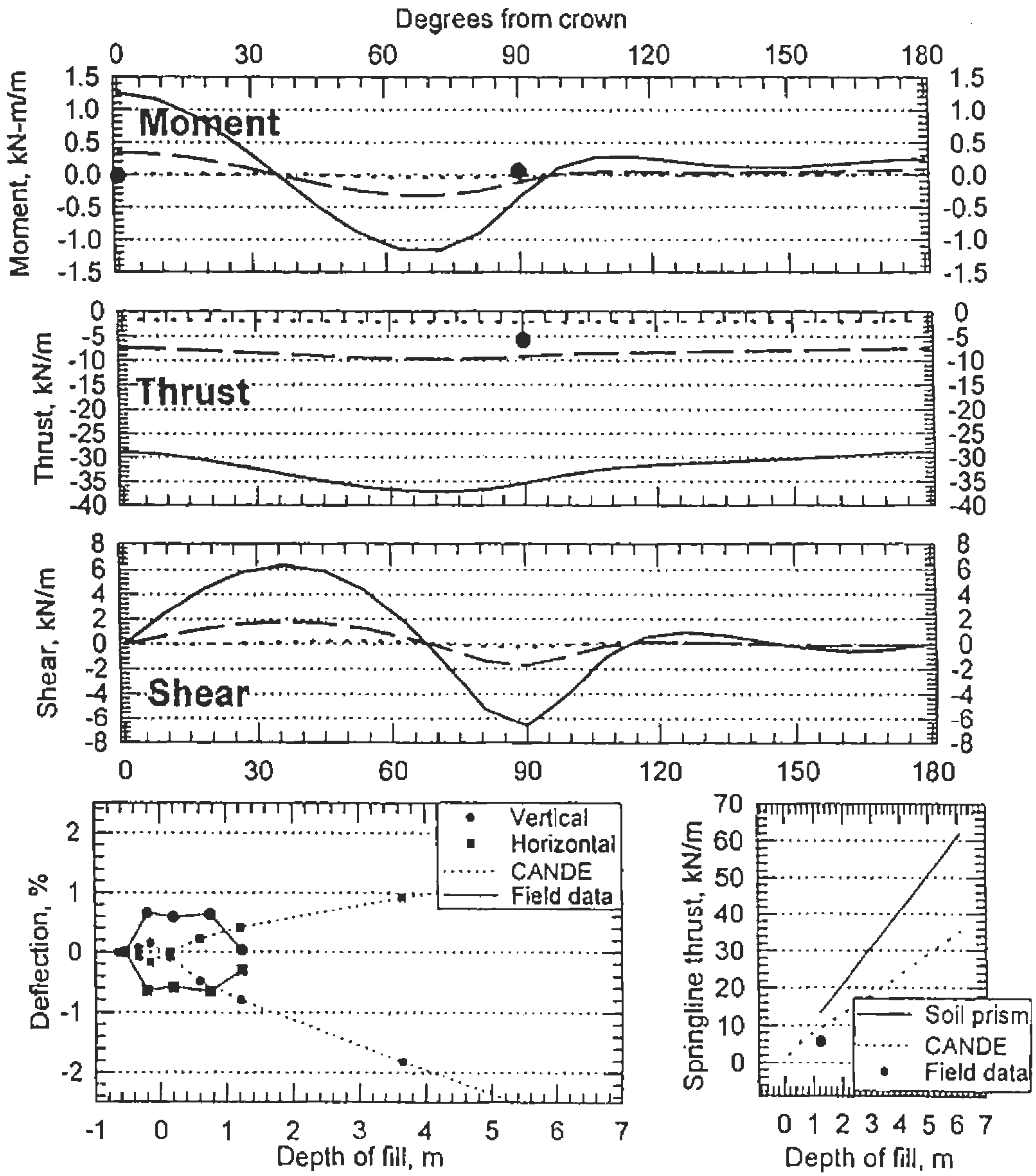

Figure A.24 CANDE Results and Field Test Data Field Test 10, Plastic Pipe

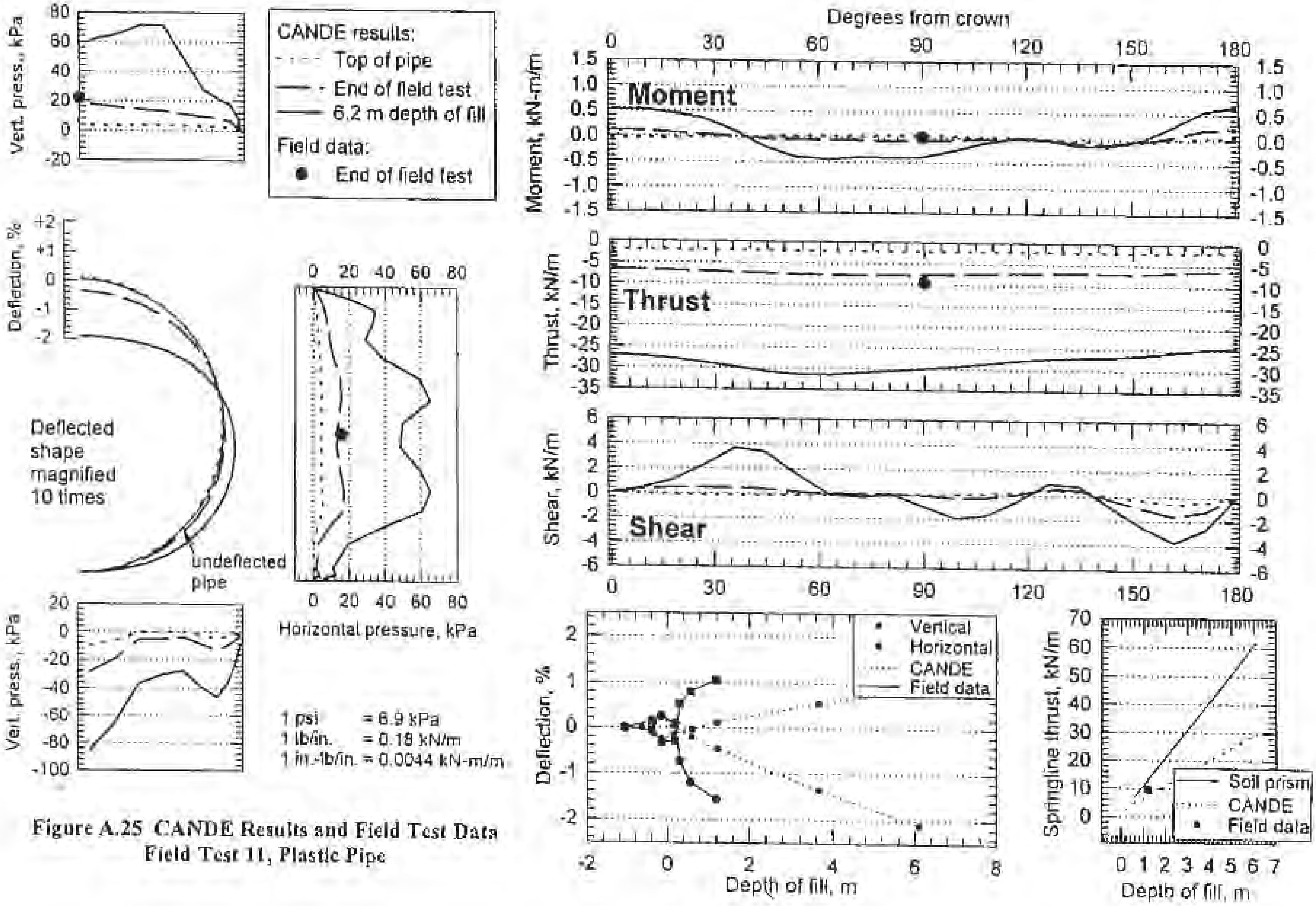

Figure A.25 CANDE Results and Field Test Data
Field Test 11, Plastic Pipe

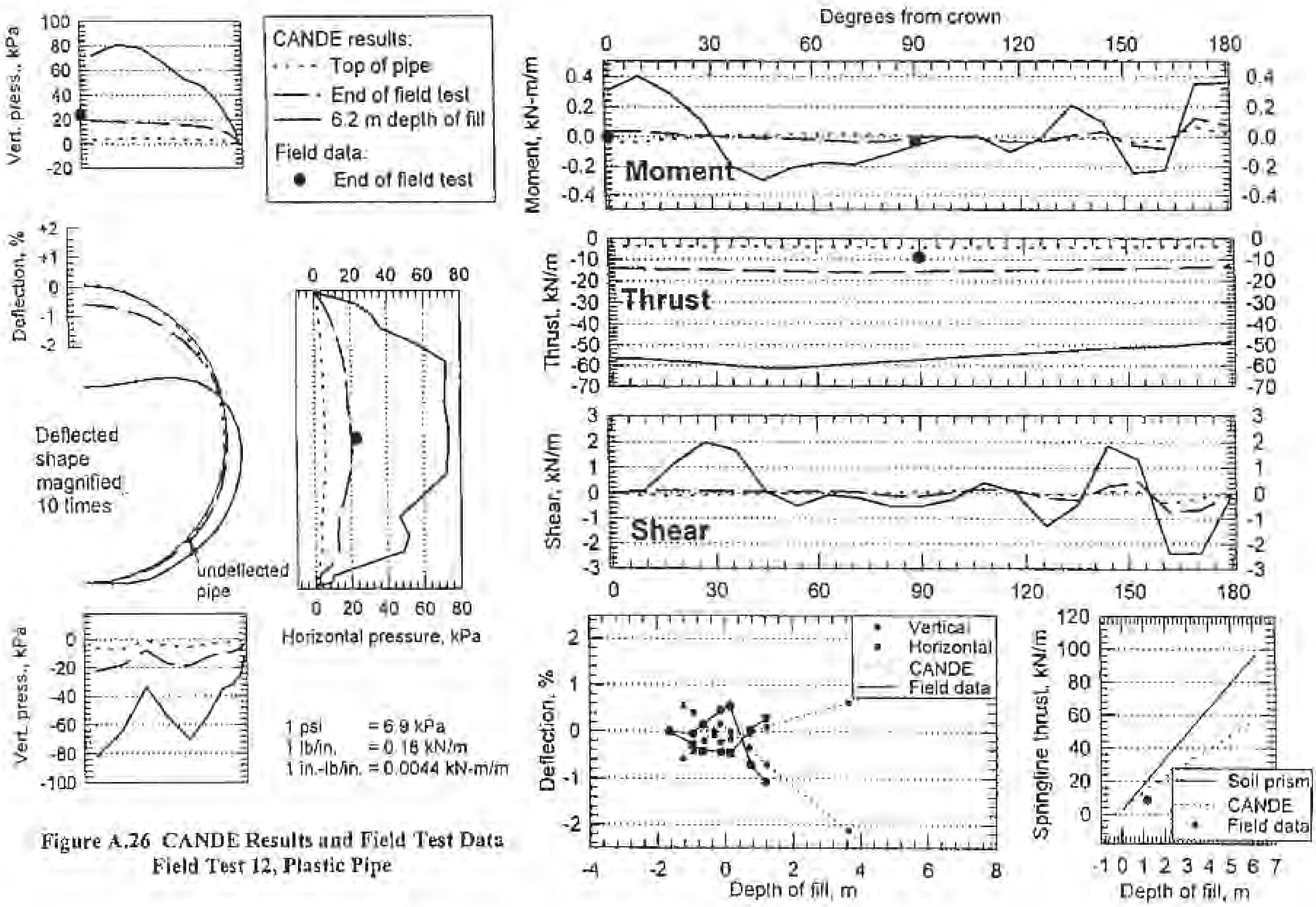

Figure A.26 CANDE Results and Field Test Data
Field Test 12, Plastic Pipe

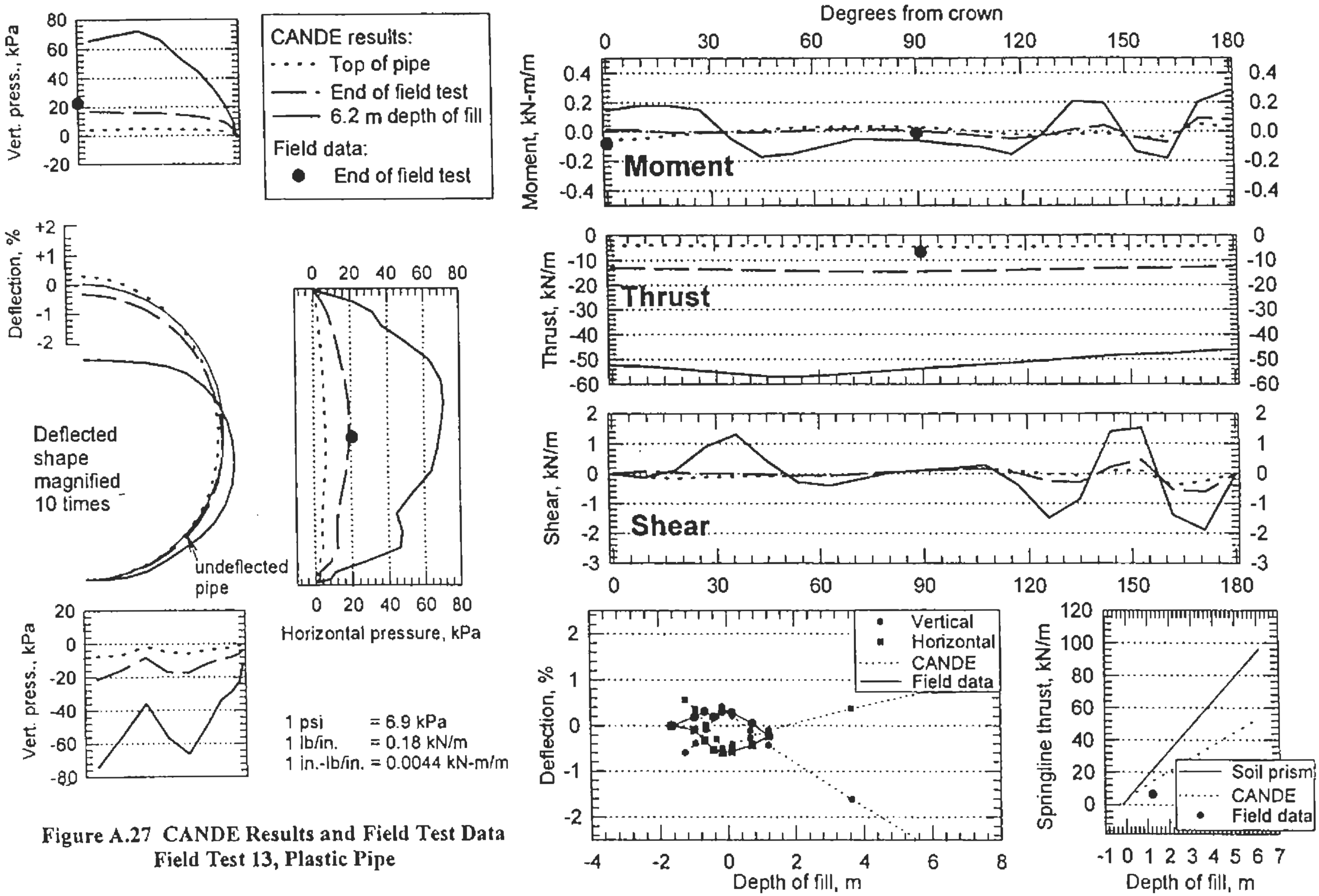

Figure A.27 CANDE Results and Field Test Data
Field Test 13, Plastic Pipe

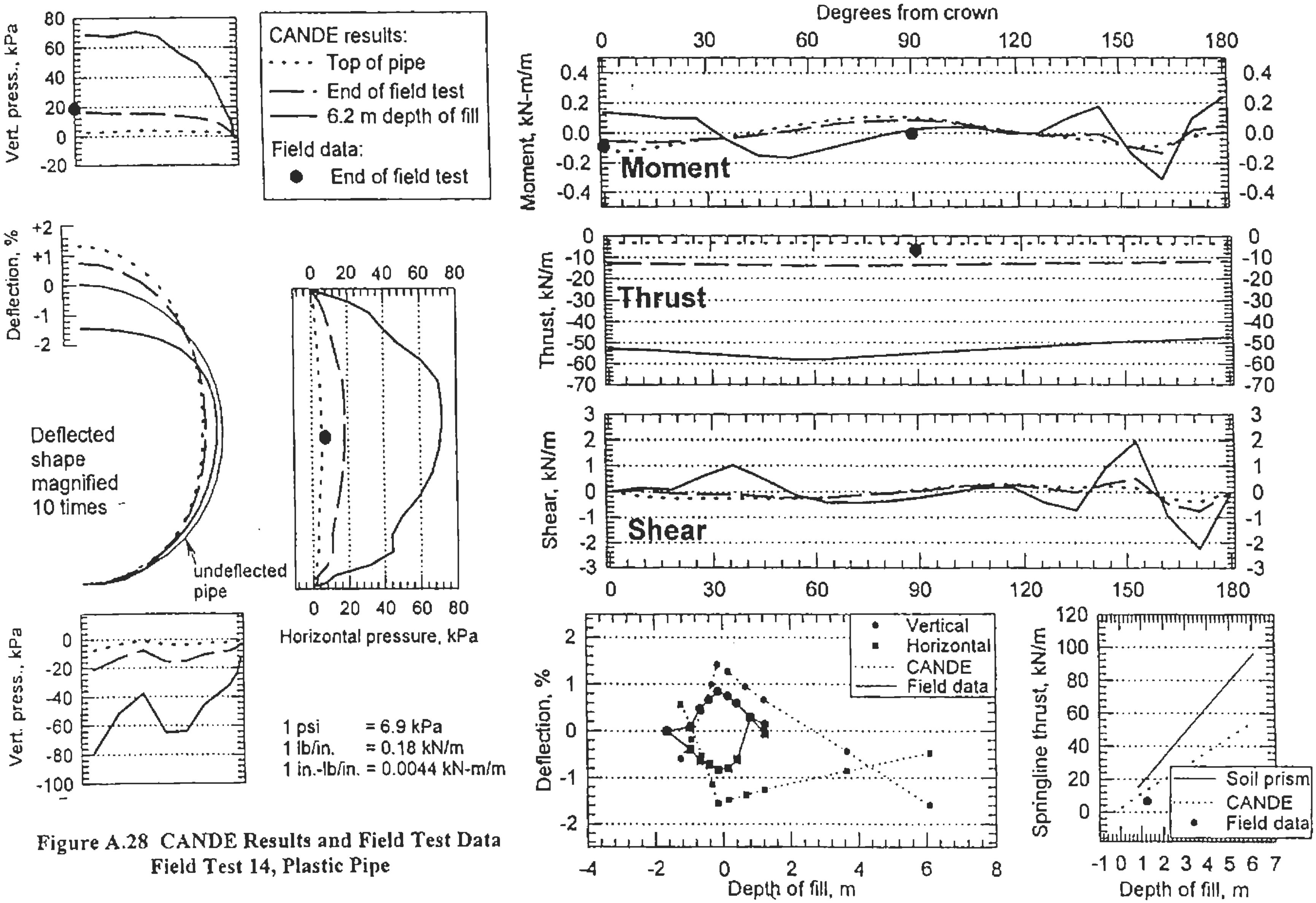

Figure A.28 CANDE Results and Field Test Data
Field Test 14, Plastic Pipe

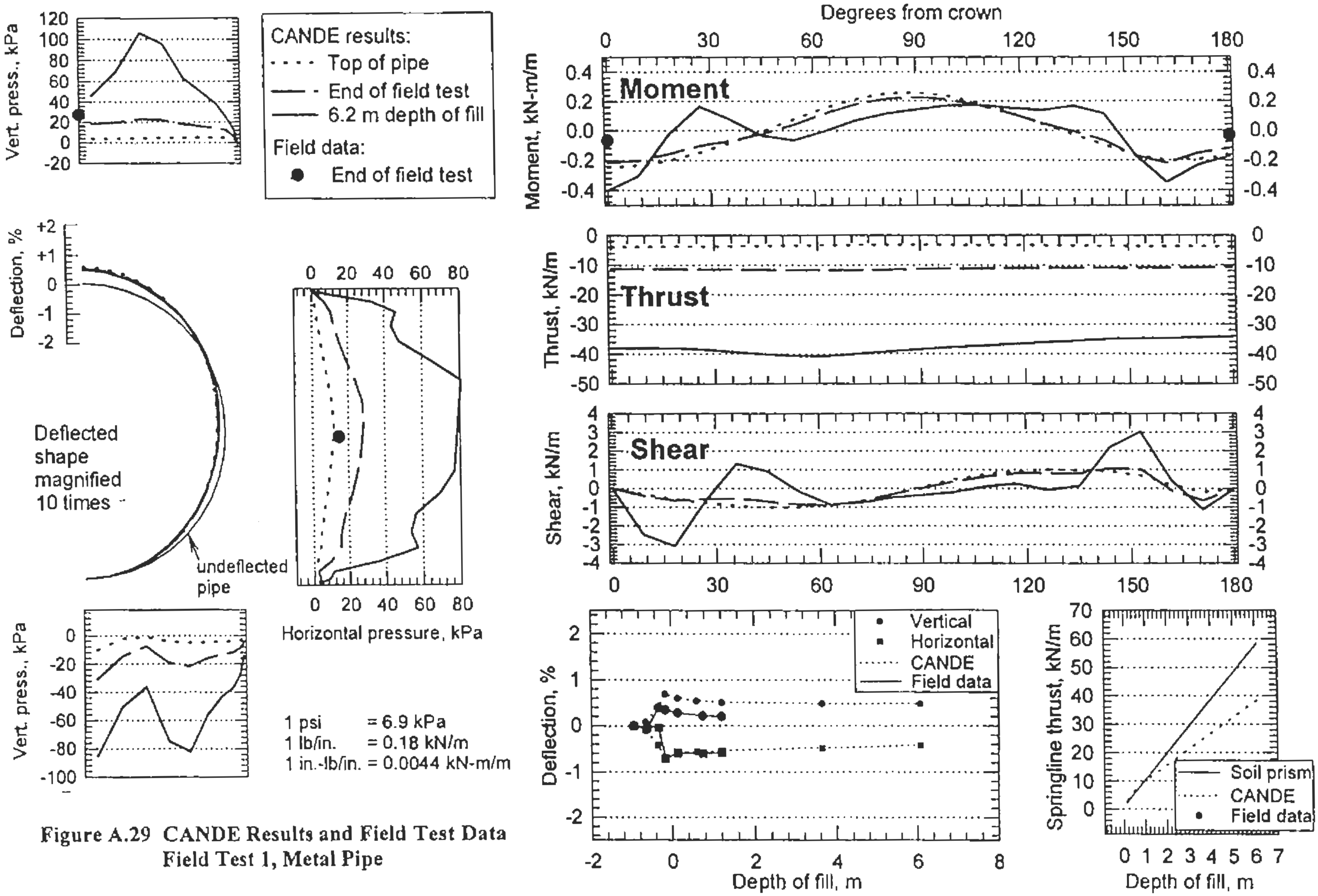

Figure A.29 CANDE Results and Field Test Data
Field Test 1, Metal Pipe

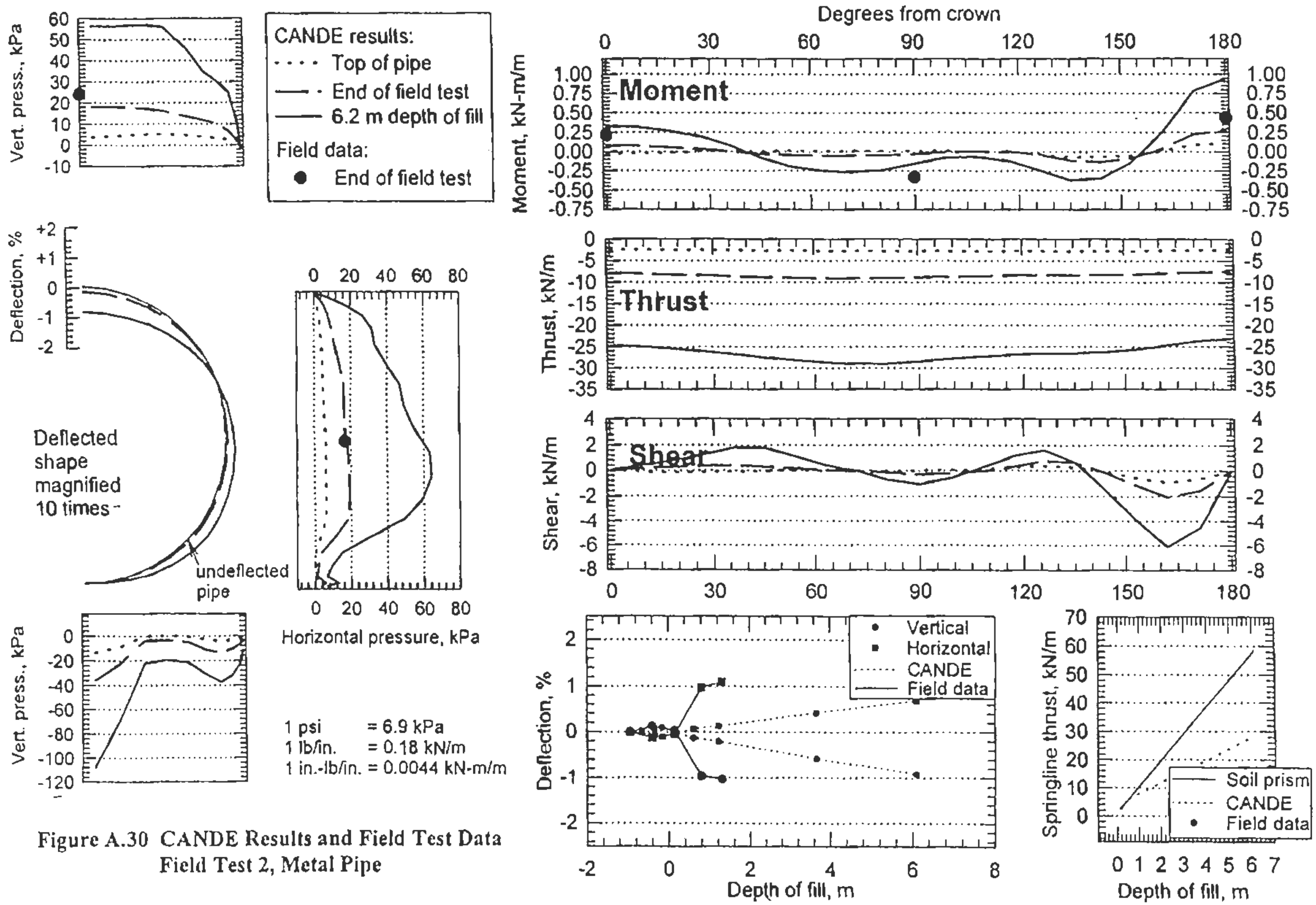

Figure A.30 CANDE Results and Field Test Data
Field Test 2, Metal Pipe

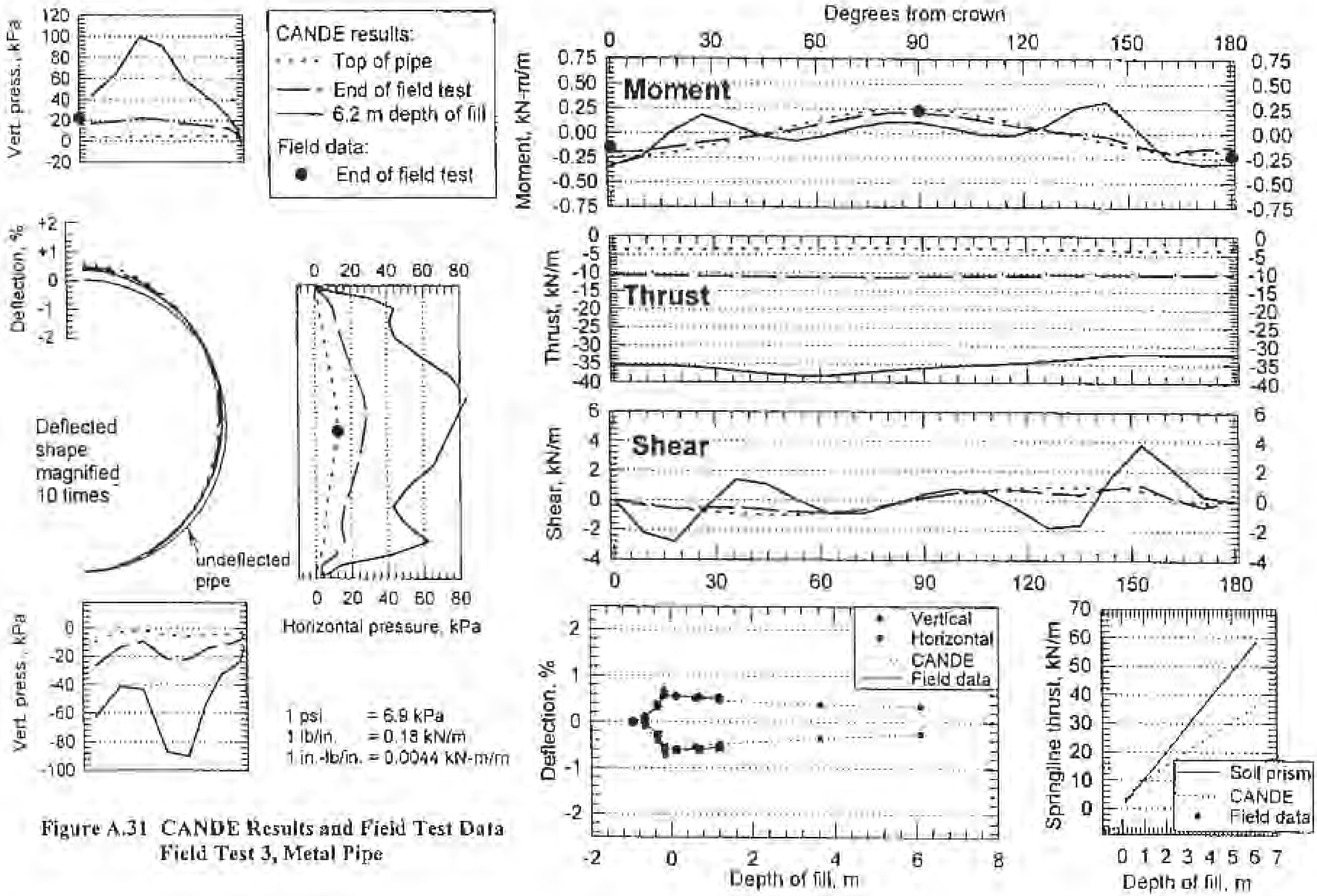

Figure A.31 CANDE Results and Field Test Data Field Test 3, Metal Pipe

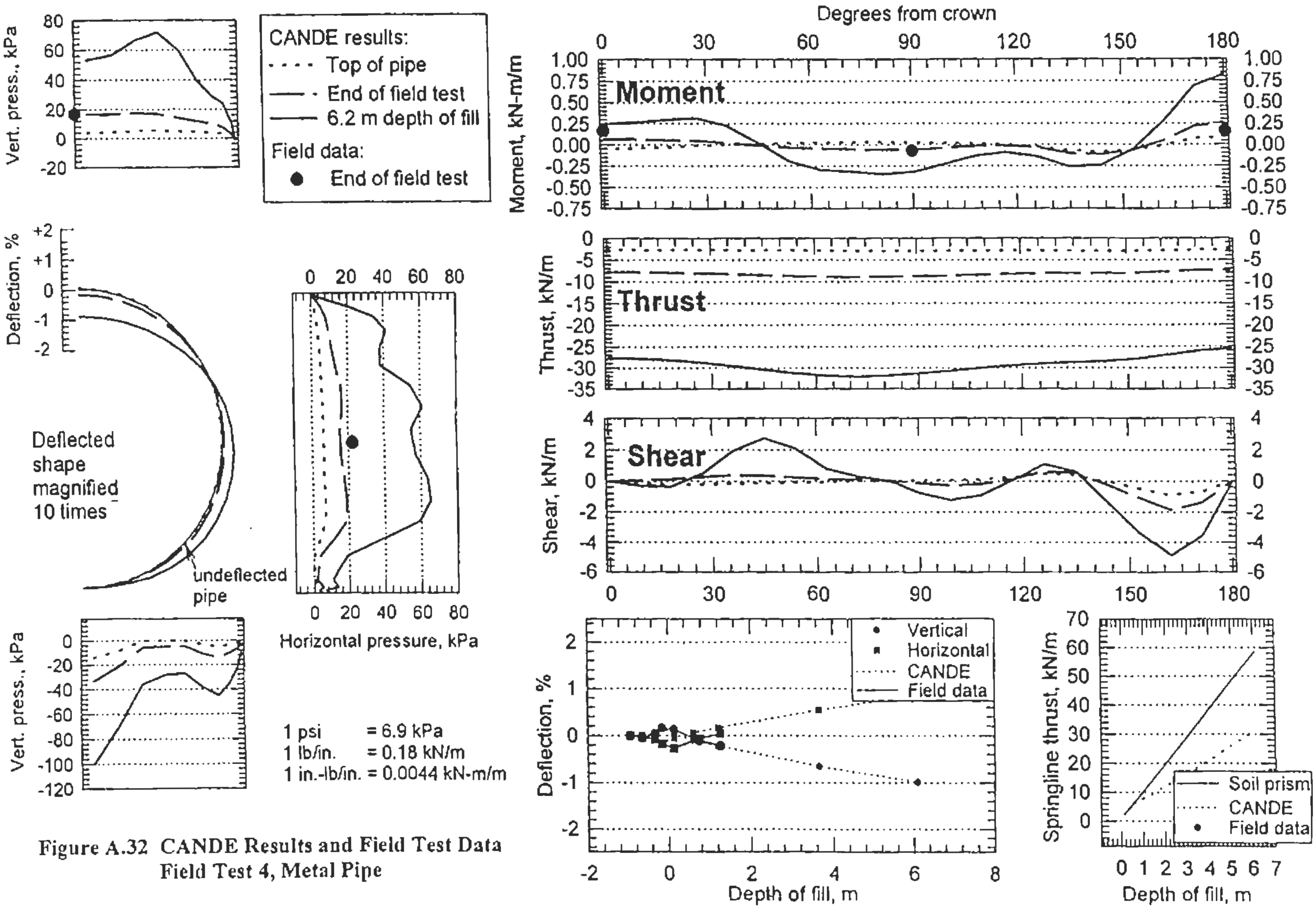

Figure A.32 CANDE Results and Field Test Data
Field Test 4, Metal Pipe

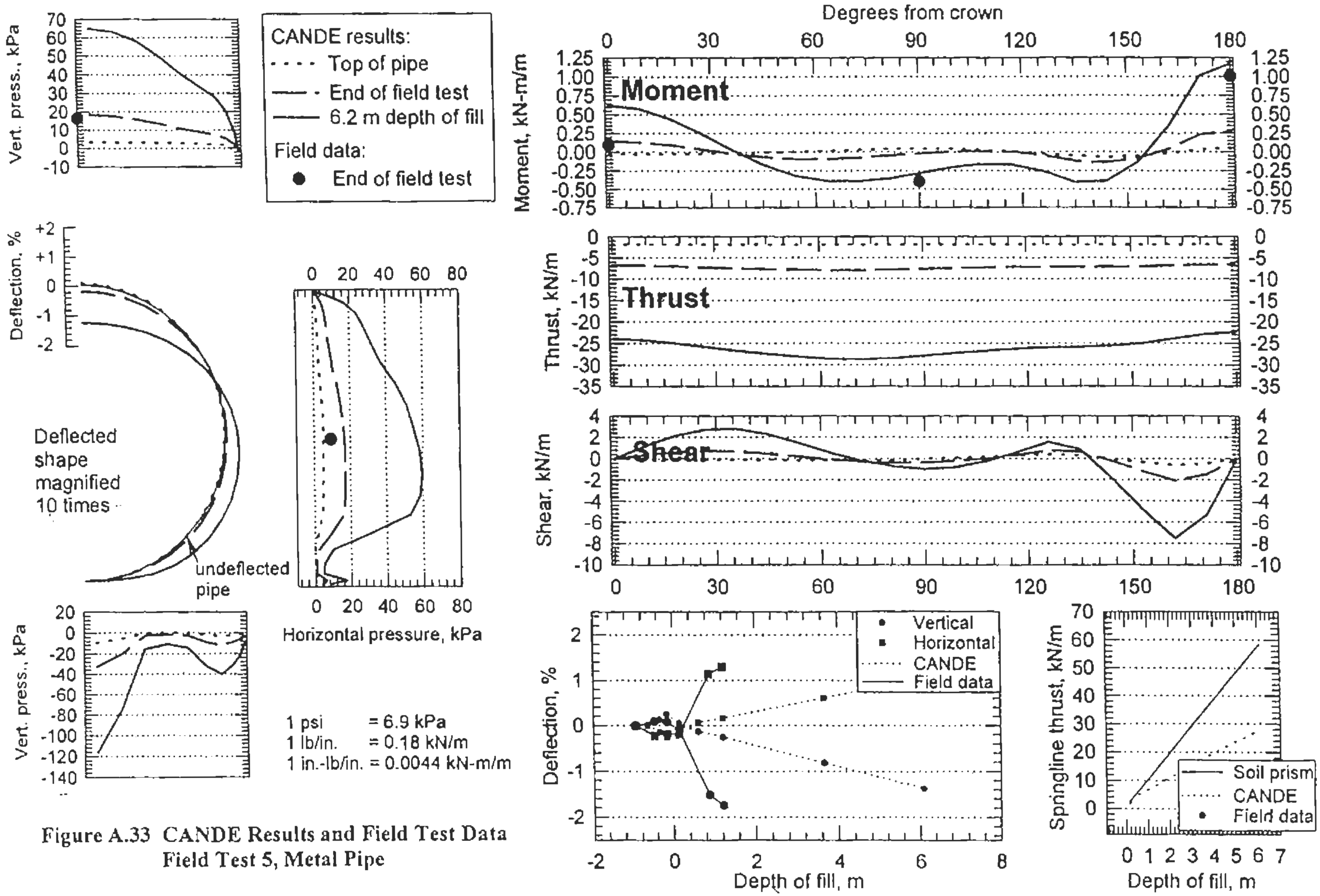

Figure A.33 CANDE Results and Field Test Data
Field Test 5, Metal Pipe

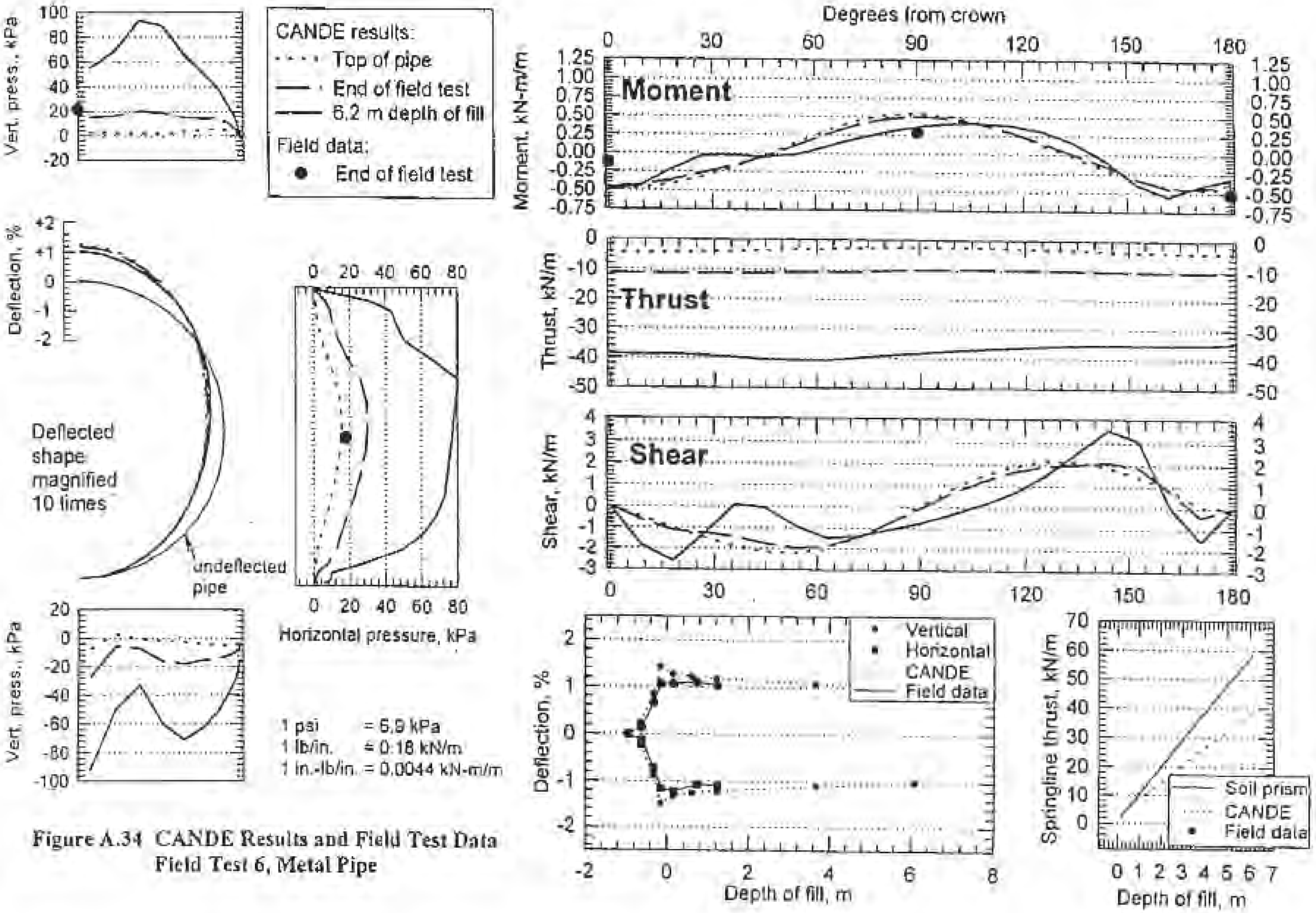

Figure A.34 CANDE Results and Field Test Data Field Test 6, Metal Pipe

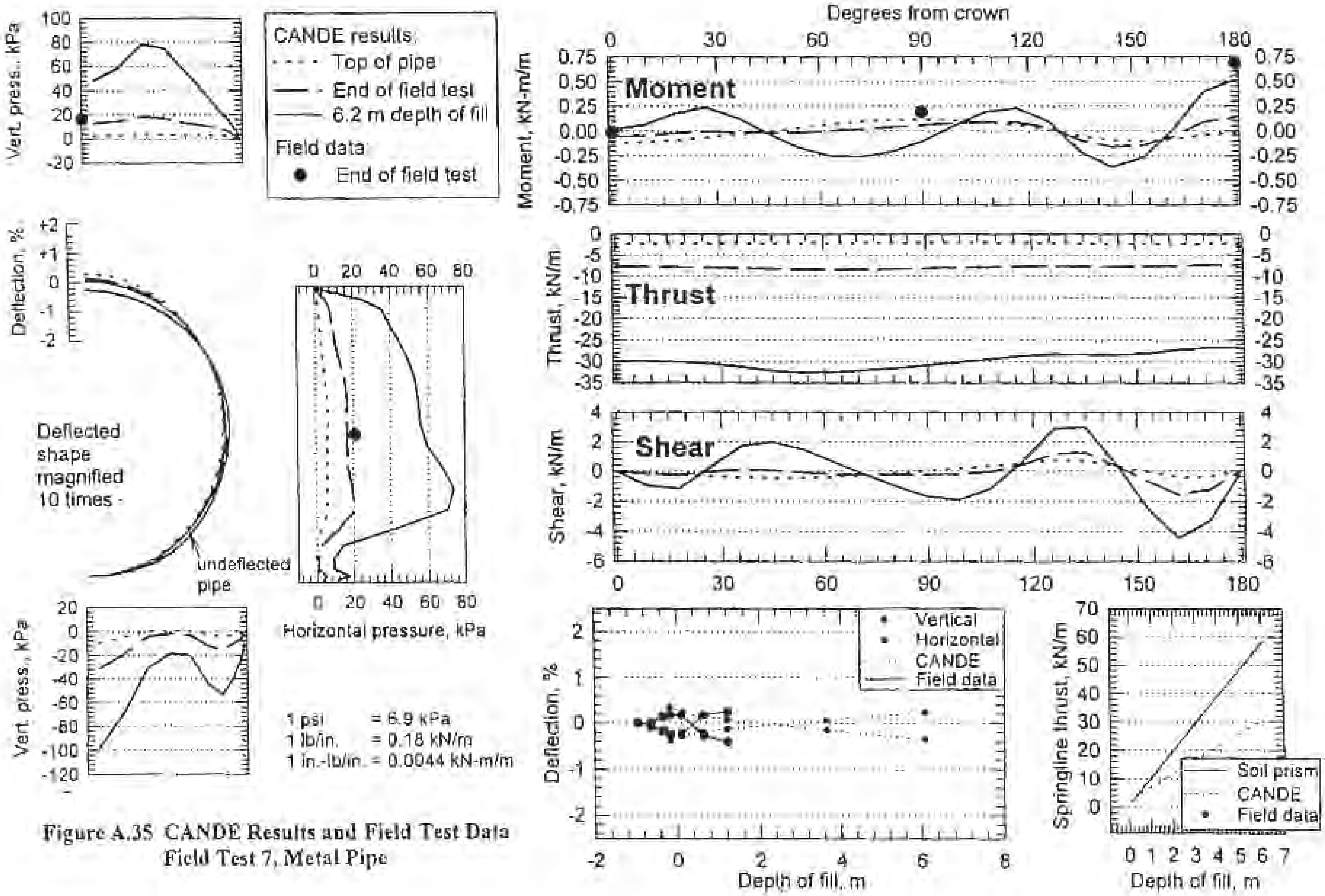

Figure A.35 CANDE Results and Field Test Data Field Test 7, Metal Pipe

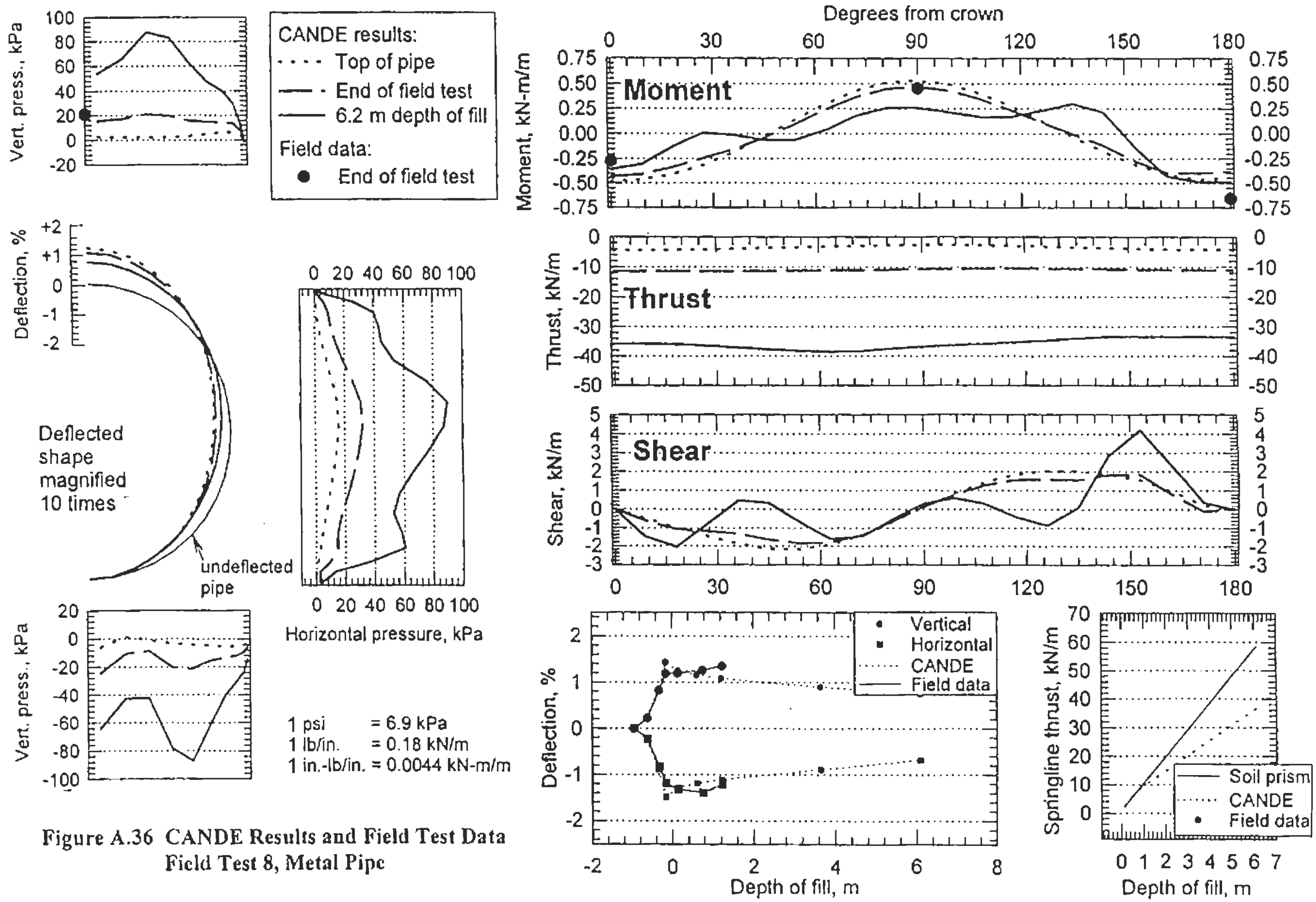

Figure A.36 CANDE Results and Field Test Data Field Test 8, Metal Pipe

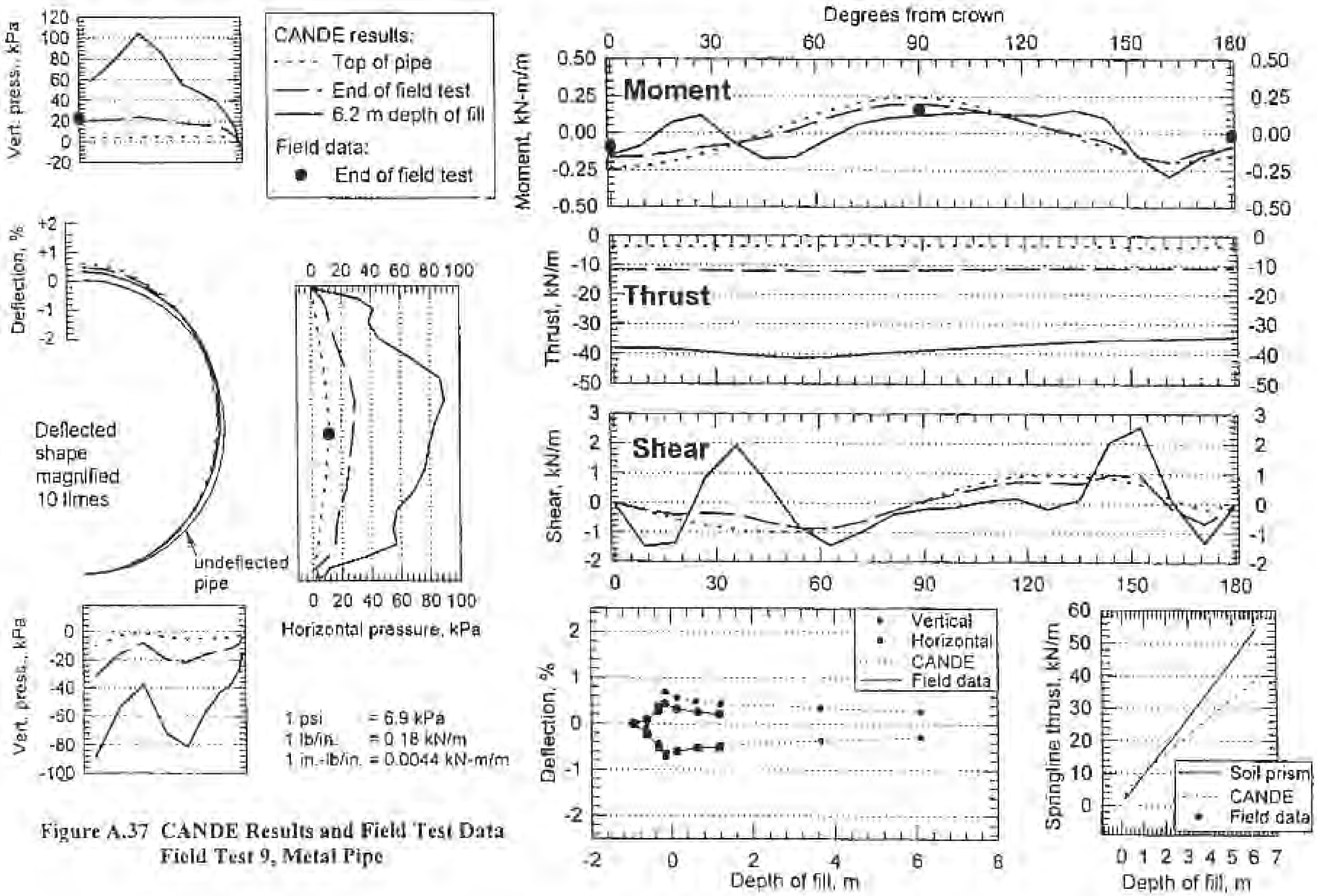

Figure A.37 CANDE Results and Field Test Data Field Test 9, Metal Pipe

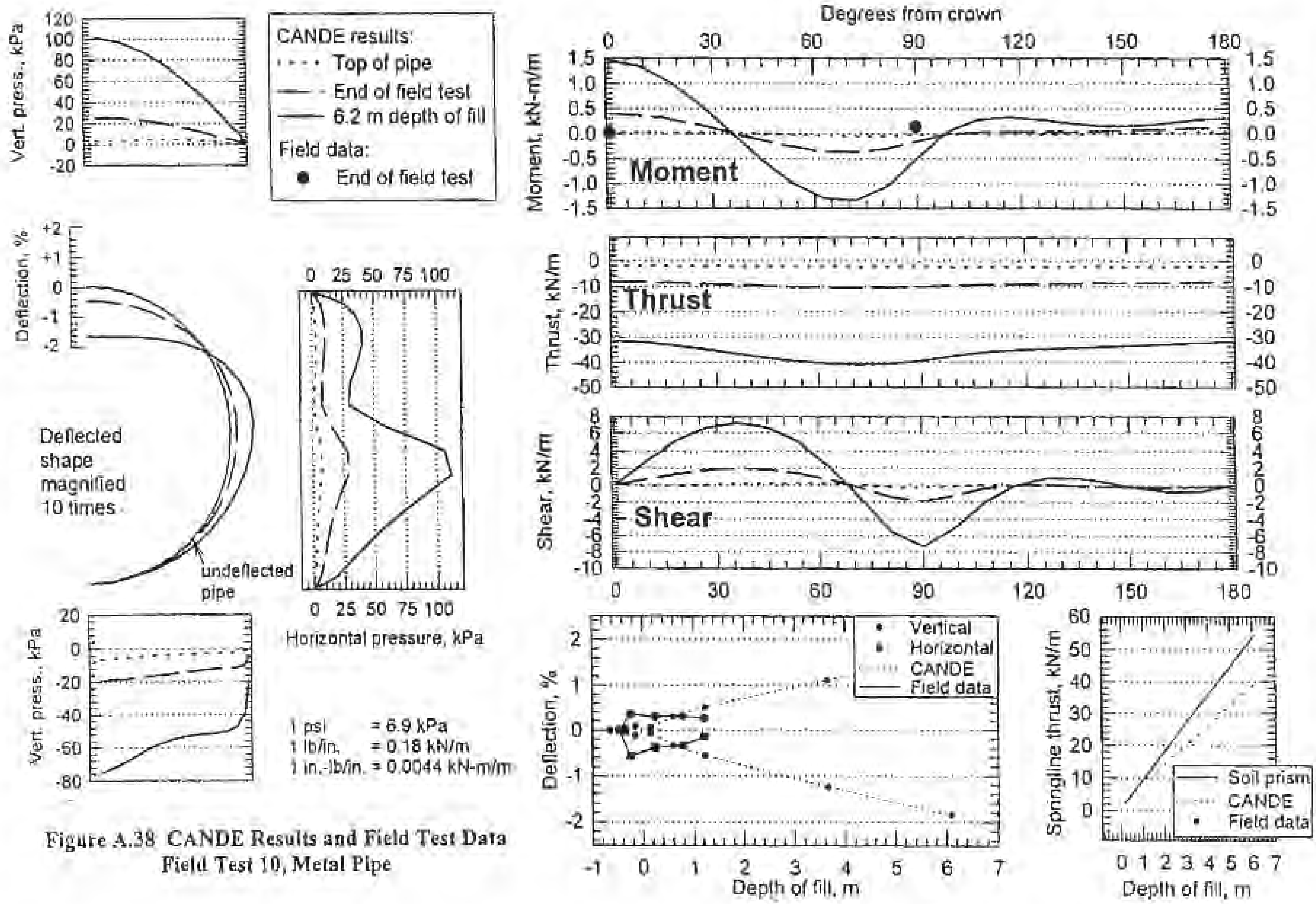

Figure A.38 CANDE Results and Field Test Data
Field Test 10, Metal Pipe

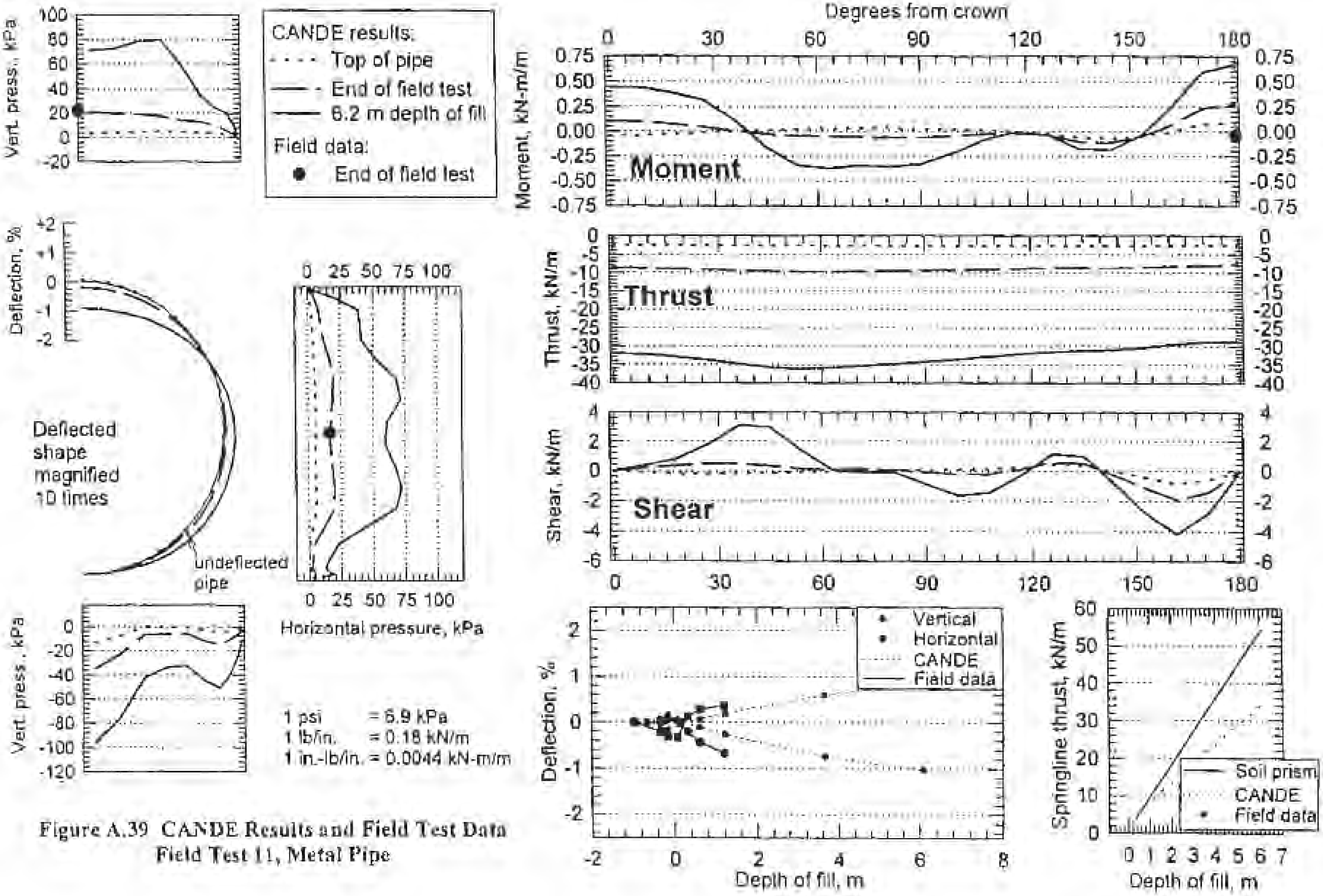

Figure A.39 CANDE Results and Field Test Data
Field Test 11, Metal Pipe

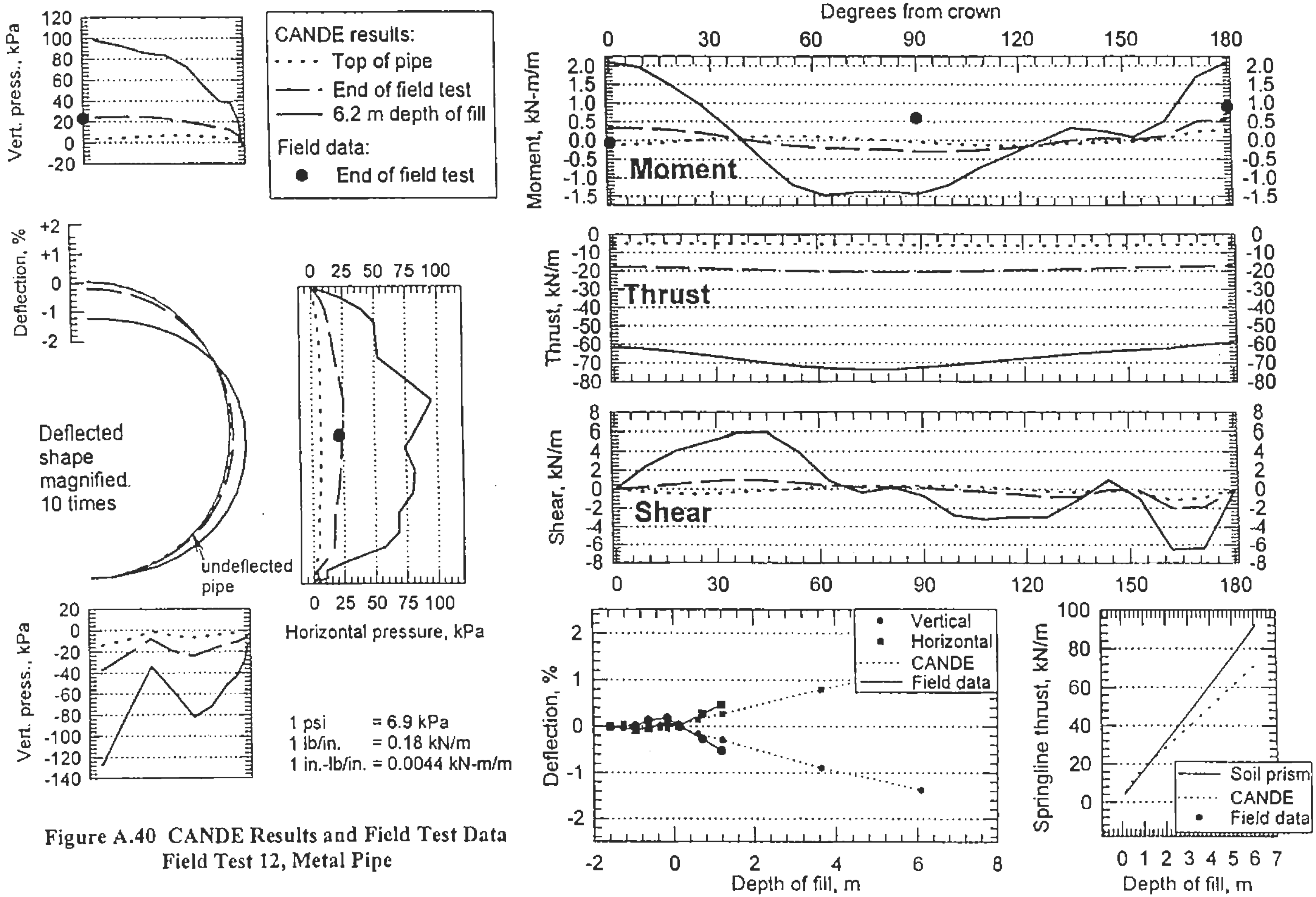

Figure A.40 CANDE Results and Field Test Data Field Test 12, Metal Pipe

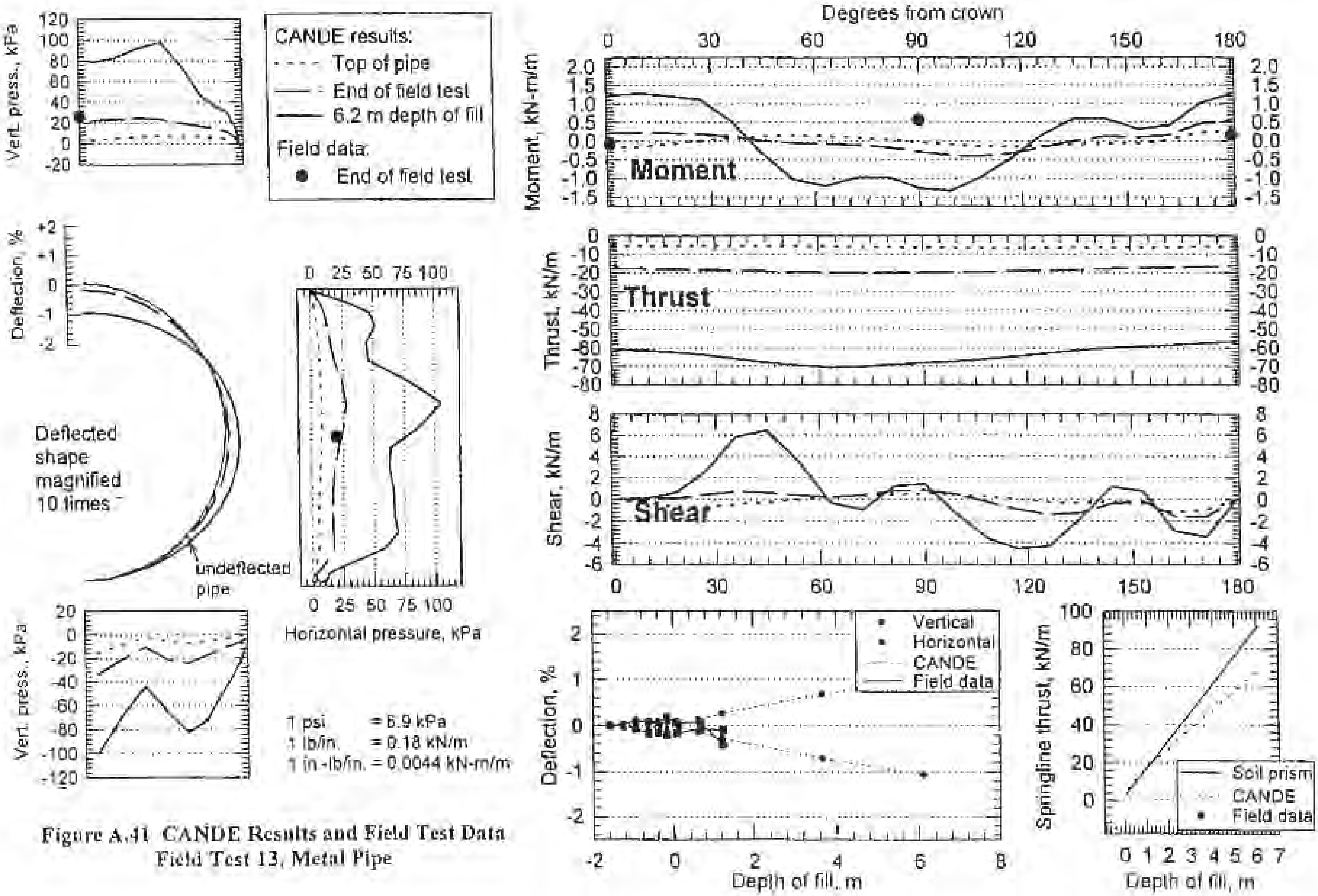

Figure A.41 CANDE Results and Field Test Data
Field Test 13, Metal Pipe

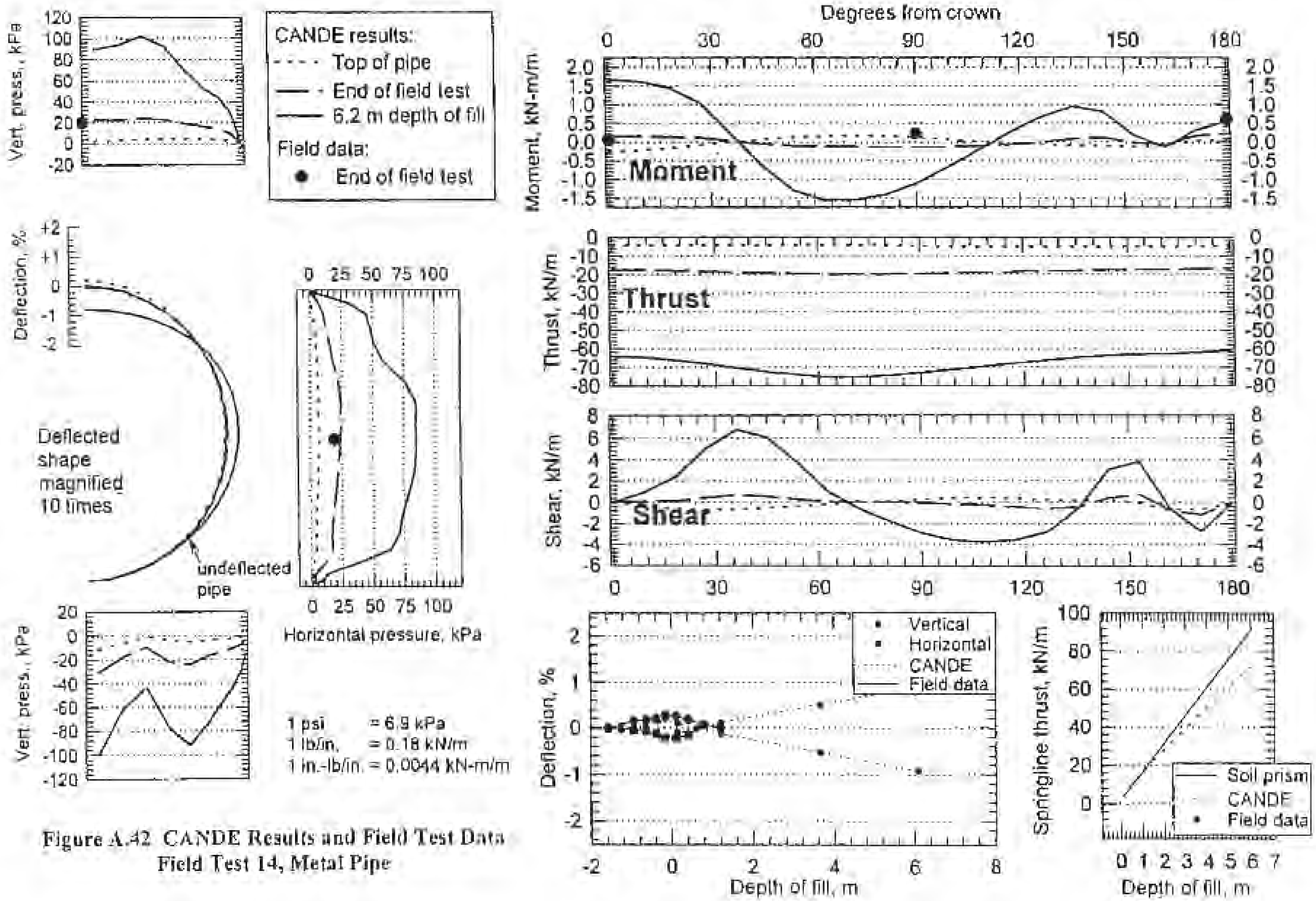

Figure A.42 CANDE Results and Field Test Data
Field Test 14, Metal Pipe

BIBLIOGRAPHY

AASHTO, (1994), *LRFD Bridge Design Specifications*, 1st Edition, American Association of State Highway and Transportation Officials, Washington, DC.

AASHTO, (1996), *Standard Specifications for Highway Bridges*, 16th Edition, American Association of State Highway and Transportation Officials, Washington, DC.

ACPA, (1987), *Concrete Pipe Design Manual*, Seventh Printing, American Concrete Pipe Association, Irving, TX.

ACPA, (1988), *Concrete Pipe Handbook*, Third Printing, American Concrete Pipe Association, Irving, TX.

ASCE, (1970), *Manual of Practice No. 37 —Design and Construction of Sanitary and Storm Sewers (also Water Pollution Control Federal Manual of Practice No. 9 — Design and Construction of Sanitary and Storm Sewers)*, American Society of Civil Engineers, New York, NY.

ASCE, (1994), "Standard Practice for Direct Design of Buried Precast Concrete Pipe Using Standard Installations," *ANSI/ASCE 15-93*, American Society of Civil Engineers, New York, NY.

AWWA, (1996), "Fiberglass Pipe Design," *AWWA Manual of Water Supply Practices M45*, American Water Works Association, Denver, CO.

Brewer, W.E. and Hurd, J.O., (1993), *Structural Performance of Pipes 93*, Balkema, Rotterdam.

Burns, J.Q. and Richard, R.M., (1964), "Attenuation of Stresses for Buried Cylinders," *Proceedings of the Symposium on Soil Structure Interaction*, University of Arizona, Tucson, AZ, pp. 378-392.

Courtney, P.M., (1995), *Performance of Pipe Backfill Materials*, Senior Honors Project Report, Department of Civil and Environmental Engineering, University of Massachusetts, Amherst, MA.

De Rosa, P.J., Hoffman, J.M. and Ollif, (1988), *Pipeline Materials Selection Manual*, Water Research Centre, Swindon, UK.

Duncan, J.M., Byrne, P., Wong, K.S., and Mabry, P., (1980), "Strength, Stress-Strain and Bulk Modulus Parameters for Finite Element Analyses of Stresses and Movements in Soil Masses," *Department of Civil Engineering Report No. UCB/GT/80-01*, University of California, Berkeley, CA.

Filz, G.M., and Brandon, T.L., (1993) *Compactor Force and Energy Measurements*, Geotechnical Testing Journal Vol. 16, No. 4, American Society for Testing and Materials, Philadelphia, PA, pp 442-449.

Filz, G.M., and Brandon, T.L., (1994) *Static and Dynamic Measurements Using Embedded Earth Pressure Cells*, Transportation Research Board, Annual Meeting, Washington, DC.

Grace Construction Products, (1996), *DaraFill Engineering Bulletin*, Grace Construction Products, Cambridge, MA.

Hartley, J.P., and Duncan, J.M., (1987), "E' and its Variations with Depth," *Journal of Transportation Engineering*, ASCE, Vol. 113, No. 5, pp. 538-553.

Hashash, N., E.T. Selig; (1994) Analysis of the Performance of a Buried High Density Polyethylene Pipe. *Proceedings of the First National Conference on Flexible Pipe*, Columbus, OH.

Hashash, N., and Selig, E.T., (1990), "Analysis of the Performance of Buried High Density Polyethyelene Pipe," *Structural Performance of Flexible Pipes*, Balkema, Rotterdam.

Heger, F.J., (1988), "New Installation Designs for Buried Concrete Pipe," *Pipeline Infrastructure — Proceedings of the Conference*, American Society of Civil Engineers, New York, NY, pp. 117-135.

Heger, F.J., Liepins, A.A., and Selig, E.T., (1985), "SPIDA: An Analysis and Design System for Buried Concrete Pipe," *Advances in Underground Pipeline Engineering — Proceedings of the International Conference*, American Society of Civil Engineers, pp. 143-154.

Hobas, (1993), *Large Diameter Centrifugally Cast Fiberglass Pipe Product Brochure 12" and Larger*, Hobas Pipe USA, Inc., Houston, TX.

Howard, A.K., (1977), "Modulus of Soil Reaction Values for Buried Flexible Pipe," *Journal of the Geotechnical Engineering*, ASCE, Vol 103, No. GT1, New York, NY, USA.

Howard, A.K. (1996), *Pipeline Installation*, Relativity Publishing, Lakewood, CO.

Katona, M.G., et al., (1976), "CANDE: Engineering Manual — A Modern Approach for the Structural Design of Buried Culverts," *Report No. FHWA/RD-77*, NCEL, Port Hueneme, CA.

Katona, M.G. and Akl, A.Y., (1987), "Structural Design of Buried Culverts and Slotted Joints, *Journal of Structural Engineering*, ASCE, Vol. 113, No. 1, pp. 44-60.

Krizek, R.J., Parmelee, R.A., Kay, N.J., and Elnaggar, H.A., (1971), "Structural Analysis and Design of Buried Culverts," *National Cooperative Highway Research Program Report 116*, National Research Council, Washington, DC.

Leonhardt, G., (1979), "Die Erdlasten bei Uberschutteten Durchlassen," *Die Bautechnik*, 56(11).

Liedberg, S. (1991), *Earth Pressure Distribution Against Rigid Pipes Under Various Bedding Conditions*, Chalmers University of Technology, Goteborg, Sweden.

Marston, A., (1930), *The Theory of External Loads on Closed Conduits in the Light of the Latest Experiments*, Bulletin 96, Iowa State College.

Marston, A., and Anderson, A.O., (1913), *The Theory of Loads on Pipes in Ditches and Tests of Cement and Clay Drain Tile and Sewer Pipe*, Bulletin 31, Iowa State College.

Marston, A., Schlick, W.J., and Clemmer, H.F., (1917), *The Supporting Strength of Sewer Pipe in Ditches and Methods of Testing Sewer Pipe in Laboratories to Determine Their Ordinary Supporting Strength,* Bulletin Number 47, Iowa State College.

McGrath, T..J., Chambers, R.E., and Sharff, P.A., (1990), "Recent Trends in Installation Standards for Plastic Pipe," *Buried Plastic Pipe Technology, ASTM STP 1093*, George S. Buczala and Michael J. Cassady, Eds., American Society for Testing and Materials, Philadelphia, PA.

McGrath, T.J., E.T. Selig, and L.C. DiFrancesco. (1994) Stiffness of HDPE Pipe in Ring Bending. *Buried Plastic Pipe Technology: 2nd Volume, ASTM STP 1222*, Dave Eckstien, Ed. American Society for Testing and Materials, Philadelphia, PA.

McGrath, T.J. and Selig, E.T. (1996), *Instrumentation for Investigating the Behavior of Pipe and Soil During Backfilling*, Geotechnical Report No. NSF96-443P. Department of Civil and Environmental Engineering, University of Massachusetts, Amherst, MA.

Musser, S.C, Katona, M.G., Selig, E.T., (1989), *CANDE-89 User Manual*, Federal Highway Administration, Turner-Fairbank Highway Research Center, McLean, VA.

Ramsay, B.R., (1994), *One Dimensional Compression of Granular Materials,* Senior Honors Project Report, Department of Civil and Environmental Engineering, Univeristy of Massachusetts, Amherst, MA.

Schlick, W.J., (1920), *Supporting Strength of Drain Tile and Sewer Pipe Under Different Pipe-Laying Conditions*, Bulletin Number 57, Iowa State College.

Schlick, W.J., and Johnson, J.W., (1926), *Concrete Cradles for Large Pipe Conduits*, Bulletin Number 80, Iowa State College.

Schlick, W.J., (1932), *Loads on Pipe in Wide Ditches*, Bulletin Number 108, Iowa State College.

Seed, R.B. and Dunan, J.M., (1984), "SSCOMP — A Finite Element Analysis Program for Evaluation of Soil-Structure Interaction and Compaction Effects," *Report No. UCB/GT/84-02*, Department of Civil Engineering, University of Berkeley, Berkeley, CA.

Selig, E.T., (1988), "Soil Parameters for Design of Buried Pipelines," *Pipeline Infrastructure — Proceedings of the Conference*, American Society of Civil Engineers, New York, NY, pp. 99-116.

Selig, E.T, (1990), "Soil Properties for Plastic Pipe Installations," *Buried Plastic Pipe Technology, ASTM STP 1093*, George S. Buczala and Michael J. Cassady, Eds., American Society for Testing and Materials, Philadelphia, PA.

Selig, E.T., L.C. DiFrancesco, and T.J. McGrath, (1994) Laboratory Test of Pipe in Hoop Compression. *Buried Plastic Pipe Technology: 2nd Volume, ASTM STP 1222*, Dave Eckstien, Ed., American Society for Testing and Materials, Philadelphia, PA.

Spangler, M.G., (1933), *The Supporting Strength of Rigid Pipe Culverts*, Bulletin 112, Iowa State College.

Spangler, M.G., (1941), "The Structural Design of Flexible Pipe Culverts." *Iowa Engineering Experiment Station, Bulletin No. 153*, Ames, IA.

Spangler, M.G., (1950), *Field Measurements of the Settlement Ratios of Various Highway Culverts*, Bulletin 170, Iowa State College.

Spangler, M.G., and Schlick, W.J., (1953), *Negative Projecting Conduits*, Report Number 14, Iowa State College.

TACA, (1989), *Suggested Guide Specification for Flowable Fill*, Texas Aggregates and Concrete Association.

Watkins, R.K. and Spangler, M.G., (1958), "Some Characteristics of the Modulus of Passive Resistance of Soil. A Study in Similitude." *Proceedings HRB*, Vol. 37, pp. 576-583.

Webb, M.C., (1995), *Field Studies of Buried Pipe Behavior During Backfilling*, Geotechnical Report No. NSF95-431P, Department of Civil and Environmental Engineering, University of Massachusetts, Amherst.

Webb, M.C., McGrath, T.J., Zoladz, G.V., and Selig, E.T., (1995), *Field Test Data from Pipe Installation Study*, Geotechnical Report No. NSF95-438I, Department of Civil and Environmental Engineering, University of Massachusetts, Amherst, MA.

Webb, M.C., McGrath, T. J., and Selig, E. T., "Field Test of Buried Pipe with CLSM Backfill, *The Design and Application of Controlled Low-Strength Materials (Flowable Fill), ASTM STP 1331*, A.K. Howard and J.L. Hitch, Eds., American Society for Testing and Materials, 1997.

White, H.L. and Layer, J.P., (1960), "The Corrugated Metal Conduit as a Compression Ring." *Proceedings HRB*, Vol. 39, pp. 389-397.

Zoladz, G.V, (1995), *Laboratory Testing of Buried Pipe*, Geotechnical Report No. NSF95-435P, Department of Civil and Environmental Engineering, University of Massachusetts, Amherst, MA.

Zoladz, G.V., T.J. McGrath, M.C. Webb, and E.T. Selig (1995), *Field Test Pipe Profiles*, Geotechnical Report No. NSF95-439I, Department of Civil and Environmental Engineering, University of Massachusetts, Amherst, MA.

Zoladz, G.V., T.J. McGrath, M.C. Webb, and E.T. Selig, (1995), *Laboratory Test Data*, Geotechnical Report No. NSF95-437I, Department of Civil and Environmental Engineering, University of Massachusetts, Amherst, MA.

HRD/S-99(441)S